JOURNAL OF POLYMER SCIENCE: PART A-1 VOL. 7, 1379–1384 (1969)

# Role of Cations in Radiation Grafting and Homopolymerization

M. B. HUGLIN and B. L. JOHNSON, *Department of Chemistry, University of Salford, Salford 5, England*

## Synopsis

The grafting of acrylic acid in aqueous solution to nylon 6 film has been studied in the presence of ferrous, ferric, and cupric salts. The mutual irradiation technique was adopted using a $^{60}Co$ source. The anions were found to have no effect on the grafting or homopolymerization, but both of these processes were suppressed by the cations in the following order of effectiveness: $Cu^{2+} > Fe^{2+} > Fe^{3+}$. The rate constant for the capture of hydroxyl radicals by acrylic acid has been determined as $6 \times 10^9$ l. mole$^{-1}$ sec$^{-1}$ by pulse radiolysis using the $CNS^-$ competition method. By invoking this result, mechanisms have been suggested for the process of chain termination by metal cations.

When the $G$(radical) value of the monomer is appreciable relative to that of the polymeric substrate, the efficiency of grafting is seriously impaired when the mutual irradiation technique is used. However, for the system poly(propylene)–acrylic acid, Ódor and Geleji[1] found that homopolymerization could be inhibited by incorporating ferrous sulfate (at an unspecified concentration), while certain salts and surface-active agents have been reported[2] to increase the rate of grafting for the same system. Subsequently Chapiro et al.[3,4] were able to follow the kinetics of grafting acrylic acid and 4-vinylpyridine to poly(tetrafluoroethylene) by suppressing homopolymerization with Mohr's salt at a fixed concentration. Although no quantitative studies appear to have been made on the effect of metal ions on radiation grafting, the situation with respect to their role in $\gamma$-initiated solution polymerization has been clarified in reports by Collinson et al.[5] and by Bengough and O'Neill[6] (containing cognate references), which provide a useful basis for this note concerned with the mutual irradiation of aqueous acrylic acid–nylon 6 in the presence of three different salts.

## EXPERIMENTAL

Radiation was effected by $\gamma$-rays from a 9 000-curie $^{60}Co$ source, and the dose rate determined by Fricke dosimetry ($G_{Fe^{3+}} = 15.5$). Nylon 6 film (thickness 75 $\mu$), donated by I.C.I. Ltd., Plastics Division, Welwyn Garden City, England, was utilized for the bulk of the work. One experiment entailed the use of thicker film (85 $\mu$), which was generously provided by Verenigd Plastic-Verkoopkantoor N.V., Zeist, Holland.

Sample tubes containing ca. 0.1 g. of film (75$\mu$) and a solution composed of 1 ml acrylic acid and 9 ml aqueous salt solution were outgassed by freeze-thaw cycles, sealed ($10^{-5}$ mm), and irradiated at 25 ± 2°C for 40 hr at 25 rad/min. After irradiation the extracted film was washed repeatedly with hot water and dried to constant weight *in vacuo*. The percentage grafting was estimated from the increase in weight. Two procedures were then adopted to determine the percentage of homopolymerization.

**Ferrous and Ferric Systems.** Aqueous sodium hydroxide was added in slight excess to the solution, the monomer and homopolymer thus being converted to their soluble sodium salts and the metal ions to their insoluble hydroxides. The latter was removed by filtration after centrifugation. The poly(sodium acrylate) was next precipitated in methanol, filtered, and weighed; the percentage of homopolymer was calculated with due allowance from a blank experiment for co-precipitated inorganic materials.

**Cupric System.** Cupric ions were reduced to cuprous ions with sulfurous acid and precipitated as the thiocyanide, which was removed by centrifugation and filtration. After adding an excess of sodium hydroxide, the sodium salt of the poly(acrylic acid) was precipitated and the percentage of homopolymer determined as for the ferrous and ferric systems.

## RESULTS

The salts utilized were ferric ammonium sulfate, ferrous ammonium sulfate, and cupric chloride. For the sake of clarity, experimental data involving ferrous sulfate and cupric sulfate have been omitted from the diagrams for, within experimental error, they were found to coincide with those for ferrous ammonium sulfate and cupric chloride, respectively. For a given concentration of cation, variations were thereby introduced in the concentration (for the ferric system) and in both the concentration and nature (for the cupric system) of the anions. It appears, therefore, that the overall effects are due primarily to the metal cations.

The three cations display similar characteristics (Fig. 1), the reduction

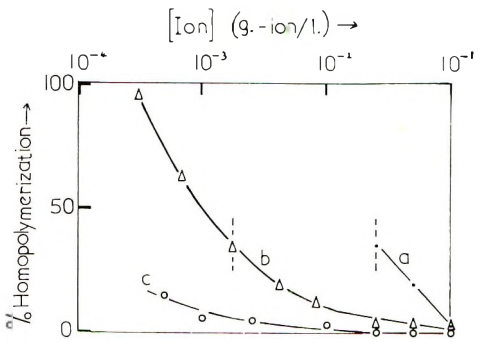


Fig. 1. Dependence of homopolymerization on concentration of added cations: (*a*) $Fe^{3+}$, (*b*) $Fe^{2+}$, and (*c*) $Cu^{2+}$.

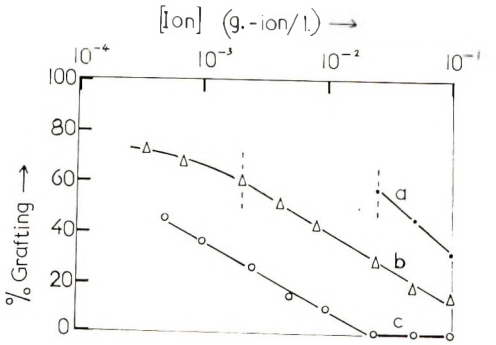


Fig. 2. Dependence of grafting on concentration of added cations: (*a*) $Fe^{3+}$, (*b*) $Fe^{2+}$, and (*c*) $Cu^{2+}$.

in homopolymerization being greater the higher the ion concentration ([ion]). At very high [ion] (ca. $10^{-1}$ g-ion/l.) the suppression is almost complete, but this practical advantage is obtained at the expense of grafting efficiency (Fig. 2). The broken vertical lines denote the points for which a marked increase in viscosity was observed, the corresponding concentration of poly(acrylic acid) being ca. 4 g/dl. The cupric medium alone remained quite fluid, for a homopolymer concentration of ca. 1.5 g/dl was attained even at the lowest $[Cu^{2+}]$ utilized. Points to the left of the line, i.e., at lower [ion], denote very high viscosity in the case of the ferrous system and a solid crosslinked gel in the ferric system. To the right of the line, i.e., at higher [ion], increasing fluidity was clearly discernible. In the absence of any metal cations gel formation proceeded very rapidly and prevented any estimation of homopolymerization or grafting.

From Figure 2 it is apparent that the cations decrease the grafting in a similar fashion to the homopolymerization. When, as in the ferrous case for example, there is a sharp increase in homopolymerization, the grafting commences to fall off correspondingly on account of the substantial depletion in monomer concentration. The order of effectiveness in suppressing homopolymerization is $Cu^{2+} > Fe^{2+} > Fe^{3+}$ and we are accordingly currently studying the kinetics of grafting in the presence of $10^{-3}M$ aqueous cupric chloride. This concentration of cupric ions is eminently suitable, for at lower ones the homopolymerization is excessive, while the suppression of grafting is too great at higher ones.

## DISCUSSION AND ANCILLARY EXPERIMENTS

As the reaction medium comprises 90% (v/v) of water, the radiolysis products of water (in the absence of oxygen: $H^{\bullet}$, $OH^{\bullet}$ and $e^{-}_{aq}$) may be expected to play a significant role. Below pH 3, the solvated electron has a very short lifetime and, as the pH of the medium is 2.5–3.0, solvated electron reactions will be omitted from consideration.

Rate constants $k$ for the reaction between hydrogen atoms and hydroxyl radicals with the cations in aqueous solution at low pH have been abstracted

from the literature compilation of Anbar and Neta,[7] and are given in Table I.

TABLE I

| Hydrogen atom | | Hydroxyl radical | |
|---|---|---|---|
| Reactant | $k$, l./mole-sec | Reactant | $k$, l./mole-sec |
| $Cu^{2+}$ | $5.9 \times 10^7$ | $Cu^{2+}$ | $3.5 \times 10^8$ |
| $Fe^{2+}$ | $2 \times 10^7$ | $Fe^{2+}$ | $2.5 \times 10^8$ |
| $Fe^{3+}$ | $9 \times 10^7$ | $Fe^{3+}$ | — |

To substantiate our argument (*vide infra*) invoking these constants we have studied the capture of OH· by the monomer via pulse radiolysis by the competition method[8] with $10^{-4}M$ KCNS as the reference solute. The relevant equation is

$$OD_0/OD_{mixt} = 1 + (k_2/k_1)\ [\text{monomer}]/[\text{reference}] \qquad (1)$$

Here $OD_0$ and $OD_{mixt}$ denote the optical densities of absorbing product ($CNS^{\cdot}$) for the pulse radiolysis of aqueous KCNS solution alone and in the presence of different concentrations of acrylic acid, respectively. The rate constants for the reaction of OH· with $CNS^-$ and with the monomer are, respectively, $k_1$ and $k_2$. The plot of eq. (1) is given in Figure 3, the slope of which yields a value of 0.91 for the ratio $k_2/k_1$. The value of $k_1$ is known[9] to be $6.6 \times 10^9$, and the derived value of $k_2$ is thus $6.0 \times 10^9$ for the reaction between hydroxyl radicals and acrylic acid.

Consideration of the value of $k_2$ in conjunction with Table I suggests that the reaction of OH· with the monomer is of prime importance compared to that with the cations. Thus typically, for $1.5M$ acrylic acid with $10^{-3}M$ cupric chloride, the reaction of OH· with $CH_2$=CHCOOH is $(6 \times 10^9 \times 1.5)/(3.5 \times 10^8 \times 10^{-3}) \simeq 3 \times 10^4$ times faster than the reaction of OH· with $Cu^{2+}$.

The effect of $Cu^{2+}$ and $Fe^{3+}$ on the $\gamma$-initiated polymerization of aqueous acrylamide in acid medium has been investigated by Collinson et al.,[5]

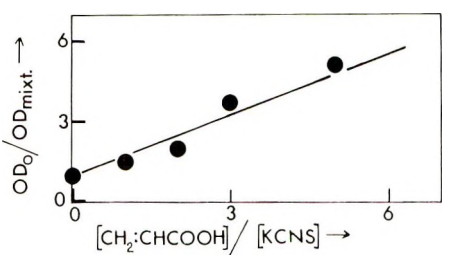


Fig. 3. Determination of the rate constant for the acrylic acid–hydroxyl radical reaction by the pulse radiolysis competition method.

who suggested that radical termination occurs by an electron transfer process from a propagating polymer to a *d*-orbital of the cation. In the light of these and our own findings it is proposed that: (1) $\gamma$-photons produce radical sites on the nylon 6 (Ny) backbone [Brodskii et al.[10] postulate—CONHC$^{\bullet}$H—$(CH_2)_4$—as the structure]; (2) grafting emanates from these sites; (3) homopolymerization is initiated by H$^{\bullet}$ and OH$^{\bullet}$ formed from radiolysis of the solvent; (4) termination by the metal (M) cations proceeds as shown in eqs. (2) and (3) for the cupric and ferric systems and as shown in eqs. (4) and (5) for the ferrous system.

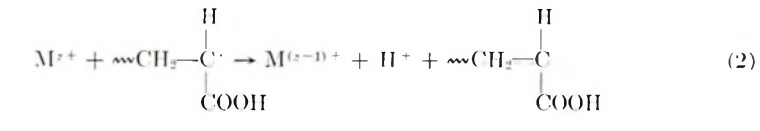

(2)

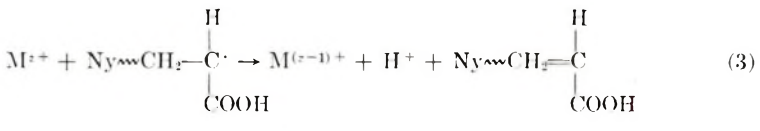

(3)

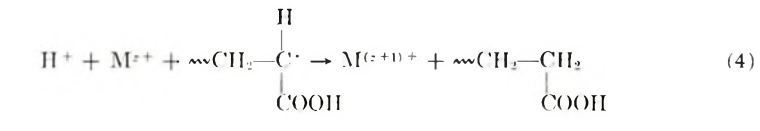

(4)

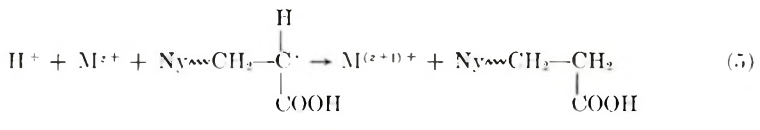

(5)

Destruction of branching loci radicals Ny$^{\bullet}$ by the cations is likely to be of minimal importance in view of the large excess of acrylic acid to which the backbone sites must be preferentially accessible (30 000 > [monomer]/[ion] > 150 for all experiments). In the absence of radiation the film had been found to swell by 20% (w/w) in 10% (v/v) aqueous monomer after $^1/_4$ hr at 25°C. Hence during the radiation grafting the swollen film constitutes a viscous barrier to diffusion of the cations and consequently, high degrees of grafting are obtained when the homopolymerization is extensively reduced over a wide range of [ion]. Complete kinetic runs (degree of grafting versus time) under the same conditions as those already described revealed that, in the presence of $[Cu^{2+}] = 10^{-3}$ g-ion/l., the rate of grafting was lower than in the presence of $[Cu^{2+}] = 5 \times 10^{-4}$ g-ion/l. Further supporting evidence is provided by the use of a thicker film (85 $\mu$) for experiments corresponding to those of Figures 1 and 2. On varying the concentration of added ferrous ions the homopolymerization behavior was identical to that found with the 75 $\mu$ film, but the degrees of grafting were higher for each $[Fe^{2+}]$, thus suggesting that the thicker film imposes a diffusive restriction to the grafting-termination process [eq. (5)].

Provision of a Science Research Council maintenance grant (to B. L. J.) is gratefully acknowledged. Pulse radiolysis facilities were kindly extended by the Christie Hospital, Manchester, England, and we are indebted to Dr. J. V. Davies for his advice and assistance in connection with this facet of the work.

## References

1. L. Ódor and F. Geleji, *Proceedings of the first Tihany Symposium on Radiation Chemistry*. (J. Dobó and P. Hedvig, Eds.) Hungarian Academy of Sciences, Budapest, 1962, p. 255.

2. S. Torikai and E. Mukoyama, *Kobunshi Kagaku* **19**, 344 (1962).

3. A. Chapiro and P. Seidler, *Europ. Polym. J.*, **1**, 189, (1965).

4. G. Bex, A. Chapiro, M. B. Huglin, A. M. Jendrychowska-Bonamour and T. O'Neill, *Macromolecular Chemistry Brussels-Louvain 1967 J. Polym. Sci. C*, **22**) G. Smets, Ed., Interscience, New York, 1968, p. 493.

5. E. Collinson, F. S. Dainton, D. R. Smith, G. J. Trudel, and (in part) S. Tazuké, *Discussions Faraday Soc.*, **29**, 188, (1960).

6. W. I. Bengough and T. O'Neill, *Trans. Faraday Soc.*, **64**, 1014 (1968).

7. M. Anbar and P. Neta, *J. Appl. Radiation Isotopes*, **18**, 493 (1967).

8. G. E. Adams, J. W. Boag, J. Currant and B. D. Michael in *Pulse Radiolysis*, M. Ebert, J. P. Keene, A. J. Swallow, and J. H. Baxendale, Eds., Academic Press, New York–London, 1965, p. 131.

9. G. E. Adams, J. W. Boag, and B. D. Michael, *Trans. Faraday Soc.*, **61**, 1417, (1965).

10. A. I. Brodskii, A. S. Fomenko, T. M. Abramova, E. P. Dar'yeva, A. A. Galina, Ye. G. Furman, L. A. Kotorlenko, and A. P. Gardenina, *Vysokomol. Soedin.* **7**, 116 (1965).

Received July 1, 1968

JOURNAL OF POLYMER SCIENCE: PART A-1 VOL. 7, 1385–1391 (1969)

# Role of Polymer Oxidation in the Adhesion of Polyethylene to Metals

J. M. SYKES and T. P. HOAR, *Department of Metallurgy, University of Cambridge, Cambridge, England*

## Synopsis

Untreated polyethylene will adhere well to aluminum only if it is applied in an oxidizing atmosphere. Peel strengths for coatings applied to various bright copper surfaces are far lower, probably because of decrease in polymer oxidation when copper is present. Preoxidized polyethylene sheet adheres well when melted on to copper in nitrogen. In view of earlier evidence for the formation of a weak interfacial layer containing short-chain material, it is proposed that the weak bond strengths so caused are substantially improved by the preferential adsorption of longer-chain surface-active oxidized species in the polymers.

## INTRODUCTION

When polyethylene is used as a hot-melt adhesive, better bond strengths are achieved with oxidized polyethylene than with unoxidized,[1] and if polyethylene is applied to metal in an oxygen-free environment poor adhesion results.[2] On the other hand, if the polyethylene is purified by selective reprecipitation from a hot solvent before use, then better bond strengths are produced in an oxygen-free atmosphere than those obtained with untreated polymer,[3] but they are not as good as those obtained with untreated polymer applied in air.[4] The improvement has been shown to be due to the removal of low molecular weight constituents that otherwise segregate to the polymer metal interface during solidification and form a weak layer.[5,6] Thus to obtain strong bonding to solid polyethylene with an epoxy adhesive, the surface of the polymer has to be crosslinked to increase its mechanical strength.[7] In the light of these results it is difficult to accept the explanation that oxidation of the polymer increases adhesion to metals merely by increasing the interaction between the polymer molecules and the metal surface; the force needed to remove the polymer from the metal is limited by its bulk strength.

## EXPERIMENTAL

Coatings of polyethylene were applied by melting to commercial grades of copper and aluminum sheet. Three grades of copper were used, electrolytic tough-pitch, phosphorus-deoxidized, and oxygen-free high con-

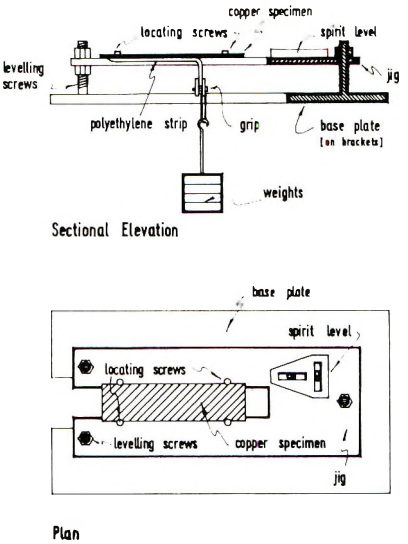


Fig. 1. Jig for peel test.

ductivity, and the results showed no significant differences between them. The polyethylene was either I.C.I. WRM-19 powder, which showed no evidence of oxidation when examined by infrared spectrophotometry,[8] or sheet fabricated commercially from Bakelite DFD 4400 powder by extrusion at 150°C in air. This showed a strong adsorption peak at ca. 1 700 $cm^{-1}$ due to C=O groups, which could not be resolved into separate peaks for carboxyl and carbonyl groups; Lancely has shown that both may be present.[9] The adhesion of the coatings was estimated by a peel test using dead loading. When coatings had been melted on to the 10 × 2.5 cm metal test pieces and had cooled again to room temperature, a 1.25 cm wide test strip was cut down the center with a sharp knife; one end of this was lifted, and a small clamp was screwed on to it. The specimen was inverted on a jig (Fig. 1) and weights were added to the clamp in small increments until peeling of the coating from the metal was first detected. This simple test gave results that agreed well with somewhat more sophisticated tests carried out at a constant peel rate on an Instron tensile testing machine.

When WRM-19 powder was spread on aluminum sheet that had been cleaned with Brasso metal polish and degreased with acetone by swabbing—a very primitive surface preparation—and then melted by heating in air for times of 5–25 min at 200°C, loads of up to 2 760 g/cm were needed to peel off the coatings (Table I). With copper the peel loads were much smaller, even after either vapor degreasing with trichlorethylene, or alkaline degreasing with hot saturated sodium carbonate. Abrading the copper to expose "clean" metal and to roughen the surface gave very little improvement in bond strength, and after etching the metal with various strengths of nitric or sulfuric acids the bond strengths were still small

TABLE I

Adhesion of Polyethylene to Aluminum[a]

| Coating time, min | Peel load, g/cm |
|---|---|
| 5 | 0 |
| 7 | 0 |
| 8 | 751 |
| 10 | 1260 |
| 15 | 1380 |
| 20 | 980 |
| | 1260 |
| 25 | 2760 |

[a] Aluminum cleaned with Brasso metal polish, degreased with acetone, and coated with WRM-19 powder in air at 200°C.

TABLE II

Adhesion of Polyethylene to Copper[a]

| Surface treatment | Maximum peel load, g/cm |
|---|---|
| Degreased | 276 |
| Etched | 700 |
| Abraded | |
| 1G paper | 386 |
| 5 0's paper | 331 |
| Electropolished | 551 |

[a] Copper treated as shown, then coated with WRM-19 powder at 200°C in air. The peel strengths in the table are the maximum obtained.

(Table II). Nor did electropolishing in 8*M* orthophosphoric acid at potentials from +600 to +1 600 mV(nhe)—aimed to modify the oxide on the metal—lead to any great improvement.

Baker and Spencer[10] have demonstrated that if copper is treated with Ebonol C to form a thick layer of cupric oxide then when polyethylene is melted on to this it adheres well. We have obtained similar results (peel loads of up to 3 970 g/cm) by anodizing the copper in 15% sodium hydroxide at 90°C;[11] details will be published elsewhere. Attempts to obtain good adhesion to thin films of cupric oxide formed by electropolishing or anodizing at high current density were not successful.

To confirm that oxidation is a prerequisite for high peel loads, coatings were applied in an oxygen-free atmosphere. Polyethylene was applied to the metal in a tube furnace connected to a gas-tight box filled with oxygen-free nitrogen (British Oxygen Co. white spot grade) in which the specimens could be manipulated with tongs. The box was purged continuously with nitrogen. When either copper or aluminum specimens were coated with WRM-19 powder in this apparatus the adhesion was too small to be

measured—the coating lifted off the substrate when a test strip was cut. If, however, the powder was spread on a clean PTFE sheet and heated for 30 min at 200°C in air, then the polyethylene sheet when bonded to aluminum even in nitrogen gave high peel strengths (Table III). Infrared absorption analysis showed that the sheet contained C=O groups. Sheet prefabricated in air also bonds well to aluminum or copper in nitrogen. This demonstrates that oxidation can cause strong adhesion of polyethylene to metal surfaces.

TABLE III

Oxidized Polyethylene Applied in Nitrogen[a]

| Coating time, min | Peel load, g/cm |
|---|---|
| 20 | 1575 |
| 25 | 2280 |
| 30 | 3150 |

[a] WRM-19 powder melted into sheet and heated for 30 min in air at 200°C, then applied to degreased aluminum at 200°C in nitrogen.

To understand why polyethylene applied to copper in air does not adhere strongly we must take account of results obtained by Bright,[12] who has shown that although most metals catalyze the oxidation of polyethylene in oxygen, copper inhibits it. He suggests that this will prevent the formation of active groups in the polymer. We have found that if polyethylene is oxidized before it is applied to the copper then the adhesion is greatly improved, which supports this suggestion (Table IV). One treatment, heating the polyethylene in a solution of 200 g/l. of sodium dichromate and 140 ml/l. of sulfuric acid at 60°C, gave particularly good results (Table V). The peel strengths are not in general higher than those found with untreated prefabricated sheet, but good bonds can be produced after much shorter heating times—the greater the degree of oxidation the faster the bonding.

TABLE IV

Oxidized Polyethylene Applied to Copper

| Treatment | Maximum peel load, g/cm |
|---|---|
| WRM-19 heated in air for 30 min at 200°C | 1570 |
| Prefabricated sheet (extruded in air) | 2520 |
| Sheet oxidized in acid $Na_2Cr_2O_7$ | 4330 |

[a] Polyethylene oxidized as shown, then applied to etched copper sheet in air at 200°C.

TABLE V

Polyethylene Sheet Oxidized in Acid $Na_2Cr_2O_7$ and Applied to Copper

| Coating time, min | Peel load, g/cm, at various oxidation times | | | | | |
|---|---|---|---|---|---|---|
| | 0 | 5 min | 10 min | 15 min | 20 min | 30 min |
| 5 | | | | 2360 | | 3150 |
| 10 | 472 | 710 | | 3550 | 1810 | 2510 |
| 20 | 1730 | 1340 | 1970 | 3150 | 2750 | 2360 |
| 30 | 2520 | 1180 | 3150 | 1970 | 2360 | 2560 |
| 40 | 2125 | 550 | 2750 | | 4330 | |

[a] The prefabricated sheet was oxidized in the solution at 60°C for the time shown, then applied to copper etched in 25% $HNO_3$ by heating at 200°C in air.

Electron-probe microanalysis of cross sections of copper coated with polyethylene was carried out. The cross sections were mounted in an acrylic resin and ground flat on wet emery papers taking care always to polish towards the metal so that metal was not smeared on to the surface of the polymer. The final polishing was carried out on a lapping wheel with 1 $\mu$ diamond paste. The microanalyzer was used to detect copper K$\alpha$ radiation emitted from the polymer. Copper was found at distances of up to 100 $\mu$ from the interface in cases of good adhesion. The polymer near the interface often contained several per cent of copper, which suggests that the copper probably reacted with carboxylic groups in the polyethylene to form a salt soluble in the polymer. Such an interaction could well also take the form of a strongly chemisorbed layer of carboxylate salt at the copper oxide surface.

## DISCUSSION

Evidently, oxidation can lead to high bond strengths, although Bikerman,[3] and also Hansen and Schonhorn,[7] have demonstrated the presence of a weak layer on the surface of polyethylene containing low molecular weight material. We have indeed found that if WRM-19 powder is purified by dissolution in boiling toluene and reprecipitation with acetone, then, provided the powder is dried slowly for several weeks and the large lumps are rejected, the polymer gives improved adhesion to metal even when applied in nitrogen (1340 g/cm to Al, 788 g/cm to Cu). These present load strengths are equivalent to those obtained by Bikerman, but (for copper) are much lower than those obtained with unpurified but oxidized polyethylene (Tables III and V).

We suggest that the function of the active groups introduced by oxidation is to nullify the effect of the weak layer by acting as links across it, between the metal (or oxide) surface and the main polymer matrix. All the oxidized polyethylene contained C=O groups; a proportion of these will be in carboxyl groups which can chemisorb on to the metal. This will certainly tend to deplete the polymer near the metal of polar molecules,

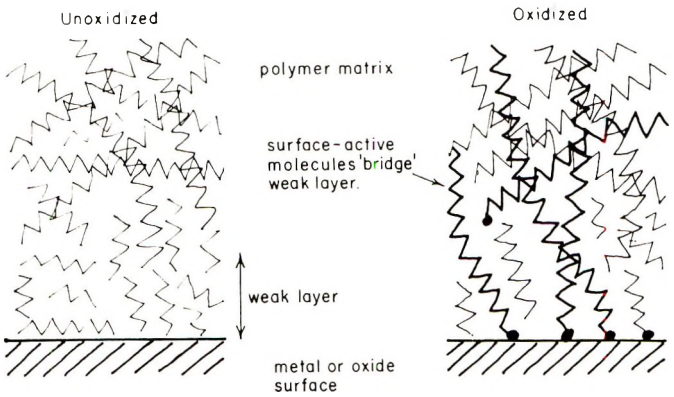


Fig. 2. Action of adsorbed polymer molecules (schematic): (*a*) unoxidized; (*b*) oxidized.

but provided that the polymer is liquid they may be replenished by diffusion until a nearly complete monolayer of adsorbed polar molecules is built up on the metal. When the polymer solidifies, impurities may well be rejected to the metal/polymer interface but will not be able to displace the strongly adsorbed oxidized molecules, which pass right through any weak layer and maintain a strong bond between the bulk of the polymer and the metal (Fig. 2). In order to remove the coating, these links must either be broken by fracturing C—C bonds, or by pulling the chain out of the polymer matrix against the van der Waals forces along the whole of their lengths. The peel strength will depend upon the number of these links formed during the time the polyethylene is molten. A high concentration of polar molecules will decrease the time taken to build up a nearly complete adsorbed monolayer.

Unless purification of the polymer can remove all the low molecular weight impurities, then a greater improvement in adhesion can be obtained by oxidation, than by purification, as shown by the experimental observations. Bikerman observed complete failure within the polymer when a load of 700 g/cm was needed to strip off a coating, but observations carried out on our specimens with the scanning electron microscope show that failure is apparently at the interface for loads of up to 2000 g/cm; presumably it occurs in the weak layer. For loads greater than 3400 g/cm, fracture occurs in the polymer, both fracture surfaces appearing completely covered with drawn out polyethylene fibers.

We acknowledge with thanks financial assistance from the International Copper Research Association, who sponsored this research and provided a grant for one of us (J.M.S.) during the period of his research studentship. We also thank them for permission to publish this work.

## References

1. F. J. Bockhoff, E. T. McDonel, and J. E. Rutzler, *Ind. Eng. Chem.*, **50,** 928 (1958).
2. H. A. Arbit, E. E. Griesser, and W. A. Haine, *Tappi*, **40,** 161 (1957).
3. J. J. Bikerman, *J. Appl. Chem.*, **11,** 81 (1961).
4. H. Schonhorn, *J. Polym. Sci. B*, **2,** 464 (1964).
5. J. J. Bikerman, *SPE Trans.*, **2,** 213 (1962).
6. J. J. Bikerman and C. R. Huang, *Trans. Soc. Rheol.*, **3,** 5 (1959).
7. R. H. Hansen and H. Schonhorn, *J. Polym. Sci. B*, **4,** 203 (1966).
8. J. M. Sykes and T. P. Hoar, to be published.
9. H. A. Lanceley, *Polymer*, **6,** 15 (1965).
10. R. G. Baker and A. T. Spencer, *Ind. Eng. Chem.*, **52,** 1015 (1960).
11. J. M. Sykes and T. P. Hoar, to be published.
12. K. A. Bright, private communication (1966).

Received August 6, 1968

JOURNAL OF POLYMER SCIENCE: PART A-1 VOL. 7, 1393–1405 (1969)

# Structure and Properties of Cellulose Graft Copolymers. III. Cellulose–Methyl Methacrylate Graft Copolymers Synthesized by the Ceric Ion Method

ROBERT Y. M. HUANG and P. CHANDRAMOULI, *Department of Chemical Engineering, University of Waterloo, Waterloo, Ontario, Canada*

## Synopsis

The ceric ion-initiated graft copolymerization of methyl methacrylate onto wood cellulose was found to depend on the concentrations of initiator, monomer, and cellulose. The structure of cellulose–methyl methacrylate graft copolymers was studied by hydrolyzing away the cellulose backbone to isolate the grafted poly(methyl methacrylate) branches. The molecular weights and molecular weight distributions of the grafted poly(methyl methacrylate) were determined by using gel-permeation chromatography. The number-average ($\bar{M}_n$) molecular weights ranged from 36000 to 160000 and the polydispersity ratios ($\bar{M}_w/\bar{M}_n$) varied from 4.0 to 7.0. The grafting frequency or the number of poly(methyl methacrylate) branches per cellulose chain calculated from the per cent grafting and molecular weight data varied from 0.38 to 3.2. The structure of cellulose–methyl methacrylate graft copolymers and the effect of stepwise addition of initiator on the structure are discussed.

## INTRODUCTION

The previous papers in this series of investigations on the structure and properties of cellulose graft copolymers were concerned with the structure of rayon–styrene graft copolymers prepared by the direct $\gamma$-ray irradiation method[1] and cellulose–styrene graft copolymers synthesized by the ceric ion method.[2] The present paper deals with the structure of cellulose–methyl methacrylate graft copolymers synthesized by the ceric ion method.

Following the work of Mino and Kaizerman[3] in 1958, many studies have been reported on the use of the ceric ion technique to initiate graft copolymerization of vinyl monomers onto cellulose. However, relatively little work has been reported on the molecular structure of the graft copolymers and the molecular weight distributions of the grafted polymer chains. In the previous paper[2], the molecular weight distributions of grafted polystyrene branches were discussed in some detail. Wellons et al.[4] reported a comparison of the molecular weight distributions of the polystyrene branches obtained from graft copolymers prepared by the mutual and pre-irradiation techniques. In the present study, gel-permeation chromatography (GPC) was used to obtain information on the molecular weights and

molecular weight distributions of the poly(methyl methacrylate) branches in cellulose–methyl methacrylate graft copolymers synthesized by the ceric ion method.

## EXPERIMENTAL

### Materials

**Cellulose.** Novocell K wood pulp obtained from International Cellulose Research Limited, Hawkesbury, Ontario, was used in all the graft copolymerization runs.

**Monomer.** Methyl methacrylate was obtained from Monomer-Polymer Laboratories, Philadelphia, Pa.

**Polymer Standards for GPC Calibration.** Monodisperse ($\overline{M_w}/\overline{M_n}$) = 1.06–1.20) standard polystyrene samples were obtained from Pressure Chemicals Ltd., Pittsburgh, Pa. Poly(methyl methacrylate) polydisperse "standards" were obtained from the Distillation Products Industries Division, Eastman Kodak Co., Rochester, New York. These standards consisted of samples from the Eastman Kodak-Brooklyn Polytechnic Institute Polymer Sample Bank having the following molecular weights: No. 6038, $\overline{M_n}$ = 19400; No. 6036, $\overline{M_n}$ = 48600; No. 6041, $\overline{M_n}$ = 160000.

**Chemicals.** Ceric ammonium nitrate (reagent grade) was obtained from J. T. Baker Chemicals Ltd.

### Purification of Monomer

Methyl methacrylate monomer was purified by washing with a 6–8% sodium hydroxide solution to remove the inhibitor. The monomer was then washed with distilled water and dried overnight over anhydrous calcium chloride, vacuum distilled and stored in a refrigerator.

### Preparation of Initiator Stock Solution

A 0.1$M$ stock solution of the initiator was prepared by dissolving the required amount of ceric ammonium nitrate [$Ce(NH_4)_2(NO_3)_6$] in a 1$M$ nitric acid solution. Stock solutions which were stored for more than 4 days were discarded, and fresh solutions were prepared.

### Grafting Procedure

The graft copolymerization reactions were carried out in standard three-necked taper joint flasks of 500 ml capacity. The samples of cellulose (1–2 g) were first swollen in water for 30 min and then dispersed in a Waring Blendor. The dispersed cellulose was transferred to the reaction flask and maintained at the reaction temperature (35°C) in a constant-temperature bath. Nitrogen was continuously bubbled through the system. After adequate purging, the required amount of monomer was added, followed by the initator. The reaction was then allowed to proceed for the required amount of time. After the completion of the reaction, the grafted cellulose

was taken out and washed with distilled water and acetone. It was then oven-dried at 60°C under vacuum to constant weight. The per cent grafting and the grafting frequency were calculated.

$$\text{Per cent grafting} = \frac{(\text{weight of grafted sample}—\text{weight of cellulose}) \times 100}{\text{weight of cellulose}}$$

$$\text{Grafting frequency} = \frac{\text{average number of PMMA chains in graft copolymer}}{\text{average number of cellulose chains in graft copolymer}}$$

$$= \frac{\text{per cent PMMA in graft copolymer}}{\text{per cent cellulose in graft copolymer}} \times \frac{\overline{M}_{n_{\text{cellulose}}}}{\overline{M}_{n_{\text{PMMA}}}}$$

All calculations are based on moisture-free cellulose weight basis.

### Grafting by Stepwise Initiator Addition

Preliminary studies were conducted with a technique of stepwise initiator addition in an attempt to control the molecular weights and the grafting frequencies of the grafted polymer chains. Cellulose was first swollen and dispersed in water. The contents were then transferred to the reaction flasks maintained at 35°C. After adequate purging with nitrogen, the monomer was added and nitrogen bubbling continued. The initiator was then added in separate steps, at regular intervals of time during the reaction. The total initial reaction mixture volume was maintained at 750 ml. Approximately 3.0 g of cellulose and 10 ml of methyl methacrylate were used in all the runs. The initiator was added in one, two, and three separate steps.

### Homopolymer Extraction

The graft copolymer samples were extracted in a Soxhlet extraction apparatus with benzene for 72 hr. In general, no homopolymer could be extracted. However, with the poly(methyl methacrylate) graft obtained by the stepwise addition of initiator, about 5% homopolymer was extracted. The molecular weight distribution of the extracted homopolymer was measured by using gel-permeation chromatography.

### Hydrolysis of Cellulose Graft Copolymers

In order to study the molecular weight distribution of the poly(methyl methacrylate) branches, the cellulose graft copolymer samples were acetolyzed to hydrolyze away the cellulose backbone. The hydrolysis was carried out for 48 hr at 45°C according to the procedure outlined in the previous paper[2] to isolate the grafted poly(methyl methacrylate) branches for characterization.

### Molecular Weight Determinations

**Viscometry.** The molecular weights of the cellulose wood pulp samples were obtained by measuring the intrinsic viscosities in 0.5*M* cupriethylene

diamine in a Cannon-Ubbelohde dilution viscometer, size 100. The relationship of Immergut et al.[5] was used to calculate the number-average molecular weights ($\overline{M}_n$) of cellulose, $[\eta] = 1.33 \times 10^{-4} \overline{M}_n^{0.905}$.

The intrinsic viscosities of poly(methyl methacrylate) standards were measured in both toluene and tetrahydrofuran in a Cannon-Ubbelohde dilution viscometer at 30 and 24°C, respectively. By using the measured intrinsic viscosities in toluene, the weight-average molecular weights ($\overline{M}_w$) were calculated from the relationship of Chinai et al.:[6]

$$[\eta] = 7.1 \times 10^{-5} \overline{M}_w^{0.73}$$

**Membrane Osmometry.** The number-average molecular weights of poly(methyl methacrylate) were obtained from osmotic measurements in toluene in a Mechrolab Model 502 high-speed membrane osmometer at 37°C.

## Molecular Weight Distribution of Grafted Poly(methyl Methacrylate) Branches

**Gel-Permeation Chromatography (GPC).** A model 200 Waters Associates gel-permeation chromatography (GPC) unit was used to obtain the molecular weight distributions of isolated poly(methyl methacrylate) branches. The eluting solvent used was tetrahydrofuran. The weight-average and number-average molecular weights ($\overline{M}_n$, $\overline{M}_w$) were calculated from the GPC chromatograms by using the calibration chart shown in Figure 1. Details of the calibration of the GPC were described in the previous paper.[2]

## Homopolymerization of Methyl Methacrylate by Using Ceric Ion Initiation

The polymerization of methyl methacrylate (10 ml) in an aqueous medium (total polymerization mixture volume 750 ml) was carried out with ceric ion initiation at 35°C. A 15-ml portion of 0.1$M$ ceric ammonium nitrate in 1$M$ nitric acid was used. After 45 min reaction time, the contents were poured into an excess of methanol containing 0.25% hydroquinone. No trace of polymer could be detected. However, in another set of experiments with 25 ml methanol in the reaction system under identical conditions, polymerization proceeded readily.

# RESULTS AND DISCUSSION

## Graft Copolymerization of Methyl Methacrylate onto Cellulose

The effect of the concentration of initator on the graft copolymerization of methyl methacrylate and other acrylic monomers was discussed in the previous paper.[2] It was observed that grafting occurred over a range of concentration of initiator, from 3.0 to 6.0 mmole/l., and the decrease in per cent grafting beyond a certain concentration of the initiator was attributed to the increasing oxidative termination rates. The effects of other factors

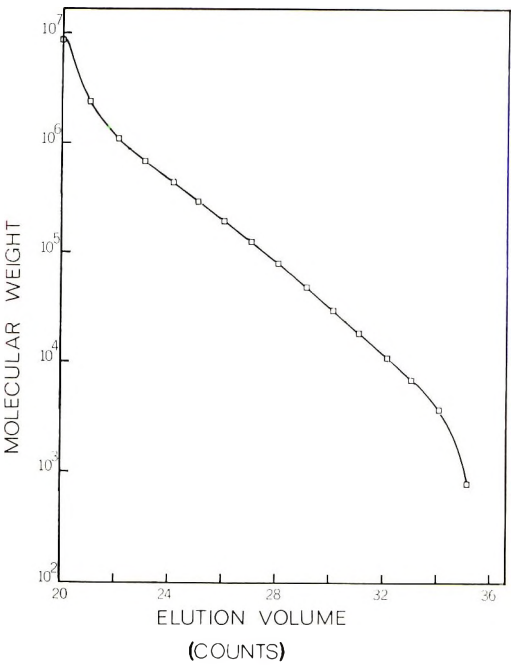


Fig. 1. Gel-permeation chromatography calibration curve.[2] Solvent flow rate, 1 ml/-min; sample concentrations, 0.5, 0.25, 0.125, and 0.0625% by weight of each standard sample in tetrahydrofuran; sample injection time, 60 sec; operating temperature, 25°C; column pore size, $3 \times 10^6$, $10^5$, $10^4$, and $10^3$ Å. Polystyrene used was from Pressure Chemical Ltd., monodisperse standards.

such as the concentration of monomer, grafting time, and cellulose content on the graft copolymerization of methyl methacrylate onto cellulose were studied in the present work. As can be seen from Figure 2, increasing the concentrations of monomer resulted in an increase in the per cent grafting. It is interesting to note that the per cent grafting tends to level off after an initial linear increase with monomer concentration. Substantial grafting occurred in a short period of time, as shown in Figure 3, and the grafting curve leveled off with further increase in time. The effect of cellulose content on methyl methacrylate grafting onto cellulose is shown in Figure 4. It can be seen that the cellulose content in the reaction mixture influences the percent grafting. This is caused by the change in the relative cellulose to ceric ion ratios. These results are in good agreement with the published data of Schwab et al.,[9] Ide,[10,11] and Ogiwara et al.[7,8] on methyl methacrylate grafting onto cellulose with ceric ion initiation.

## Characterization of Methyl Methacrylate Graft Copolymers

### *GPC Calibration Curve for Poly(methyl Methacrylate)*

In GPC practice, it is necessary to obtain the experimental log molecular weight versus elution volume calibration curve in order to convert the raw

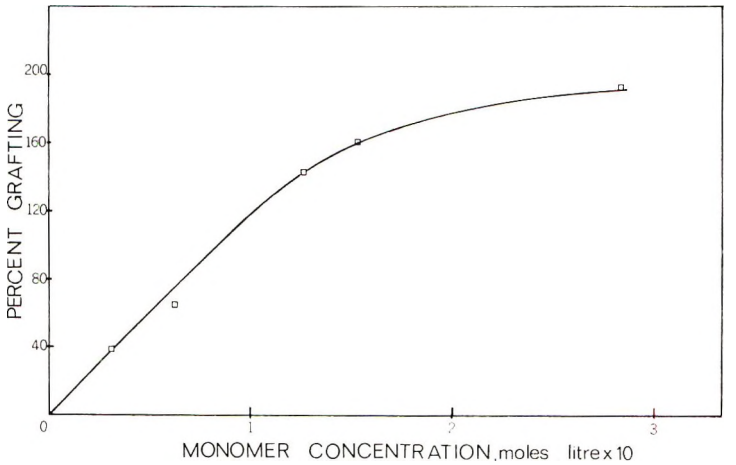


Fig. 2. Effect of monomer concentration on the graft copolymerization of methyl methacrylate onto cellulose. Grafting time, 45 min; grafting temperature, 35°C; initiator concentration, 4 mmole/l.; total polymerization mixture volume, 300 ml; amount of cellulose used, 1.0 g.

GPC chromatograms into actual molecular weights. The calibration curve should be based on elution volumes of monodisperse polymers of known molecular weight. However, at the present time monodisperse polymer standards are not available for polymethyl methacrylate. A universal calibration method which is based on considerations of the equivalent hydrodynamic radii of polymers has recently been proposed by Boni et al.[12] In order to compare molecular weight data from GPC by using the polystyrene calibration curves and the universal calibration curve with molecu-

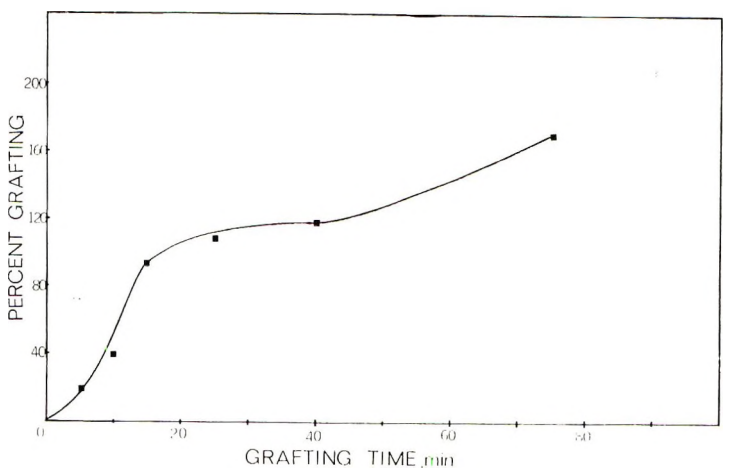


Fig. 3. Effect of grafting time on the graft copolymerization of methyl methacrylate onto cellulose. Grafting temperature, 35°C; initiator concentration, 4 mmole/l.; amount of monomer used, 4.0 g; amount of cellulose used, 1.0 g.

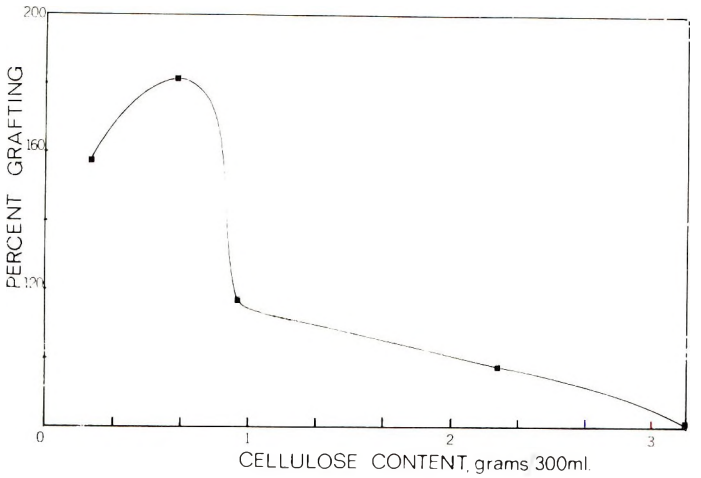


Fig. 4. Effect of cellulose content on the graft copolymerization of methyl methacrylate onto cellulose. Grafting time, 45 min; grafting temperature, 35°C; initiator concentration, 4.0 mmole/l.; amount of monomer used, 4.0 g; total polymerization mixture volume, 300 ml.

lar weights obtained by other independent methods, a series of measurements on the three Polymer Sample Bank poly(methyl methacrylate) samples were carried out. The results of the measurements and computations are summarized in Table I. As can be seen, the data indicate that the use of the polystyrene calibration curve gives calculated molecular weight values for poly(methyl methacrylate) which are in reasonable agreement with values of $\overline{M}_n$ and $\overline{M}_w$ measured by osmometry and viscometry. The GPC results computed from the polystyrene calibration curve also appear to be somewhat better than those based on the universal calibration curve. In view of these results, and in the absence of a proper calibration curve

TABLE I
Comparison of $\overline{M}_w$ and $\overline{M}_n$ of Poly(methyl Methacrylate) Measured by Different Methods

| Sample number | Osmometry and intrinsic viscosity | | | GPC with polystyrene calibration[d] | | GPC with universal calibration method[e] | |
|---|---|---|---|---|---|---|---|
| | $\overline{M}_w$[a] | $\overline{M}_n$[b] | $\overline{M}_n$[c] | $\overline{M}_w$ | $\overline{M}_n$ | $\overline{M}_n$ | $\overline{M}_n$ |
| 1(6038) | 55900 | 22700 | 19400 | 49800 | 27000 | 49000 | 35000 |
| 2(6036) | 111700 | 49800 | 48600 | 106800 | 58000 | 96000 | 70000 |
| 3(6041) | 228200 | 115500 | 160000 | 254300 | 141300 | 255000 | 152000 |

[a] $[\eta]_{30°C} = 7.1 \times 10^{-5}\ Mw^{0.73}$ (Chinai et al.), $[\eta]$ measured in toluene.
[b] Membrane osmometry.
[c] Polymer Sample Bank values (provided by Eastman Kodak).
[d] GPC calculated values from polystyrene calibration curve.
[e] GPC calculated values by the universal calibration method of Boni et al.[12]

based on monodisperse PMMA standards, it was decided to use the polystyrene calibration curve for computing the molecular weights from GPC data. It should be pointed out that this is justified only on an empirical basis.

## Molecular Weights of Grafted Branches

**Effect of Initiator Concentration.** The effect of the concentration of initiator on the number-average and weight-average molecular weights, the polydispersity ratios, and grafting frequencies of the poly(methyl methacrylate) branches was investigated. The results are shown in Table II. Ogiwara et al.[7] reported an inverse relationship of the molecular

TABLE II
Effect of Initiator Concentration on the Molecular Weights and Molecular Weight Distributions of Grafted Poly(methyl Methacrylate) Branches[a]

| Run number | Grafting, % | $[Ce^{IV}]$, mmole/l. | $\overline{M_w} \times 10^{-5}$ | $\overline{M_n} \times 10^{-5}$ | $\overline{M_w}/\overline{M_n}$ | Grafting frequency |
|---|---|---|---|---|---|---|
| MCe 1 | 85.6 | 0.99 | 3.71 | 1.53 | 2.43 | 0.528 |
| MCe 2 | 109.0 | 1.66 | 1.83 | 0.81 | 2.63 | 1.267 |
| MCe 3 | 96.4 | 2.33 | 3.03 | 0.84 | 3.59 | 1.081 |
| MCe 4 | 112.0 | 5.00 | 2.38 | 0.37 | 6.44 | 2.883 |
| MCe 5 | 101.0 | 7.33 | 2.20 | 0.60 | 3.66 | 1.613 |
| MCe 6 | 76.2 | 8.33 | 7.58 | 1.14 | 6.64 | 0.630 |

[a] Cellulose molecular weight ($\overline{M_n}$) 94600; grafting time, 45 min; grafting temperature, 35°C; total polymerization mixture volume, 300 ml; methyl methacrylate, 5 ml; cellulose, 1.0 g.

weight with the concentration of initiator. They investigated a ceric ion concentration range up to 5.0 mmole/l. The present studies cover a wider range of concentration of ceric ion initiator up to 8.33 mmole/l. As can be seen from the data in Table II, the trend is in agreement with that of Ogiwara et al.[7,8] Up to 4.0 mmoles/l., $\overline{M_n}$ decreased with initiator concentration, resulting in a rise in grafting frequency. Beyond this concentration, $\overline{M_n}$ starts to increase again with a resulting decrease in grafting frequency. This can be explained by the increased oxidative termination rates at higher initiator concentrations.[10,11]

**Effect of Grafting Time.** The effect of grafting time on the molecular weights and grafting frequencies is shown in Table III. In the initial stages of the graft copolymerization reaction the ceric ion initiates a large number of growing PMMA branches. This is reflected by the rise in the grafting frequency. However, with increasing grafting time, the grafting frequency remains more or less constant. The grafting frequency is essentially the ratio of the amount of grafted polymer to its $\overline{M_n}$ assuming the cellulose content and molecular weight to be constant. Therefore, the increase in the polymer add on is offset by a proportionate increase in

TABLE III
Effect of Grafting Time on the Molecular Weights and Molecular Weight Distributions of Grafted Poly(methyl Methacrylate) Branches[a]

| Run number | Grafting, % | Time, min | $\overline{M}_w \times 10^{-5}$ | $\overline{M}_n \times 10^{-5}$ | $\overline{M}_w/\overline{M}_n$ | Grafting frequency |
|---|---|---|---|---|---|---|
| MTm 1 | 169.2 | 75 | 3.98 | 1.62 | 2.46 | 1.463 |
| MTm 2 | 117.2 | 40 | 4.97 | 0.79 | 6.29 | 1.405 |
| MTm 3 | 107.2 | 25 | 5.08 | 0.66 | 7.74 | 1.555 |
| MTm 4 | 90.0 | 15 | 1.95 | 0.69 | 2.80 | 1.262 |
| MTm 5 | 39.8 | 10 | 1.89 | 0.36 | 5.24 | 1.043 |
| MTm 6 | 19.6 | 5 | 3.46 | 0.52 | 6.67 | 0.357 |

[a] Cellulose molecular weight ($\overline{M}_n$) 94600; grafting temperature, 35°C; total polymerization mixture volume, 300 ml; methyl methacrylate, 5 ml; ceric ion concentration, 4 mmole/l.; cellulose, 1 g.

the $\overline{M}_n$ of the grafted chains due to the gel effect. This results in grafts with constant grafting frequencies.

**Effect of Cellulose Content.** The effect of the amount of cellulose used on the molecular weights of the grafted PMMA branches is shown in Table IV. The number-average molecular weight of the grafted branches generally decreased with increasing cellulose content.

**Molecular Weight Distributions of Grafted Poly(methyl Methacrylate) Branches.** A typical chromatogram of grafted PMMA is shown in Figure 5. Cumulative weight distribution curves calculated from experimental chromatograms of isolated poly(methyl methacrylate) branches are shown in Figure 6. The corresponding differential weight distribution curves calculated from the GPC experimental chromatograms are shown in Figure 7. It is of considerable interest to note that a high proportion of the grafted polymer lies in the molecular weight region below 200000. However, the averaging of the high concentration of relatively low molecular weight polymer chains and the less densely populated high molecular

TABLE IV
Effect of Cellulose Content on the Molecular Weights and Molecular Weight Distributions of Grafted Poly(methyl Methacrylate) Branches[a]

| Run number | Grafting, % | Cellulose content, g | $\overline{M}_w \times 10^{-5}$ | $\overline{M}_n \times 10^{-5}$ | $\overline{M}_w/\overline{M}_n$ | Grafting frequency |
|---|---|---|---|---|---|---|
| MCl 1 | 154.70 | 0.11343 | 3.45 | 0.79 | 4.38 | 2.001 |
| MCl 2 | 202.06 | 0.65887 | 3.11 | 0.58 | 7.59 | 3.294 |
| MCl 3 | 72.93 | 0.93340 | 2.46 | 0.48 | 5.21 | 1.446 |
| MCl 4 | 34.04 | 2.23200 | 2.33 | 0.44 | 5.29 | 0.942 |

[a] Cellulose molecular weight ($\overline{M}_n$) 94600; grafting temperature, 35°C; total polymerization mixture volume, 300 ml; methyl methacrylate, 5 ml; ceric ion concentration, 4 mmole/l.; grafting time, 45 min.

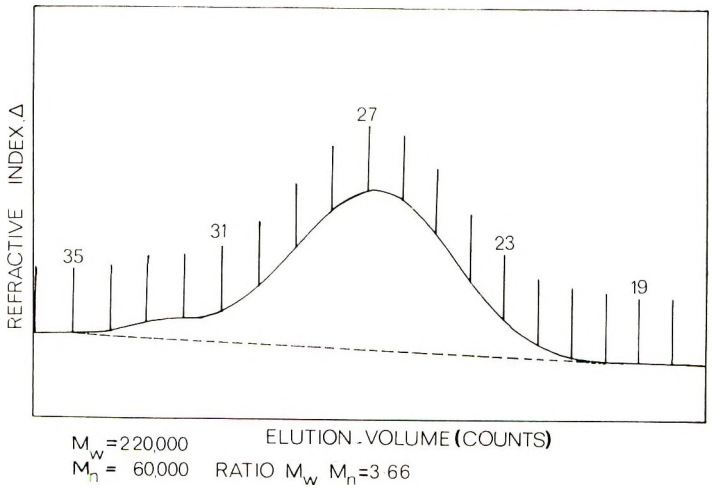


Fig. 5. Typical gel-permeation chromatogram of grafted poly(methyl methacrylate) branches. Sample concentration, 0.25%; injection time, 60 sec; oven temperature, 25°C; sensitivity, 8×; column size, 3 × $10^6$, $10^5$, $10^4$, $10^3$ Å; elution solvent, tetrahydrofuran; $\bar{M}_w$ = 220,000; $\bar{M}_n$ = 63,000; ratio $\bar{M}_w/\bar{M}_n$ = 3.66.

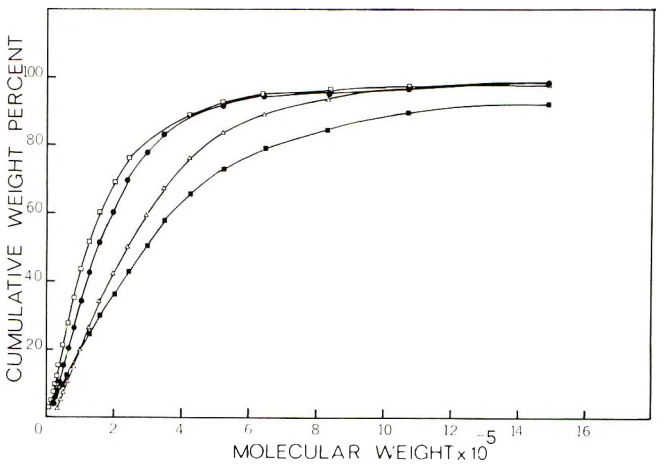


Fig. 6. Integral molecular weight distribution curves of grafted poly(methyl methacrylate) branches calculated from gel-permeation chromatograms for various initiator concentrations: (△) 0.99 mmole/l.; (●) 2.33 mmole/l.; (□) 7.33 mmole/l.; (■) 8.33 mmole/l.

weight chains results in a broad molecular weight distribution. As can be seen from Figure 6, the amount of grafted PMMA having $\bar{M}_n < 200000$ increases from approximately 30% to 60% as the concentration of initiator was varied from 0.99 to 7.33 mmole/l. It can also be observed from Figure 7 that the distribution in the lower molecular weight regions narrows down considerably with increasing concentrations of initiator. While the $\bar{M}_n$ of

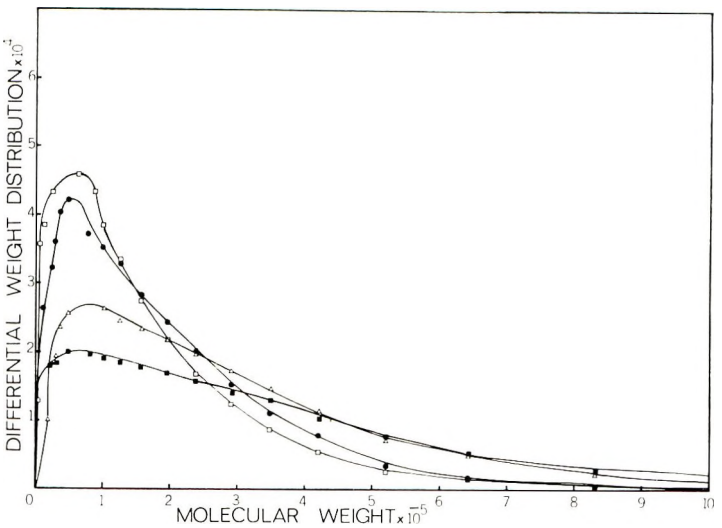


Fig. 7. Differential weight distribution curves of isolated poly(methyl methacrylate) branches calculated from the experimental GPC chromatograms for various initiator concentrations: (△) 0.99 mmole/l.; (●) 2.33 mmole/l.; (□) 7.33 mmole/l.; (■) 8.33 mmole/l.

the grafted polystyrene branches reported in the previous study[2] varied from 23000 to 460000, the $\bar{M}_n$ of the grafted polymethyl methacrylate branches were in the region of 36000 to 160000. The weight-average molecular weights found in the present study ranged from 183000 to 758000. Polydispersity ratios obtained for grafted PMMA were of the order of 4–7, although some lower polydispersity ratios were obtained with changes in ceric ion concentration. Compared to styrene grafting considerable improvement in the grafting frequencies was obtained with methyl methacrylate. Grafting frequencies ranged from 0.38 to 3.2 for methyl methacrylate compared to those for styrene grafting,[2] which varied from 0.05 to 0.4.

## Effect of Stepwise Addition of Initiator

Preliminary studies were carried out using the stepwise initiator addition technique to see if the grafting frequency could be improved. The results are shown in Table V. These results show that no appreciable improvements in grafting frequencies were obtained. This suggests that most of the grafted chains are initiated in the early stages of grafting and the additional stepwise addition of ceric ion initiator has little effect, other than participating in chain termination. Approximately 5% homopolymer was extracted from the cellulose–PMMA grafts by benzene extraction in a Soxhlet apparatus. The molecular weights of the extracted homopolymer are shown in Table VI, together with the values for methyl methacrylate homopolymerized in the presence of methanol. As can be seen, the $\bar{M}_n$ of

TABLE V
Effect of Stepwise Addition of Initiator on the Graft Copolymerization of Methyl Methacrylate onto Cellulose[a]

| Run number | Grafting after extraction, % | Time, min | No. of stepwise additions | Amount initiator added in each step, ml | $\overline{M_w} \times 10^{-5}$ | $\overline{M_n} \times 10^{-5}$ | $\overline{M_w}/\overline{M_n}$ | Grafting frequency |
|---|---|---|---|---|---|---|---|---|
| MSt 2 | 119.30 | 45 | 1 | 5 | 11.50 | 3.57 | 3.24 | 0.316 |
| MSt 3 | 83.20 | 45 | 2 | 5,5 | 7.11 | 2.44 | 3.17 | 0.351 |
| MSt 8 | 76.88 | 45 | 1 | 10 | 4.65 | 1.41 | 3.30 | 0.516 |
| MSt 9 | 67.90 | 45 | 1 | 15 | 3.33 | 0.80 | 4.14 | 0.800 |
| MSt 5 | 55.42 | 45 | 2 | 7.5,7.5 | 5.59 | 1.09 | 5.12 | 0.480 |
| MSt 6 | 70.40 | 45 | 3 | 5,5,5 | 5.86 | 1.40 | 4.19 | 0.476 |

[a] Cellulose molecular weight ($\overline{M_n}$) 94,600; cellulose, 3.0 g; methyl methacrylate, 10 ml; initial polymerization mixture volume, 750 ml; grafting temperature, 35°C; grafting time, 45 min.

TABLE VI
Molecular Weight Distributions of Extracted Poly(methyl Methacrylate) from Graft Copolymer Samples Obtained by Stepwise Initiator addition Technique

| Run number | Grafting after extraction, % | Homopolymer extracted, % | Conversion % | Time, min | $\overline{M_w} \times 10^{-5}$ | $\overline{M_n} \times 10^{-5}$ | $\overline{M_w}/\overline{M_n}$ |
|---|---|---|---|---|---|---|---|
| MHp 1[a] | 119.30 | 6.71 | | | 12.65 | 1.52 | 8.29 |
| MHp 2 | 83.20 | 6.54 | | | 7.19 | 1.44 | 5.00 |
| MHp 4 | 67.90 | 5.42 | | | 4.42 | 0.94 | 4.71 |
| MHp 5 | 55.42 | 3.28 | | | 3.44 | 1.08 | 3.20 |
| MHp 6 | 70.40 | 7.24 | | | 3.23 | 0.71 | 4.57 |
| CeM 1[b] | | | 10.23 | 45 | 3.62 | 0.48 | 7.60 |
| CeM 2 | | | 16.92 | 45 | 2.33 | 0.52 | 4.48 |

[a] MHp 1 to 6, extracted homopolymer from graft copolymer samples shown in Table V.
[b] Homopolymerized methyl methacrylate; ceric ion initiator, 15 ml; methyl methacrylate, 10 ml; methanol, 25 ml; total polymerization mixture volume, 750 ml.

the homopolymer polymerized in the presence of methanol was very low, but the $\overline{M_n}$ of the extracted polymer from the grafts was quite high and generally of the same order as the $\overline{M_n}$ of the grafted polymers.

The financial support of the National Research Council of Canada and the Department of University Affairs, Province of Ontario for this research program is gratefully acknowledged.

## References

1. R. Y. M. Huang, *J. Appl. Polym. Sci.*, **10**, 325 (1966).
2. R. Y. M. Huang and P. Chandramouli, *J. Appl. Polym. Sci.*, **12**, 2549 (1968).
3. G. Mino and S. Kaizerman, *J. Polym. Sci.*, **31**, 242 (1958).
4. J. D. Wellons, A. Schindler, and V. Stannett, *Polymer*, **5**, 499 (1964).
5. E. H. Immergut, B. G. Rånby, and H. F. Mark, *Ind. Eng. Chem.*, **45**, 2483 (1953).
6. J. Chinai, J. Matlock, and A. Rensik, *J. Polym. Sci.*, **17**, 391 (1955).
7. Y. Ogiwara, Y. Ogiwara, and H. Kubota, *J. Polym. Sci. A-1*, **5**, 2791 (1967).
8. Y. Ogiwara, Y. Ogiwara, and H. Kubota, *Kogyo Kagaku Zasshi*, **70**, 1, 103 (1967).
9. E. V. Schwab, V. Stannett, D. H. Rakowitz, and J. M. Magrane, *Tappi*, **45**, 390 (1962).
10. F. Ide and U. Takayama, *Kogyo Kagaku Zasshi*, **64**, 213 (1961).
11. F. Ide, R. Handa, and K. Nakatuka, *Kobunshi Kagaku*, **21**, 57 (1963).
12. K. A. Boni, F. A. Sliemers, and P. B. Stickney, Proceedings, Fourth International GPC Seminar, Miami Beach, May, 1967.

Received August 12, 1968

JOURNAL OF POLYMER SCIENCE: PART A-1 VOL. 7, 1407–1414 (1969)

# Vinyl Polymerization with Fe(III)–Thiourea as Initiator System. Part I. General Features and Kinetics of $Fe(ClO_4)_3$–Thiourea Reaction*

B. M. MANDAL, U. S. NANDI, and S. R. PALIT, *Department of Physical Chemistry, Indian Association for the Cultivation of Science, Jadavpur, Calcutta 32, India*

## Synopsis

Initiation of polymerization of methyl methacrylate, styrene, and acrylonitrile with the redox system Fe(III)–thiourea has been examined. For the heterophase polymerization any of the ferric salts, such as $FeCl_3$, $Fe_2(SO_4)_3$, and $Fe(ClO_4)_3$ can be used as oxidant, but there is no polymerization in the homogeneous phase when $FeCl_3$ is used as oxidant. It was also observed that $Fe(ClO_4)_3$ retards the radical polymerization of styrene, though this salt has hardly any effect on the radical polymerization of methyl methacrylate. Further, the reaction between $Fe(ClO_4)_3$ and thiourea was found to be kinetically of second order. The rate is largely influenced by the nature of the solvent. It is concluded that apart from the dielectric constant of the solvents, specific effects like complex formation of Fe(III) with solvents should have a marked influence on the rate of this reaction.

## INTRODUCTION

The reaction between Fe(III) and monomercaptides[1–3] has been studied quite extensively. It was shown that complexes formed between Fe(III) and monomercaptides such as thioglycolate or cysteinate invariably undergo oxidation–reduction reaction in which the monomercaptide is oxidized to disulfide and iron(III) is reduced to iron(II). Recently Wallace[4] studied in some detail the reaction between ferric soap and mercaptans in organic solvents like xylene and acetone, at temperatures near 35°C and observed a rapid oxidation–reduction reaction. Wallace considered also that the reaction involves free radicals. The intermediate thiyl (RS) radicals were trapped by olefins. Initiation of polymerization by thiyl radicals generated in the reactions of mercaptans with hexacyanoferrate[5–7](III) or pentacyanonitritoferrate(III)[8] was also realized.

By virtue of its existence in the tautomeric equilibrium[9] (1), thiourea (TU) can be considered a potential thiol.

* Presented in part at the International Symposium of Macromolecular Chemistry, Tokyo-Kyoto, Japan, 1966.

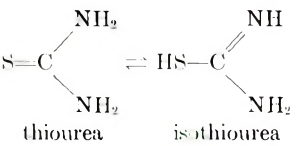


(1)

The reaction of thiourea with Fe(III) is therefore likely to be analogous to that between Fe(III) and mercaptans. The free radical generated in the reaction between Fe(III) and TU has been identified earlier[10] as $\dot{S}C(=NH)$-$NH_2$. For a large number of redox initiator systems containing TU as the reductant, the same radical, $\dot{S}C(=NH)NH_2$, was shown to be largely responsible for the initiation of vinyl polymerization in the aqueous medium.[11] As the instances of redox initiation in organic solvents are rather few (limited largely by the solubility of the initiators) this work is undertaken to examine the potential of the Fe(III)–TU redox system as a polymerization initiator in an organic base. As an integral part of the work the kinetics of the $Fe(ClO_4)_3$–TU reaction have also been studied.

## EXPERIMENTAL

### Materials

Methyl methacrylate (MMA), styrene (St), and acrylonitrile (AN) were purified, dried, and distilled *in vacuo* according to the normal procedure.[12]

*N*,*N*-Dimethylformamide (DMF) (E. Merck) wastre ated twice with $P_2O_5$ for 5–6 hr and then distilled. *tert*-Butyl alcohol (TBA) (British Drug House) was first distilled, then refluxed with sodium for 8–10 hr and distilled from sodium. Ethyl acetate (ETOAC), (British Drug House), and acetonitrile (Fischer certified reagent) were used after simple distillation.

Thiourea (TU), (E. Merck), was used after crystallizations three times from distilled water, mp 180°C.

$Fe(ClO_4)_3$ was prepared from analytical reagent grade ferric chloride hexahydrate (British Drug House) by first precipitating $Fe(OH)_3$ with ammonia, washing with distilled water until free from $Cl^-$, and then dissolving the precipitate in 70% $HClO_4$. The resulting solution was carefully evaporated. The first portions of the crystals deposited were rejected; the rest, having a pale lilac tint, were filtered under suction and kept in a vacuum desiccator. Ferric acetate was prepared by dissolving the hydroxide in glacial acetic acid and concentrating carefully. All solutions on ferric salts were allowed to equilibriate for about 10 days at room temperature and then stored in a refrigerator for future use. In the polymerization experiments the concentration of Fe(III) ranged between $10^{-4}$ and $10^{-2}$ mole/l.

### Technique

In general, the rates of polymerization were measured dilatometrically. At 40°C, contraction per centimeter of the capillary of the dilatometer was equivalent to 0.72 mmole of methyl methacrylate polymerized. When the

measurement of the rate of polymerization was not necessary (as in the tests for anion specificity and monomer selectivity) the polymerization experiments were conducted in ampoules sealed *in vacuo*. Occurrence of a polymerization reaction was evident from the isolation of the polymer on pouring the contents of the sealed ampoules into methanol. Polymerization in the aqueous phase was carried out under nitrogen.

### Estimation of Ferrous Ion

At the end of the desired period of reaction the contents of the vacuum-sealed ampoules (5 ml) were poured immediately in a solution mixture (65 ml) of equal volumes of methyl alcohol and 0.1*M* acetate buffer (pH 3.5) to which 1 ml of 1*M* sodium fluoride and 5 ml of 0.5% *o*-phenanthroline hydrate had been added. Fluoride was added to arrest any further reaction between Fe(III) and TU. It should be noted that fluoride can not totally arrest the reaction in the presence of *o*-phenanthroline, though it can do so in the absence of *o*-phenanthroline. Again, *o*-phenanthroline can not be added in the later stage because in its absence Fe(II) is rapidly oxidized by air in the presence of $F^-$ ion. The solution was then filtered (when there was a polymer) in a 100 ml volumetric flask, washed throughly with the acetate buffer (pH 3.5) and made up to the mark with the buffer. The optical density of the suitably diluted solution was measured without delay at 510 m$\mu$ in a Hilger UV spectrophotometer using 1 cm cells, and the concentration of the ferrous ion in the solution was computed from a calibration curve similarly prepared with a standard ferrous (Mohr salt) solution ($\epsilon_{510}$ = 11310). The maximum Fe(II) measured was 1.3 mg with the above reagent concentrations and the maximum Fe(III) used was 3.8 mg.

### Rate Measurement for the Reaction Between $Fe(ClO_4)_3$ and TU

The experiments were carried out in vacuum-sealed ampoules with the use of equimolar concentrations ($10^{-3}$–$10^{-2}$ mole/l, depending on the speed of the reaction) of $Fe(ClO_4)_3$ and TU. At the end of the desired periods of the ampoules were broken open and Fe(II) measured as above.

## RESULTS AND DISCUSSION

Neither TU nor any of the ferric salts used could alone initiate the polymerization reaction in aqueous or in TBA medium. The polymerization reaction effected by Fe(III) and TU is inhibited by 2,2′-diphenyl-1-picryl hydrazyl, indicating a radical mechanism for the reaction.

### Influence of the Anion of the Fe(III) Salt

From Table I it is evident that ferric salts such as $FeCl_3$, $Fe_2(SO_4)_3$, and $Fe(ClO_4)_3$ constitute efficient initiating systems in combination with thiourea for the heterophase polymerization of monomers like MMA, styrene, and acrylonitrile. Ferric acetate is inefficient in this regard. On the contrary, initiation of polymerization in the homogeneous phase exhibits

TABLE I
Influence of the Anion of the Ferric Salt and the Medium on the Polymerization of Vinyl Monomers with the Use of Fe(III) and Thiourea as Initiator in the Absence of Oxygen at 35–40°C

| | | Polymerization[b] | | |
|---|---|---|---|---|
| Initiator[a] | Monomer | Nonaqueous homogeneous medium[c] | Nonaqueous heterogeneous medium[d] | Aqueous heterogeneous medium |
| $Fe(ClO_4)_3$–TU | MMA | + | + | + |
| | St | − | + | |
| | AN | −(DMF) | +[e] | + |
| $FeCl_3$–TU | MMA | − | + | + |
| | St | − | + | |
| | AN | −(DMF) | +[e] | + |
| $Fe_2(SO_4)_3$–TU | MMA | +[f] | + | + |
| | St | +[f] | + | |
| | AN | +[f] | + | + |
| $Fe(OOCCH_3)_3$–TU | MMA | — | — | — |
| | St | — | — | |
| | AN | — | — | — |

[a] Concentration of Fe(III) ranged between $10^{-4}$ and $10^{-2}$ mole/l. and that of TU varied between $10^{-3}$ and $10^{-2}$ mole/l.

[b] Code: + indicates polymerization (as evident from the isolation of polymer); − indicates no polymerization (polymer not isolable by the addition of MeOH).

[c] Solvents used are DMF, TBA, and acetonitrile.

[d] Mainly lower alcohols or aquated TBA.

[e] in DMF with [M] > 6.48 mole/l. when the polymer precipitates out.

[f] moist DMF as solvent.

greater specificity on the anion associated with Fe(III). Thus while $FeCl_3$ and TU fail, $Fe_2(SO_4)_3$ or $Fe(ClO_4)_3$ and TU succeed to effect the polymerization of MMA in the solution phase (with TBA, DMF, or acetonitrile as solvents). The anion specificity exhibited in the solution phase parallels the radical-scavenging power of the Fe(III) salts in the solution phase. Polymerization in the solution phase is best effected with the aid of those salts, i.e., $Fe(ClO_4)_3$ and $Fe_2(SO_3)_3$, which have been shown to be incapable to scavenge the poly(methylmethacrylate) radical.[13]

### Selectivity of Monomers and the Effect of the Polymerization Phase

Unlike the aqueous or nonaqueous heterophase polymerization, the solution polymerization shows some selectivity to monomers (Table I). With the $Fe(ClO_4)_3$–TU initiator system, styrene or acrylonitrile, for example, cannot be polymerized in the solution phase, while MMA can be easily polymerized. Independent experiments (Fig. 1) have proved that $Fe(ClO_4)_3$ can retard the azobisisobutyronitrile-initiated solution polymerization of styrene, though this salt does not affect the radical polymerization of MMA.[13]

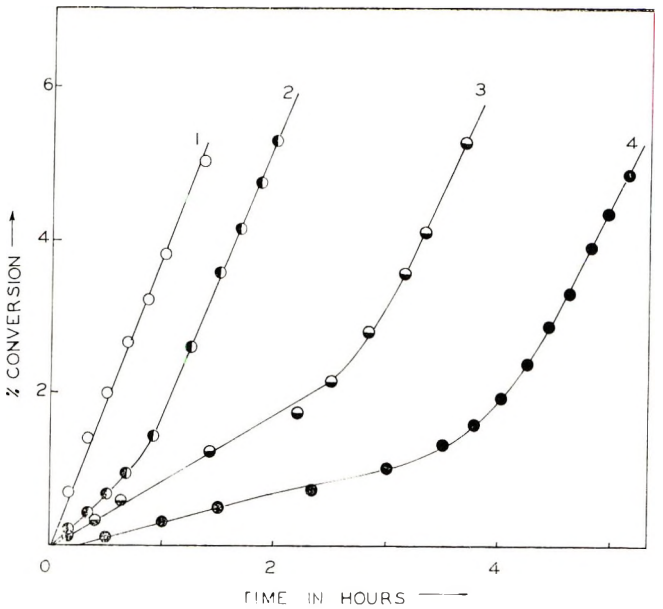


Fig. 1. Retardation of styrene polymerization by various concentrations of $Fe(ClO_4)_3$: (*1*) no $Fe(ClO_4)_3$; (*2*) 1.78 mmole/l.; (*3*) 4.44 mmole/l.; (*4*) 6.22 mmole/l. [Styrene] = 3.48 mole/l. in DMF; [AIBN] = $2 \times 10^{-2}$ mole/l. 60°C.

## Effect of Solvent on the Shape of the Conversion–Time Plot

The per cent conversion–time plot for the polymerization of MMA in the solution phase (DMF, TBA, acetonitrile) effected by $Fe(ClO_4)_3$–TU, shown in Figure 2, indicates that in the solvents of high dielectric constant such as DMF or acetonitrile ($D$ about 37) the rate of polymerization ($R_p$) falls off with time while in TBA ($D$ = 10.6) $R_p$ remains steady for a long time. The fall-off of the rates in DMF or acetonitrile is probably due to the rapid decay of the initiator in such solvents, as discussed below.

## Kinetics of the Reaction between $Fe(ClO_4)_3$ and Thiourea

Prior to the kinetic study of the polymerization reaction proper, it was desirable to study the reaction between Fe(III) and TU. For this purpose, the $Fe(ClO_4)_3$–TU system was chosen as ideal, as this system permits the polymerization of MMA in the homogeneous phase. The reaction was followed in five solvents, ie., TBA, DMF, acetonitrile, mixture of TBA and MMA (60:40 v/v), and mixture of TBA and ethyl acetate (60:40 v/v), by measuring the formation of Fe(II) ion at various time intervals starting with equimolar concentrations of the reactants.

The reaction was found to be of the second order, and the values of the second-order rate constant in various solvents at 40°C are given in Table II. The oxidation product form TU might be tentatively considered as formamidine disulfide,[9,14] which has also been considered to be formed in the oxi-

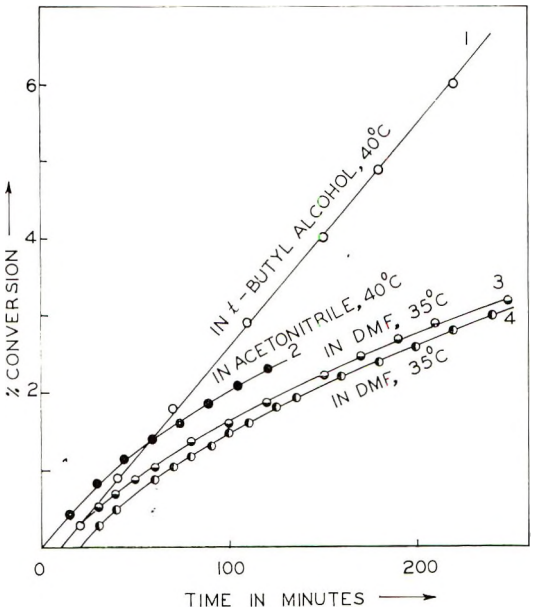


Fig. 2. Yield–time curves for the $Fe(ClO_4)_3$–TU initiated polymerization of MMA in different solvents at various $Fe(ClO_4)_3$ and TU concentrations, respectively: (*1*) 10, 10 mmole/l.; (*2*) 1,1 mmole/l.; (*3*) 1, 10 mmole/l.; (*4*) 0.5, 10 mmole/l. [MMA] = 3.92 mole/l.

dation of TU by Cu(II) in acetonitrile[15] in an analogous reaction sequence represented here by reactions (2) and (3).

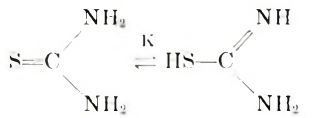


(2)

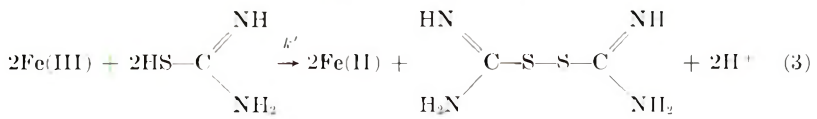


(3)

The proton liberated in reaction (3) is taken up by the formamidine disulfide base.[15,16] The rate constant ($k$) reported in Table II represents that for the overall reaction and not for reaction (3). However, $k$ and $k'$ are interrelated by the equilibrium constant $K$, as given by the eq. (4).

$$k = k'K \tag{4}$$

From Table II it is evident that the rate increases with the increase in the dielectric constant of the solvent which is expected for an oxidation–reduction reaction.[16] Wallace also observed a pronounced increase in the rate of the ferric soap–thiol reaction as the polarity of the medium is increased.[4]

TABLE II
Second-Order Rate Constants for the Reaction Between $Fe(ClO_4)_3$ and TU in Various Solvents at 40°C

| Solvent | Dielectric constant $D$ | $k$, l./mole-min |
|---|---|---|
| *tert*-Butyl alcohol | 10.6 | 0.023 |
| *N*,*N*-Dimethylformamide | 36 | 1.52 |
| Acetonitrile | 36 | 14.5 |
| *tert*-Butyl alcohol (60% v/v) + MMA | | 0.03 |
| *tert*-Butyl alcohol (60% v/v) + ethyl acetate | 6.3 for ethyl acetate | 0.24 |

The solvent effect in the present case is due to two reasons: (*a*) the effect of the solvent on the tautomeric equilibrium constant $K$ and (*b*) the effect on the rate constant $k'$. Solvents of high dielectric constant probably increase both.

However, that the dielectric constant of the solvent is not the only determining factor is evident from a comparison of the values of the rate constant in DMF and in acetonitrile (both having almost equal $D$) or in TBA and in the mixed solvents of TBA and an ester (the ester having lower $D$ than TBA). Specific effects like complexation of Fe(III) by solvents must have a major influence on the rate. The rate constant in DMF is about one tenth that in acetonitrile, which points out that $Fe(ClO_4)_3$ is strongly complexed by DMF. That nitriles are much less effective than DMF as complexing agents for $FeCl_3$ was suggested also by Bamford etal.,[12] who found that the rate for the oxidation of the polyacrylonitrile radical by $FeCl_3$ is about 37 times as fast in pure acrylonitrile as in a mixture of DMF and acrylonitrile at 60°C. The higher rate of the reaction in a solvent mixture of TBA and MMA than that in pure TBA prompted us to measure the rate in an analogous mixture of TBA and a nonpolymerizable ester solvent, ethyl acetate (EtOAc). Table II shows that the rate in a TBA–EtOAc solvent mixture is much greater than that in a TBA–MMA mixture. The higher rate in a solvent mixture of an alcohol and an ester than that in a pure alcohol can be interpreted on the basis of stronger complex formation in the latter solvent than in the former. In view of the "hard base nature[17]" of the alcohols compared to the esters and the "hard acid" nature[17] of $Fe^{3+}$, the above reasoning may be allowed.

The above study shows that the decay rate of the initiator in acetonitrile and DMF is much higher than that in TBA, and hence the yield–time curves are not linear in the former solvents. With this background the kinetics of the polymerization reaction in the solution phase may be studied, and this will be discussed in Part II.

This work is supported by National Bureau of Standards (U.S.) in the form of a research grant, PL-480.

## References

1. M. P. Schubert, *J. Amer. Chem. Soc.*, **54**, 4077 (1932).
2. D. L. Leussing and I. M. Kolthoff, *J. Amer. Chem. Soc.*, **75**, 3904 (1953).
3. N. Tanaka, I. M. Kolthoff, and W. Stricks, *J. Amer. Chem. Soc.*, **77**, 1996 (1955).
4. T. J. Wallace, *J. Org. Chem.*, **31**, 3071 (1966).
5. I. M. Kolthoff and W. J. Dale, *J. Polym. Sci.*, **3**, 400 (1948).
6. I. M. Kolthoff and W. J. Dale, *J. Polym. Sci.*, **5**, 301 (1950).
7. R. W. Hobson and J. D. D'Ianni, *Ind. Eng. Chem.*, **42**, 1572 (1950).
8. I. M. Kolthoff and E. J. Meehan, *J. Polym. Sci.*, **11**, 71 (1953).
9. H. Gilman, *Organic Chemistry*, Wiley, New York, 2nd Ed., Vol. 1, p. 940.
10. B. M. Mandal, U. S. Nandi, and S. R. Palit, *J. Polym. Sci. A-1*, **4**, 3115 (1966).
11. A. R. Mukherjee, R. Pal, A. M. Biswas, and S. Maiti, *J. Polym. Sci. A-1*, **5**, 135 (1967).
12. C. H. Bamford, A. D. Jenkins, and R. Johnston, *Proc. Roy. Soc.* (London), **A239**, 214 (1957).
13. E. R. Entwistle, *Trans. Faraday Soc.*, **56**, 284 (1960).
14. E. A. Werner, *J. Chem. Soc.*, **101**, 2166 (1912).
15. B. Kratochvil, D. A. Zatko, and R. Markuszewski, *Anal. Chem.*, **38**, 770 (1966).
16. B. Kratochvil, *Record Chem. Progr.*, **27**, 253 (1966).
17. R. G. Pearson, *J. Amer. Chem. Soc.*, **85**, 3534 (1963); *Science*, **151**, 172 (1966).

Received April 17, 1968
Revised August 22, 1968

JOURNAL OF POLYMER SCIENCE: PART A-1 VOL. 7, 1415–1424 (1969)

# Thermal Stabilities of Homopolymers of Amino Acids

HIROKO OBATA and SHIGEO OGAWA, *The Textile Research Institute of Japanese Government, Kanagawa-ku, Yokohama, Japan*

## Synopsis

In order to study the thermal stabilities of the α-helical polyamino acids in the solid state, measurements of the infrared spectra at high temperature, weight loss by thermogravimetry, and the expansion of the α-helix by x-ray diffractometry were carried out on poly(γ-methyl D-glutamate), poly(γ-benzyl L-glutamate), poly-L-alanine, poly-(β-benzyl L-aspartate), poly-δ-carbobenzoxy-L-ornithine and poly-ε-carbobenzoxy-L-lysine. The thermal degradation temperatures of these polymers lie between 140°C and 230°C. The α-helical conformation is stable at high temperature in these polyamino acids, except for poly(β-benzyl L-aspartate), unless thermal degradation takes place. As temperature rises, the amide A and the amide I bands of the infrared spectra shift slightly to higher frequencies and the amide II band to lower frequencies. At the same time, the intensities of these amide bands decrease. These changes differ among the different molecules. From the x-ray measurement, it was found that the α-helix expands along the helical axis with temperature. It is expected that the intramolecular hydrogen bonds of the α-helix become weak with increasing temperature and that the state of the hydrogen bonds of the α-helices depends upon the molecules.

## INTRODUCTION

Some physical properties of the α-helical polyamino acids in the solid state depend upon the side chains of the molecules. This dependence has been attributed mainly to the motion of the side chains through studies of the viscoelasticity[1–3] the dielectric dispersion,[3,4] and the broad line nuclear magnetic resonance.[3,5,6] The dynamic modulus, for instance, decreases according to the motion of the side chains. This decrease is generally great in helical polyamino acids with large side chains, such as poly(γ-benzyl L-glutamate).

On the other hand, second or higher order structures of the polyamino acids are also affected by their side chains. The problem of the side chain, especially a correlation between the main chain and the side chain, is very interesting in many points.

In order to study the conformational stability of the helical structure of the polyamino acids in the solid state, the infrared spectra, the x-ray diffraction at high temperature, and the thermal degradation were measured on six polyamino acids which have different side chains.

TABLE I
Solvents

| Sample | Solvent used | |
|---|---|---|
| | Films for thermal degradation and infrared spectra | Films or fibers for x-ray diffraction |
| PMDG | Chloroform | Chloroform (fiber) |
| PBLG | Chloroform | Dioxane (fiber) |
| PCBZLOrn | Chloroform | Dioxane (fiber) |
| PCBZLLys | Chloroform | Dioxane (oriented film) |
| PBLAsp | Chloroform | |
| PLAla | Dichloroacetic acid | |

## EXPERIMENTAL

The six polyamino acids examined were as follows: poly(γ-methyl D-glutamate) (PMDG), poly(γ-benzyl L-glutamate) (PBLG), poly-L-alanine (PLAla), poly-ε-carbobenzoxy-L-lysine (PCBZLLys), poly-δ-carbobenzoxy-L-ornithine (PCBZLOrn), and poly(β-benzyl L-aspartate) (PBLAsp). PMDG was prepared at Ajinomoto Inc. and the others at Pilot Chemicals Inc. These polyamino acids were dissolved in the solvents listed in Table I and were made into films or fibers. The films for the infrared measurement were prepared by casting from chloroform solutions on sodium chloride disks. Also, a thin film that was made from dichloroacetic acid solution by substituting the dichloroacetic acid with ethyl alcohol was put between the disks. Oriented films were prepared by stroking concentrated solutions on the disks until the solvents were evaporated. These films or fibers were all found to be in the α-helical form from the x-ray and the infrared spectral examinations.

The infrared spectra were measured at a constant temperature at intervals from 20°C to 300°C with a Japan Spectroscopic Co., Ltd., Model DS-402G spectrophotometer which was equipped with a Hitachi heating cell. The peak intensities of the amide bands and the shift of their frequencies are discussed in this paper. Emission from film and sodium chloride disks was observed at high temperature. However, no emission was observed in the region of the N-H stretching band at 3300 $cm^{-1}$ (amide A). Therefore especially this band is discussed; the C-O stretching (amide I) and the N-H deformation (amide II) bands after correction for the emission are also discussed.

The thermal degradation was measured with a Shimazu differential thermal analyzer, Type DT-IO which was fitted with an attachment of a thermobalance. The films examined were tens of microns in thickness and from 100 to 500 mg in weight. The temperature was raised at a rate of 3°C/min. In order to compare this result with that of the infrared spectra, the experiment was carried out in the air.

Ni-filtered CuK$\alpha$ radiation was used for the measurement of the x-ray diffraction. The x-ray diffraction curve for the residue translation of the $\alpha$-helix was measured at various temperatures by an x-ray diffractometer A bundle of fibers or oriented films was fixed in a heating cell to be tilted at 30° from normal to the x-ray beam. Then the cell was heated to a constant temperature at intervals between 20°C and 200°C. At each temperature, $2\theta$ was measured by rotating a goniometer from 67° to 59°. The cylindrical photographs were taken with a Weissenberg camera. The sample was tilted 30° from normal to the beam and was oscillated between 25° and 35°. Samples made from PMDG, PBLG, PCBZLOrn, and PCBZLLys were examined.

## RESULTS

### Changes in the Infrared Spectra at High Temperature

According to the infrared spectra of PMDG, PBLG, PLAla, PCBZLOrn and PCBZLLys, the $\alpha$-helical conformation is stable in these polyamino acids, even at high temperature, unless thermal degradation takes place. In the infrared spectra of these polyamino acids, a shift in the frequencies and a decrease in the intensities of the amide bands were observed as the temperature rose. The amide A and the amide I bands shift slightly to higher frequencies and the amide II band to lower frequencies. Figure 1 shows the changes in the frequencies of the amide A bands of the unoriented films. Figures 2, 3, and 4 show the relative intensities of the amide A, the amide I, and the amide II bands of the unoriented films on the basis of the intensities at 20°C. The relative intensities of the amide A bands shown

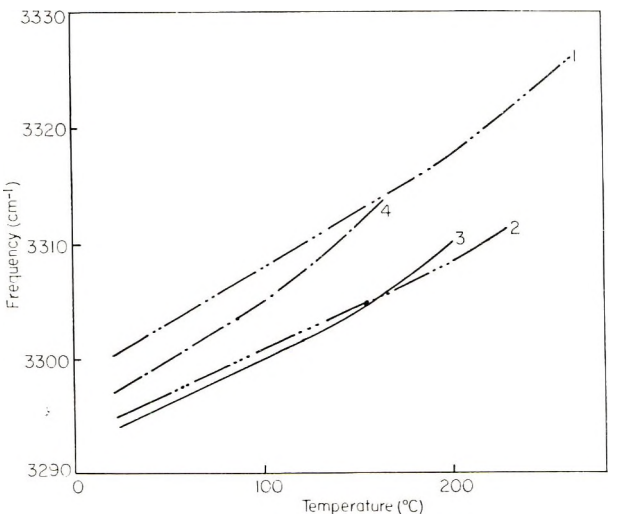


Fig. 1. Changes in freqeuncies of the amide A bands of the $\alpha$-helical polyamino acids: (*1*) PLAla; (*2*) PMDG; (*3*) PBLG; (*4*) PCBZLLys.

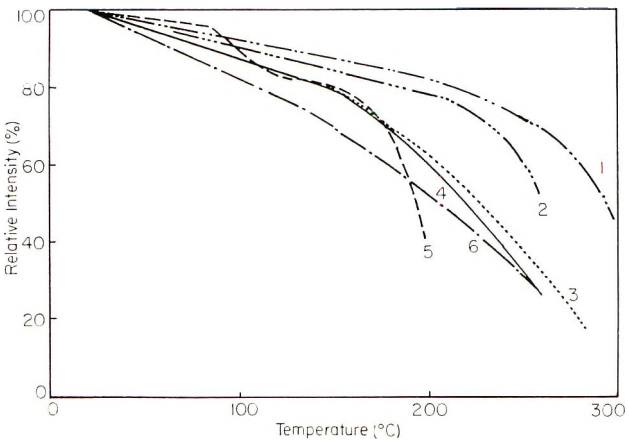


Fig. 2. Changes in the relative intensities of the amide A bands of $\alpha$-helical polyamino acids: (*1*) PLAla; (*2*) PMDG; (*3*) PCBZLOrn; (*4*) PBLG; (*5*) PBLAsp; (*6*) PCBZLLys.

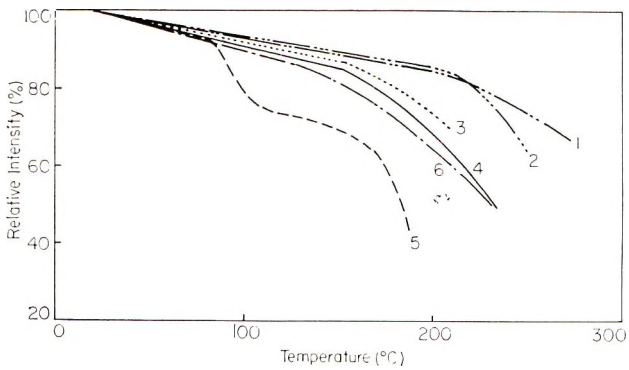


Fig. 3. Changes in the relative intensities of the amide I bands of $\alpha$-helical polyamino acids: (*1*) PLAla; (*2*) PMDG; (*3*) PCBZLOrn; (*4*) PBLG; (*5*) PBLAsp; (*6*) PCBZLLys.

in Figure 2 decrease linearly in low-temperature regions. This decrease was almost reversible on cooling. In the case of PMDG, the relative intensity that was measured at 20°C on cooling after the first run increased slightly. However, details beyond this have not been discussed. The temperature regions in which the intensities of the amide A bands change reversibly are as follows: PLAla, 200°C; PMDG, 210°C; PBLG, 150°C; PCBZLOrn, 140°C; and PCBZLLys, 130°C. In the regions above these temperatures, the intensities do not return to the initial values.

The results for PBLAsp are also shown in Figures 2 and 3. In the case of PBLAsp, the transition from $\alpha$- to $\omega$-helical conformation on heating is well known.[7–9] The decreases in the intensities of the amide A and the amide I bands around 100°C correspond to this transition. The amide II band at 1560 $cm^{-1}$ decreases abruptly near 90°C, as shown in Figure 3.

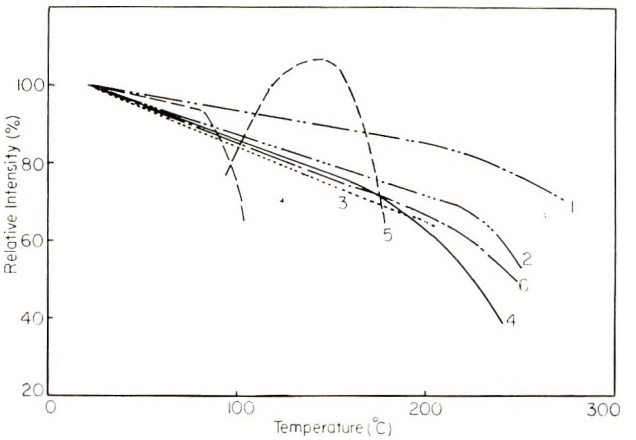


Fig. 4. Changes in the relative intensities of the amide II bands of $\alpha$-helical polyamino acids: (*1*) PLAla; (*2*) PMDG; (*3*) PCBZLOrn; (*4*) PBLG; (*5*) PBLAsp; (*6*) PCBZLLys.

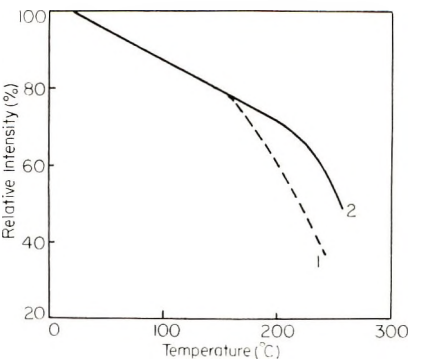


Fig. 5. Relative intensity of the amide A band of PBLG: (*1*) unoriented film; (*2*); oriented film.

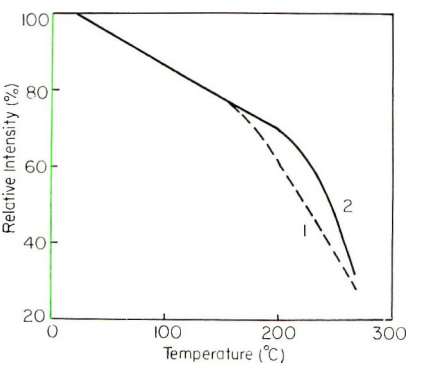


Fig. 6. Relative intensity of the amide A band of PCBZLOrn: (*1*) unoriented film; (*2*) oriented film.

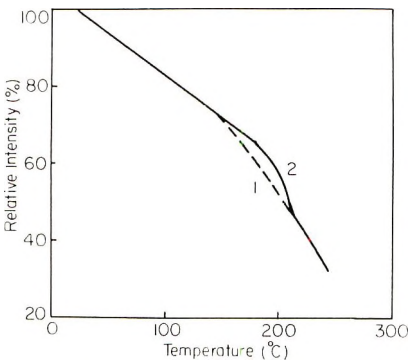


Fig. 7. Relative intensity of the amide A band of PCBZLLys: (*1*) unoriented film; (*2*) oriented film.

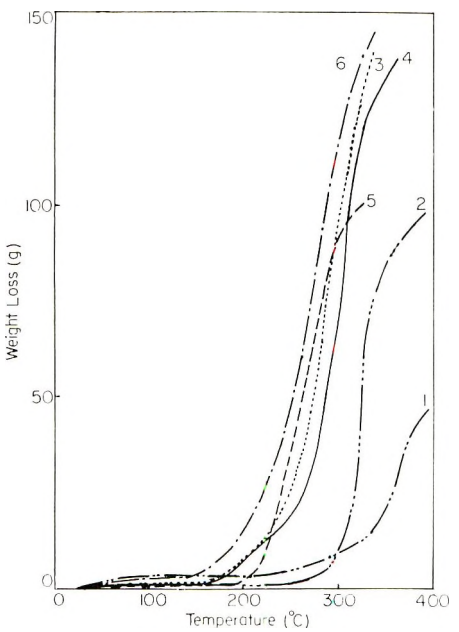


Fig. 8. Thermal degradation curves of the unoriented films of $\alpha$-helical polyamino acids: (*1*) PLAla; (*2*) PMDG; (*3*) PCBZLOrn; (*4*) PBLG; (*5*) PBLAsp; (*6*) PCBZLLys.

At the same time, this band shifts to 1539 $cm^{-1}$, and its intensity increases gradually. This change is not reversible. The thermal degradation of PBLAsp begins about at 170°C.

The infrared spectra of the oriented films were measured in the same way as those of the unoriented films. Only PLAla was not measured because we failed to obtain an oriented film from dichloroacetic acid solution. In the case of PMDG and PBLAsp, no difference was observed in the intensities between the oriented and the unoriented films under the similar mea-

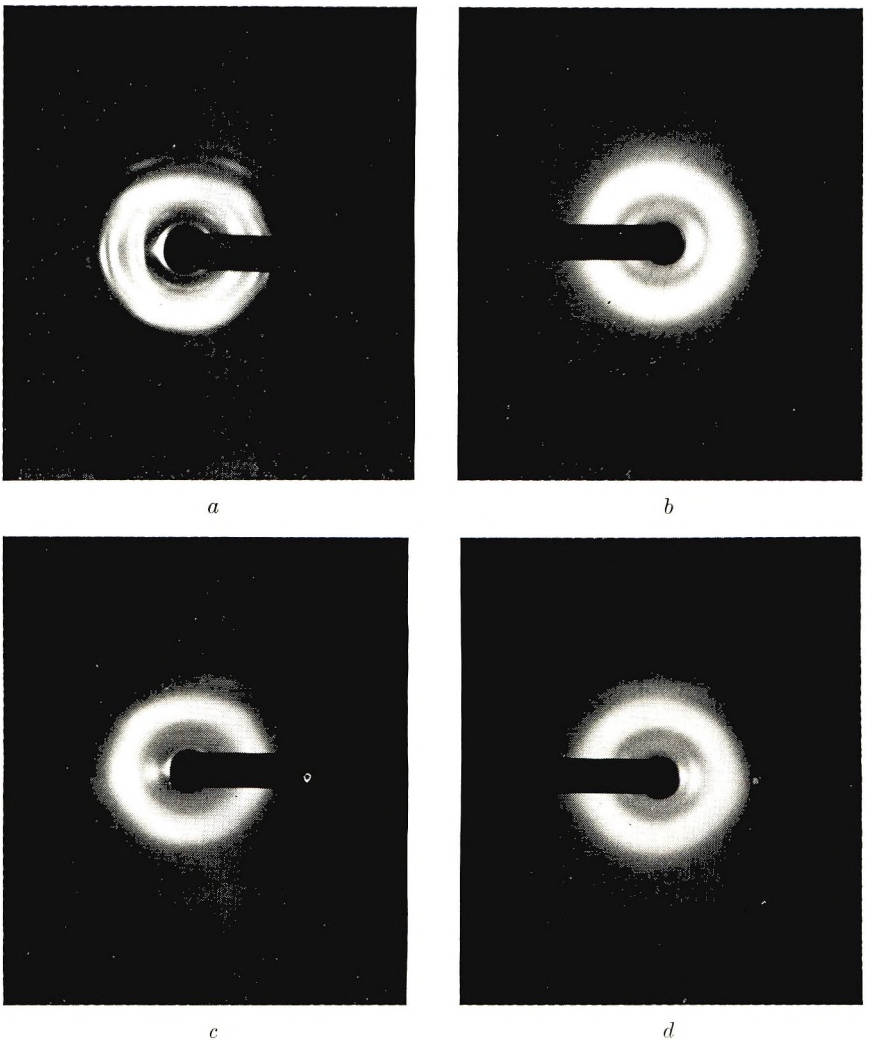

Fig. 9. X-ray diffraction patterns of the α-helical polyamino acids: (*a*) PMDG fibers; (*b*) PBLG fibers; (*c*) PCBZLOrn fibers; (*d*) oriented PCBZLLys films. Cylindrical photographs of normal diameter 57.3 mm. Fiber axis or oriented direction of the film was tilted at 30° from the normal to the beam and oscillated between 25° and 35°.

surement conditions. On the other hand, in the case of PBLG, PCBZLLys, and PCBZLOrn, there was a difference between the oriented and unoriented films. These results are shown in Figures 5, 6, and 7, respectively. The relative intensity in the low-temperature regions is unchanged by increased orientation of the molecules. However the relative intensity of the oriented film still continues to decrease reversibly beyond a temperature at which changes for the unoriented film become irreversibly.

On surveying the infrared spectra from 4000 to 700 $cm^{-1}$, it was found that the spectra measured at 20°C after heating almost agree with the

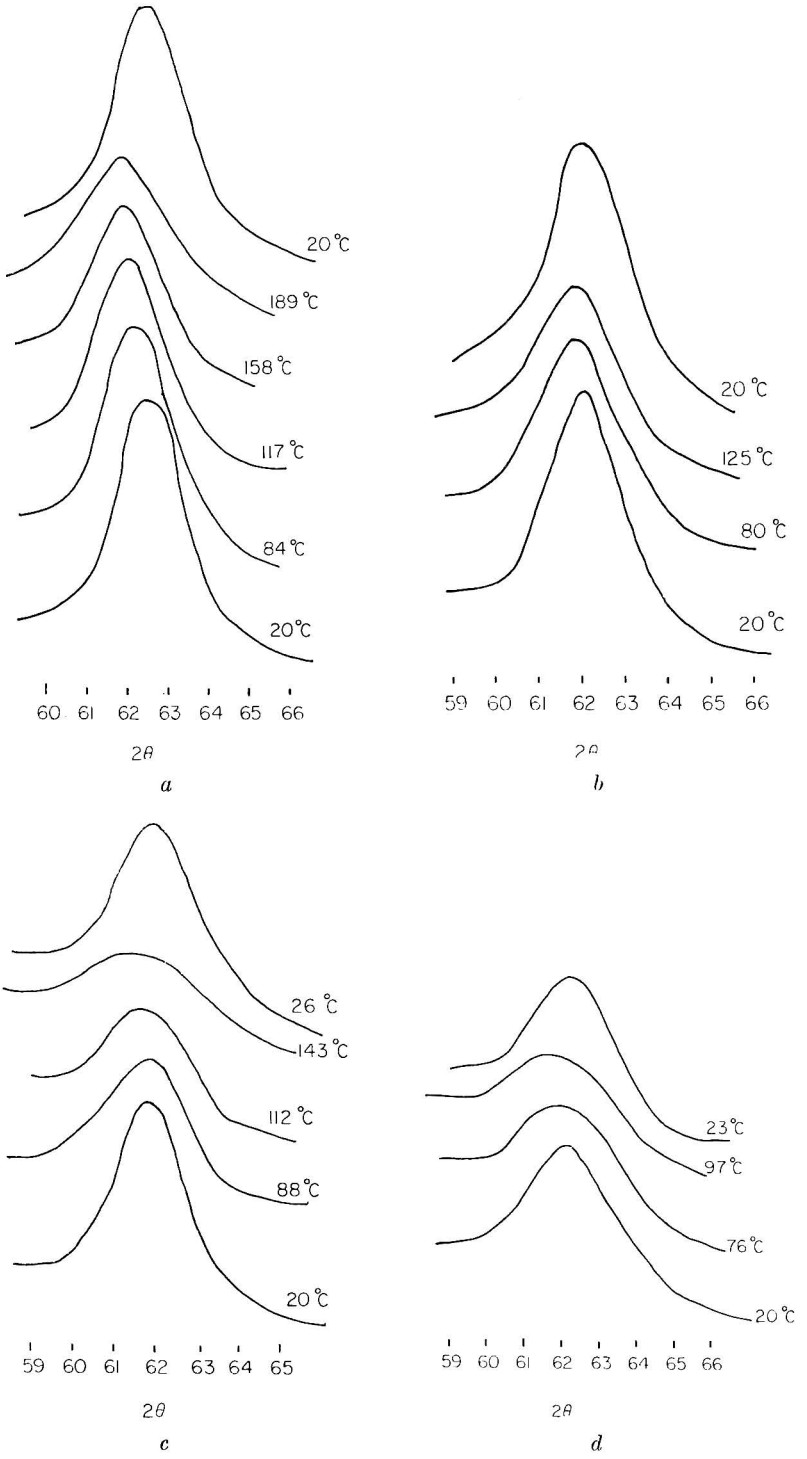


Fig. 10. X-ray diffraction curves for residue translation of $\alpha$-helical polyamino acids at various temperatures: (*a*) PMDG fibers; (*b*) PBLG fibers; (*c*) PCBZLOrn fibers; (*d*) PCBZLLys films.

original ones if it is in the temperature region at which the amide A band changes reversibly. This result applies not only to the unoriented films but also to the oriented ones.

### Thermal Degradation

The irreversible decreases in the intensities of the infrared spectra in the high-temperature regions are related to thermal degradation, because the samples changed color in these regions. Therefore thermal degradation was examined by the thermogravimetric method. Results are shown in Figure 8. The weight loss given on the ordinate is on the basis of 1 gram molecular weight of the residue of each polyamino acid. The weight loss up to 100°C may be due to the loss of absorbed water and that above 100° C to thermal degradation. The thermal degradation temperatures are about as follows: PLAla, 190°C; PBLAsp, 170°C; PMDG, 230°C; PCBZLLys, 140°C; PBLG, 160°C; PCBZLOrn, 150°C.

These temperatures nearly correspond with the temperatures at which the irreversible changes in the infrared absorption bands begin.

### Thermal Expansion of the $\alpha$-Helix along the Direction of the Helical Axis

The x-ray diffraction photographs of the polyamino acids at room temperatures are shown in Figure 9. The meridional diffraction of the residue translation of 1.5 Å is found. The diffraction curves for 1.5 Å measured with a diffractometer at various temperatures are shown in Figure 10. The diffraction curves shift to lower angles as temperature rises. This change is also reversible on cooling.

## DISCUSSION

It was found that the thermal stabilities of the $\alpha$-helical polyamino acids differ among the different molecules. The thermal degradation temperatures for PMDG, PBLG, PCBZLOrn, PCBZLLys, PLAla, and PBLAsp were observed about at 230, 160, 150, 140, 190, and 170°C, respectively, as shown in Figure 8. The $\alpha$-helical conformation of these polyamino acids except PBLAsp is stable at high temperature unless thermal degradation takes place. In the case of PBLAsp, a transition from $\alpha$- to $\omega$-helical conformation was observed.

The changes in the intensities and the frequencies of the amide bands observed in the infrared spectra at high temperature agree with the general observation of such changes which have been explained as a result of weakening of the hydrogen bonds. From the fact that the amide A band shifts to higher frequency with increasing temperature, it is expected that the $\alpha$-helix expands along the helical axis. This expansion of the $\alpha$-helix was qualitatively determined by the x-ray measurement as shown in Figure 10.

As shown in Figures 2–4, the relative intensities of the amide bands differ among the different molecules. However there is a general tendency that the faster the relative intensity of the amide A band decreases, the lower is

the thermal degradation temperature. Moreover this fast decrease in the intensity of the amide A band is observed in polyamino acids that have large side chains, such as PCBZLLys, PCBZLOrn, and PBLG. Except for PBLAsp, the decrease in intensity is reversible on cooling unless thermal degradation takes place.

Although further examination is necessary, the relationship described above indicates that the decrease in the intensity of the amide A band at high temperature is related to the motion of the side chains. As a result of such motion, it is expected that the intramolecular thermal vibration of the main chain of the $\alpha$-helix increases in polyamino acids such as PCBZLLys, PCBZLOrn, and PBLG.

It was found that the thermal stabilities of PBLG, PCBZLLys, and PCBZLOrn increase on orientation of the $\alpha$-helices. The temperature at which the intensity of the amide A band begins to decrease irreversibly shifts about 20 or 30°C to a higher value with increased orientation of the molecules, as shown in Figures 5–7. Also, from the measurement of the infrared spectra between 4000 and 700 $cm^{-1}$, it is clear that the thermal degradation temperature shifts to higher temperatures with increasing orientation of the molecules. It may be that the motion of the bulky side chains is inhibited by the orientation of the molecules and that this inhibition improves the thermal stability of the main chains.

Generally the motion of the side chains has a great effect on the thermal stabilities of polyamino acids.

The authors would like to thank Prof. Tatsuo Miyazawa of the Institute for Protein Research for valuable advice and discussion on the infrared spectroscopy; to Dr. Saburo Ishikawa of Textile Research Institute of Osaka Prefecture for valuable advice and discussion on the infrared spectra at high temperature; to Dr. Yukio Mitsui of Faculty of Pharmaceutical Sciences, University of Tokyo for valuable advice on the x-ray diffraction experiment; to Toshio Kurita of The Textile Research Institute of Japanese Government for valuable advice and help on the x-ray diffraction studies.

## References

1. Y. Hashino, M. Yoshino, and K. Nagamatsu, *Repts. Progr. Polym. Phys. Japan*, **8**, 212 (1965); *ibid.*, **9**, 297 (1966).

2. H. Obata, S. Ogawa, and T. Hatakeyama, *Senkoshi Hokoku*, **No. 73**, 41 (1965); *ibid.*, **No. 74**, 7 (1965); *Repts. Progr. Polym. Phys. Japan*, **8**, 119 (1965); *ibid.*, **9**, 301 (1966).

3. S. Sugai, K. Kamashima, S. Makino, and T. Noguchi, *J. Polym. Sci. A-2*, **4**, 183 (1966).

4. S. Sugai and K. Kamashima, *Kobunshi Kagaku*, **22**, 84 (1965).

5. K. Hikichi, *J. Phys. Soc. Japan*, **19**, 2169 (1964).

6. J. A. E. Kail, J. A. Sauer, and A. E. Woodward, *J. Phys. Chem.*, **66**, 1292 (1962).

7. E. M. Bradbury, L. Brown, A. R. Downie, A. Elliott, W. E. Hanby, and T. R. R. McDonald, *Nature*, **183**, 1736 (1959).

8. W. L. Bragg, J. C. Kendrew, and M. F. Perutz, *Proc. Roy. Soc.* (London), **A203**, 321 (1950).

9. E. M. Bradbury, L. Brown, A. R. Downie, A. Elliott, R. D. B. Fraser, and W. E. Hanby, *J. Mol. Biol.*, **5**, 230 (1962).

Received November 22, 1967
Revised May 10, 1968
Revised August 28, 1968

JOURNAL OF POLYMER SCIENCE: PART A-1 VOL. 7, 1425–1435 (1969)

# Photodegradation of Copolymers of Methyl Methacrylate and Methyl Acrylate at Elevated Temperatures

N. GRASSIE, B. J. D. TORRANCE,* and J. B. COLFORD,
*Chemistry Department, The University of Glasgow, Glasgow, W2, Scotland*

## Synopsis

Four methyl methacrylate–methyl acrylate copolymers with molar ratios, MMA/MA, of 112/1, 26/1, 7·7/1, and 2/1 have been photodegraded at 170°C by 2537 Å radiation. The changes which occur in the molecular weight of the copolymers are typical of a random scission process and from these and volatilization data the extent of chain scission during the course of the reaction has been calculated. The pattern of volatile products is the same as that previously obtained in the thermal reaction at 300°C although there are a number of differences in detail. For example, only one in ten of the methyl acrylate units is liberated as monomer compared with one in four in the thermal reaction and the ratio $CO_2$/chain scissions is considerably greater than the strict 1/1 ratio observed in the thermal reaction. Zip lengths are also very much greater in the photo reaction. These minor differences between the two reactions have been accounted for in terms of the mechanism previously presented to account for the thermal reaction, bearing in mind the differences in the temperature (170 and 300°C) at which the two investigations were carried out.

## INTRODUCTION

Recent publications[1–3] have demonstrated how the presence of the comonomers, acrylonitrile and methyl acrylate, influence the thermal degradation of poly(methyl methacrylate). In both systems the depolymerization reaction is initiated by random scission in the methyl methacrylate segments of the polymer chains. Like pure poly(methyl methacrylate) these copolymers also depolymerize at elevated temperatures under the influence of 2537 Å radiation. In the acrylonitrile polymer,[4] however, the initiation process consists of chain scission specifically at acrylonitrile units, and the principal differences between the thermal and photo reaction have been accounted for in terms of the different sites of initiation and the influence of the temperature (280°C and 160°C for the thermal and photo reactions, respectively) and viscosity of the medium upon the relative rates of the subsequent constituent processes comprising the total reaction. In the present paper the principal features of the

* Present address: Research Department, Courtaulds Ltd., Coventry, England.

photodegradation of the methyl methacrylate–methyl acrylate copolymer system are described and differences from the thermal reaction discussed.

## EXPERIMENTAL

### Copolymers

The four copolymers studied were those whose preparations have previously been described.[2] Their molar compositions are (MMA/MA) 112/1, 26/1, 7·7/1, 2/1.

### Molecular Weights

Number-average molecular weights were measured by use of a Mechrolab high-speed membrane osmometer.

The amounts of material available for the measurement of molecular weights were of the order of only a few milligrams. Molecular weight measurements are therefore subject to considerable error and this accounts for the scatter of points in Figures 4 and 5.

### Photodegradation Techniques

Photodegradations, except those involving the measurement of $CO_2$ produced, were carried out as previously described,[4] the polymer (2–4 mg), in the form of a thin transparent film, being irradiated *in vacuo*, through silica, by a source of 2 537 Å radiation.

Because of the very small amounts of $CO_2$ involved it was found more convenient to make the $CO_2$ evolution measurements in the apparatus used for thermal studies[2] with a suitably modified reaction vessel. The exit tube was situated at the side of the reaction vessel, being replaced at the top of the reaction vessel by a silica window through which the polymer was irradiated.

All product analyses were carried out exactly as described for the thermal reaction.[2]

## RESULTS

### Influence of Temperature on Rate of Volatilization

The primary influence of ultraviolet radiation on poly(methyl methacrylate) is to cause chain scission, the radicals,

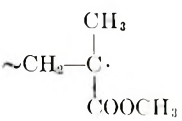

ultimately appearing in the system.[5] The overall characteristics of the photolysis depends upon the subsequent reactions of these radicals, which in turn depends upon the temperature. At high temperatures, at which

the polymer is in the liquid state, monomer produced in the equilibrium,

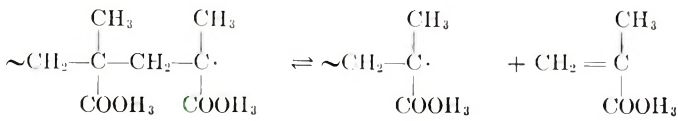

can easily escape, so that the reaction tends to the right and quantitative conversion to monomer occurs. On the other hand, at low temperatures when the polymer is in the form of a rigid solid, monomer can not readily escape, appreciable depolymerization does not occur, and the polymer radicals subsequently mutually destroy each other. At low temperatures, therefore, the photolysis is characterized by chain scission and at high temperatures by monomer production. It is the high-temperature reaction with which this paper is concerned. Unfortunately, however, the range of temperature in which this reaction can be studied is restricted, the lower limit (≃150°C) being governed by the softening point of the polymer and the upper limit (≃200°C) by the onset of thermal degradation. Clearly, in this temperature range the viscosity of the polymer is changing rapidly with temperature, and since the viscosity could have a profound influence on the above equilibrium it is important to obtain some assessment of the influence of the viscosity on the overall reaction. The data in Figure 1 demonstrate that there is no significant change in the rate of photodegradation of PMMA in the temperature range 150–170°C. Since the reaction consists of photoinitiation followed by complete unzipping of the polymer chains the rate of the reaction should be governed by the rate of initiation and since photoinitiation should be associated with an activation energy close to zero, the constant rate is accounted for and in turn implies that

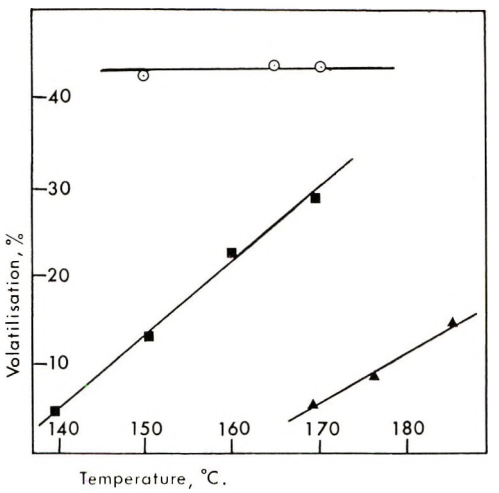


Fig. 1. Extent of volatilization in 30 min at various temperatures: (○) poly(methyl methacrylate; (■) methyl methacrylate–methyl acrylate copolymer (26/1); (▲) methyl methacrylate–methyl acrylate copolymer (7·7/1).

there is no significant viscosity effect which should be expected to cause an increase in rate with temperature. In turn, it may be concluded that the increase in the rate of photodepolymerization of the two copolymers with temperature, illustrated in Figure 1, is not associated with a viscosity effect but is a direct manifestation of the modification of the overall reaction by the presence of the comonomer.

As a result of these experiments, 170°C was chosen as a suitable temperature for a general study of the reaction since an appreciable rate of reaction was obtained over the whole copolymer composition range without interference from thermal degradation. All subsequent data were obtained at this temperature and are summarized in Table I. Chain scissions per

TABLE I
Photodegradation Data Obtained at 170°C

| Co-polymer | Time, min | Volatilization, % | MW of residue | Chain length of co-polymer ($CL_0$) | Scissions Per molecule ($N$) | Scissions Per chain unit ($n=N/CL_0$) × $10^4$ |
|---|---|---|---|---|---|---|
| 112/1 | 0 | 0 | 600000 | 6000 | 0 | 0 |
| | 10 | 5·4 | 250000 | | 1·27 | 2·11 |
| | 30 | 20·7 | — | | — | — |
| | 60 | 41·4 | 237000 | | 0·47 | 0·78 |
| | 90 | 53·6 | — | | — | — |
| | 120 | 60·8 | — | | — | — |
| 26/1 | 0 | 0 | 600000 | 6030 | 0 | 0 |
| | 5 | 1·7 | 376000 | | 0·12 | 0·19 |
| | 15 | 4·0 | 248000 | | 1·32 | 2·19 |
| | 23 | 13·4 | 229000 | | 1·27 | 2·11 |
| | 30 | 30·4 | 172000 | | 1·50 | 2·49 |
| | 45 | 34·2 | 180000 | | 1·19 | 1·98 |
| | 60 | 36·2 | 145000 | | 1·65 | 2·73 |
| | 90 | 46·2 | 118000 | | 1·68 | 2·79 |
| | 120 | 54·0 | 125000 | | 1·21 | 2·01 |
| 7·7/1 | 0 | 0 | 425000 | 4370 | 0 | 0 |
| | 5 | 1·5 | 411000 | | 0·02 | 0·05 |
| | 15 | 2·9 | 321000 | | 0·27 | 0·62 |
| | 23 | 4·4 | 181000 | | 1·25 | 2·86 |
| | 30 | 5·2 | 263000 | | 0·53 | 1·21 |
| | 45 | 16·2 | 168000 | | 1·12 | 2·56 |
| | 65 | 20·3 | 144000 | | 1·35 | 3·09 |
| | 75 | 22·3 | 157000 | | 1·10 | 2·52 |
| | 90 | 27·8 | 150000 | | 1·05 | 2·40 |
| | 120 | 29·8 | 140000 | | 1·13 | 2·58 |
| | 300 | 40·0 | 81000 | | 1·96 | 4·47 |
| 2/1 | 0 | 0 | 370000 | 3880 | 0 | 0 |
| | 30 | 1·75 | 149000 | | 1·46 | 3·76 |
| | 60 | 5·8 | 78000 | | 3·08 | 7·95 |
| | 150 | 13·0 | 49000 | | 5·52 | 14·22 |
| | 300 | 28·2 | 45000 | | 4·91 | 12·65 |
| | 600 | 39·6 | 47000 | | 3·75 | 9·65 |

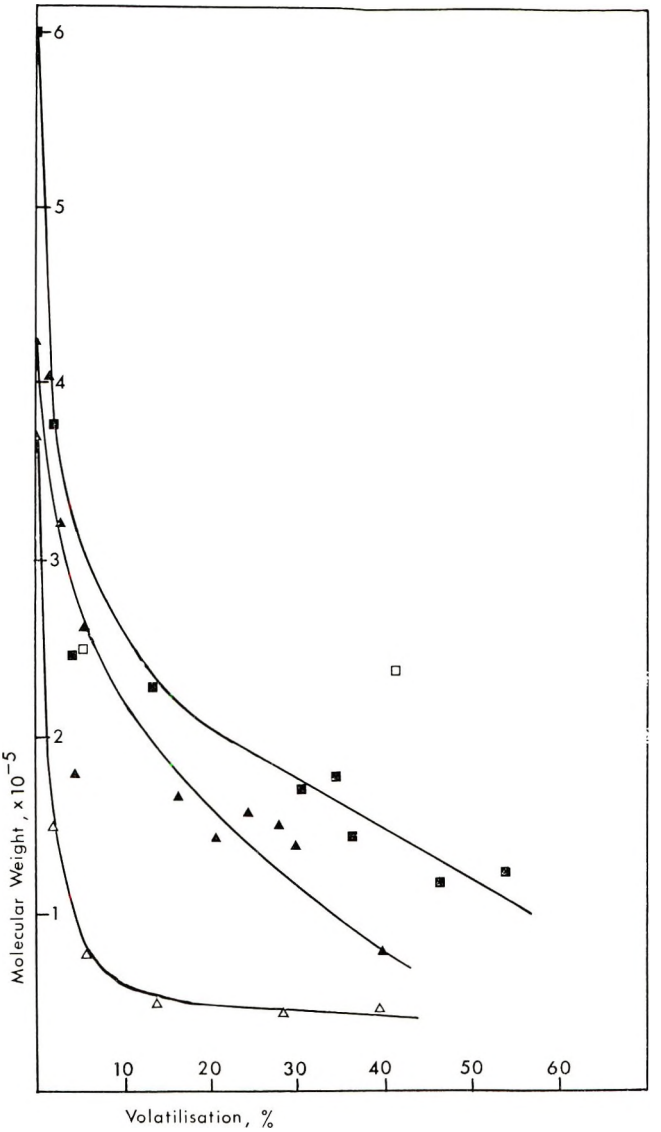


Fig. 2. Change in molecular weight with volatilization for photodegradation of methyl methacrylate–methyl acrylate copolymers at 170°C: (□) 112/1; (■) 26/1; (▲) 7·7/1; (△) 2/1.

molecule of polymer were calculated by using the formula,[3]

$$N = CL_0(1 - x)/CL - 1$$

in which $CL_0$ and $CL$ are the original chain length and the chain length at an extent of volatilization $x$, respectively. The number of chain scissions per unit length of chain, $n$, given by

$$n = N/CL_0 = [(1 - x)/CL] - (1/CL_0)$$

must be used as a comparative measure of the extent of chain scission, however, since the copolymers have substantially different molecular weights.

## Molecular Weight Changes

The changes in molecular weight which occur during photodegradation are related to the extent of volatilization in Figure 2. Like the results of thermal degradation[2,3] they are characteristic of a reaction in which random chain scission is involved. Even in the 2/1 copolymers there is no direct evidence of the crosslinking which is typical of poly(methyl acrylate), the residual material being completely soluble in all cases.

## Volatile Products of Degradation

The pattern of volatile products is closely comparable with that produced in the thermal reaction. The only significant difference concerns the ratio of the monomers. The gas-liquid chromatographic analysis of the monomer fractions are presented in Table II, from which it is clear that approximately one in ten of the MA units is liberated as monomer, compared with one in four in the thermal reaction.

TABLE II
Molar Composition of Monomeric Products (MMA/MA)

| Copolymer | Products |
|---|---|
| 112/1 | >1000/1 |
| 26/1 | 320/1 |
| 7·7/1 | 80/1 |

## Rates of Volatilization

Volatilization versus time curves for the four copolymers and PMMA are compared in Figure 3. It is obvious that, as in the thermal reaction, increasing concentrations of MA increasingly stabilize the copolymers.

## Chain Scission and the Production of Carbon Dioxide

The data in Table III summarize the results of experiments designed to determine the relationship between chain scissions and $CO_2$ production.

In the thermal reaction a strict 1/1 ratio was found throughout the polymer composition range which made it possible to use $CO_2$ production as a direct measure of chain scission. A mechanism for chain scission was proposed which accounted for these experimental observations. From the data in Table III it is clear that the $CO_2$/chain scission ratio is considerably greater than unity in the photo reaction. There appears to be some tendency for the ratio to fall as the MA content of the copolymer is increased, but the very small amounts of material available make it difficult

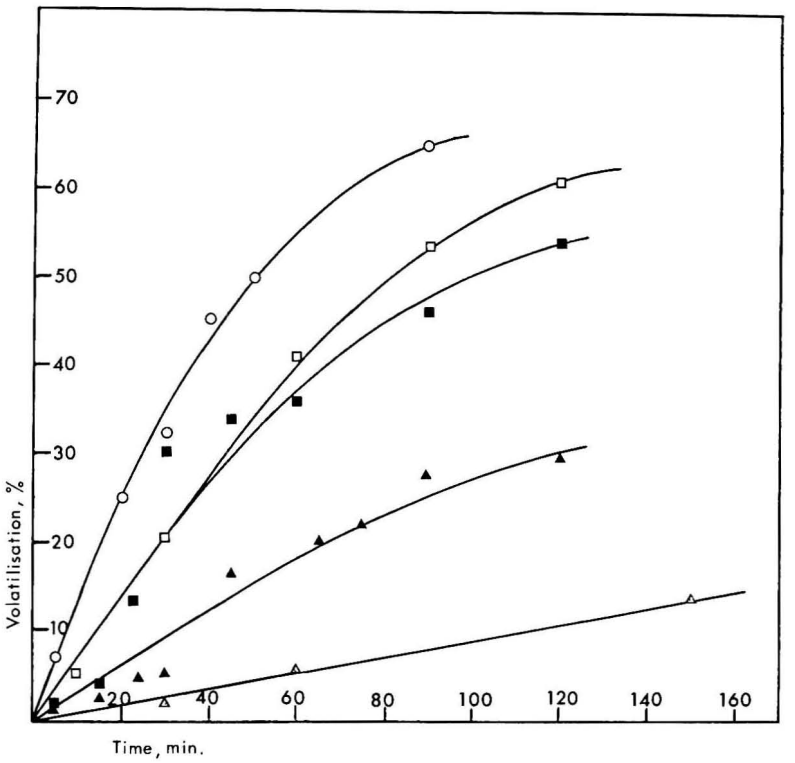


Fig. 3. Volatilization–time curves for the photodegradation of poly(methyl methacrylate) and methyl methacrylate–methyl acrylate copolymers at 170°C: (○) PMMA; (□) MMA/MA, 112/1; (■) MMA/MA, 26/1; (▲) MMA/MA, 7·7/1; (△) MMA/MA, 2/1.

TABLE III
Chain Scission and the Production of Carbon Dioxide

| Copolymer | Temp, °C | Volatilization, % | MW of residue | Scissions/molecule | $CO_2$/molecule | $CO_2$/scission |
|---|---|---|---|---|---|---|
| 26/1 | 160 | 11·6 | 244,000 | 1·062 | 4·84 | 4·5 |
| | 170 | 11·5 | 292,000 | 0·82 | 4·46 | 5·4 |
| 7·7/1 | 170 | 24·8 | 118,000 | 1·71 | 5·15 | 3·0 |
| | 170 | 46·2 | 70,000 | 2·26 | 10·6 | 4·7 |
| 2/1 | 170 | 7·4 | 75,000 | 3·57 | 7·47 | 2·1 |

to obtain values of molecular weight of sufficient accuracy to study the effect with high precision.

## Chain Scission and Volatilization

The relationship between chain scission and volatilization is illustrated in Figure 4, the data in Table I being used. Once again, the scatter of the experimental points can be attributed to the difficulty of obtaining accurate values of molecular weight, but, taken as a whole, the results are

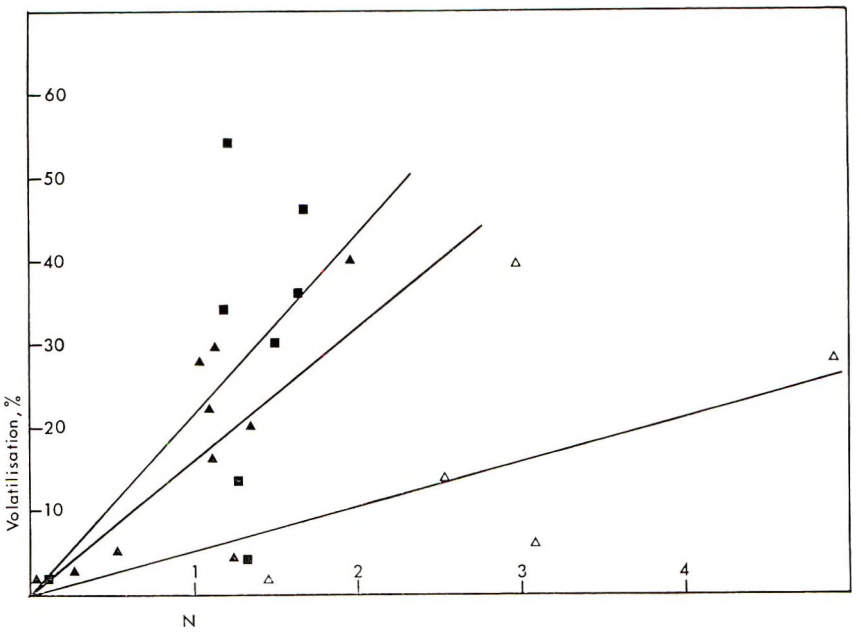


Fig. 4. Relationship between chain scissions and volatilization in the photodegradation of methyl methacrylate–methyl acrylate copolymers at 170°C: (■) 26/1; (▲) 7·7/1; (△) 2/1.

best interpreted as demonstrating a linear relationship as represented in the figure. Thus it may be concluded that, as in the thermal reaction, radicals are formed as a direct result of chain scission and that volatilization occurs by depolymerization of these radicals. Zip lengths may be calculated as in Table IV, and the values are seen to be very much greater than those observed in the thermal reaction which are presented in the last column of Table IV. However, as before, blockage of the depropagation reaction by the MA units is clearly occurring, since zip lengths decrease with increasing MA content.

## Chain Scission and Copolymer Composition

The time dependence of chain scission for the four copolymers is represented in Figure 5. There is no clear trend with copolymer composition,

TABLE IV
Zip Lengths for Depolymerization

| Co-polymer | Slope (Fig. 4) $A$, % volatilization/scission/molecule | MW | MW lost/scission (MW × $A$) | Average wt. of monomer unit ($B$) | Zip Length MW × $A/B$ | Zip Length Thermal |
|---|---|---|---|---|---|---|
| 26/1 | 22 | 600,000 | 132,000 | 99·5 | 1327 | 74 |
| 7·7/1 | 17 | 425,000 | 72,000 | 97·2 | 741 | 74 |
| 2/1 | 5·5 | 370,000 | 20,300 | 95·3 | 214 | 34 |

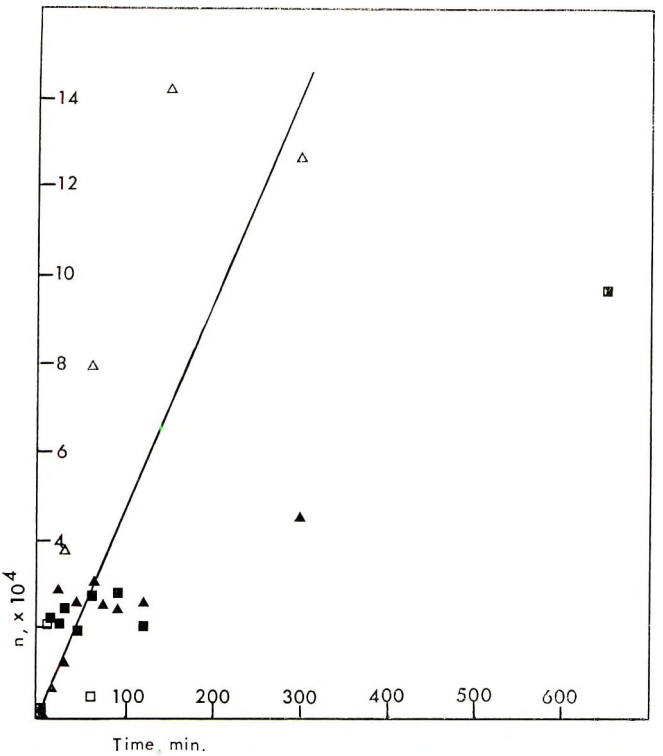


Fig. 5. Time dependence of chain scission in the photodegradation of methyl methacrylate–methyl acrylate copolymers at 170°C: (□) 112/1; (■) 26/1; (▲) 7·7/1; (△) 2/1.

and all the experimental points may be reasonably represented by a single straight line. Thus the rate of chain scission is independent of the MA content of the polymer.

## DISCUSSION

Figure 2 demonstrates that the photolysis of MMA/MA copolymers at elevated temperatures involves the successive scissioning of the chain. Although the data in Figure 5 are of limited reliability, it is clear that the rate of chain scission is not strongly dependent upon MA content and thus that the scission reaction does not occur preferentially at MA units but rather at random. Since the rate of volatilization is progressively retarded by increasing MA content, it may be deduced that MA units block the monomer producing depropagation process. This blocking action is not complete, however, since small amounts of MA monomer do appear among the volatile products. In all these aspects the photo reaction is identical with the thermal reaction.[2,3]

There are, however, some well defined differences between the two

processes and the following are probably the most significant. Firstly, the zip length in the photo reaction is very much greater than in the thermal reaction. Secondly, the strict 1/1 ratio between $CO_2$ molecules produced and chain scissions in the thermal reaction does not apply to the photo reaction. In this case a very much higher proportion of $CO_2$ appears. Thirdly, a very much smaller proportion of the MA is liberated as monomer in the photo reaction—1 in 10 units compared with 1 in 4 in the thermal reaction.

The reaction mechanism shown in Scheme I was presented previously[3] to account for the principal features of the thermal reaction. The minor differences mentioned above between the thermal and photo reactions can be accounted for in terms of this mechanism bearing in mind the differences in the temperatures at which the two reactions were studied. These were 170°C and approximately 300°C for the photo and thermal reactions, respectively. In the present instance this difference in temperature may manifest itself through the direct influence of temperature on the relative rates of constituent reactions or these relative rates may be even more strongly influenced by the very great difference in the viscosity of the medium at the two temperatures. At 170°C the polymer is in the form of a highly viscous mass, while at 300° it is a relatively mobile liquid.

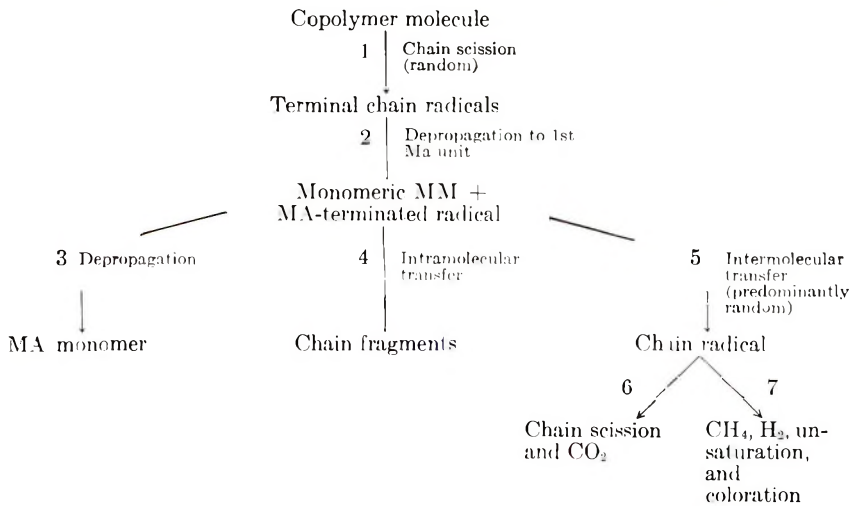


Scheme I.

Thus the greater zip length in the photo reaction can be accounted for by the fact that the more viscous medium, by suppressing thermal motion, should be expected to favor intramolecular transfer [reaction (4)] at the expense of intermolecular transfer [reaction (5)]. On the other hand, the greater $CO_2$/chain scission ratio in the photo reaction may result from the higher viscosity, favoring reaction (7) at the expense of reaction (6). These may be represented in more detail as shown in Scheme II,

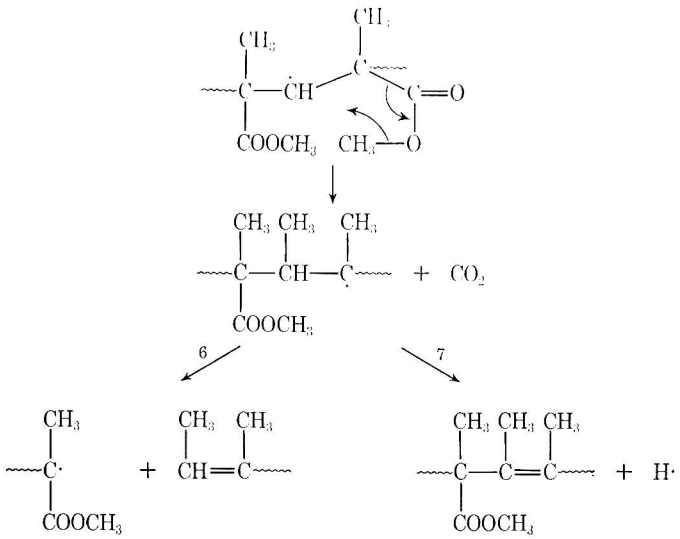

Scheme II

and the lower molecular mobility at the temperature of the photo reaction should be expected to favor separation of a mobile hydrogen atom at the expense of the diffusion apart of two long chain species. Finally the smaller relative amount of monomeric MA produced at the lower temperature may be a measure of the direct relative influence of temperature on reactions (3) and (4). Alternatively it may result from the greater viscosity of the medium inhibiting diffusion from the site of the reaction of monomer produced in depropagation. This would favor the back-reaction in the equilibrium,

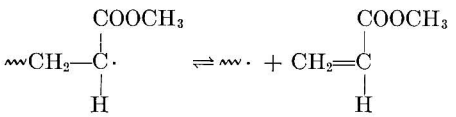

and thus in turn favor reaction (4) at the expense of reaction (3).

This research work has been sponsored by the United States Air Force under Contract AF 61 (052)-883 through the European Office of Aerospace Research, OAR, United States Air Force.

We also record our thanks to Messrs. R. Smith and G. Perrit who carried out molecular weight measurements and gave general technical assistance.

## References

1. N. Grassie and E. Farish, *Europ. Polym. J.*, **3**, 619 (1967).
2. N. Grassie and B. J. D. Torrance, *J. Polym. Sci., A-1*, **6**, 3303 (1968).
3. N. Grassie and B. J. D. Torrance, *J. Polym. Sci., A-1*, **6**, 3315 (1968).
4. N. Grassie and E. Farish, *Europ. Polym. J.*, **3**, 627 (1967).
5. R. B. Fox, *Progr. Polym. Sci.*, **1**, 45 (1967).

Received September 5, 1968

JOURNAL OF POLYMER SCIENCE: PART A-1 VOL. 7, 1437–1445 (1969)

# Sodium Hydride-Initiated Polymerizations of Vinyl Monomers in Aprotic Solvents

H. L. NEEDLES,* *Western Regional Research Laboratory, U.S. Department of Agriculture, Albany, California 94710*

## Synopsis

Polymerizations of several vinyl monomers at 25°C in aprotic solvents (dimethyl sulfoxide, *N,N*-dimethylacetamide, and hexamethylphosphoric triamide) using sodium hydride dispersion as initiator yield low to intermediate molecular weight polymers. The molecular weight of the resulting polymer as well as the mode of initiation depends on the monomer and aprotic solvent used. Initiation of polymerization of monomers with available $\alpha$ hydrogens (methyl acrylate, acrylonitrile) involves monomer anion, while initiation of a monomer with no $\alpha$ hydrogen (methyl methacrylate) proceeds by a more complex mechanism. In contrast, initiation of styrene and $\alpha$-methylstyrene proceeds by dimsyl anion addition to monomer in dimethylsulfoxide. Although the triad tacticities and number-average molecular weights of poly(methyl methacrylate) samples obtained from all three aprotic solvents are nearly the same, poly(methyl methacrylates) prepared in dimethyl sulfoxide and *N,N*-dimethylacetamide give polymers having polydispersities of ~3, while a very polydisperse polymer is obtained in hexamethylphosphoric triamide.

## INTRODUCTION

During recent studies of amide anion-initiated polymerizations of methyl acrylate in aprotic solvents,[1] we noted that reaction of sodium hydride with amide must be complete, otherwise sufficient quantities of unreacted sodium hydride initiated polymerization of monomer in aprotic solvents. Now, we wish to report that polymerization of several representative acrylic monomers is initiated by sodium hydride dispersions in aprotic solvents at room temperature to yield polymers of low to intermediate molecular weights. The nature of polymerization initiation and of the resultant polymer is dependent on the monomer used and the specific solvent employed. Although sodium hydride-initiated polymerizations[2–6] are known, we believe this to be the first study of initiation by sodium hydride dispersions in polar aprotic solvents (dimethyl sulfoxide, *N,N*-dimethylacetamide, and hexamethylphosphoric triamide).

* Present Address: Dept. of Consumer Sciences, University of California, Davis, Calif. 95616.

## EXPERIMENTAL

### Monomers and Reagents

The sources and purification of monomers, reagents, and solvents have been described previously.[1] Materials used in this study which were not used previously are from the same sources and were purified as before.

### Polymerization Procedure

The previously described procedure[1] for amide anion-initiated polymerizations was used with the following modifications. After removing mineral oil from NaH (0.01–0.001 mole), solvent (40 ml) and subsequently monomer (0.10 mole) were added to the vigorously stirred solution. The solution was stirred for 2–5 hr at room temperature and immediately quenched by addition of 1 ml of acetic acid. The resulting solutions were poured into 400 ml of water to precipitate the polymer. The poly(methyl acrylate), polystyrene, and poly-$\alpha$-methylstyrene oils were dissolved in ethyl acetate or benzene, washed with water, dried, and solvent removed to yield the polymer. Poly(methyl acrylate) and polyacrylonitrile samples were isolated by filtration after precipitation, washed thoroughly with hot water, and dried. Some poly(methyl methacrylate) samples were further purified by dissolving in acetone and reprecipitating with water and drying.

### Analyses and Spectra

Nitrogen and sulfur analyses were determined in this laboratory by standard techniques. Infrared spectra of polymer films and of polymers in Nujol were taken on a Perkin-Elmer Infracord 137 spectrophotometer. The tacticities of representative poly(methyl methacrylates) were determined by the NMR procedure of Hatada et al.[7] at 55°C in chloroform. Gel-permeation chromatographic runs were made by ArRo Laboratories, Inc. in tetrahydrofuran at 25°C on a Waters Associates chromatograph.

## RESULTS AND DISCUSSION

### General Considerations

Sodium hydride dispersions initiate polymerization of a number of vinyl monomers in polar aprotic solvents at 25°C (Tables I–III). Polymerizations have been successfully carried out in the polar aprotic solvents *N*,*N*-dimethylacetamide (DMA), dimethyl sulfoxide (DMSO), and hexamethylphosphoric triamide (HMPT), while no polymerization is observed in tetrahydrofuran (THF) or heptane. The molecular weights of the resultant polymers vary with the nature of monomer as well as the aprotic solvent used. Although the properties and molecular weights of the resultant polymers are similar to those from amide anion[1] and dimethylsulfinyl anion-initiated[8–15] polymerizations in aprotic solvents, the mode of initiation is different in many cases and varies with the monomer and solvent

TABLE I
Sodium Hydride-Initiated Polymerizations of Methyl Acrylate in Aprotic Solvents[a]

| Run no. | Ratio monomer to sodium hydride | Aprotic solvent | Reaction time, hr | Conversion of monomers, % | $[\eta]$, dl/g |
|---|---|---|---|---|---|
| 1 | 10 | DMSO | 2 | 76 | 0.04 |
| 2 | 10[b] | DMSO | 2 | 85 | 0.06 |
| 3 | 20[c] | DMSO | 2 | 86 | 0.04 |
| 4 | 100 | DMSO | 2 | 41 | 0.05 |
| 5 | 10 | HMPT | 2 | 74 | 0.13 |
| 6 | 20 | HMPT | 2 | 85 | 0.19 |
| 7 | 100 | HMPT | 5 | 5 | — |

[a] Initial methyl acrylate concn = 2.5$M$.
[b] Carbon dioxide bubbled in at 2 hr, then acetic acid.
[c] Half of monomer at $T$ = 0, then other half at $T$ = 1 hr.

TABLE II
Sodium Hydride-Initiated Polymerizations of Methyl Methacrylate[a]

| Run no. | Ratio monomer to initiator | Solvent | Reaction time, hr | Conversion of monomer, % | $[\eta]$, dl/g |
|---|---|---|---|---|---|
| 10 | 10 | DMSO | 2 | 99 | 0.09 |
| 11 | 10[b] | DMSO | 2 | 92 | 0.10 |
| 12 | 20 | DMSO | 2 | 98 | 0.12 |
| 13 | 20[c] | DMSO | 2 | 96 | 0.12 |
| 14 | 50 | DMSO | 2 | 45 | 0.07 |
| 15 | 50 | DMSO | 5 | 98 | 0.12 |
| 16 | 100 | DMSO | 5 | 0 | — |
| 17 | 20 | DMA | 2 | 0 | — |
| 18 | 20 | DMA | 5 | 93 | 0.12 |
| 19 | 20 | HMPT | 2 | 98 | 0.23 |
| 20 | 40 | HMPT | 2 | 52 | 0.23 |
| 21 | 20 | THF | 5 | Trace | — |
| 22 | 20[d] | THF | 5 | 0 | — |
| 23 | 20 | Heptane | 5 | 0 | — |
| 24 | 40 | Heptane | 5 | 0 | — |
| 25 | 40[d] | Heptane | 5 | 0 | — |

[a] Initial methyl methacrylate concn = 2.5$M$.
[b] $CO_2$ bubbled through solution at 2 hr followed by acetic acid.
[c] Half of monomer at $T$ = 0, then other half at $T$ = 1 hr.
[d] Reaction run at −78°C.

used. Apparently, very little of the sodium hydride suspension is involved in initiation of polymerization, since large amounts of hydrogen are evolved when these polymerizations are quenched. The molecular weights of the polymers were found to increase somewhat as the ratio of monomer to initiator ($M/I$) became larger; however, at the highest ratios, no polymerization of monomers was observed in a 2–5 hr period.

TABLE III
Sodium Hydride-Initiated Polymerizations of Selected Monomers in Aprotic Solvents[a]

| Run no. | Monomer | Ratio of monomer to initiator | Aprotic solvent | Time, hr | Conversion of monomer, % | $[\eta]$, dl/g |
|---|---|---|---|---|---|---|
| 30 | Styrene | 10 | DMSO | 2 | 100 | 0.02 |
| 31 | Styrene | 100 | DMSO | 2 | 0 | — |
| 32 | Styrene | 20 | HMPT | 5 | 4 | 0.10 |
| 33 | α-Methylstyrene | 20 | DMSO | 2 | 67 | 0.02 |
| 34 | α-Methylstyrene | 20 | DMSO | 5 | 92 | 0.02 |
| 35 | α-Methylstyrene | 20 | HMPT | 5 | 0 | — |
| 36 | Acrylonitrile | 10 | DMSO | 2 | 96 | 0.12 |
| 37 | Acrylonitrile | 100 | DMSO | 2 | 98 | 0.17 |
| 38 | Acrylonitrile | 10 | HMPT | 2 | 98 | 0.14 |
| 39 | Acrylonitrile | 100 | HMPT | 2 | 0 | — |

[a] Initial monomer concn = 2.5 *M*.

In general, the molecular weight of a given polymer will be higher if run in HMPT than in DMSO or DMA; however, polymerizations proceed most readily in DMSO and least readily in HMPT.

Initiation of methyl acrylate and acrylonitrile probably involves monomer anion, while polymerization initiation of styrene and α-methylstyrene in DMSO involves dimsyl anion. Initiation of polymerization of methyl methacrylate is complex and probably involves more than one mode of initiation.

## Polymerization of Methyl Acrylate

Sodium hydride-initiated polymerization of methyl acrylate proceeds rapidly at 25°C to yield low molecular weight poly(methyl acrylate) oils (Table I) similar to those isolated from amide anion-initiated polymerizations.[1] On introduction of methyl acrylate into solution, immediate hydrogen evolution and a mild exothermic reaction is observed in both DMSO and HMPT.

The resulting polymeric oils contain only traces of sulfur or nitrogen, depending on the solvent in which the polymerizations were run; therefore, dimethylsulfinyl or hexamethylphosphoric triamide anions are not involved to any extent. Infrared spectral analyses of the oils reveal that monomer anion initiation occurs to yield polymers containing a double bond head unit, as has been found for amide anion initiated polymerization of methyl acrylate.[1] In addition to strong carbonyl bands (1 740 $cm^{-1}$) characteristic of poly(methyl acrylate),[16] ester conjugated vinylic olefin bands (1 625–1 640 $cm^{-1}$)[16] varying in intensity with apparent molecular weight are observed.

No bands characteristic of dimethyl sulfoxide or hexamethylphosphoric triamide substituents are observed.

In DMSO increase of the monomer to initiator ratio has little effect on the molecular weight of the resultant polymer as reflected in intrinsic viscosity measurements, although the yield of polymer is lower as the ratio is increased. In HMPT, an increase in monomer to initiator ratio gives a higher molecular weight product, but the yield of polymer drops off much more sharply than in DMSO.

Anionic polymerization in polar aprotic solvents is usually not considered to constitute a "living" system.[8-15,17,18] We have carried out the following experiments in order to gain more insight into this consideration in DMSO. Adding additional monomer to solution after reaction of initial monomer addition (run 3) did not increase the molecular weight of the resultant polymer. Furthermore, addition of carbon dioxide (run 2) does not introduce carboxyl groups into the polymer. Gel-permeation chromatographic (GPC) analysis of poly(methyl acrylate) from run 6 in HMPT revealed that the resultant polymer possessed a number-average ($\bar{A}_n$) and weight-average ($\bar{A}_w$) molecular size of 153.0 and 491.4 Å, respectively, and therefore a moderate degree of polydispersity, as reflected by a heterogeneity factor ($\bar{A}_w/\bar{A}_n$) of 3.21. These results suggest that the system is not a living system.[19]

## Polymerization of Methyl Methacrylate

Unlike sodium hydride-initiated polymerization of methyl acrylate in aprotic solvents, polymerization of methyl methacrylate (Table II) does not begin immediately on addition of monomer. Mild exothermic polymerization is noted after stirring the solution for a period of 15 min to 2 hr time. Since initiation of methyl methacrylate cannot occur through formation of monomer anion, initiation must occur by some other means, i.e., addition of sodium hydride or another anion across the double bond of methyl methacrylate. In the presence of sufficient sodium hydride, polymerization of methyl methacrylate is nearly quantitative in aprotic solvents if sufficient time is allowed for complete polymerization. As observed for methyl acrylate, increasing the ratio of monomer to initiator slightly increases the intrinsic viscosity $[\eta]$ of the resultant polymer, while percentage conversion for a given reaction time drops.

Polymerization of methyl methacrylate proceeds more readily in DMSO than DMA or HMPT. While the molecular weights of poly(methyl methacrylate) polymerized in DMSO and DMA are the same, polymerization in HMPT gives significantly higher molecular weight products. Since it is known that dimysl anions[8-15,17,18] and *N*,*N*-dimethylacetamide anions[1] can be formed and initiate polymerizations, it is possible that polymerizations in both DMSO and DMA are terminated by abstraction of hydrogen from solvent by the growing polymer anion thereby decreasing the molecular weight of polymer. Although formation of radical anions are known for HMPT, formation of anions of HMPT at room temperature by

strong bases has not been observed,[20] and termination by abstraction from HMPT is not expected in this solvent. It seems doubtful that dimsyl anion and *N*,*N*-dimethylacetamide anion is the sole initiator for methyl methacrylate in DMSO and DMA. Analyses of reprecipitated samples of poly(methyl methacrylate) contain very small amounts of sulfur and nitrogen, which correspond to much less than 25% initiation by these anions.[1] Furthermore, it is quite possible that these analyses actually represent traces of residual solvent which cannot be excluded from the polymer even after repeated precipitations. Infrared spectra of the poly(methyl methacrylate) samples were identical to samples prepared by free-radical initiation, and no bands attributable to DMSO or DMA incorporation or to vinylic unsaturation into the polymer could be detected. At this point it appears to be impossible to determine the exact nature of initiation, however, the following is proposed. Sodium hydride particles suspended in an aprotic solvent are greatly polarized[20] and conceivably could slowly react with methyl methacrylate by adding across the double bond to give a resonance-stabilized saturated monomer anion,

$$(CH_3)_2\text{—}\overset{\ominus}{C}\text{—}\overset{\displaystyle O}{\overset{\|}{C}}OCH_3$$

which in turn initiates polymerization to yield a polymer with a saturated head unit. Very little of the total concentration of sodium hydride would actually initiate polymerization and therefore extensive hydrogen evolution on quenching the reaction is explained. Initiation by addition of sodium hydride across monomer in nonpolar solvents has been suggested previously.[5]

Adding monomer a second time (run 13) has little effect on the molecular weight of the polymer, and attempts to carboxylate the polymer (run 11) failed. Also, sodium hydride-initiated polymerization of methyl methacrylate in tetrahydrofuran (runs 21,22) and *n*-heptane (runs 23–25) failed even at reduced temperatures. These observations further serve to indicate that these are not "living" systems.[19]

In order to compare poly(methyl methacrylates) from polymerizations in the three aprotic solvents, further characterization of products (Table IV) from reaction of 20:1 monomer to initiator have been made (Table II, runs 12, 18, 19). Analyses of these samples by gel-permeation chromatography (GPC) showed that the poly(methyl methacrylates) varied in molecular size and therefore in molecular weight from solvent to solvent. Although the number-average molecular sizes varied only by a factor of about 2, there were large differences in the weight-average molecular sizes of the polymers and therefore the polydispersities of the samples. Samples run in DMSO and DMA gave similar heterogeneity factors of moderate polydispersity, although not nearly so low as found in "living" systems.[19] Poly(methyl methacrylate) polymerized in HMPT was of higher molecular weight but had a very wide molecular weight distribution, as reflected in the heterogeneity factor of 17.03. It is thought that these differences in

TABLE IV
Molecular Weights, Distributions, and Tacticities of
Poly(methyl Methacrylates) from 20:1 Monomer to Initiator in Aprotic Solvents

| Run no. | Aprotic solvent | Molecular size | | Heterogeneity factor | Molecular weight[a] | | Tacticity[b] | | |
|---|---|---|---|---|---|---|---|---|---|
| | | $\bar{A}_n$, Å | $\bar{A}_w$, Å | $\bar{A}_n/\bar{A}_w$ | $\bar{M}_n$ | $\bar{M}_w$ | I, % | H, % | S, % |
| 12 | DMSO | 126.63 | 337.54 | 2.67 | 4,940 | 13,100 | 8 | 37 | 55 |
| 18 | DMA | 84.85 | 247.85 | 2.92 | 3,300 | 9,690 | 8 | 40 | 52 |
| 19 | HMPT | 165.75 | 2823.42 | 17.03 | 6,540 | 111,000 | 9 | 39 | 52 |

[a] Molecular weight units per angstrom ($Q$) assumed to be 39.
[b] See reference 7.

polymers reflect that growing polymer anions are terminated by hydrogen abstraction from the solvent DMSO and DMA to give polymers of lower molecular weight and polydispersity, whereas polymerization of methyl methacrylate in HMPT, although initiated by sodium hydride in the same manner as in DMSO and DMA, is terminated by other means than hydrogen abstraction from solvent, thereby giving a higher molecular weight polymer of broad distribution. Determination of the triad tacticity of the polymers[7] showed that each possessed nearly the same percentages of isotactic, heterotactic, and syndiotactic units, with syndiotactic units favored over isotactic units, and solvent having no effect on the tacticity of the polymer. The tacticities of these samples were similar to tacticities of poly(methyl methacrylates) formed by dimsyl anion-initiated polymerizations in DMSO.[11] Furthermore, preference for syndiotactic placement suggests free-ion growth.

### Polymerization of Styrene and α-Methylstyrene

Both sytrene and α-methylstyrene polymerize in DMSO at low monomer/sodium hydride ratios to yield oils of low molecular weight (Table III). Only styrene could be polymerized in HMPT (run 32) to give a low yield of crystalline polymer. Recently, Stannett and co-workers[15] found that butyllithium-initiated polymerization of styrene in DMSO yields an oil, the major product of which contained a sulfinyl head unit attached to three styrene units. Surprisingly, the oil we obtained from sodium hydride-initiated polymerization of styrene also contained a high percentage of sulfur (S = 7.96%)* and gave an infrared spectrum identical to that for polystyrene except for a strong absorption at 1050 cm.$^{-1}$ characteristic of the sulfoxide group. In all properties including infrared spectra it was identical with the product reported by Stannett. The oil from similar polymerization of α-methylstyrene contained sulfur and also gave a strong absorption band at 1050 cm$^{-1}$ in addition to a characteristic spectrum of poly-α-methylstyrene. We must therefore conclude that sodium hydride-

* Calcd for dimsyl anion plus 3 styryl residues, $S$ = 8.23%.

initiated polymerization of both styrene and α-methylstyrene in DMSO proceeds by addition of dimsyl anion to monomer followed by rapid termination to give a low molecular weight product. Dimsyl anion does not appear to cause significant initiation of any other polymerizations in this study. Certainly significant quantities of dimsyl anion exist in our system, since it is known that reaction of sodium hydride in DMSO to form dimsyl anion is 15% complete in 2 hr at 27°C.[21] It is presently unknown why styrene and α-methylstyrene encourages dimsyl anion formation, but it seems logical that abstraction of hydrogen from DMSO solvent by the short growing polymer chain results in a chain effect which will generate sufficient dimsyl anions for complete dimsyl anion-initiated polymerization of monomer.

## Polymerization of Acrylonitrile

On addition of acrylonitrile to a stirred suspension of sodium hydride the solution turns yellow-green, and hydrogen evolution is observed accompanied by mild exothermic reaction (Table III). Within 2 hr the solution turns dark brown-purple; acetic acid quenching gives nearly quantitative yields of yellow to red polymers. Polymerization proceeds more readily in DMSO than HMPT, and the polymers from DMSO are less colored. Also, as the monomer to initiator ratio increases lighter colored products and less nitrogen loss from the polymer are found.

Infrared spectra of these anionically polymerized polyacrylonitriles are identical to polyacrylonitrile with the following exceptions. In addition to the expected cyanide stretching vibration at 2 260 $cm^{-1}$, a band at 2 225 $cm^{-1}$ due to vinyl conjugated cyanide[22] and/or ketonitrile groups[23,24] is observed. The intensities of these two bands vary in the polymers with the ratio of monomer to initiator, the 2 225 $cm^{-1}$ band being strongest at low monomer/initiator ratios. Also, diffuse wide bands between 1 650 and 1 550, a region where carbon–carbon and carbon–nitrogen double bonds absorb,[22–24] are observed. The presence of vinyl conjugated nitrile groups and observed rapid hydrogen evolution during polymerization of acrylonitrile point to initial hydrogen abstraction from acrylonitrile by sodium hydride[17,18] followed by initiation of polymerization by acrylonitrile anion. The presence of possible ketonitrile carbon–nitrogen unsaturation in the polyacrylonitriles, the presence of color in the polymers increasing as the monomer/initiator ratio is lowered, and percentage nitrogen loss suggest that significant base-catalyzed condensation and cyclization reactions occur. Ottolenghi and Zilka[17] have previously shown the anionic polymerization of acrylonitrile in *N*,*N*-dimethylformamide is terminated by cyclization of the growing polymer anion to yield a stable six-membered ring which loses nitrogen on addition of a proton source. These polymers gave similar infrared spectra to those of our present study. In addition, base-catalyzed cyclizations of polyacrylonitrile are well known,[23,24] and could occur through attack of polyacrylonitrile by excess sodium hydride, followed by condensation to yield highly colored products containing partially hydrogenated naphthylidine type structures.[23,24]

I wish to thank Dr. William L. Wasley for helpful discussions and encouragement throughout the course of this work, and Dr. V. T. Stannett and J. E. Mulvaney for disclosure of research results prior to publication.

Reference to a company or product name does not imply approval or recommendation of the product by the U.S. Department of Agriculture to the exclusion of others that may be suitable.

## References

1. H. L. Needles, *J. Polym. Sci. B*, **6**, 377 (1968).
2. J. L. R. Williams, T. M. Laakso, and W. J. Dulmage, *J. Org. Chem.*, **23**, 638 (1958).
3. E. G. Kastning and K. Bronstert, Ger. Pat. 1,066,742 (Oct. 8, 1959).
4. P. P. Thomas and G. J. Tyler, Brit. Pat. 886,958 (Jan. 10, 1962).
5. H. T. Feng, N. F. Ch'iu, and T. C. Chiang, *Ko Fen Tzu T'ung Hsun*, **7**, 48, 112 (1965); *Chem. Abstr.*, **63**, 16478 (1965); *Chem. Abstr.*, **64**, 2172 (1966).
6. R. Wakasa, S. Ishida, and Y. Kitahama, Japan Pat. 15,622 (1967).
7. K. Hatada, K. Ota, and H. Yuki, *J. Polym. Sci. B*, **5**, 225 (1967).
8. L. Trossarelli, M. Guaita, A. Priola, and G. Saini, *Intern. Symp. Macromol. Chem., Prague*, 1965, preprint 578.
9. L. Trossarelli, M. Guaita, and A. Priola, *Atti Acad. Sci. Torina*, **100**, 367 (1966).
10. L. Trossarelli, M. Guaita, and A. Priola, *J. Polym. Sci. B*, **5**, 535 (1967).
11. J. E. Mulvaney and R. L. Markham, *J. Polym. Sci. B*, **4**, 343 (1966).
12. G. E. Molau and J. E. Mason, *J. Polym. Sci. A-1*, **4**, 2336 (1966).
13. G. E. Molau and J. E. Mason, Brit. Pat. 1,097,239 (Jan. 3, 1968).
14. C. E. H. Bawn, A. Ledwith, and N. R. McFarlane, *Polymer*, **8**, 484 (1967).
15. A. B. Gosnell, J. A. Gervasi, and V. Stannett, *Makromol. Chem.*, **109**, 62 (1967).
16. W. H. T. Davison and G. R. Bates, *J. Chem. Soc.*, **1953**, 2607.
17. A. Ottolenghi and A. Zilkha, *J. Polym. Sci. A*, **1**, 687 (1963).
18. R. B. Cundall, J. Driver, and D. D. Eley, *Proc. Chem. Soc.*, **1958** 170.
19. M. Szwarc, *Makromol. Chem.*, **35**, 132 (1960).
20. H. Normant, T. Cuvigny, J. Normant, and B. Angelo, *Bull. Soc. Chim. France*, **1965**, 3441.
21. W. I. Lyness, D. E. O'Connor, and J. S. Berry, U.S. Pat. 3,288,860 (1966).
22. L. J. Bellamy, in *The Infra-red Spectra of Complex Molecules*, Wiley, New York, 1958.
23. J. R. Kirby, J. Brandrup, and L. H. Peebles, Jr., *Macromolecules*, **1**, 53 (1968).
24. H. N. Friedlander, L. H. Peebles, Jr., J. Brandrup, and J. R. Kirby, *Macromolecules*, **1**, 79 (1968).

Received September 11, 1968
Revised November 14, 1968

JOURNAL OF POLYMER SCIENCE: PART A-1 VOL. 7, 1447–1454 (1969)

# Structure and Reactivity of $\alpha,\beta$-Unsaturated Ethers. V. Cationic Copolymerizations of Ring-Substituted Phenyl Vinyl Ethers

T. FUENO,* T. OKUYAMA,* I. MATSUMURA, and J. FURUKAWA,
*Department of Synthetic Chemistry, Kyoto University, Kyoto, Japan*

## Synopsis

Phenyl vinyl ether ($M_1$) has been copolymerized with its various ring-substituted derivatives ($M_2$) in toluene at $-78°C$ with stannic tetrachloride as catalyst. The substituents investigated include *p*-$CH_3O$, *m*-$CH_3O$, *p*-$CH_3$, *m*-$CH_3$, *p*-Cl, and *m*-Cl. The course of copolymerization was followed by gas chromatographic determinations of residual monomers, and the monomer reactivity ratios were evaluated by use of the integral form of the Mayo-Lewis copolymerization equation. Except for the unusual case of the *m*-$CH_3O$ derivative, the observed values of log $(1/r_1)$ were found to be linearly correlated with Hammett's $\sigma$ constants, the reaction constant being $\rho = -1.76$ with the correlation coefficient $r = 0.990$. Comparisons of these results with the existing data for the styrene copolymerizations have enlightened the behavior of the oxygen atom in transmitting the electronic effects of ring substituents onto the reaction center.

## INTRODUCTION

In previous papers of this series,[1,2] we have reported the results of cationic copolymerizations of various alkenyl alkyl ethers (R′CH=CHOR) and discussed the effects of the $\beta$-alkyl substituents, R′, as well as those of geometrical isomerism on the polymerizability. Another factor that clearly influences the reactivity of unsaturated ethers is the electronic effect of the $\alpha$-alkoxyl groups, OR; the cationic polymerizability of vinyl ethers is recognized to diminish in the order: *t*-$C_4H_9O$ > *i*-$C_3H_7O$ > *i*-$C_4H_9O$ > *n*-$C_4H_9O$ > $C_2H_5O$ > $CH_3O$.[3,4]

The origin of this order of the alkoxyl groups in affecting the vinyl ether reactivity is still a matter open to inquiry.[3,4] Although several factors will need to be considered, it appears to be a particular advantage to first establish the consequences of a well-defined mesomeric effect of the ethereal groups on the vinyl ether polymerizability.

One of the most pertinent experimental approaches to the above-stated proposition is perhaps to examine possible electronic effects of ring substituents on the polymerizability of an alkenyl aryl ether. Although cationic polymerization and copolymerization of phenyl vinyl ether, for

* Present address: Faculty of Engineering Science, Osaka University, Toyonaka, Osaka, Japan.

instance, have already been reported by several workers,[5-9] mutual copolymerizations of substituted phenyl vinyl ethers have never received attention. It is known only that cationic polymerizability of phenyl vinyl ether is somewhat smaller than that of alkyl vinyl ether[4,5] but is markedly greater than that of styrene.[9]

Thus, in the present paper, we have undertaken to investigate copolymerizations of phenyl vinyl ether with several of its ring-substituted derivatives. The specific aim of this work is twofold: one goal is to examine whether possible electronic effects of substituents may be correlated with the well-accepted Hammett constants of substituents; the other is to gain an insight into the nature of an oxygen atom in transmitting across it the electronic effects of substituents onto the reaction center. Although the substituents selectively adopted for these purposes have only been modest in number, special cautions have been taken to carry out precision measurements of the monomer reactivity ratios so that they suffice to disclose general trends.

## EXPERIMENTAL

### Materials

Phenyl vinyl ether (PVE) and its *p*-$CH_3O$, *m*-$CH_3O$, *p*-$CH_3$, *m*-$CH_3$, *p*-Cl, and *m*-Cl derivatives were prepared as described previously.[10] Gas chromatography showed that all these ethers were over 99.5% pure. They were distilled over calcium hydride under dry nitrogen immediately before use.

Toluene and Tetralin were distilled over metallic sodium under a nitrogen atmosphere. Stannic chloride was refluxed over phosphorus pentoxide and distilled.

### Procedure

PVE was copolymerized with each of its ring-substituted derivatives by stannic chloride in toluene at −78°C. Copolymerization was conducted under dry nitrogen in a flask equipped with a stirrer. Toluene, Tetralin, and monomers were successively introduced into the flask immersed in a Dry Ice–methanol bath. The total volume of the solution was usually 20 ml, and the total monomer concentration was 1.25 mole/l. The concentration of Tetralin used as the internal standard was 0.5 mole/l. After the monomer solution having been cooled down to the Dry Ice–methanol temperature, 2 ml of a toluene solution of stannic chloride (1.00 mole-% with respect to the monomer mixture) was added by use of a syringe under stirring, and the reaction was started. After a specified time of reaction, a small portion of the reaction mixture was sampled out by a syringe and poured into methanolic potassium hydroxide to stop the reaction.

The concentrations of comonomers, both before and after the reaction, were determined by gas chromatography. A Yanagimoto gas chromatograph, Model GCG-3DH, was operated at the column temperature of ca. 140°C with hydrogen as carrier gas. Silicone DC 550 or Apiezon Grease L

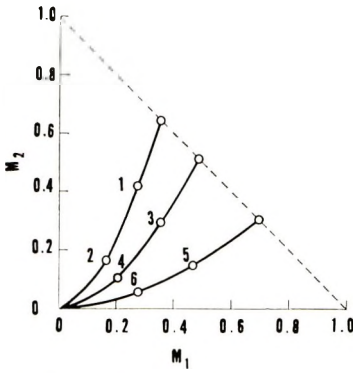


Fig. 1. Monomer consumption curves for the copolymerization of PVE ($M_1$) with *p*-$CH_3$-PVE ($M_2$). The numbers appended to the plots correspond to the runs given in Table I.

was used as column packing. It was confirmed by calibration that the half-height width evaluation of the peak areas coupled with the internal standard technique fully sufficed for determining the monomer concentrations. The monomer reactivity ratios were obtained by the aid of the integral form of the Mayo-Lewis copolymerization equation.[11]

## RESULTS

Listed in Table I are the copolymerization data for the system, PVE ($M_1$)–*p*-$CH_3$-PVE ($M_2$), as an example. The quantities $M_1^0$ and $M_2^0$ are the molar compositions of the monomer mixture for the copolymerization experiments, while $M_1$ and $M_2$ are the molar fractions of the residual monomers after the reaction has been terminated. The magnitude $1 - M_1 - M_2$ thus stands for the extent of reaction for a given run. The change of $M_1$ and $M_2$ with copolymerization is shown in Figure 1.

TABLE I
Copolymerization of Phenyl Vinyl Ether ($M_1$) with *p*-Methylphenyl Vinyl Ether ($M_2$)[a]

| Run no. | Monomer feed[b] | | Polymerization time, min | Residual monomer[c] | | Extent of reaction, % | $m$[d] | $b$[d] |
|---|---|---|---|---|---|---|---|---|
| | $M_1^0$ | $M_2^0$ | | $M_1$ | $M_2$ | | | |
| 1 | 0.352 | 0.648 | 5 | 0.275 | 0.420 | 30.5 | 0.949 | −1.098 |
| 2 | 0.352 | 0.648 | 75 | 0.167 | 0.166 | 66.7 | 0.739 | −0.798 |
| 3 | 0.485 | 0.515 | 9 | 0.352 | 0.294 | 35.4 | 0.531 | −0.361 |
| 4 | 0.485 | 0.515 | 300 | 0.205 | 0.109 | 68.6 | 0.428 | −0.215 |
| 5 | 0.694 | 0.306 | 15 | 0.465 | 0.149 | 38.6 | 0.204 | 0.187 |
| 6 | 0.694 | 0.306 | 210 | 0.278 | 0.0594 | 66.3 | 0.172 | 0.247 |

[a] Experimental conditions: initial monomer concentration, 1.25 mole/l; catalyst, $SnCl_4$ (12.5 mmoles/l); solvent, toluene; temp, −78°C.

[b] Initial molar compositions of the monomer mixture.

[c] Molar fractions of the residual monomers with respect to the total monomer feeds.

[d] Calculated by use of the integral form of the Mayo-Lewis copolymerization equation (see text).

The $r_1$–$r_2$ relationships which resulted from the introduction of the observed values of $M_1^0$, $M_2^0$, $M_1$, and $M_2$ into the integrated copolymerization equation were essentially linear, i.e., of the form $r_1 = mr_2 + b$, in the regions of interest. The quantities $m$ and $b$ are constants characteristic of each run. The monomer reactivity ratios $r_1$ and $r_2$ for a given monomer pair may thus be evaluated by the least-squares treatments of an expected linear relationship between the observed quantities $m$ and $b$, i.e., $b = -r_2m + r_1$. This latter linearity has been substantiated with fair precision for all the monomer combinations investigated. Figure 2 represents a typical example of such linear plots.

Monomer reactivity ratios obtained for the various pairs of PVE ($M_1$) and its derivatives ($M_2$) are summarized in Table II. The uncertainties appended to the $r_1$ and $r_2$ values are the probable errors[12] involved in the intercepts and the slopes of the linear $m$–$b$ plots.

It may be seen in Table II that the observed monomer reactivities run parallel to the Hammett $\sigma$ constants of the substituents. The trend that the cationic polymerizability of PVE derivatives increases with the increase in electron-donating character of the substituents is readily understandable.

The $m$-$CH_3O$ derivative showed a somewhat unusual behavior. At $-78°C$ it did not undergo copolymerization with PVE, and the reaction system turned yellowish red in color, with formation of red-brown precipitates. Apparently, this indicates the occurrence of some intermolecular reaction between the $m$-$CH_3O$ derivative and stannic chloride. Since the type of copolymerization desired was found to be somehow feasible at $-40°C$, the monomer reactivities of this derivative were evaluated at this temperature. However, because the undesirable side reaction mentioned above could not be avoided, the monomer reactivity ratios obtained for this particular system are not reliable.

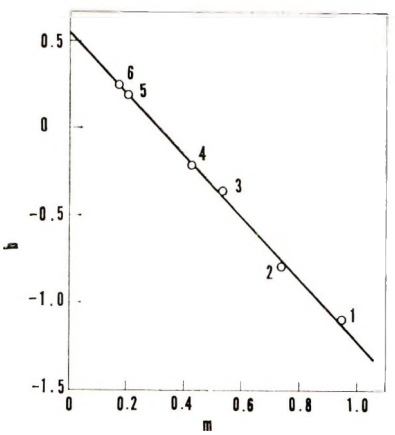


Fig. 2. Linear relationship, $b = -r_2m + r_1$, for the copolymerization of PVE ($M_1$) and $p$-$CH_3$-PVE ($M_2$). The numbers appended to the plots correspond to the runs given in Table I.

TABLE II
Monomer Reactivity Ratios for the Cationic Copolymerizations of Phenyl Vinyl Ether ($M_1$) with its Ring-Substituted Derivatives ($M_2$)

| Substituent | σ | No. of runs | $r_1$[a] | $r_2$[a] | $r_1r_2$ |
|---|---|---|---|---|---|
| *p*-$CH_3O$ | −0.268 | 7 | 0.42 ± 0.061 | 2.1 ± 0.14 | 0.88 ± 0.19 |
| *p*-$CH_3$ | −0.170 | 6 | 0.55 ± 0.014 | 1.76 ± 0.032 | 0.97 ± 0.05 |
| *m*-$CH_3$ | −0.069 | 6 | 0.79 ± 0.067 | 1.50 ± 0.056 | 1.19 ± 0.21 |
| *m*-$CH_3O$ | 0.115 | 7 | 0.71 ± 0.058 | 1.1 ± 0.07 | 0.78 ± 0.11 |
| *p*-Cl | 0.227 | 8 | 3.6 ± 0.34 | 0.27 ± 0.023 | 0.97 ± 0.20 |
| *m*-Cl | 0.373 | 6 | 4.6 ± 0.50 | 0.19 ± 0.021 | 0.87 ± 0.19 |

[a] Uncertainties are the probable errors in the intercepts and the slopes of the linear plots of $b$ vs. $m$; $b = -r_2m + r_1$.

## DISCUSSION

### Phenomenology of the Copolymer Chain Growth

The final column of Table II gives the product values, $r_1r_2$, of the observed monomer reactivity ratios. The uncertainties appended to these entries have been obtained as such that the percentage error of each $r_1r_2$ value is simply the sum of the percentage errors attached to its composite $r_1$ and $r_2$ values.

Inspection of the $r_1r_2$ products listed in Table II shows that, apart from the anomalous case of *m*-$CH_3O$-PVE, the probable values within the error limits encompass the value of unity in all the copolymerization systems. This is an indication that the instantaneous selection of adding monomers exercised by growing chain ends is not influenced at all by the substituents attached to the chain ends. The indication, in turn, guarantees the occurrence of copolymerization reactions even though copolymers have not really been identified as such.

In all cases, the resulting copolymers consisted of a fraction of methanol-insoluble white powders and a small, yet not negligible, amount of methanol-soluble fraction. Nonetheless, in the case of the *m*-Cl-PVE system (which was selected as a representative case), the methanol-insoluble fraction of the copolymers formed in the low conversion region (<5 %) gave elemental analysis data that checked quite well with those calculated back from the observed monomer reactivity ratios and the starting comonomer compositions. These results show that the two fractions of the copolymer formed were of the same composition, indicative of the statistical randomness of the monomer selection during the chain growth. Thus the present determination of the monomer reactivity ratios by following the variation in composition of the residual comonomers is perfectly legitimate.

### Effects of Substituent on the Polymerizability

Figure 3 represents a plot of the observed values of log $(1/r_1)$ against Hammett σ constants of the substituents. Although the substituents adopted for the plot have only been modest in number, it still may be safe

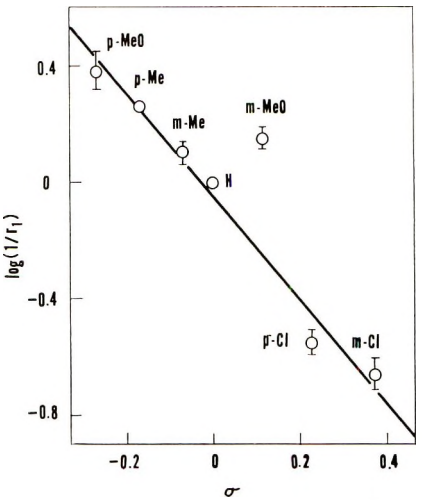


Fig. 3. Plots of $\log(1/r_1)$ vs. Hammett $\sigma$. The vertical lines drawn on the circles indicate the range of the probable error.

to conclude that a linear relationship holds between the two quantities. Aside from the anomalous *m*-$CH_3O$ plot, the least-squares treatment of the linearity has led to a reaction constant $\rho = -1.76 \pm 0.13$ with the correlation coefficient $r = 0.990$.

The fact that the substituent effects conform to the Hammett $\sigma$ values is a clear indication that the anomalous exalting effect of some electron-donating *para* substituents on electrophilic reactions, as has been observed in the cationic copolymerizations of styrenes,[13,14] is not operative in the chain-propagation step of the phenyl vinyl ether copolymerizations. Undoubtedly, this is because the oxygen atom between the benzene ring and the reaction center in this latter class of monomers suppresses direct conjugation. Sufficient conjugation would have permitted a correlation of log $(1/r_1)$ with Brown's $\sigma^+$ values,[15] as in the case of the styrene copolymerizations.[14] The differences in behavior of the two classes of monomers may best be understood from the difference in the most dominant limiting structures that will contribute to their electronic ground states.

Styrenes:

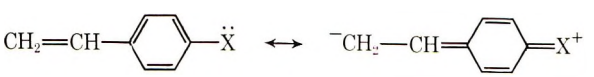

Phenyl vinyl ethers:

The situation remains the same[10] when one considers the resulting carbonium ions, which may be regarded as a general extrapolation of the transition states for electrophilic addition reactions.

Nevertheless, the oxygen atom certainly transmits the mesomeric effect of substituents onto the reaction center, even though only slightly. This

is clear[16] from the comparisons of the effects of ring substituents on the NMR chemical shifts of the *trans*-β-protons of phenyl vinyl ether and allylbenzene, both having been found to be linearly correlated with Hammett's σ (greater upfield shifts for more electron-donating substituents), but the sensitivity toward σ is greater in the former family of compounds than in the latter. If, in phenyl vinyl ethers, no such conjugation between the extracyclic reaction center and substituents had been possible at all, then the values of $\log(1/r_1)$ here reported would probably have been better correlated with Taft's normal substituent constants, $\sigma^0$.[17] The substituent effects observed in the present copolymerization studies imply that such a conjugation across the intervening oxygen atom is significant just to the same extent as the interaction between the carboxylate group and ring substituents in benzoic acid dissociations.[18] The situation is formally analogous to that encountered in our previous studies of the acid-catalyzed hydrolysis rates of substituted phenyl vinyl ethers.[10]

### Carbonium Ion Character of Monomers in the Transition State

A brief discussion of the reaction constant ρ now seems to be in order. The value of $\rho = -1.76$ observed here is somewhat smaller in magnitude than the corresponding value of $\rho = -2.03$ obtained for the styrene copolymerizations.[14] This change in ρ brought about by the intervention of an oxygen atom between the vinyl group and the benzene ring is qualitatively understandable in view of the generalization that the effects of substituents should diminish with increasing distance between the substituents and the reaction center. A similar comparison can also be made between the acid-catalyzed hydrolysis of substituted phenyl vinyl ethers ($\rho = -2.14$)[10] and the acid-catalyzed hydration of styrene derivatives ($\rho = -3.4$).[19] Although these latter two reactions are different in type as well as in the experimental conditions adopted, both of them have in common that they have been established to involve the rate-determining proton transfer from the hydronium ion to the β-carbon of the substrates.

Of particular interest to us is the magnitude of the "fall-off" factor in ρ due to the presence of the intervening oxygen atom. In the cationic polymerizations of our present concern, this factor is $-1.76/-2.03 = 0.87$, while it is as small as $-2.14/-3.4 = 0.63$ in the above-mentioned β-carbon protonation reactions. Although no quantitative interpretation of the variation of these factors appears possible, it may at least partly be ascribable to some difference in the nature of the transition states of the two types of reactions.

Noteworthy in this connection is the observation that this factor takes on a value of approximately unity in the case of the silver ion complexation equilibria of phenyl vinyl ethers[20] and styrene derivatives[21] (Table III). The fall-off factor might then be regarded as an empirical quantity reflecting a possible difference in the carbonium ion character of the transition states involved, which tends to diminish as this character becomes greater. Sakurai has noted a similar trend in the comparisons of the substituent effects on the rates of some radical reactions of toluene and anisole deriv-

TABLE III
Comparisons of the $\rho$ Values between Some Types of Reactions of Phenyl Vinyl Ethers and of Styrenes

| | $\rho$[a] | | |
|---|---|---|---|
| | Phenyl vinyl ether | Styrene | $\rho_{pve}/\rho_{st}$ |
| Protonation[b] | $-2.14$ ($\sigma$)[10] | $-3.4$ ($\sigma^+$)[19] | 0.63 |
| Cationic copolymerization[c] | $-1.76$ ($\sigma$) | $-2.03$ ($\sigma^+$)[14] | 0.87 |
| Silver ion complexation[d] | $-0.79$ ($\sigma$)[20] | $-0.77$ ($\sigma$)[21] | 1.03 |

[a] Shown in the parentheses are the substituent constants with which the rate data have been correlated.

[b] In 80% dioxane–water at 25°C.

[c] In toluene at Dry Ice–methanol temperature.

[d] In water of ionic strength of unity at 25°C.

atives.[22] However, little can be said at present concerning the physical basis of the proposed relationship between the carbonium ion character and the fall-off tendency.

## References

1. T. Okuyama, T. Fueno, and J. Furukawa, *J. Polym. Sci. A-1*, **6**, 993 (1968).
2. T. Okuyama, T. Fueno, J. Furukawa, and K. Uyeo, *J. Polym. Sci. A-1*, **6**, 1001 (1968).
3. C. E. Schildknecht, A. O. Zoss, and F. Grosser, *Ind. Eng. Chem.*, **41**, 2691 (1949).
4. H. Yuki, K. Hatada, and M. Takeshita, *J. Polym. Sci. A-1*, in press.
5. W. Chalmers, *Can. J. Res.*, **7**, 464, 472 (1932).
6. A. E. Favorskii and M. F. Shostaskovokii, *J. Gen. Chem. USSR*, **13**, 1 (1943).
7. I. F. Losev, O. Y. Fedotova, and B. E. Trostyanskaya, *J. Gen. Chem. USSR*, **15**, 353 (1945).
8. M. Imoto and J. Takenaka, *Chem. High Polymers Japan (Kobunshi Kagaku)*, **13**, 268 (1956).
9. S. Okamura, T. Higashimura, and K. Fujii, *Chem. High Polymers Japan (Kobunshi Kagaku)*, **15**, 425 (1958).
10. T. Fueno, I. Matsumura, T. Okuyama, and J. Furukawa, *Bull. Chem. Soc. Japan*, **41**, 818 (1968).
11. F. R. Mayo and F. M. Lewis, *J. Amer. Chem. Soc.*, **66**, 1594 (1944).
12. H. Margenau and G. M. Murphy, *The Mathematics of Physics and Chemistry*, D. van Nostrand Co., New York, N. Y. (1943), pp. 500–502.
13. C. G. Overberger, L. H. Arond, D. Tanner, J. J. Taylor, and T. Alfrey, Jr., *J. Amer. Chem. Soc.*, **74**, 4848 (1952).
14. J. P. Kennedy, in *Copolymerization*, G. E. Ham, Ed., Interscience, New York, N. Y. (1964), p. 308.
15. H. C. Brown and Y. Okamoto, *J. Amer. Chem. Soc.*, **80**, 4979 (1958).
16. O. Kajimoto and T. Fueno, paper presented at the Symposium on the Hammett Relationship, Kyoto, October 1967, preprint p. 51.
17. R. W. Taft, Jr., *J. Phys. Chem.*, **64**, 1805 (1960).
18. T. Fueno, T. Okuyama, and J. Furukawa, *Bull. Chem. Soc. Japan*, **39**, 569 (1966).
19. W. M. Schubert, B. Lamm, and J. R. Keeffe, *J. Am. Chem. Soc.*, **86**, 4727 (1964).
20. O. Kajimoto and T. Fueno, unpublished work.
21. T. Fueno, T. Okuyama, T. Deguchi, and J. Furukawa, *J. Amer. Chem. Soc.*, **87**, 170 (1965).
22. H. Sakurai, private communication.

Received November 15, 1968

JOURNAL OF POLYMER SCIENCE: PART A-1 VOL. 7, 1455–1465 (1969)

# Studies of Japanese Lacquer: Urushiol Dimerization by the Coupling Reaction between Urushiol Quinone and a Triolefinic Component of Urushiol

TAKASHI KATO and JU KUMANOTANI, *The Engineering Research Institute, Faculty of Engineering, The University of Tokyo, Tokyo, Japan*

## Synopsis

Previously, the formation of urushiol quinone from urushiol was demonstrated in the laccase-catalyzed oxidation process of the sap of the Japanese lacquer tree (*Rhus vernicifera D.C.*) or of lacquer formed from it. This paper presents the results of the investigation on the participation of urushiol quinone in the oxidative polymerization and crosslinking of the sap or the lacquer. The polymeric urushiol was obtained by the fractionation of the mildly oxidized sap (Japanese lacquer), and a specific dimeric urushiol was isolated from it by thin-layer chromatography (TLC). Structural analysis of the dimer illustrated that it has a conjugated triene structure and may be formed by a coupling reaction between urushiol quinone and a triolefinic component of urushiol. Further support for this was given by the spectroscopic study of the reaction between 4-*tert*-butyl-*o*-quinone and the triolefinic component of dimethylurushiol, and by the isolation and identification of the coupling product between them.

## INTRODUCTION

Previously it was demonstrated by the present authors[1] that the initial oxidative reaction course of the sap of the Japanese lacquer tree or of Japanese lacquer formed from the sap involves a specific laccase-catalyzed oxidation of urushiol into the corresponding *o*-quinone and the subsequent reaction of the quinone thus formed with the remaining urushiol, another quinone, or other components of the sap or the lacquer.

To illustrate the behavior of the urushiol quinone thus formed, the present authors have now attempted to examine the polymeric urushiol obtained by the fractionation of the enzymatically oxidized sap (Japanese lacquer) by means of thin-layer chromatography (TLC) and by infrared and ultraviolet spectroscopy. It was found that a specific dimer of urushiol with a conjugated triene structure was present in the polymeric urushiol as one of the major products. Therefore, the present paper has focussed attention on the following items: (a) the separation of a specific dimeric urushiol from a mildly oxidized sap, (b) the characterization of the dimeric urushiol, and (c) the elucidation of the pathway of the formation of the dimeric urushiol by model reactions.

The results obtained offer information as to the specific contribution of urushiol to the laccase-catalyzed drying process of Japanese lacquer.

## Separation of a Specific Dimeric Urushiol From Mildly Oxidized Sap

A mildly oxidized sap was prepared from the sap of the lacquer tree (*Rhus vernicifera D.C.*, Japan) under conditions similar to commercial practice for making Japanese lacquer. The polymerized urushiol was obtained by the fractionation of the treated sap. The components of the polymerized urushiol were determined by means of TLC. Ultraviolet and infrared spectroscopy and molecular weight measurements were carried out on each spot of the chromatogram. A specific dimeric urushiol with a conjugated triene structure was found. This was then collected, purified by TLC, and identified.

### Preparation and Fractionation of a Mildly Oxidized Sap

The sap (63.6 g) was stirred in air at 30–40°C for 7 hr in a wooden vessel (diameter, 20 cm; height, 5 cm) with the use of a stirrer especially designed to keep the sap in good contact with air. (This process involves the laccase-catalyzed oxidation of urushiol and the evaporation of water from the sap.[1]) The sap thus treated (50.9 g) was shaken with ethanol (300 ml). The resultant ethanolic solution was separated from insoluble substances by centrifugation (4000 rpm) for 15 min. A dark brown, oily material, obtained after the removal of the ethanol at 30–40°C with a rotary vacuum evaporator, was dissolved in petroleum ether (bp 40–60°C, 100 ml). The resulting solution was washed with water (100 ml) and dried over calcium chloride. After the calcium chloride was filtered off, the solution was further diluted with petroleum ether (2 l.) and then allowed to stand overnight. The waxy polymeric material that precipitated was collected by decanting the supernatant and weighed; the yield was 9.6 g (15.1% based upon the sap).

### Separation of a Specific Dimeric Urushiol

The polymeric urushiol was dissolved in chloroform and applied as a spot on the silica-gel layer (thickness, 0.25 mm), which was made from Silica Rider (silica gel with 12–14% calcium sulfate, purchased from the Daiichi Pure Chemicals Co.), and was activated at 105°C for 1.5 hr before use. It was then chromatographed in a chloroform–ethyl acetate (87:13v/v) solvent tank by the ascending technique. The developing distance was 12–14 cm. A filter paper (20 × 20 cm) impregnated with the developing solvent was inserted into the tank in order to saturate the atmosphere with the solvent vapor. After the plate was taken out of the tank, it was dried in air for 15 min.

The chromatogram gave, when sprayed with a methanol–1% $FeCl_3$ solution, spots with $R_f$ values of 0.50(urushiol, dark violet), 0.37(dark brownish green), 0.27(dark violet), and 0.20(dark violet), and others with

smaller $R_f$ values, including a spot at the starting point; no other spots appeared when the chromatogram was further sprayed with an aqueous sulfuric acid solution (1:1) and heated at 150°C for 30 min. Besides urushiol ($R_f$ 0.50), the three components with $R_f$ values of 0.37, 0.27, and 0.20 (1:1:0.5 by weight), were found to be the major polymeric materials. The component with $R_f$ 0.37 had an infrared spectral band at 997 $cm^{-1}$ characteristic of a conjugated triene. It was collected by TLC, except that a silica gel plate (1.5 mm thick) was used and the sample was applied in line. The position of the separated zone was detected by spraying a methanol–1% $FeCl_3$ solution on the strip (0.5 cm wide), along one edge of the plate, and then the separated zone was immediately scraped off from the plate and extracted with ether (20 ml). The dark yellow product obtained by removing the ether from the solution at reduced nitrogen pressure was still contaminated with small amounts of urushiol and the component with $R_f$ 0.27, and it was chromatographed twice more. A yield of 0.29 of the purified material (hereafter designated as B), which gave only one spot (with $R_f$ 0.37) in its TLC, was obtained from 4 g of the fractionated polymeric urushiol. Analysis showed C, 78.97%; H, 9.48%; molecular weight 684 (measured in MEK by a vapor-pressure osmometer, Model 301-A, Mechrolab, Inc.). Infrared absorptions of the liquid film appeared at 3600–3200(vs, broad), 3010(m), 2925(vs), 2855(s), ca 1650(w), 1623(m), 1596(m), 1497(s), 1478(s), 1280(vs), 1182(s), 997(vs), 984(shoulder), 947(m), 826(w), 803(w), 776(m), and 734(s) $cm^{-1}$. Ultraviolet absorptions (ethanol) were found at 225(absorptivity, 57.0), 263(38.6, shoulder), 272.5(47.4) and 284 m$\mu$(39.5). The hydroxyl content (ratio to the unit value of urushiol) was estimated to be 0.83 ± 0.06 by the near infrared spectroscopy (hydroxyl overtones at 1.41 $\mu$ and 1.43 $\mu$ in carbon tetrachloride) on the assumption that the extinction coefficients of urushiol and B were equal.

The results of both the elementary analysis and the molecular weight measurement indicate that B is a dimer of urushiol.

## CHARACTERIZATION OF DIMERIC URUSHIOL

The conjugated triene B was characterized by comparing its ultraviolet and infrared spectral data with those of related compounds. The suggested mechanism of the formation of B is based on its structure and on the already known reactivities of *o*-quinoid compounds toward the compounds with active hydrogens.

### Ultraviolet and Infrared Spectral Data of Compounds Related to B

The ultraviolet and infrared spectra of the compounds related to B were determined with a Hitachi spectrophotometer, EPS-2, and a Nihon Bunko IR-spectrophotometer, Model IR-S, respectively. The preparation of standard materials were made as follows.

**Hydrogenated B.** This was obtained from the hydrogenation of the polymeric urushiol, followed by the TLC in the manner similar to that described in the collection of B.

ANAL. Calcd for $C_{42}H_{76}O_4$: C, 78.94%; H, 11.04%. Found: C, 78.44%; H, 10.92%.

Infrared absorptions in the range 1000–900 $cm^{-1}$ (liquid film) were at ca. 960 $cm^{-1}$ (w, broad); Ultraviolet absorptions were at 266 (absorptivity, 9.1) and 278 m$\mu$ (9.0). The hydroxyl content was 0.80 ± 0.06.

The hydrogenation of polymeric urushiol was performed as follows. The polymeric urushiol (5 g) was dissolved in ethanol (10 ml) and hydrogenated at room temperature under 1 atm of hydrogen over 5% Pd on charcoal (1 g). Absorption of hydrogen ceased after 2 days, and the catalyst was filtered off. The ethanol was then distilled off from the filtrate at a reduced pressure, and a dark brown substance was obtained as residue.

**Urushiol.** Urushiol (bp 175–180°C/0.01 mm, $n_D^{25}$ 1.5342) was obtained from the sap according to the method described in the literature,[2] and it was further purified by molecular distillation. Infrared absorptions (liquid film) were at 3600–3200(vs, broad), 3010(m), 2925(vs), 2855(s), ca 1650(w), 1623(m), 1596(m), 1478(s), 1280(vs), 1182(s), 984(s), 947(s), 826(w), 776(m), and 734(s) $cm^{-1}$. Ultraviolet absorptions were at 225 (absorptivity, 40.5) and 277 m$\mu$ (6.6).

**Hydrourushiol.** Hydrourushiol (3-pentadecylcatechol, mp 58–59°C) was prepared by the hydrogenation of urushiol at 132 $kg/cm^2$ of hydrogen over 5% Pd on charcoal and recrystallized from toluene. Infrared absorption (1000–900 $cm^{-1}$, carbon tetrachloride) was at 968 $cm^{-1}$(m); ultraviolet absorption was at 277 m$\mu$(absorptivity, 5.4).

**Dimethylurushiol.** Dimethylurushiol (dimethyl ether of urushiol, bp 175–183°C/0.2–0.3 mm, $n_D^{25}$ 1.5163) was prepared according to the method of Majima.[2] Ultraviolet absorptions: 225(absorptivity, 60.0), 273(4.6), and 278 m$\mu$(4.5).

**Alkali-Isomerized Dimethylurushiol.** This was prepared according to a method similar to that employed for the conjugation of polyunsaturated fatty acids.[3] In an atmosphere of oxygen-free nitrogen, dimethylurushiol (275 mg) was added to 6.6% of a KOH–ethylene glycol solution (162 g), and the mixture was kept at 180°C under stirring for 30 min, cooled to room temperature, and diluted with the water saturated with sodium chloride. The mixture was then extracted three times with *n*-hexane (100 ml, and twice with 50 ml); the combined *n*-hexane extracts were washed three times with 50-ml portions of a saturated sodium chloride solution and dried over sodium sulfate. The removal of the *n*-hexane from the solution at 40°C *in vacuo* gave a colorless oil (238 mg). Ultraviolet absorptions were at 223(absorptivity, 32.0), 260(60.3, shoulder), 270(80.7), and 280 m$\mu$(64.5). The identity of this alkali-isomerized dimethylurushiol was confirmed by its derivation to 3-pentadecylveratrole; the alkali-isomerized dimethylurushiol (99 mg) was hydrogenated over 5% Pd on charcoal (51 mg) in *n*-hexane (10 ml) at room temperature at 120 $kg/cm^2$

of hydrogen for 5 hr, and the *n*-hexane filtrate was evaporated to dryness, giving 3-pentadecylveratrole (89 mg; mp 35–36°C, undepressed by admixture with an authentic sample prepared by the catalytic hydrogenation of dimethylurushiol in the same manner).

## Character of Conjugated Triene B

The ultraviolet spectrum of B is quite similar to that of a compound with a conjugated triene structure such as alkali-isomerized dimethylurushiol or eleostearic acid,[4] and this suggests that B contains a conjugated triene structure. This finding is consistent with the infrared spectral absorption band characteristic of the conjugated triene[5] at 997 $cm^{-1}$.

The molecular extinction coefficient ($\epsilon$) due to the conjugated triene of B was estimated at $2.62 \times 10^4$ (272.5 m$\mu$) from the observed molecular weight of 684 and the difference between the absorptivities (38.4) observed before and after the hydrogenation of the olefinic parts of B. This value agrees approximately with those of the compounds with conjugated triene structure such as octadeca-*cis*-9,*cis*-11,*trans*-13-trienoic acid[6] (271 m$\mu$, $3.23 \times 10^4$), octadeca-*cis*-9,*trans*-11,*trans*-13-trienoic acid[6] ($\alpha$-eleostearic acid; 271 m$\mu$, $4.70 \times 10^4$), and octadeca-*trans*-9,trans-11,trans-13-trienoic acid[6] ($\beta$-eleostearic acid; 268 m$\mu$, $6.10 \times 10^4$). From these results it can be concluded that B has one conjugated triene per molecule. Moreover, the relatively low value of $\epsilon$ (272.5 m$\mu$) of B may be interpreted in terms of the greater contents of *cis* structure in B or in terms of the presence of the substituted phenoxyl group in the vicinity of the conjugated triene (see Scheme I).

**Bonding Site.** Another possible pathway of the autoxidative dimerization to B is the reaction between the triolefinic side chains of urushiol. But this possibility can be rejected on the basis of the finding that the catalytic hydrogenation of the conjugated triene of B over 5% Pd on charcoal yielded a product absorbing at 266 and 278 m$\mu$, while each of urushiol and hydrourushiol showed only one absorption at 277 m$\mu$, in ethanol.

Concerning the reaction of *o*-quinoid compounds with the unsaturated hydrocarbons which contain active methylenes or methines, it is well known that *o*-quinone abstracts a hydrogen from the latter.[7,8] It has been found (1) that urushiol quinone is formed at an early stage of the laccase-catalyzed oxidative polymerization of the sap,[1] (2) that 50% or so of the urushiol in the sap is the triolefinic components,[9] and (3) that the hydroxyl content of B decreases in comparison with that of urushiol. On the basis of these findings, it seems reasonable to consider that B is formed by a coupling reaction between the urushiol quinone and the triolefinic component of urushiol, as is shown in Scheme I (I).

The formation of B may involve a dehydrogenation from the active methylene in the triolefinic component (Ia) by the urushiol quinone (Ib), and a simultaneous conjugation and coupling between the possible intermediates derived from the quinone and the triolefinic component of

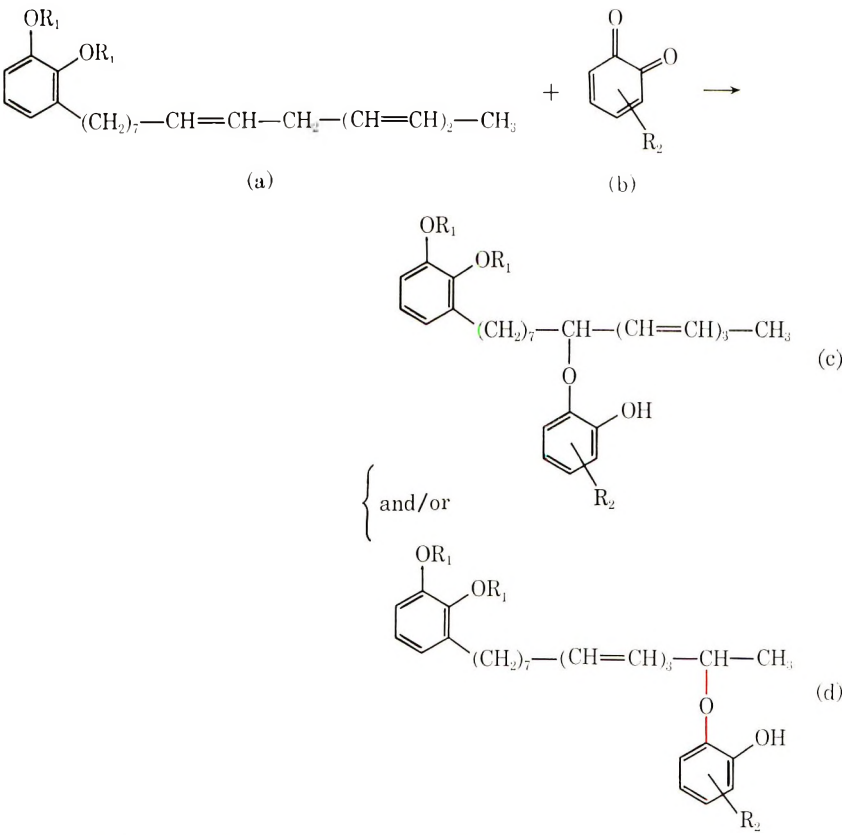


(I): $R_1$=H, $R_2$=arbitrary side chain of urushiol attached to 3 or 6 position.
(II): $R_1$=$CH_3$, $R_1$=*tert*-butyl attached to 4 or 5 position.

Scheme I

urushiol. An attempt to confirm the phenoxy methine proton (H—C—O—$C_6H_5$) in B by NMR spectroscopy failed, presumably due either to the low ratio of this proton to all the protons involved in B or to the overlapping of the signal of this proton with that of the hydroxyl protons to form a broad signal centered at $\tau$ 4.7.

## COUPLING REACTION OF 4-*tert*-BUTYL-*O*-QUINONE AND A TRIOLEFINIC COMPONENT OF DIMETHYLURUSHIOL

In order to elucidate the pathway of the formation of B by the coupling reaction of urushiol quinone and the triolefinic component of urushiol, a model study was attempted by use of an *o*-quinone derivative and the triolefinic component of urushiol.

*o*-Quinones substituted at the 3- or 4-position with a primary or secondary alkyl or an alkenyl group, are usually quite unstable.[1,10] These quinones,

including urushiol quinone, may cause complexity. Therefore, as a relatively stable quinone component, *tert*-butyl-*o*-quinone was used.

Dimethylurushiol was used as convenient triolefinic component for the reaction, since it contains about 50% of a triolefinic component (Ia).[9] In comparison with urushiol, we may avoid complicated reactions between the catechol nucleus of urushiol and the *o*-quinone.

The reaction of the *o*-quinone with the triolefinic component was followed in chloroform and ethanol by infrared and ultraviolet spectroscopy, respectively. Then the coupling product was separated and identified.

4-*tert*-Butyl-*o*-quinone was prepared according to the Goldschmidt and Graef method[11] from 4-*tert*-butylcatechol (bp 129–131°C/3 mm).

## Spectroscopic Study

**Infrared Spectroscopy.** The reaction was started at 27–28°C by quick dissolution of the quinone (ca 50 mg) in chloroform (1 ml) containing dimethylurushiol (ca. 90 mg); the reaction was followed in a rock salt cell by infrared spectroscopy. As the reaction between 4-*tert*-butyl-*o*-quinone and dimethyl-urushiol proceeded, the absorption bands of the quinoid carbonyl group at 1696 and 1670 $cm^{-1}$ and the olefinic absorption bands of dimethylurushiol at 983 and 948 $cm^{-1}$ decreased, and the absorption bands due to hydroxyl groups (ca. 3600 $cm^{-1}$), benzene ring (1508 $cm^{-1}$) and conjugated triene (998 and 964 $cm^{-1}$) appeared and gradually increased. These results obviously indicate that a conjugated triene system is formed in the reaction of the *o*-quinone with the triolefinic component. Further, these results suggest the formation of a 2-hydroxyphenyl ether-type structure such as that indicated in B.

**Ultraviolet and Visible Spectroscopy.** A 2-ml portion of an ethanolic dimethylurushiol solution (ca 90 g/l.) was mixed with 2 ml of an ethanolic quinone solution (ca 20 g/l.) in a 20-ml glass stoppered flask; the flask was then maintained at 30 ± 0.1°C in a water bath. From time to time, 0.1-ml portions of the reacting solution were pipetted out and diluted suitably with ethanol. The ultraviolet and visible spectra of the solutions thus prepared were taken in a quartz cell with an optical path length of 1 cm. The amount of 4-*tert*-butyl-*o*-quinone in the reacting mixture was determined by measuring the intensity of the absorption band at 386 mμ ($\epsilon$ = 1430, in ethanol).

As may be seen in Figure 1, the progress of the reaction between the *o*-quinone (IIb) and the triolefinic component (IIa) of dimethylurushiol brought about the appearance and the subsequent increase of the absorption band at 272.5 mμ, with inflections at 263 and 284 mμ, which is characteristic of a conjugated triene. With this spectral change, the band at 386 mμ characteristic of the *o*-quinone, as well as that at 225 mμ characteristic of the conjugated diene of dimethylurushiol, decreased markedly. These results are in agreement with those obtained from the infrared spectral measurements described above; that is, the conjugated triene system was apparently formed in this reaction. Moreover, from the decreased

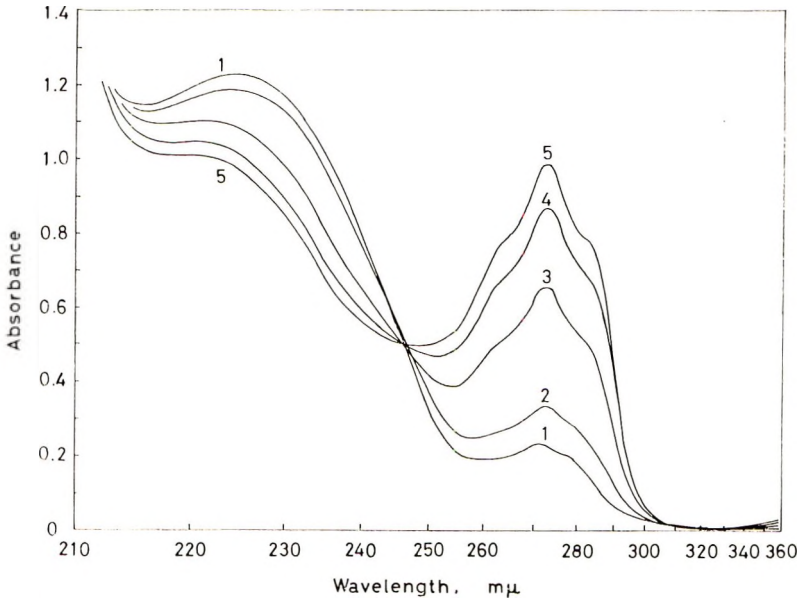


**Fig. 1.** Ultraviolet spectral change in the reaction between 4-*tert*-butyl-*o*-quinone and dimethylurushiol: (1) just after mixing; (2) 0.28 hr; (3) 2.4 hr; (4) 4.2 hr; (5) 8.4 hr. The concentrations of reaction mixture were 19.8 g/l. for 4 *tert*-butyl-*o*-quinone and 89.8 g/l. for dimethyurushiol, and the spectrum was taken after 0.1 ml of each reacting solution was diluted with ethanol to $2.27 \times 10^{-2}$ g/l.

amounts of 4-*tert*-butyl-*o*-quinone (56% in 2.4 hr) and the increase in the absorbance at 272.5 mμ (0.42 in 2.4 hr), the molecular extinction coefficient of a conjugated triene formed was tentatively estimated to be $3.0 \times 10^4$, assuming that one molecule of 4-*tert*-butyl-*o*-quinone causes one triene conjugation. This value was in good agreement with that obtained with the conjugated triene of the coupling reaction product ($3.97 \times 10^4$ at 272.5 mμ), which was separated and identified as will be described below. This finding indicates that this reaction occurred quantitatively.

## Separation and Identification of the Reaction Product

The 4-*tert*-butyl-*o*-quinone (1.02 g) was allowed to react with dimethylurushiol (4.09 g) in ethanol (20 ml) at room temperature for 17.5 hr. After the reaction, the composition of the reaction mixture was examined by TLC (thickness of the gel layer, 0.25 mm; solvent system, *n*-hexane–ether, 85:15v/v). Guaiacol was used as the standard material for the determination of the $R_f$ value, and each spot was located by $R[R_f$ (spot)/$R_f$(guaiacol)]. When the chromatographed (12–14 cm) plate was dried and sprayed with a methanol-1% $FeCl_3$ solution, spots appeared at $R$ = 0.99 (green, trace), 0.84 (green, main), 0.24 (dark brown, small amounts), and the starting point (trace). When the plate thus treated was further sprayed with aqueous sulfuric acid (1:1) and then heated at

160°C for 30 min, a new spot appeared at $R$ = 1.61 (unreacted dimethylurushiol). The compound with R = 0.84 ($R_f$ 0.48) was collected by TLC in the manner similar to that described in the case of B; the chromatography was done twice on a silica gel plate (thickness, 1 mm) in order to obtain a pure product (0.82 g; 26% based on the quinone).

ANAL. Calcd for $C_{33}H_{46}O_4$: C, 78.22%; H, 9.15%; molecular weight, 506.7. Found: C, 78.49%; H, 9.48%; molecular weight, 527.

The hydrogen absorption was 3.1 mole/mole, measured volumetrically at 30.0°C. Infrared absorptions (liquid film) were found at 3600–3400 (s, broad), 2925(vs), 2855(s), 1590(m), 1510(s), 1479(vs), 1430(m), 1369(m), 1274(vs), 1221(vs), 1174(w), 1125(w), 1087(vs), 1005(s), 997(vs), 967(m), 872(w), 814(w) and 746(m) $cm^{-1}$. Ultraviolet absorptions were at 263 ($\epsilon$, 3.2 × $10^4$, shoulder), 272.5(4.25 × $10^4$), and 284 m$\mu$(3.25 × $10^4$). NMR signals(carbon tetrachloride) were at $\tau$ 3–3.6(6H), $\tau$ 3.4–4.7(broad), $\tau$ 4.62 and 4.52(sharp), $\tau$ 5.27(1H, broad), $\tau$ 6.21 and 6.23(6H), $\tau$ 7.43(2H, triplet, $J$ = 8 cps), $\tau$ 7.6–8.1(broad), $\tau$ 8.1–8.9, $\tau$ 8.57(doublet, J = 6.6 cps).

The hydrogenated sample was obtained by hydrogenation of the coupling product in *n*-hexane at room temperature for 5.4 hr at 64 $kg/cm^2$ of hydrogen over 5% Pd on charcoal.

ANAL. Calcd for $C_{33}H_{52}O_4$: C, 77.30%; H, 10.22%; molecular weight, 512.8. Found: C, 77.37%; H, 10.77%; molecular weight, 557.

Infrared absorption (1000–900 $cm^{-1}$, liquid film): was at 964 $cm^{-1}$(w). Ultraviolet absorption was at 279 m$\mu$($\epsilon$, 3.6 × $10^3$). NMR signals were at $\tau$ 3–3.6(6H), $\tau$ 4.66 and 4.58(1H), $\tau$ 5.74(1H, broad), $\tau$ 6.21 and 6.23(6H), $\tau$ 7.43(2H, triplet, J = 8 cps), $\tau$ 8.1–9.0(36H).

From the results of both the elemental analyses and the molecular-weight measurements, it is obvious that the reaction product is a coupling product of 4-*tert*-butyl-*o*-quinone (IIb) and the triolefinic component (IIa) of dimethylurushiol. The ultraviolet absorptions at 272.5 m$\mu$ ($\epsilon$, 4.25 × $10^4$) and 284 m$\mu$($\epsilon$, 3.25 × $10^4$) with a shoulder at 263 m$\mu$ indicate the presence of the conjugated triene structure in this compound. This result is in agreement with that of the infrared spectral measurements. The infrared spectrum of the compound had a strong absorption band at 997 $cm^{-1}$ characteristic of a conjugated triene. The compound absorbed hydrogen equivalent to three double bonds upon catalytic hydrogenation over 5% Pd on charcoal in ethyl acetate. The infrared spectrum also showed an absorption of the hydroxyl group, indicating that this compound contains a phenolic hydroxyl group. From these data, the structure of the reaction product can evidently be represented by IIc or IId.

In the NMR spectrum of the coupling product, the signal at $\tau$ 5.27 due to a phenoxy methine proton[12] undoubtedly supports the idea that the two reactants are combined by a phenyl ether bond. On catalytic hydrogenation, this signal shifted to an appreciably higher field at $\tau$ 5.74.

This indicates that the phenyl ether bond is adjacent to the conjugated triene. The signals at $\tau$ 4.62 and $\tau$ 4.52 were assigned to a phenolic proton: the signals of phenolic and olefinic protons overlap in the NMR spectrum of the reaction product. Therefore, the phenolic hydrogen of the hydrogenated compound was replaced with deuterium. The signals of phenolic protons disappeared as expected. As for the conjugated triene, the signals due to the olefinic protons shifted to a field lower than those of the triolefinic component. Moreover, the signal at $\tau$ 7.19 ($J$ = 6 cps) due to the $=C—CH_2—C=$ structure which is present in the triolefinic component is absent in the reaction product. On the basis of the methoxy protons ($\tau$ 6.23, $\tau$ 6.21), the contents of hydroxyl protons and phenoxy methine protons

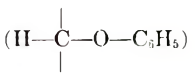

were estimated from the integrated NMR spectrum; it was proved that the compound contains one hydroxyl group and one phenyl ether bond.

From these results it is evident that the compound contains: (1) a conjugated triene, (2) a phenoxyl group, and (3) a phenyl ether bond; its structure can thus be represented by IIc or IId. The identity of this product with IId was established as follows. The terminal methyl of IId has the

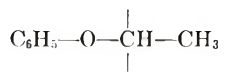

structure, the chemical shift of which is expected[12] to be about $\tau$ 8.7. This $\tau$-value is in good agreement with that of $\tau$ 8.57 (doublet, $J$ = 6.6 cps) observed with the compound, considering the effect of the neighboring conjugated triene. On the other hand, the terminal methyl of IIc has the $—(C=C)_3—CH_3$ structure, for which a doublet at $\tau$ 8.3 may be expected from the value of $\tau$ 8.3 for the $—C=C—CH_3$ structure[13] and that of $\tau$ 8.30 for the $—(C=C)_2—CH_3$ structure. Thus, the compound was proved not to have the IIc structure. The NMR spectrum of a reaction mixture of an excess of 4-*tert*-butyl-*o*-quinone and a triolefinic component (IIa; bp 180–186°C/0.4–0.5 mm; $n_D^{25}$ 1.5243; obtained by a method described in the literature[14]) did not show a detectable signal at $\tau$ 8.3, indicating that this reaction gives mainly the compound represented by IId. The two signals from phenolic protons observed at $\tau$ 4.62 and $\tau$ 4.52 may be attributed to two isomeric structures of IId, namely, 4- and 5-*tert*-butyl-substituted isomers.

## CONCLUSION

From the enzymatically oxidized sap, a specific dimeric urushiol (B) was separated. The information on the structure of B indicated that urushiol quinone and a triolefinic component of urushiol react to give the

coupling product, B. The structure of this product was elucidated by the finding that 4-*tert*-butyl-*o*-quinone and a triolefinic component of dimethylurushiol actually react to yield a coupling product of the same type under such mild conditions as are adopted for the natural lacquer system. Thus, regarding the formation of B, its nonenzymic character has become clear.

The authors wish to express their gratitude to the Saito Co., Ltd., Tokyo, for supplying the sap used in this investigation.

## References

1. J. Kumanotani, T. Kato, and A. Hikosaka, paper presented at International Symposium on Macromolecular Chemistry, Tokyo and Kyoto, 1966; *J. Polym. Sci. C*, in press.

2. R. Majima, *Ber. Dtsch. Chem. Ges.*, **42**, 1418 (1909).

3. P. L. Nichols, S. F. Herb, and R. W. Riemenschneider, *J. Amer. Chem. Soc.*, **73**, 247 (1951).

4. J. S. Hoffmann, R. T. O'Connor, D. C. Heinzelman, and W. G. Bickford, *J. Amer. Oil Chem. Soc.*, **34**, 338 (1957).

5. N. H. E. Ahlers, R. A. Brett, and N. G. McTaggart, *J. Appl. Chem.*, **3**, 432 (1953).

6. L. Crombie and A. G. Jacklin, *J. Chem. Soc.*, **1957**, 1632.

7. E. A. Braude, A. G. Brook, and R. P. Linstead, *J. Chem. Soc.*, **1954**, 3569.

8. L. M. Jackman and D. T. Thompson, *J. Chem. Soc.*, **1961**, 4794.

9. S. V. Sunthankar and C. R. Dawson, *J. Amer. Chem. Soc.*, **76**, 5070 (1954).

10. H. J. Teuber and G. Staiger, *Chem. Ber.*, **88**, 802 (1955).

11. S. Goldschmidt and F. Graef, *Ber. Dtsch. Chem. Ges.*, **61**, 1858 (1928).

12. R. M. Silverstein and G. C. Bassler, *Spectrometric Identification of Organic Compounds*, New York, 1967, p. 136.

13. M. Hidai, Y. Uchida, and A. Misono, *Bull. Chem. Soc. Japan*, **38**, 1243 (1965).

14. M. Sato and S. Shoji, *Nippon Kagaku Zasshi*, **89**, 814 (1968).

Received April 24, 1968
Revised November 25, 1968

JOURNAL OF POLYMER SCIENCE: PART A-1 VOL. 7, 1467–1478 (1969)

# Fluorocyclopropanes. IV. Copolymers of Perfluorocyclopropene

P. B. SARGEANT* and C. G. KRESPAN, *Central Research Department Experimental Station, E. I. du Pont de Nemours and Company, Wilmington, Delaware 19898*

## Synopsis

Perfluorocyclopropene undergoes free-radical copolymerization with ethylene, isobutylene, *cis*- and *trans*-2-butene, vinyl acetate, methyl vinyl ether, vinyl chloride, styrene, acrylonitrile, tetrafluoroethylene, vinyl fluoride, and vinylidene fluoride. The copolymerization proceeds most readily with electron-rich olefins such as methyl vinyl ether (to yield a 1:1 copolymer), but conditions were found to give copolymers with electron-deficient olefins such as tetrafluoroethylene and vinylidene fluoride. Copolymers with methyl vinyl ether, tetrafluoroethylene, vinyl fluoride, and vinylidene fluoride were examined in detail. Evidence is presented that the perfluorocyclopropyl ring is incorporated intact into the copolymer and can be subsequently isomerized to a perfluoropropenyl unit by heating at 200–300°C.

## INTRODUCTION

Cyclopropene readily polymerizes at −36°C, presumably via a free-radical mechanism.[1,2] The NMR spectrum indicates the polymer to be a polycyclopropane.[1] Recently copolymers of tetrachlorocyclopropene have been reported.[3] We have previously reported[4,5] the synthesis, properties, and reactions of perfluorocyclopropene, and this paper describes copolymerizations of perfluorocyclopropene.

## EXPERIMENTAL

### Materials

The preparation of perfluorocyclopropene has been previously described.[4] Commercial reagent-grade comonomers were distilled from inhibitor and used without further purification. Perfluoropropionyl peroxide was obtained from D. P. Carlson of the E. I. du Pont de Nemours and Company.

### Polymerizations

Two general polymerization techniques were used. In the first, equimolar quantities of perfluorocyclopropene and comonomer (~3 mmole

* Present address: Dacron Research Laboratory, Textile Fibers Department, E. I. du Pont de Nemours and Company, Kinston, N.C. 28501.

each) were charged to a glass tube (18 mm × 4 mm i.d.) containing benzoyl peroxide (5 mg, 2 × $10^{-5}$ mole). The tube was degassed, sealed, and heated at 80–85°C for 8 hr. The tube was opened on the vacuum system and the volatile products were isolated; the solid polymer was filtered off and characterized. Copolymers of perfluorocyclopropene with ethylene, isobutylene, vinyl chloride, styrene, acrylonitrile, methyl vinyl ether, vinyl acetate, *cis*-2-butene, and *trans*-2-butene were prepared in this manner. The second procedure was used to prepare copolymers with tetrafluoroethylene, vinyl fluoride, and vinylidene fluoride. Perfluorocyclopropene and comonomer were transferred to a platinum tube (7 in. × $^1/_4$ in. or $^3/_8$ in.) containing initiator. The tube was degassed, sealed, and heated at the prescribed temperature at 3000 atm for 8 hr. The initiators and temperatures were: azobisisobutyronitrile (AIBN), 75°C; benzoyl peroxide, 85°C; dinitrogen difluoride, 70°C; perfluoropropionyl peroxide, 45°C; aqueous ammonium persulfate, 90°C. The tube was opened, volatile products were collected, and the solid polymer was isolated and characterized.

### Polymer Characterization

Infrared spectra were obtained on a Perkin-Elmer Infracord calibrated with polystyrene. DTA was performed on a Du Pont 900 differential thermal analyzer. Thermogravimetric analysis was obtained from an Ainsworth thermobalance equipped with a Type AV-2 recorder unit. Inherent viscosities were measured in 0.1% benzene solution with a Fenske viscometer. Fluorine elemental analysis was used to calculate mole percent perfluorocyclopropene in the copolymers derived from nonfluorinated monomers.

## RESULTS AND DISCUSSION

Copolymers of perfluorocyclopropene were obtained with a variety of comonomers by using free-radical catalysts. The copolymers were characterized by their infrared spectra, differential thermal analysis, and in most cases by fluorine elemental analysis. All copolymers had infrared absorptions absent in the respective homopolymers. Absorptions evidently characteristic of the perfluorocyclopropene copolymer appear at 1700–1770 and 1100–1200 $cm^{-1}$ (C-F stretch). The 1700 $cm^{-1}$ absorption is attributed to fluorinated carbon–carbon double-bond stretch. An alternative possibility is carbon–carbon double-bond stretch from an exo methylenecyclopropane unit, such as I, resulting from hydrogen fluoride elimina-

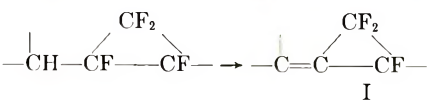

I

tion from an initially formed copolymer. This possibility is unlikely, since no HF was produced in the polymerization. The 1700 $cm^{-1}$ band, sub-

stantially decreased upon reprecipitation, is probably due to low molecular weight polymer. Differential thermal analysis charts of the copolymers were different from those of the homopolymers. Glass transition temperatures were frequently lower in copolymer than in homopolymer, melting endotherms shifted, and in copolymers containing a perfluorocyclopropene: comonomer mole ratio of at least 1:3 a substantial exotherm was observed at approximately 300°C. The mole ratios of perfluorocyclopropene in copolymers with hydrocarbon comonomers were determined by fluorine analysis. Examination of the volatile material after each polymerization showed mostly unchanged starting olefin and perfluorocyclopropene with only traces of other fluorine-containing materials.

## Reaction Scope

Table I shows the results of benzoyl peroxide-catalyzed copolymerizations of perfluorocyclopropene with several comonomers. In general, the electron-rich olefins such as methyl vinyl ether and the hydrocarbons incorporated more perfluorocyclopropene than electron-deficient olefins like vinyl chloride and acrylonitrile. Fluorinated olefins did not readily copolymerize under these conditions; however, copolymers could be obtained with other initiators, as described below.

TABLE I
Perfluorocyclopropene (PFCP) Copolymers[a]

| Comonomer | Amt monomer, mmole[b] | Polymer, g | F, % | Mole monomer/mole PFCP | Appearance |
|---|---|---|---|---|---|
| Ethylene[c] | 3.6 | 0.15 | 38.3 | 3.1 | Dark solid |
| Isobutylene[c] | 2.7 | 0.17 | 27.7 | 2.9 | Sticky, tough solid |
| *trans*-2-Butene | 3.4 | Trace | 25.9 | 3.2 | White solid |
| *cis*-2-Butene[c] | 3.4 | Trace | 33.8 | 2.0 | White solid |
| Vinyl acetate | 2.1 | 0.19 | 38.3 | 3.1 | Clear solid |
| Methyl vinyl ether[c] | 2.1 | 0.20 | 39.9 | 1.3 | White solid |
| Vinyl chloride | 1.4 | 0.05 | 6.2 | 18 | Tan solid |
| Tetrafluoroethylene | 2.9 | 0.02 | — | — | Dark solid |
| Vinyl fluoride | 2.1 | 0.02 | — | — | Dark solid |
| Vinylidene fluoride | 1.4 | Trace | — | — | Dark oil |
| Styrene | 1.3 | 0.13 | 2.9 | 24 | Tan solid |
| Acrylonitrile[c] | 2.1 | 0.11 | 1.2 | 117 | White solid |

[a] Initiator, $Bz_2O_2$ ($2 \times 10^{-5}$ mole), 80–85°C, 8 hr.
[b] Used equimolar quantities PFCP and comonomer.
[c] Additional runs yielded similar results.

The copolymer infrared spectra and DTA charts are described in the experimental section. The methyl vinyl ether copolymer was chosen for further study, and copolymers with fluorinated monomers were obtained under conditions to be discussed.

### Perfluorocyclopropene–Methyl Vinyl Ether Copolymers

Perfluorocyclopropene and methyl vinyl ether (MVE) copolymerize in nearly a 1:1 ratio in good yield (Table I). This copolymer was used as a model to establish the effect of initiator, starting material ratio, and solvent upon the reaction, and to determine the structure and properties of the copolymer. The results (Table II), show that the mole ratio of methyl vinyl ether in the copolymer increases as expected as the ratio of methyl vinyl ether in the reaction mixture increases. The molecular weight (from $\eta_{inh}$ or the physical state of the copolymer) is sensitive to the initiator concentration. Increasing the initiator concentration decreases the molecular weight and can yield an oil instead of a solid copolymer. Polymerization in benzene yields a copolymer of approximately 3:1 MVE:PFCP ratio, and in 1,1,2-trichloro-1,2,2-trifluoroethane the copolymer is colored, possibly because it decomposes slightly during polymerization. Bulk polymerization with azobisisobutyronitrile readily yields copolymer of approximately 1:1 mole ratio of moderate molecular weight ($\eta_{inh}$ = 0.6).

The copolymer is soluble in acetone, benzene, dimethylformamide, tetrahydrofuran, and other common solvents. Clear, self-supporting films were cast from benzene solution. The infrared spectrum (Fig. 1) shows weak unsaturated fluorocarbon absorption at 1730 $cm^{-1}$ and strong C-F stretching around 1200 $cm^{-1}$. The copolymer stick temperature is approximately 140°C, but the bulk copolymer may be heated slowly to 250°C without flowing. Thermogravimetric analysis showed 5% weight loss at 277°C in nitrogen and 292°C in air with significant weight loss beginning at 375°C. Differential thermal analysis showed a glass transition at 75°C, several shallow endotherms between 100 and 180°C, and a very large exotherm starting at 250°C and reaching a maximum at 325°C. Heating copolymer films in air at 200–250°C for 18 hr resulted in yellowing, increased brittleness, and insolubility (crosslinking). No direct evidence for elimination of hydrogen fluoride was observed, and the TGA data showed significant weight loss only after the large DTA endotherm. This behavior is consistent with the postulate that polymerization occurs without destruction


II

of the perfluorocyclopropyl ring to form polymer with repeating structure II; heating isomerizes the fluorocyclopropyl ring to the fluoroolefin structures III (and/or their positional isomers). Tetrachlorocyclopropene is reported to copolymerize with styrene and vinyl acetate without destruction of the cyclopropyl ring; no evidence for isomerization was found.[3]

TABLE II
Perfluorocyclopropene–Methyl Vinyl Ether Copolymers

| PFCP, mmole | MVE, mmole | Initiator Type | Initiator Amt, mole × $10^5$ | Polymer, g | F, % | Ratio MVE:PFCP | Appearance |
|---|---|---|---|---|---|---|---|
| 2.1 | 2.1 | $Bz_2O_2$[a] | 2 | 0.20 | 39.9 | 1.3 | Tan solid |
| 2.6 | 1.2 | $Bz_2O_2$ | 6.5 | — | — | — | Dark oil |
| 3.0 | 2.7 | $Bz_2O_2$ | 6.5 | — | — | — | Viscous oil |
| 3.0 | 2.7 | $Bz_2O_2$ | 2 | 0.27 | — | — | Tan solid |
| 3.0 | 3.0 | $Bz_2O_2$ | 2 | 0.25 | — | — | White solid |
| 1.5 | 4.6 | $Bz_2O_2$ | 2 | 0.40 | 21.0 | 4.3 | White solid |
| 3.0 | 3.0 | $Bz_2O_2$ | 0.6 | 0.38 | 27.5 | 2.8 | White solid |
| 16 | 16.7 | $Bz_2O_2$ | 4.5 | 1.94 | 41.6 | 1.2 | $\eta_{inh}$ = 0.3[b] |
| 16 | 18 | $Bz_2O_2$ | 8.4 | 2.46 | — | — | White solid |
| 16 | 17 | $Bz_2O_2$ | 17 | 2.29 | — | — | $\eta_{inh}$ = 0.2[b] |
| 2 | 2 | $Bz_2O_2$ | 2 | 0.21 | 25.3 | 3.2 | White solid[c] |
| 2 | 2 | $Bz_2O_2$ | 2 | 0.23 | 28.5 | 2.7 | White solid[d] |
| 2 | 2 | $Bz_2O_2$ | 2 | 0.25 | 26.1 | 3.1 | White solid[e] |
| 2 | 2 | $Bz_2O_2$ | 2 | 0.13 | 30.0 | 2.4 | Black solid[f] |
| 2 | 2 | $Bz_2O_2$ | 2 | 0.19 | 29.5 | 2.5 | Black solid[f] |
| 2 | 2 | $Bz_2O_2$ | 2 | 0.23 | 29.0 | 2.6 | Black solid[g] |
| 2 | 2 | $Bz_2O_2$ | 2 | 0.19 | 32.6 | 2.1 | Black solid[h] |
| 2.6 | 2.6 | $(t\text{-BuO})_2$[i] | 8 | 0.40 | 36.6 | 1.6 | Black solid |
| 2.6 | 2.6 | $(t\text{-BuO})_2$ | 8 | 0.40 | 36.2 | 1.7 | Black solid |
| 3 | 3 | AIBN[j] | 2 | 0.59 | 42.2 | 1.2 | White solid |
| 3 | 3 | AIBN | 2 | 0.56 | 42.8 | 1.1 | White solid, $\eta_{inh}$ = 0.6[b] |
| 100 | 100 | AIBN | 40 | 14.0 | 44.7 | 1.0 | White solid, $\eta_{inh}$ = 0.6 |

[a] Benzoyl peroxide, 85°C, 8 hr.
[b] Polymer dissolved in ether and reprecipitated in methanol. $\eta_{inh}$ in 0.1% benzene solution at 25°.
[c] 0.9 ml benzene solvent.
[d] 1.8 ml benzene solvent.
[e] 2.7 ml benzene solvent.
[f] 0.9 ml 1,1,2-trichloro-1,2,2-trifluoroethane solvent.
[g] 1.8 ml 1,1,2-trichloro-1,2,2-trifluoroethane solvent.
[h] 2.7 ml 1,1,2-trichloro-1,2,2-trifluoroethane solvent.
[i] *tert*-Butyl peroxide, 135°C, 8 hr.
Azobisisobutyronitrile, 65°C, 8 hr.

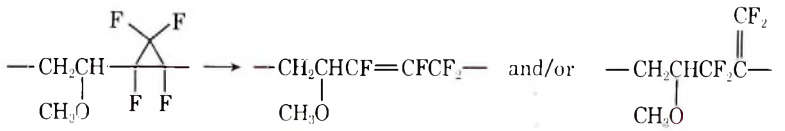


III

We have previously observed fluorocyclopropane geometrical isomerization[6] and ring-opening isomerization in some Diels-Alder cycloadducts of perfluorocyclopropene.[5] Evidence of this transformation is the absence of hydrogen fluoride elimination and the increase in intensity of the 1730 $cm^{-1}$ unsaturated fluoroolefin stretching band in the infrared spectrum of the heated polymer. Figures 1 and 2 compare the infrared spectra of unheated and heated polymer, illustrating the dramatic increase in fluorocarbon unsaturation. The polymer when heated may crosslink through the unsaturation or possibly through the hydrocarbon portion of the polymer.

## Perfluorocyclopropene–Tetrafluoroethylene Copolymers

Perfluorocyclopropene and tetrafluoroethylene did not copolymerize in sealed glass tubes at autogenous pressures; only polytetrafluoroethylene was isolated. When the reaction was performed in platinum tubes at 3000 atm, copolymer was obtained with several free radical catalysts (Table III).

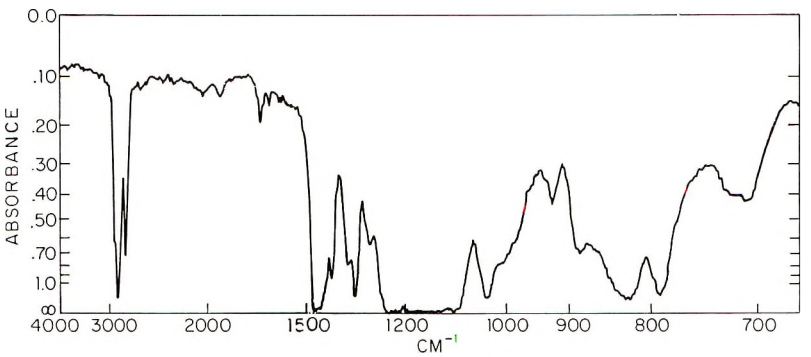


Figure 1. Perfluorocyclopropene/Methyl Vinyl Ether Copolymer 3 mil. Film.

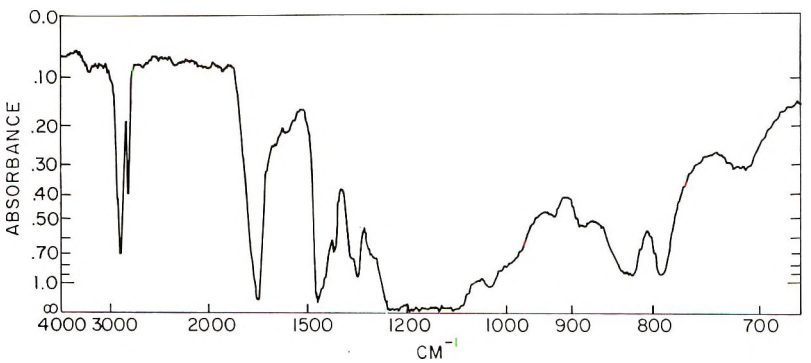


Figure 2. Perfluorocyclopropene/Methyl Vinyl Ether Copolymer 3 mil Film Heated 20 Hr. at 200°C.

TABLE III. Perfluorocyclopropene–Tetrafluoroethylene Copolymers

| PFCP, mmole | TFE, mmole | Initiator | | Polymer, g | Yield, %[a] |
|---|---|---|---|---|---|
| | | Type | Amt, mole × $10^6$ | | |
| 0 | 2.4 | AIBN | 12 | 0.19 | 78 |
| 0 | 4.8 | AIBN | 5 | 0.51 | 106 |
| 0 | 4.8 | $Bz_2O_2$ | 5 | 0.47 | 98 |
| 0 | 4.8 | $Bz_2O_2$ | 10 | 0.45 | 95 |
| 0 | 4.5 | $N_2F_2$ | 1 | 0.42 | 92 |
| 0[b] | 7.0 | $N_2F_2$ | 10 | 0.55 | 78 |
| 0[c] | 7.0 | $N_2F_2$ | 10 | 0.45 | 64 |
| 0[d] | 7.0 | 3P[d] | 15 | 0.78 | 110 |
| 0[e] | 7.0 | $(NH_4)_2S_2O_8$ | 5 | 0.28 | 40 |
| 1.2 | 3.6 | AIBN | 5 | 0.34 | 68 |
| 1.2 | 3.6 | AIBN | 5 | 0.36 | 72 |
| 1.2 | 3.6 | AIBN | 5 | 0.37 | 75 |
| 2.4 | 2.4 | AIBN | 2.4 | 0.15 | 31 |
| 2.4 | 2.4 | AIBN | 10 | 0.16 | 32 |
| 2.4 | 2.4 | AIBN | 5 | 0.18 | 36 |
| 2.4 | 2.4 | AIBN | 5 | 0.16 | 32 |
| 2.4 | 2.4 | AIBN | 5 | 0.17 | 34 |
| 2.4 | 2.4 | AIBN | 5 | 0.16 | 32 |
| 3.6 | 1.2 | AIBN | 5 | 0.08 | 16 |
| 3.6 | 1.2 | AIBN | 5 | 0.08 | 16 |
| 5.9 | 2.3 | AIBN | 5 | 0.17 | 19 |
| 9.4 | 2.3 | AIBN | 5 | 0.06 | 4 |
| 2.4 | 2.4 | $Bz_2O_2$ | 2 | 0.08 | 17 |
| 2.4 | 2.4 | $Bz_2O_2$ | 5 | 0.13 | 26 |
| 2.4 | 2.4 | $Bz_2O_2$ | 10 | 0.14 | 29 |
| 2.4 | 2.4 | $Bz_2O_2$ | 20 | 0.19 | 38 |
| 5.9 | 2.3 | $Bz_2O_2$ | 5 | 0.08 | 9 |
| 9.4 | 2.3 | $Bz_2O_2$ | 5 | 0.02 | 2 |
| 2.4 | 2.4 | $N_2F_2$ | 1 | 0.09[f] | 0 |
| 2.4 | 2.4 | $N_2F_2$ | 1 | 0.09[f] | 0 |
| 3.5[b] | 3.5 | $N_2F_2$ | 10 | 0.33 | 45 |
| 3.5[b] | 3.5 | $N_2F_2$ | 10 | 0.33 | 45 |
| 3.5[c] | 3.5 | $N_2F_2$ | 10 | 0.35 | 48 |
| 3.5[c] | 3.5 | $N_2F_2$ | 10 | 0.33 | 45 |
| 4.7 | 2.3 | $N_2F_2$ | 10 | 0 | 0 |
| 4.7[c] | 2.3 | $N_2F_2$ | 10 | 0.20 | 26 |
| 3.5[b] | 3.5 | 3P[d] | 1.5 | 0.27 | 36 |
| 3.5[b] | 3.5 | 3P[d] | 3.8 | 0.29 | 39 |
| 3.5[b] | 3.5 | 3P[d] | 7.6 | 0.29 | 39 |
| 3.5[b] | 3.5 | 3P[d] | 15 | 0.28 | 37 |
| 3.5[b] | 3.5 | 3P[d] | 15 | 0.29 | 39 |
| 3.5[b] | 3.5 | 3P[d] | 15 | 0.30 | 41 |
| 4.7[b] | 2.3 | 3P[b] | 15 | 0.16 | 21 |
| 3.5[e] | 3.5 | $(NH_4)_2S_2O_8$ | 5 | 0.23[g] | 31 |
| 3.5[e] | 3.5 | $(NH_4)_2S_2O_8$ | 5 | 0.18[g] | 24 |
| 7.0[b] | 0 | 3P[d] | 15 | 0 | 0 |
| 7.0[b] | 0 | 3P[d] | 15 | 0 | 0 |
| 7.0[c] | 0 | $N_2F_2$ | 10 | 0 | 0 |

[a] Yield based on weight per cent polymer isolated.

[b] 1,1,2-Trichloro-1,2,2-trifluoroethane was used as solvent.

[c] Hexafluoropropylene cyclic dimer was used as solvent.

[d] 3P represents perfluoropropionyl peroxide.

[e] Water was used as solvent.

[f] Residue was identified as carbon.

[g] Polymer contained black particles. A rapid temperature increase was recorded early in the reaction.

All initiators gave satisfactory copolymer; perfluoropropionyl peroxide was consistently good. Dinitrogen difluoride occasionally gave runaway polymerizations and ruptured tubes or yielded carbonaceous product. Aqueous persulfate also gave some runaway polymerizations. Equimolar charges of monomers gave copolymer in about 40% yield. The increased yield as the ratio of tetrafluoroethylene was increased and the decreased yield when the ratio of perfluorocyclopropene was increased suggest the slowest reaction is the addition of the perfluorocyclopropyl radical to tetrafluoroethylene. With perfluoropropionyl peroxide initiation the relatively constant yield as the initiator concentration decreases indicates the maximum copolymer molecular weight was not observed in most reactions.

The copolymer resembles polytetrafluoroethylene in many ways, including insolubility in many potential solvents. That copolymer is actually obtained is shown by the infrared spectrum and differential thermal analysis. Authentic polytetrafluoroethylene (Table III) was prepared under all reaction conditions used. The infrared spectrum of polytetrafluoroethylene

TABLE IV
Differential Thermal Analysis of PFCP–TFE Copolymers

| Initiator | | | | | Melt endotherm, °C | | |
|---|---|---|---|---|---|---|---|
| Type | Amt, mole × $10^5$ | PFCP, mmole | TFE, mmole | $T_g$, °C | Onset | Ex. onset[a] | Peak |
| | Commercial polytetrafluoroethylene | | | 14 | 280 | 325 | 335 |
| AIBN | 5 | 0 | 4.8 | 14 | 310 | 320 | 328 |
| 3P[b,c] | 15 | 0 | 7.0 | 11 | 300 | 314 | 325 |
| $N_2F_2$[c] | 10 | 0 | 7.0 | −6 | 300 | 313 | 323 |
| $N_2F_2$[d] | 10 | 0 | 7.0 | −6 | 260 | 313 | 324 |
| AIBN | 5 | 1.2 | 3.6 | −9 | 285 | 308 | 320 |
| AIBN | 10 | 2.4 | 2.4 | | 282 | 295 | 306 |
| AIBN | 5 | 2.4 | 2.4 | −25 | 197 | 295 | 300 |
| $Bz_2O_2$ | 10 | 2.4 | 2.4 | −31 | 280 | 290 | 304 |
| $h\nu$[e] | | 6.0 | 6.0 | −28 | 280 | 297 | 310 |
| $N_2F_2$[c] | 10 | 3.5 | 3.5 | −38 | 280 | 305 | 318 |
| $N_2F_2$[c,f] | 10 | 3.5 | 3.5 | −30 | 275 | 303 | 312 |
| $N_2F_2$ | 10 | 3.5 | 3.5 | −26 | 300 | 309 | 318 |
| 3P[b,c] | 15 | 3.5 | 3.5 | −29 | 280 | 308 | 317 |
| 3P[b,c,g] | 15 | 3.5 | 3.5 | −16 | 290 | 306 | 313 |
| $N_2F_2$[d] | 10 | 4.7 | 2.3 | −38 | 263 | 295 | 314 |
| 3P[b,c] | 15 | 4.7 | 2.3 | −30 | 275 | 295 | 310 |
| 3P[b,g] | 15 | 4.7 | 2.3 | −30 | 255 | 297 | 315 |

[a] Extrapolated onset of melting point.
[b] 3P represents perfluoropropionyl peroxide.
[c] 1,1,2-Trichloro-1,2,2-trifluoroethane was used as solvent.
[d] Hexafluoropropylene cyclic dimer was used as solvent.
[e] Initiation was by photolysis at atmospheric pressure.
[f] Copolymer was heated in concentrated nitric acid before analysis.
[g] Copolymer was heated 24 hr at 200°C before analysis.

has very strong bands at 1200–1260 and 1160 $cm^{-1}$ and a weak band at 720 $cm^{-1}$. Occasionally, samples had a weak absorption at 960 $cm^{-1}$. The copolymer infrared spectrum exhibits the two strong bands at 1200–1260 $cm^{-1}$ and 1160 $cm^{-1}$ and has, in addition, weak bands at 1020, 960, and 803 $cm^{-1}$. Differential thermal analysis clearly showed a copolymer; major transitions are reported in Table IV. The glass transition temperature of 14°C for polytetrafluoroethylene is lowered to approximately −30°C in the copolymer, and the polytetrafluoroethylene melting point of 313–325°C was lowered to 290–309°C in the copolymers. The copolymer derived from a 3:1 tetrafluoroethylene:perfluorocyclopropene charge, which presumably contains more polytetrafluoroethylene units than copolymers derived from equimolar charges has a glass transition and melting point intermediate between those of polytetrafluoroethylene and most of the copolymers (−9 and 308°C, respectively). Thermal gravimetric analysis (Table V) indicates the copolymer approaches polytetrafluoroethylene in thermal stability.

TABLE V
Thermal Gravimetric Analysis of PFCP–TFE Copolymers

| Initiator | Temp of 5% weight loss, °C | Temp at which significant degradation begins, °C |
|---|---|---|
| $N_2F_2$ | 283 | 525 |
| $N_2F_2$ | 313 | 525 |
| 3P[a] | 300 | 525 |
| 3P[a,b] | 287 | 525 |
| [c] | 525 | 550 |

[a] 3P represents perfluoropropionyl peroxide.
[b] Polytetrafluoroethylene control polymer.
[c] Commercial polytetrafluoroethylene.

The lower temperature observed for 5% weight loss for the copolymers and for the polytetrafluoroethylene prepared under our conditions is probably due to low molecular weight polymer.

No evidence regarding the structure or composition of the copolymer is available. Examination of low molecular weight materials showed only unreacted starting materials in significant amount. Since tetrafluoroethylene readily polymerizes under our reaction conditions but the copolymer yield is only ~40% and decreases with increasing perfluorocyclopropene, and since the infrared spectrum shows no major new absorptions, the amount of perfluorocyclopropene incorporated into the copolymer is probably low. When heated at 210°C for 24 hr, the copolymer yellowed slightly, but the infrared spectrum and DTA (Table IV) indicated little, if any, change.

### Perfluorocyclopropene–Vinyl Fluoride Copolymers

Azobisisobutyronitrile-initiated copolymerization of perfluorocyclopropene and vinyl fluoride readily occurred in platinum tubes at 3000 atm and

TABLE VI
Perfluorocyclopropene–Vinyl Fluoride Copolymers

| PFCP, mmole | VF, mmole[a] | Polymer, g | Yield, %[b] |
|---|---|---|---|
| 0 | 7.0 | 0.30 | 95 |
| 2.3 | 4.7 | 0.47 | 100 |
| 3.5 | 3.5 | 0.44 | 80 |
| 3.5 | 3.5 | 0.42 | 76 |
| 3.5 | 3.5 | 0.42 | 76 |
| 4.7 | 2.3 | 0.32 | 50 |

[a] Initiated by AIBN, $5 \times 10^{-5}$ mole at 75°C, 3000 atm, 8 hr.
[b] Per cent yield on a weight basis.

TABLE VII
Differential Thermal Analysis of PCFP–VF Copolymers

| PFCP, mmole | VF, mmole | $T_m$, °C | Exothermic activity, °C | | | |
|---|---|---|---|---|---|---|
| | | | Starts | Crests | | |
| 0 | 7.0 | 33[a] | 290 | 300[b] | 350[c] | 434 |
| 2.3 | 4.7 | 20 | 250 | 313[c] | 370 | |
| 3.5 | 3.5 | 23,52 | 235 | 314[c] | 380 | |
| 3.5 | 3.5 | 34 | 243 | 309[c] | 385 | |
| 3.5 | 3.5 | 23 | 230 | 300[c] | 390 | |
| 4.7 | 2.3 | 44 | 250 | 312[c] | 408 | |

[a] Melting endotherm observed at 207°C.
[b] Sharp exotherm, characteristic of poly(vinyl fluoride).
[c] Largest exotherm on chart.

75°C (Table VI). In at least one case, the copolymer is clearly 2:1 VF:PFCP, and the yields suggest that all the copolymerizations gave roughly 2:1 VF:PFCP copolymer.

The elastomeric copolymer was insoluble in the many solvents tested. The infrared spectrum was clearly different from that of polyvinyl fluoride and had new absorptions at 1490, 1250, 1190 (C—F), 918, and 803 $cm^{-1}$. The absorption at 1490 $cm^{-1}$ has been suggested as due to the fluorocyclopropyl ring system.[7] Differential thermal analysis (Table VII) is clearly different from that of poly(vinyl fluoride). No melting endotherm is observed for the copolymer, but some endothermic activity appears between 100 and 150°C. The exotherm at 350°C in poly(vinyl fluoride) and 370–400°C in the copolymers is believed due to the normal elimination of HF from the vinyl fluoride units of the polymer.

Of particular interest is the very large exotherm at approximately 310°C in the copolymers and absent in polyvinyl fluoride. This exotherm is several orders of magnitude larger than any other transition observed in the copolymer. It is believed this exotherm results from the fluorocyclopro-

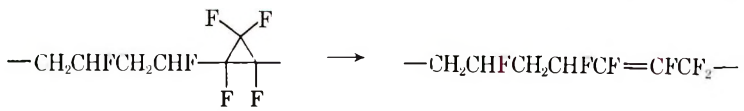

pane isomerization previously discussed for the perfluorocyclopropene–methyl vinyl ether copolymer. It is also possible that the 310°C exotherm is HF elimination involving the cyclopropane ring. The copolymer turned dark and became brittle when heated at 190°C for 24 hr; however, the infrared spectrum did not show any fluorocarbon unsaturation.

### Perfluorocyclopropene–Vinylidene Fluoride Copolymers

Perfluorocyclopropene and vinylidene fluoride copolymerized in platinum tubes at 3000 atm with azobisisobutyronitrile or perfluoropropionyl peroxide catalysis. The results (Table VIII) indicate perfluoropropionyl peroxide is the most effective initiator. Increasing the vinylidene fluoride ratio

TABLE VIII
Perfluorocyclopropene–Vinylidene Fluoride Copolymers

| PFCP, mmole | $VF_2$, mmole | Initiator | | Polymer, g | Yield, %[a] |
|---|---|---|---|---|---|
| | | Type | Amt, mole × $10^5$ | | |
| 0 | 7.0 | AIBN | 5 | 0.24 | 53 |
| 0[b] | 7.0 | 3P[c] | 15 | 0.45 | 101 |
| 0[b] | 7.0 | 3P[c] | 15 | 0.50 | 107 |
| 2.3 | 4.7 | AIBN | 5 | 0.36 | 62 |
| 2.3[b] | 4.7 | 3P[c] | 15 | 0.48 | 86 |
| 3.5 | 3.5 | AIBN | 5 | 0.12 | 20 |
| 3.5 | 3.5 | AIBN | 5 | 0.25 | 40 |
| 3.5[b] | 3.5 | 3P[c] | 15 | 0.41 | 66 |
| 3.5[b] | 3.5 | 3P[c] | 15 | 0.40 | 65 |
| 3.5[b] | 3.5 | 3P[c] | 7.5 | 0.39 | 64 |
| 3.5[b] | 3.5 | 3P[c] | 15 | 0.35 | 57 |
| 3.5[b] | 3.5 | 3P[c] | 15 | 0.40 | 65 |
| 3.5[b] | 3.5 | 3P[c] | 15 | 0.37 | 60 |
| 3.5[b] | 3.5 | 3P[c] | 15 | 0.37 | 60 |
| 3.5[b] | 3.5 | 3P[c] | 15 | 0.37 | 60 |

[a] Per cent yield on a weight basis.
[b] 1,1,2-Trichloro-1,2,2-trifluoroethane was used as solvent.
[c] 3P represents perfluoropropionyl peroxide.

in the reaction mixture increased the yield. The elastomeric copolymer is soluble in solvents such as dioxane, methyl ethyl ketone, dimethylacetamide, dimethyl sulfoxide, and diglyme. Elastomeric films may be cast from solution or pressed at 65°C. The infrared spectra of the copolymers had absorption at 1490 (fluorocyclopropyl ring?) $cm^{-1}$. Differential thermal analysis (Table IX) shows a low-temperature glass transition absent in poly(vinylidene fluoride) and a second transition at approximately 40°C. A distinct difference was noted between the sharp melting point endotherm for poly(vinylidene fluoride) and the copolymer endotherms; the copolymer had a definite, but broad and shallow endotherm at approximately 100°C. The exothermic activity of poly(vinylidene fluoride) and

TABLE IX
Differential Thermal Analysis of PFCP–$VF_2$ Copolymers

| PFCP, mmole | $VF_2$, mmole | $T_g$, °C | Endotherm, °C | Exothermic activity, °C | | |
|---|---|---|---|---|---|---|
| | | | | Start | Crests | |
| 0 | 7.0 | 56 | 167[a] | 382 | 397 | 421 |
| 0 | 7.0 | 43 | 177[b] | 350 | 390 | 405 |
| 2.3 | 4.7 | −30 | 123[c] | 250 | 328 | 397 |
| 2.3 | 4.7 | −44 | 110[c] | 250 | 333 | 387 |
| 3.5 | 3.5 | −6, 40 | [d] | 252 | 330 | 403 |
| 3.5 | 3.5 | −10, 45 | 100[c] | 265 | 327 | 387 |
| 3.5 | 3.5 | −20 | 92[c] | 300 | 340 | 382 |
| 3.5 | 3.5 | −17 | 100[c] | 300 | 335 | 375 |
| 3.5 | 3.5 | −20 | 101[c] | 300 | 334 | 380 |

[a] Melting endotherm; extrapolated onset, $T_m$ 155°C.
[b] Melting endotherm; extrapolated onset, $T_m$ 158°C.
[c] Could be melting endotherm, but is broad and shallow.
[d] Temperature range 60–200°C was not recorded.

the copolymer is similar, but the copolymer exotherm started at a lower temperature (250–300 compared to 350°C) and the first crest appeared at a lower temperature (327–340 compared to 390°C). The exotherms in poly(vinylidene fluoride) are believed due to HF elimination; the copolymer exotherms at 327–340°C and at 375–400°C are believed due to the fluorocyclopropane ring isomerization and the normal HF elimination, respectively.

The authors wish to acknowledge the suggestion of A. E. Barkdoll that perfluorocyclopropene should form polymers.

## References

1. K. B. Wiberg and W. J. Bartley, *J. Amer. Chem. Soc.*, **82**, 6375 (1960).
2. F. L. Carter and V. L. Frampton, *Chem. Rev.*, **64**, 497 (1964).
3. J. K. Hecht, *J. Polym. Sci. B*, **6**, 395 (1968).
4. P. B. Sargeant and C. G. Krespan, *J. Amer. Chem. Soc.*, **91**, 415 (1969).
5. P. B. Sargeant, *J. Org. Chem.*, in press.
6. P. B. Sargeant, *J. Amer. Chem. Soc.*, in press.
7. R. A. Mitsch, *J. Heterocyclic Chem.*, **1**, 271 (1964).

Received December 2, 1968

JOURNAL OF POLYMER SCIENCE: PART A-1 VOL. 7, 1479–1488 (1969)

# Relationship Between Reduction of Ceric Ion with Poly(vinyl Alcohol) and Graft Copolymerization

YOSHITAKA OGIWARA and MASAHIRO UCHIYAMA,
*Faculty of Engineering, Gunma University, Kiryu, Japan*

## Synopsis

Various poly(vinyl alcohol) samples were preliminarily subjected to oxidation treatment with sodium hypochlorite, and the reduction of ceric ion and subsequently initiation in the graft copolymerization in the system containing methyl methacrylate were investigated. The reduction behavior of ceric ion could be subdivided into three parts, each of different reaction rate. In the initial stage of the reaction, there was observed rapid cleavage of the backbone chain of poly(vinyl alcohol) with ceric salts. The amount $A$ of cleavage was proportional to the amount of ceric ion reduced at the initial fastest rate for various samples of different extents of oxidation; cleavage of 1 mole required ca. 10 moles of reduction of ceric ion. Higher carbonyl contents of the sample caused increased $A$. Graft polymerization was carried out in the same system with the addition of the monomer. The amounts of grafted chains produced were determined, and approximately one mole of grafted chains was obtained for per mole of cleavage. The copolymer is concluded to be blocklike in structure. The contribution of the carbonyl groups in poly(vinyl alcohol) sample to the initiation of the polymerization should be emphasized.

## INTRODUCTION

It has been widely considered[1,2] that, in the graft copolymerizations of vinyl monomers onto poly(vinyl alcohol) with the use of ceric salt as initiator, free radicals produced by oxidation of 1,2-glycol initiate polymerization, since 1,2-glycol is particularly susceptible to ceric ion oxidation among the hydroxyl groups in poly(vinyl alcohol).[1]

Since by nature many 1,2-glycol groups are present in cellulosic materials, graft copolymerizations onto cellulosic materials are also considered to be initiated by free-radical polymerization mechanisms due to the oxidation of 1,2-glycol. In our previous reports,[3,4] however, we found that the number of active groups in the reaction toward ceric ion was considerably smaller as compared with that of 1,2-glycol present in cellulosic materials, and concluded from kinetic discussion that the main groups participating in polymerization reaction were aldehyde and carbonyl.

It is reported that oxidized poly(vinyl alcohol) contains carbonyl groups in the backbone chains,[5] which readily induce the cleavage of the chains by the attack with an oxidant such as hydrogen peroxide.[6] At the present time, however, little is known about the effects of such groups on graft copolymerization onto poly(vinyl alcohol).

The purpose of this study was to investigate, the reduction of ceric ion with various samples of poly(vinyl alcohol) of different carbonyl contents and the initiation of graft copolymerization in the case of the coexistence of methyl methacrylate in this system, and to examine the correlations of the two reactions.

## EXPERIMENTAL

### Sample

Commercial poly(vinyl alcohol) powder was rinsed with distilled water and acetone, followed by drying to obtain a sample containing very few carbonyl groups. The sample was oxidized with sodium hypochlorite weakly acidified with hydrochloric acid to yield poly(vinyl alcohol) samples of various degrees of oxidation. Shiraishi et al.[5] reported that these samples contained carbonyl groups in the backbone chains. The amount of carbonyl groups was determined by hydroxylamine method.[7] Oxidation conditions, amounts of carbonyl groups, and degrees of polymerization are indicated in Table I.

TABLE I
Preparation and Analysis of Poly(vinyl Alcohol) Samples

| Sample | Amount of sodium hypochlorite for PVA, %[a] | Total carbonyl content, mmole/100 g PVA | Average degree of polymerization |
|---|---|---|---|
| 1 | 0[b] | 0.0 | 1 180 |
| 2 | 1.30[c] | 5.0 | 1 050 |
| 3 | 0.32[d] | 11.4 | 1 450 |
| 4 | 0.64[d] | 18.8 | 1 490 |
| 5 | 1.71[d] | 22.1 | 589 |

[a] Values are presented as weight per cent of available chlorine for PVA.
[b] Rinsed with water and acetone.
[c] Oxidation time 1 hr.
[d] Oxidation time 2 hr.

Methyl methacrylate was prepared by purifying a commercial product, and a commercial ceric ammonium nitrate of the highest purity was employed.

### Reduction of Ceric Ion with Poly(vinyl Alcohol)

A 90-ml portion of 0.1*N* nitric acid containing a given amount of ceric salt was added to a vessel in which was placed 150 ml of an aqueous solution of 3.00 g of poly(vinyl alcohol); the resulting solution was maintained at 45°C with stirring and 20-ml aliquots were taken at given intervals for measurement. The reaction was brought to a stop by adding 20 ml of an aqueous ferrous salt solution of a known concentration to the aliquot, and the amount of unreacted ceric ion was determined. The viscosities of

aqueous solutions at 30°C were also measured to determine the degrees of polymerization of poly(vinyl alcohol) according to Nakajima's equation.[8]

$$[\eta]_{30°C} = 7.50 \times 10^{-4} P^{0.64}$$

### Graft Copolymerization

Under nitrogen, 15 ml of 0.1*N* nitric acid containing a given amount of ceric salt was added to 25 ml of an aqueous solution containing 0.5 g of poly(vinyl alcohol) and 2.5 ml of methyl methacrylate. The polymerization was carried out at 45°C. The resulting product was first extracted with water at 70°C for 1 hr to remove the unreacted poly(vinyl alcohol), then the residue was extracted with acetone for 48 hr by means of a Soxhlet extractor to obtain the graft copolymer. The grafted chains were separated according to the procedure of Danelyan et al.[9] by treating the graft copolymer with 30% nitric acid at 70°C for 5 hr and then boiling in water for 40 min and subsequently by rinsing and drying. The molecular weight of the grafted chains was determined from the viscosity of acetone solution according to the following equation:[10]

$$[\eta]_{25°C} = 0.96 \times 10^{-4} M^{0.69}$$

The per cent grafting, defined as follows:

$$\text{Per cent grafting} = \frac{\text{wt. grafted chains separated by nitric acid, g}}{\text{wt. poly(vinyl alcohol) used in the reaction, g}} \times 100$$

was found, and the number of grafted chains was determined from the average molecular weight of the branches and the per cent grafting.

## RESULTS AND DISCUSSION

### Reduction of Ceric Ion with Poly(vinyl Alcohol)

Figure 1 indicates the change of ceric ion concentration with time in the reduction of ceric ion with two kinds of poly(vinyl alcohol) of differing carbonyl contents.

It was clearly observed that the logarithm of the change of ceric ion concentration with reaction time was represented by three straight lines, each indicating a different coefficient of reaction rate; during several minutes at the initial stage of the reaction, very rapid reduction of ceric ion took place, followed by subsequent 20–30 min stage of the reaction at the second rate and a third reduction at a very slow rate. By extrapolating each straight line to the ordinate, the intersecting points were determined, from which the amounts of ceric ion (in mmole/100 g) reduced most rapidly and with the second rate were obtained (I and II respectively).

### Fastest Reduction of Ceric Ion

As shown in Figure 2, the amount of I was affected strongly by the kind of poly(vinyl alcohol) sample as well as ceric ion concentration. I increases

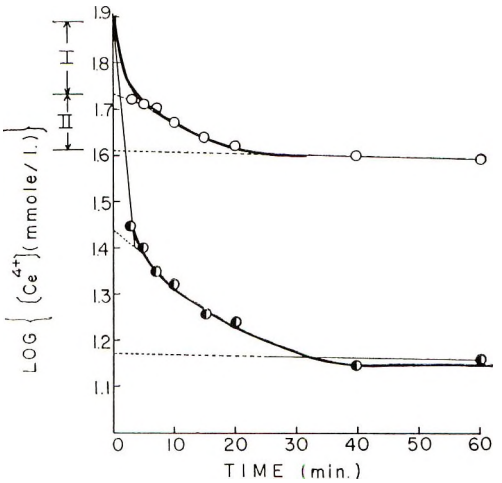


Fig. 1. Changes of the concentration of ceric ion with time at various total carbonyl contents of PVA: (O) 0; (◐) 22.1 mmole/100 g PVA. Reaction temperature, 45°C; initial concentration of ceric ion, 10 mmole/l.

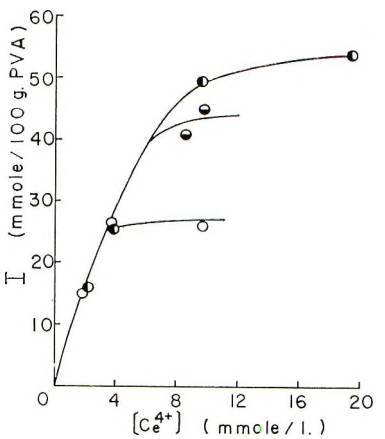


Fig. 2. Relationship of the amount of ceric ion reduced at the fastest rate (I) to the concentration of ceric ion at various total carbonyl contents of PVA: (O) 0; (◒) 11.4 (◐) 22.1 mmole/100 g PVA. Reaction temperature, 45°C; concentration of ceric ion, 10 mmole/l.

tendency with ceric ion concentration, while its value at equilibrium is higher the higher the carbonyl content of the sample.

Ide[2] and Iwakura et al.[11] reported that, in the formation of the graft copolymer of poly(vinyl alcohol) with the use of ceric salt as initiator, the cleavage of the backbone chain occurred. Hence, in this study, the cleavage of poly(vinyl alcohol) with ceric salt in the absence of monomer was investigated. Average degrees of polymerization for poly(vinyl

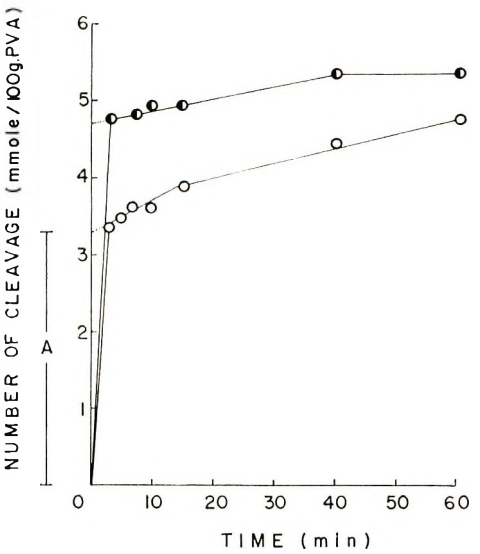


Fig. 3. Changes of the number of cleavage of PVA chain with time at various total carbonyl contents of PVA: (○) 0; (◐) 22.1 mmole/100 g PVA. Reaction temperature, 45°C; concentration of ceric ion, 10 mmole/l.

alcohol) were determined by the solution viscosities, and the amount of the cleavage was calculated according to the equation:

$$\text{Cleavage(mmole/100g PVA)} = (100/44)[(1/\bar{P}_t) - (1/\bar{P}_0)]$$

where $\bar{P}_t$ and $\bar{P}_0$ represent the average degree of polymerization at time and initially, respectively. The relation between the change and time is shown in Figure 3.

It is clear from this figure that rapid cleavage reaction of the backbone chain to an amount $A$, takes place during the initial several minutes; $A$ is greater the higher the carbonyl content of the sample.

Figure 4 indicates the relationships between $A$ and ceric ion concentration in various poly(vinyl alcohol) samples. $A$ increased with ceric ion concentration to an equilibrium value which was dependent upon the kind of sample was higher, the higher the carbonyl content of the sample. Since it is clear that I and $A$ are dependent upon the kind of poly(vinyl alcohol) sample and ceric salt concentration, these relationships are indicated in Figure 5. In spite of the change of ceric ion concentration as well as the carbonyl content in poly(vinyl alcohol), a linear relationship passing through the origin held between I and $A$.

The slope of this straight line indicates that the cleavage of one mole of the backbone chain was induced by the reduction of ca. 10 moles of ceric ion. Sakurada et al.[12] examined the oxidation mechanism with hydrogen peroxide and described that the cleavage of one mole of the backbone chain linkage required 10–20 moles of hydrogen peroxide, the 1,2-glycol bond being susceptible to oxidative decomposition. Takayama[6] reported that

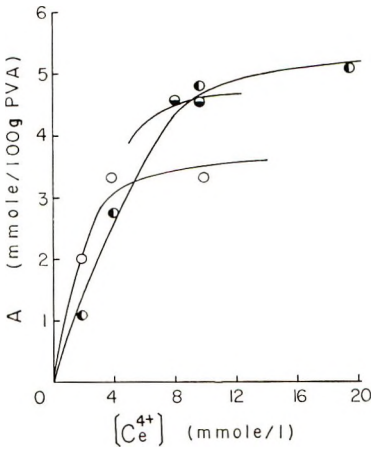


Fig. 4. Relationship of the number of cleavages of PVA chain A to the concentration of ceric ion at various total carbonyl contents of PVA: (○) 0; (◒) 11.4; (◐) 22.1 mmole/100 g PVA. Reaction temperature, 45°C; reaction time, 60 min.

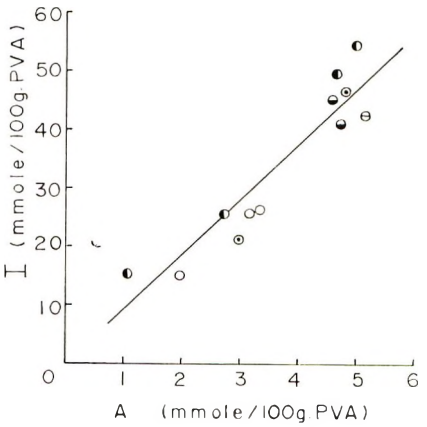


Fig. 5. Relationship of the amount of ceric ion reduced at the initial rate (I) to the amount of cleavage of PVA chain A at various total carbonyl contents of PVA: (○) 0; (⊙) 5.0; (◒) 11.4; (⊖) 18.8; (◐) 22.1 mmole/100 g PVA. Reaction temperature, 45°C; reaction time, 60 min; concentration of ceric ion, 2–20 mmole/l.

in such a system the bond adjacent to a carbonyl group was susceptible to oxidative cleavage.

## Reduction of Ceric Ion at the Second Rate

It is apparent that there exists a reduction of ceric ion at a second rate. Figure 6 shows an excellent linear relationship between II and carbonyl content over the range 0–22 mmole/100 g PVA in various poly(vinyl alcohol) samples.

Unlike the case of I, however, it is clear that II is almost independent of

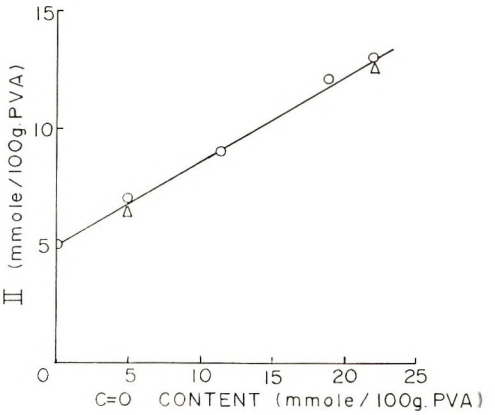


Fig. 6. Relationship of the amount of ceric ion reduced at the second rate (II) to the total carbonyl content at various concentrations of ceric ion: (O) 10; (Δ) 20 mmole/l. Reaction temperature, 45°C; reaction time, 60 min.

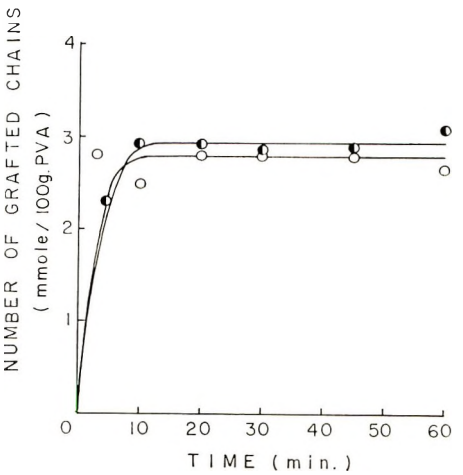


Fig. 7. Change of the number of grafted chains with time at various total carbonyl contents of PVA: (O) 0; (◐) 22.1 mmole/100 g PVA. Reaction temperature, 45°C; concentration of ceric ion, 10 mmole/l; amount of monomer, 2.5 ml.

ceric salt concentration and the amount of II indicates an approximately equal value to the carbonyl content in sample. As discussed below, this reaction takes place considerably later than graft copolymerization, so it is considered that the reduction of ceric ion at the second rate has little relation to the initiation reaction.

## Graft Copolymerization of Methyl Methacrylate

Graft copolymerization of methyl methacrylate onto poly(vinyl alcohol) with the use of ceric salt as initiator was carried out. The relation between the number of grafted chains of the copolymer and the polymerization time is indicated in Figure 7.

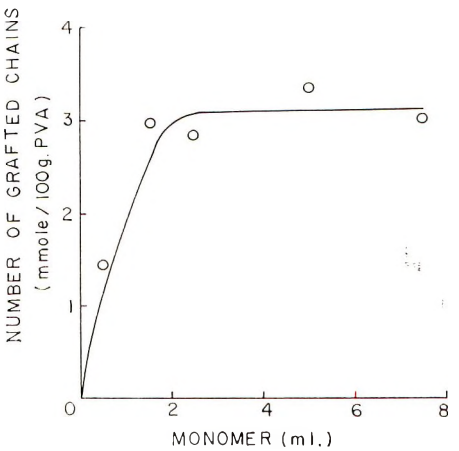


Fig. 8. Relationship of the number of grafted chains to the amount of monomer. Reaction temperature, 45°C; reaction time, 30 min; concentration of ceric ion, 10 mmole/l; total carbonyl contents of PVA, 0 mmole/100 g PVA.

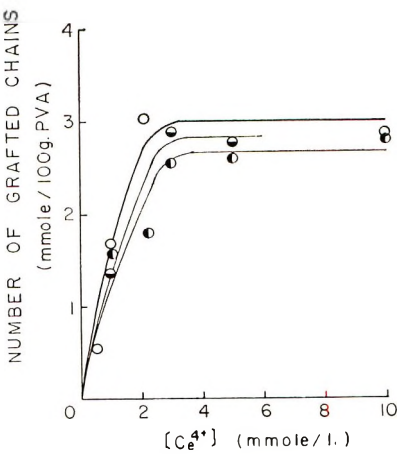


Fig. 9. Relationship of the number of grafted chains to the concentration of ceric ion at various total carbonyl contents of PVA: (○) 0; (◒) 11.4; (◐) 22.1 mmole/100 g PVA. Reaction temperature, 45°C; reaction time, 30 min; amount of monomer, 2.5 ml.

It is apparent from this that the formation of grafted chains nearly ends several minutes after the initiation of the reaction, and the increase in the number of grafted chains is very small after the initial vigorous branch formation subsides. This indicates that the fastest reduction of ceric ion is directly related to the initiation of graft copolymerization, which is considered to be induced by cleavage of the backbone chain. The effects of the amount of monomer employed and ceric salt concentration on the number of grafted chains are shown in Figures 8 and 9. The number of

grafted chains increases in proportion to the amount of the monomer when the latter is employed in small quantity, reaching an almost constant value above 2 ml. Therefore 2.5 ml, as employed in this study, is considered to be an optimum amount for the discussion of the number of grafted chains. Although the number of grafted chains increased almost linearly with ceric ion concentration, a tendency to reaching a saturated value for the poly-(vinyl alcohol) sample was observed above a ceric ion concentration of 3 mmole/l. The average molecular weights of the grafted chains as determined by the solution viscosity measurements are considered to be close to the weight-average ones. If it is assumed that twice the number- average molecular weight is equal to the weight-average molecular weight, the number of grafted chains determined by us becomes half the value obtained from the number-average molecular weight. On the other hand, Nakajima's equation has been reported to give molecular weight values close to number-average ones,[6,12] so that at the initial stage of graft copolymerization, below ceric salt concentration of 2 mmole/l, the amount of grafted chains produced is approximately one mole for the cleavage of one mole of the backbone chain (cf. Figs. 4 and 9).

From these results and the fact that poly(vinyl alcohol) participating in graft copolymerization is about 50% in the scope of this study, it can be concluded that the structure of the copolymer is somewhat like that of a block copolymer, as also indicated by Iwakura et al.[11]

## CONCLUSION

The results of the investigation of the reaction of poly(vinyl alcohol) with ceric salt in homogeneous aqueous system indicate that poly(vinyl alcohol) samples with higher carbonyl contents reduced more ceric ion at the fastest initial rates and afforded more cleavage of the backbone chain at the fastest initial rates. Also, in graft copolymerization in the system containing methyl methacrylate, the formation of grafted chains almost ceased after the initial several minutes where the preceding reactions predominated. From the time correspondence of these reactions, therefore, it is considered that the formation of branches in poly(vinyl alcohol) is induced by the oxidative cleavage of the backbone chain and this cleavage reaction is largely dependent upon the carbonyl group of the backbone chain. Hence, it is concluded that the graft copolymerization onto cellulosic materials is considered to be dependent upon the associations with the carbonyl groups rather than the 1,2-glycol groups.

## References

1. G. Mino, S. Kaizerman, and E. Rasmussen, *J. Polym. Sci.*, **39**, 523 (1959).
2. F. Ide, *Kogyo Kagaku Zasshi*, **64**, 1671 (1961).
3. Y. Ogiwara, H. Kubota, and Y. Ogiwara, *Kogyo Kagaku Zasshi*, **70**, 103 (1967).
4. Y. Ogiwara, Y. Ogiwara, and H. Kubota, *J. Polym. Sci. A-1*, **5**, 2791 (1967).
5. M. Shiraishi and S. Matsumoto, *Kogyo Kagaku Zasshi*, **65**, 1430 (1962).

6. G. Takayama, *Kobunshi Kagaku*, **17**, 698 (1960).
7. M. Kadooka, N. Nakajo, M. Tanaka, and N. Murata, *Kobunshi Kagaku*, **23**, 451 (1966).
8. A. Nakajima and K. Furudate, *Kobunshi Kagaku*, **6**, 460 (1949).
9. G. G. Danelyan and R. M. Livshits, *Vysokomolekul. Soedin.*, **8**, 1501 (1966).
10. S. Chinai, J. Matlack, and A. Resink, *J. Polym. Sci.*, **17**, 391 (1955).
11. Y. Iwakura and Y. Imai, *Makromol. Chem.*, **98**, 1 (1966).
12. I. Sakurada and S. Matsuzawa, *Kobunshi Kagaku*, **16**, 565 (1959).

Received September 5, 1968
Revised December 9, 1968

JOURNAL OF POLYMER SCIENCE: PART A-1 VOL. 7, 1489–1496 (1969)

# Polymerization of Tetrahydrofuran: A Radiochemical Study of the Initiation Mechanism

WALLACE M. PASIKA, *Macromolecular Research Center, Texas A & M University, College Station, Texas 77843* and JOHN W. WYNN, *Chemistry Department, East Texas State University, Commerce, Texas 75428*

## Synopsis

$^{14}C$-tagged triphenylmethyl hexachloroantimonate was used to initiate the polymerization of THF. An activity count on the polymers indicated no incorporation of initiator fragments into the macromolecule. On ascertaining the fate of the tagged trityl fragment it was found that the activity resided in the triphenylmethane isolated from the methanol supernatant. This indicates that at least one sequence of the initiation reaction in this polymerization involves hydride ion abstraction.

## INTRODUCTION

Tetrahydrofuran(THF) can be polymerized to a high molecular weight polyether by employing the salt triphenylmethyl hexachloroantimonate. Several mechanisms have been postulated for the initiation step. One[1] mechanism (I) involved a trityl–THF complex which suffers nucleophilic attack at the $\alpha$ carbon of the THF segment by a molecule [eqs. (1) and (2)];

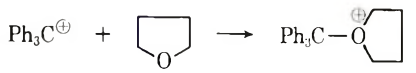

(1)

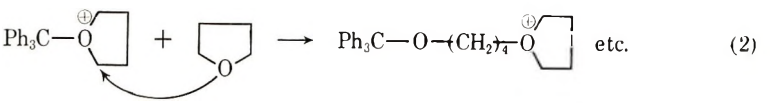

(2)

the other initiation mechanism (II)[1] involved hydride ion abstraction by the trityl cation, complexation of the THF cation with monomer, and subsequent nucleophilic attack by monomer molecules to produce a polymer [eqs. (3) and (4)].

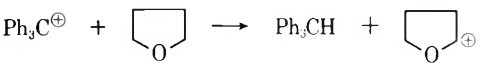

(3)

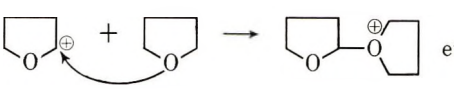

(4)

Kuntz,[2] who carried out a molecular weight study on the polymers obtained when the monocation $Ph_3CSbCl_6$ and dication $(Ph_2CC_6H_4CH_2)_2$ $(SbCl_6)_2$

salts were used as initiator, found that for equimolar amounts of cation the molecular weights of the polymers produced by these initiators were identical. Employing NMR and pinpointing the tertiary hydrogen of $Ph_3CH$ at 5.7 ppm, Kuntz[3] also demonstrated that $Ph_3CH$ is formed readily in the interaction of trityl salt with THF. Dreyfuss[4] has suggested that the initiation scheme of Kuntz is incomplete. With regard to his experimental evidence, this author postulates that the gegenion abstracts a proton from the THF cation to form hexachloroantimonic acid and a dihydrofuran. The acid protonates a THF molecule, forming a species which then complexes with a free THF molecule to produce the species which is actually the "initiator" of the polymerization. The experimental evidence of Kuntz and Dreyfuss, which is strongly dependent on NMR evidence, indicates trityl complexation cannot be considered as the initiation step. It appears that the role of the trityl moiety is primarily that of hydride abstracter. NMR arguments, however, leave a 5% margin in the establishment of the mechanism. It may be that mechanism I [eqs. (1) and (2)] is operative to this extent which would result in some polymer that has an incorporated trityl group. A much more precise technique is required to determine the extent of reaction I. Radiotracer techniques offer the precision needed.

We wish to report some data that bear on the above question. We have synthesized trityl hexachloroantimonate radio-tagged at the tertiary carbon, counted the formed polymer, and ascertained the fate of the trityl fragment in the THF polymerization.

## EXPERIMENTAL

### Preparation of Initiator

Benzoic acid labeled in the carboxyl group (0.125 mc) was added in benzene solution to 10 g of unlabeled benzoic acid. By using the procedure of Fieser[5] a yield of 4.5 g of radio-tagged triphenylcarbinol, mp 163–165°C (lit. mp 164.2°C), was obtained. The labeled $Ph_3COH$ (4.5 g) reacted with 2.7 ml of a cetyl chloride in benzene produced 2.1 g of triphenylchloromethane, mp 110.5–112°C (lit. 112–113°C). The 2.1 g of triphenylchloromethane was dissolved in dry carbon tetrachloride and 2.26 g of antimony pentachloride were added. After washing with carbon tetrachloride and drying in a vacuum oven for 24 hr, the orange-yellow precipitate, $Ph_3{}^{14}CSbCl_6$, had a melting point range of 219–227°C. Unlabeled $Ph_3CSbCl_6$ prepared in a similar manner melted in the range 220–227°C. The infrared spectra of the two salts were identical.

### Preparation of Polymer

After drying with calcium chloride and sodium, the THF was refluxed for 6 hr over lithium aluminum hydride and then distilled (66–67°C) into a receiver containing a mixture of sodium and naphthalene. The monomer was deoxygenated by a series of freezing–thawing cycles under vacuum until the green sodium naphthalene was in evidence. Measured aliquots

of the monomer were transferred under vacuum to tubes containing various concentrations of the labeled initiator. The tubes were vacuum-sealed and placed in thermostatically controlled water baths at 35°C. After the desired polymerization period the reaction tubes were opened and the contents dissolved in benzene. The polymer was precipitated by slowly pouring the benzene solution into 600 ml of stirred methanol. A second set of tubes was prepared in a similar fashion with the use of labeled initiator with the exception that the monomer was distilled from the sodium naphthalene complex under vacuum into a receiver containing 2 g of unlabeled initiator, $Ph_3CSbCl_6$, and then transferred on the vacuum line into the reaction tubes containing labeled initiator. These tubes were thermostated at 35°C. The polymer was twice precipitated in methanol and dried in a vacuum oven at 50°C for 24 hr.

### Treatment of the Methanol Supernatant

The methanol supernatants of the second set of tubes polymerized at 35°C were all treated in the following manner. The 1 200 ml of methanol were evaporated to "dryness" on a rotary evaporator, and carefully weighed quantities of nonlabeled triphenylmethane and triphenylcarbinol were introduced. The oily semisolid was dissolved in 30 ml of ether and transferred by pipet to a 30-cm activated alumina chromatographic column and eluted with ethyl ether; 2-ml portions were collected and evaporated to dryness. The first fraction to pass through the column was triphenylmethane, mp 91–92.5°C (lit. mp 94°C). Further elution was carried out with 1:1 ethyl ether–methanol. The 2-ml fractions collected and evaporated to dryness resulted in an oily fraction. Elution with methanol gave a third fraction which was triphenylcarbinol. The $Ph_3CH$ and $Ph_3COH$ were radio assayed.

### Radio Counting

Liquid scintillation was employed in counting the polymer samples. The equipment used was a Model 186 Nuclear Chicago scaler, a Model DS-5-Nuclear Chicago scintillation detector, a 2-in. thick lead castle and a counting cell that could be flushed with helium.

The liquid scintillating solution consisted of 4 g of *p*-terphenyl and 0.1 g of POPOP dissolved in 1 liter of dry toluene.[7]

Deoxygenation[8] was effected by bubbling helium through the 20 ml of scintillator solution taken as standard volume for all radiochemical assays and counted for three 5-min periods. The gas inlet and outlet tubes were clamped during a count.

Mineral oil was used to make optical contact between the cell bottom and the photomultiplier face.

Counting data on the trityl salt were not directly obtainable because the orange color imparted to the scintillation solution acted as a quenching agent.[8]

In order to obtain a count on the labeled initiator, some of it was converted to $Ph_3COH$ by treating 0.1 g with 5 ml of 6*N* ammonium hydroxide and extracting with a 1:1 petroleum ether–benzene solution. The labeled $Ph_3COH$ was recovered and purified; mp 165°C (lit. mp 164.2°C).

## RESULTS AND DISCUSSION

Table I summarizes the polytetrahydrofuran preparative aspects of this study.

Counting data on polymer samples (0.2 g) recovered from the first and second set of tubes polymerized at 35°C are presented in Table II.

The polymer samples obtained from the second set of tubes were counted at a reduced scaler sensitivity.

Triphenylmethane and triphenylcarbinol (added and any formed in the reaction) isolated from the methanol supernatants were counted in the standard manner. These data are presented in Table III.

TABLE I
Initiator Concentration and Polymer Yield Data

| Sample | Reaction temp, °C | Wt initiator, mg | Initiator, mole | THF, ml | Initiator concn, *M* | Reaction time, days | Polymer yield, g |
|---|---|---|---|---|---|---|---|
| 2A | 35 | 5.789 | $1 \times 10^{-5}$ | 10 | $1 \times 10^{-3}$ | 1 | 1.0552 |
| 2B | 35 | 5.789 | $1 \times 10^{-5}$ | 10 | $1 \times 10^{-3}$ | 3 | 1.4367 |
| 2C | 35 | 5.789 | $1 \times 10^{-5}$ | 10 | $1 \times 10^{-3}$ | 8 | 3.9316 |
| 3A | 35 | 57.89 | $1 \times 10^{-4}$ | 5 | $2 \times 10^{-2}$ | 1 | 1.3510 |
| 3B | 35 | 57.89 | $1 \times 10^{-4}$ | 5 | $2 \times 10^{-2}$ | 2.5 | 1.5307 |
| 3C | 35 | 57.89 | $1 \times 10^{-4}$ | 5 | $2 \times 10^{-2}$ | 5 | 2.8016 |
| 2Q | 35 | 12.0 | $2.07 \times 10^{-5}$ | 5 | $4.14 \times 10^{-3}$ | 3.5 | 1.2906 |
| 3Q | 35 | 12.0 | $2.07 \times 10^{-5}$ | 5 | $4.14 \times 10^{-3}$ | 7.5 | 1.4870 |
| 4Q | 35 | 57.0 | $0.983 \times 10^{-4}$ | 5 | $1.97 \times 10^{-2}$ | 7.5 | 2.8360 |

TABLE II
Counting Data for Polytetrahydrofuran

| Series | Sample | Weight of polymer counted, g | Count, cpm | Corrected count, cpm[a] | Background count, cpm[a] |
|---|---|---|---|---|---|
| First set | 2A | 0.2016 | 394 | 492 (22.2) | 458 (36.6) |
| | 2B | 0.2010 | 390 | 488 (22.0) | 458 (36.6) |
| | 2C | 0.2142 | 416 | 520 (22.8) | 458 (36.6) |
| | 3A | 0.2165 | 408 | 507 (22.4) | 458 (36.6) |
| | 3B | 0.2037 | 394 | 492 (22.2) | 458 (36.6) |
| | 3C | 0.2003 | 388 | 485 (22.0) | 458 (36.6) |
| Second set | 2Q | 0.1000 | 74 | 82 (9.1) | 72 (8.1) |
| | 3Q | 0.1000 | 68 | 76 (8.5) | 72 (8.1) |
| | 4Q | 0.1000 | 70 | 78 (8.7) | 72 (8.1) |

[a] Standard deviation[9] in parentheses.

TABLE III
Counting Data for Triphenylmethane and Triphenylcarbinol

| Sample | $Ph_3CSbCl_6$, mole | Time, days | Weight $Ph_3CH$, g[a] | Weight of $Ph_3CH$ derived from $Ph_3CSbCl_6$, g[b] | Total weight $Ph_3CH$, g[c] | Weight $Ph_3CH$ counted, g[d] | $Ph_3CH$ count/min | $Ph_3CH$ corrected count/min[e] | Calculated expected initiator count/min[e] |
|---|---|---|---|---|---|---|---|---|---|
| 2Q | $2.07 \times 10^{-5}$ | 3.5 | 0.0100 | 0.0051 | 0.0151 | 0.0019 | 3 306 | 26 270 (162) | 33 170 (182) |
| 3Q | $2.07 \times 10^{-5}$ | 7.5 | 0.0441 | 0.0051 | 0.0492 | 0.0153 | 8 580 | 27 590 (167) | 33 170 (182) |
| 4Q | $0.983 \times 10^{-4}$ | 7.5 | 0.0161 | 0.0240 | 0.0401 | 0.0340 | 120 500 | 142 120 (375) | 157 540 (394) |

[a] Unlabeled $Ph_3CH$ added to concentrated methanol supernatant.
[b] Labeled $Ph_3CH$.
[c] Total amount being chromatographed.
[d] Weight of chromatographed material counted.
[e] Standard deviation[9] in parentheses.

Labeled $Ph_3COH$ (0.0022 g) obtained directly from the initiator and used as a standard for this class of compound counted for three 5-min intervals gave an average count of 14,566 ± 118 cpm.

In order to investigate the possibility of trityl carbinol self-quenching, labeled $Ph_3COH$ was counted before and after increments of unlabeled $Ph_3COH$ were added (Fig. 1). A 12% decrease in count per milligram of $Ph_3COH$ is evident for amounts counted of less than 20 mg.

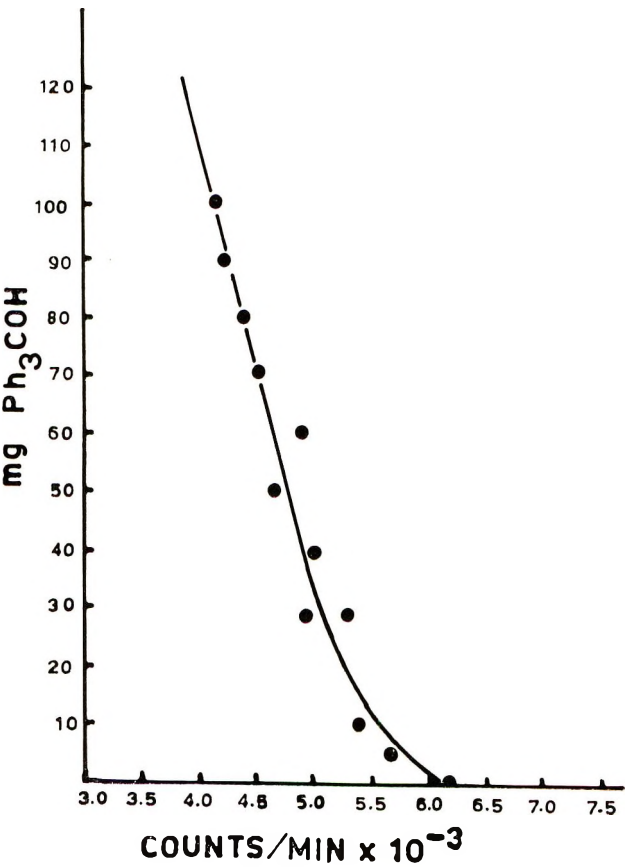


Fig. 1. Quenching by $Ph_3COH$.

Figure 2 shows the self-quenching characteristics of the polymer. An average decrease of 10% in the count per 0.1 g increment of polymer was experienced. This was taken into account in correcting the counting data on the polymers of Table II. At the 68% probability level, good agreement results between columns 4 and 5 except with samples 2C and 3A. However, at the 75% probability level total agreement between the two columns is obtained.[9] This indicates that the counts in the two columns agree within the standard deviation.

The corrected counts for the polymer samples therefore are identical with

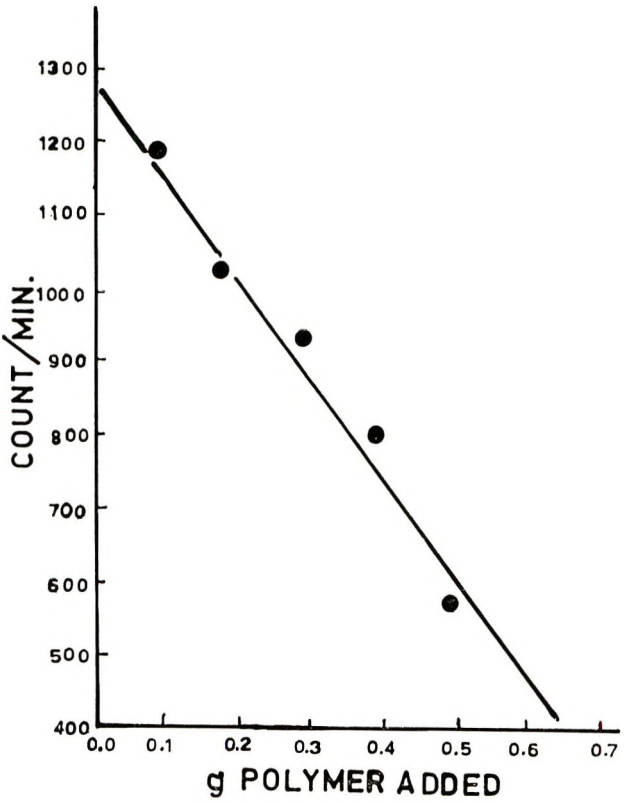


Fig. 2. Quenching by polytetrahydrofuran.

that of the background, indicating negligible activity in the polymer; this totally precludes mechanism I [eqs. (1) and (2)] as an initiation reaction.

The radiochemical activity obviously resides in some other chemical species. Initiation mechanism II [eqs. (3) and (4)] suggests that the species might be $Ph_3CH$. Isotropic dilution and isolation of $Ph_3CH$ and $Ph_3COH$ from the methanol supernatant allowed radio assay of these species. These species separated from the supernatant were characterized by melting point. Since there was a small amount of tailing in the chromatographic process only the middle, purest portion of the $Ph_3CH$ and $Ph_3COH$ were used in counting. The count was scaled up by the ratio of the sum of trityl compound in the supernatant (that introduced and that derived from the initiator) to that counted. No activity was found in the triphenyl carbinol recovered. All the activity resided in the triphenylmethane. Therefore no trityl carbinol was formed in the polymerization reaction.

The corrected count for the $Ph_3CH$ in the methanol supernatant derived from the initiator and the calculated "expected count" for $Ph_3CH$ derived from the amount of initiator used are found in Table III. It was assumed that $Ph_3CH$ would not quench sufficiently and hence no corrections were applied to the counting data for this species. This can be ascertained from

a comparison of the amounts of $Ph_3CH$ counted for samples 2Q and 3Q. These samples have the same initial initiator concentration and therefore should have the same activity deriving from this amount of initiator. The amount of isotropically diluted $Ph_3CH$ counted is different by a factor of approximately 10. Sample 3Q, if $Ph_3CH$ quenches, should have an activity lower than proportionately expected relative to the count obtained for 2Q. The corrected counts for the total activity are 26 720 for 2Q and 27 590 for 3Q. The agreement between these values indicates that $Ph_3CH$ does not self-quench. Agreement is lacking between columns 9 and 10 at the 99.99% probability level,[9] where the error range for each count is about as large as can be accounted for on a statistical basis. These differences suggest that there might be yet another species which contains some of the $^{14}C$—some species other than $Ph_3CH$ or $Ph_3COH$ which incorporated some of the tagged trityl fragments—possibly $Ph_3C^{14}Cl$ for which we did not assay.

We are appreciative of the support extended us by the Robert A. Welch Foundation during the course of this investigation.

## References

1. C. E. H. Bawn, C. Fitzsimmons and A. Ledwith, *Proc. Chem. Soc.*, **1964**, 391.
2. I. Kuntz, *ACS Polymer Preprints*, **7**, **1966**, 187.
3. I. Kuntz, *J. Polym. Sci. A-1*, **5**, 193 (1967).
4. M. P. Dreyfuss, J. C. Westfahl, and P. Dreyfuss, *Macromolecules*, **1** (5), 437 (1968).
5. L. F. Fieser, *Organic Experiments*, 2nd ed., Raytheon Education Co., N. Y., 1966, p. 92.
6. L. E. Smith, *Org. Syn.*, **23**, 100 (1947).
7. B. M. Tolbert and W. E. Siri, in *Physical Methods of Organic Chemistry*, 3rd ed., Weissberger, Ed., Vol. 1, Interscience, N. Y., 1960, p. 3335.
8. R. T. Overman and H. M. Clark, in *Radioisotope Techniques*, McGraw-Hill, Inc., N. Y., 1960, p. 187.
9. J. H. Harley and S. E. Wiberly, *Instrumental Analysis*, J. Wiley and Sons, N. Y., 1954, p. 369.

Received October 29, 1968
Revised December 16, 1968

JOURNAL OF POLYMER SCIENCE: PART A-1 VOL. 7, 1497–1508 (1969)

# Polymerization of Vinyl Compounds with Heterocyclic Groups. IV. Thermal Polymerization of 2-Vinylthiophene*

C. ASO, T. KUNITAKE, M. SHINSENJI, and H. MIYAZAKI,
*Department of Organic Synthesis, Faculty of Engineering, Kyushu University, Fukuoka, Japan*

## Synopsis

2-Vinylthiophene was found to undergo thermal polymerization. With benzene as diluent, the overall rate of polymerization was proportional to the 2.5 power of monomer concentration, suggesting that the thermal initiation is a termolecular process. The following Arrhenius equation was obtained from the polymerization data for the range 55–100°C:

$$k \text{ (overall rate)} = 9.4 \times 10^3 \exp\{-15\,600/RT\}$$

The activation energy of the thermal initiation was estimated to be 28.2 kcal/mole, which was similar to those values obtained for styrene and 2-vinylfuran. When a dilute solution of the monomer in bromobenzene was heated in an ampoule at 151°C, a dimer, mp 82°C, was obtained in a good yield. The spectroscopic data indicated that the dimer was a Diels-Alder type adduct. The initiation of the thermal polymerization was considered to involve hydrogen abstraction by monomer from the Diels-Alder dimer, in common with the initiation of other vinylaromatic monomers.

## INTRODUCTION

Although many investigations have been carried out of thermal polymerization of styrene, corresponding studies on other vinyl compounds are few. The authors previously found that 2-vinylfuran underwent thermal polymerization. The thermal initiation for 2-vinylfuran was a termolecular process,[1] and a Diels-Alder type dimer was formed thermally in bromobenzene.[2] Thus, the initiation mechanism of the thermal polymerization of 2-vinylfuran was considered to involve hydrogen abstraction by monomer from a dimer intermediate, as is the case with styrene.

These results suggest that thermal polymerization will be observed not only for styrene but generally for vinylaromatic monomers and that a common mechanism may exist for the thermal initiation of these monomers. Thus, the thermal polymerization of 2-vinylthiophene was investigated in order to see if the same mechanism was observed.

* Presented in part at the 20th Annual Meeting of the Chemical Society of Japan, Tokyo, Japan, March 1967.

## EXPERIMENTAL

### Preparation of Monomer

2-Vinylthiophene was obtained by chloroethylation of thiophene with paraldehyde and hydrochloric acid, followed by dehydrochlorination with pyridine.[3] The monomer, purified by repeated distillation and dried with Linde molecular sieve 3A, showed a single peak on a gas chromatogram over poly(ethylene glycol) 6 000, bp 60.0°C/42 mm Hg (lit.[3] bp 65–67°C/50 mm Hg).

### Thermal Polymerization

Purified monomer was transferred in a vacuum system ($10^{-5}$ mm Hg) to a Schlenk-type ampoule equipped with breakseal, degassed, and sealed. A small portion of monomer was prepolymerized thermally at 100°C in order to remove impurities which might interfere with the thermal polymerization, and then the breakseal was broken and portions of the unreacted monomer were transferred to polymerization ampoules in the vacuum system. In solution polymerization, ampoules equipped with a stopcock were used. Benzene, carefully purified and dried with $CaH_2$, was used as diluent. Upon transfer of monomer or benzene, the stopcock was closed and the ampoule was detached from the vacuum line, and the quantities of monomer and benzene were determined from the weight difference of the ampoule. In all the polymerizations, the contents of the ampoules were degassed several times by the freeze-pump-thaw method with liquid nitrogen, and the ampoules were sealed under vacuum. After given periods, ampoules were opened and given amounts of toluene were added. The amount of the unreacted monomer was determined by gas chromatography with the use of toluene as an internal standard. The conversions of runs 4–7 (Table II) were, however, determined from the amounts of polymer recovered on pouring the reaction mixture into excess methanol.

### Thermal Dimerization

A bromobenzene solution of monomer (0.306 mole/l.) was placed in an ampoule and degassed. The ampoule was sealed under vacuum, and then heated for 136 hr at 151 ± 1°C in an oil bath. After the reaction, solvent and unreacted monomer were removed under vacuum and the residue was poured into methanol. The precipitate (5 wt-% yield) was separated by centrifugation. Colorless crystals were obtained from the methanol solution upon evaporation of solvent; yield, 69.6 wt-% of monomer. The crystals, mp 81.1–82.1°C after recrystallization from ethanol, showed a single peak on a gas chromatogram.

Anal. Calcd for $(C_6H_6S)_2$: C, 65.41%; H, 5.49%. Found: C, 65.20%; H, 5.59%; Molecular weight, 210 (Vapor Pressure Osmometer, Mechrolab Model 301A).

The methanol-insoluble product was found to be polyvinylthiophene from its infrared spectrum. The molecular weight was 2 100.

### Radical Polymerization of Styrene

Given amounts of azobisisobutyronitrile, styrene, and the dimer of 2-vinylthiophene were added to an ampoule and weighed. The content was degassed in a Dry Ice–methanol bath, and the ampoule was sealed. After a given period, the reaction mixture was poured into methanol and then the white precipitate formed was washed with methanol and dried.

### Miscellaneous

Benzene was washed with sulfuric acid and aqueous alkali, refluxed over sodium, and distilled. Bromobenzene was washed with concentrated sulfuric acid, refluxed several days over $P_2O_5$, and distilled. Measurements of infrared and NMR spectra were made on a Nippon-Bunko DS 301 spectrometer and a Varian A-60 spectrometer, respectively.

## RESULTS

### Structure of the Thermal Dimer

The colorless needles obtained thermally in bromobenzene was shown to be a dimer of 2-vinylthiophene from the results of elemental analysis and molecular weight determination. The infrared spectrum of the dimer, shown in Figure 1, possesses the characteristic absorptions of the thiophene ring[4] at 3 130, 1 520, 1 040, and 700 $cm^{-1}$, in common with those in the monomer and polymer spectra. On the other hand, characteristic peaks of the vinyl group in monomer (1 623, 975, and 895 $cm^{-1}$) were lost in Figure 1.

TABLE I
NMR Spectral Assignment

| | Peak A | Peak B | Peak C | Peak D |
|---|---|---|---|---|
| Chemical shift, ppm[a] | 6.80 (multiplet) | 4.20 (triplet) | 2.78 (triplet) | 1.93 (multiplet) |
| Area ratio | 5.0 | 1.1 | 1.9 | 4.1 |
| Assignment | a | b | c | d |
| Number of protons | 5 | 1 | 2 | 4 |

[a] TMS internal standard; $J_{bd}$ = 6 cps.

The NMR pattern of the dimer (Fig. 2) is quite similar to that of 1-phenyltetralin[5] (the Diels-Alder type dimer of styrene) and to that of the thermal dimer of 2-vinylfuran.[2] Thus, similar assignments may be made as in Table I. The area ratios obtained from the integration curve agreed with the proposed structure (I).

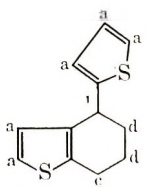


I

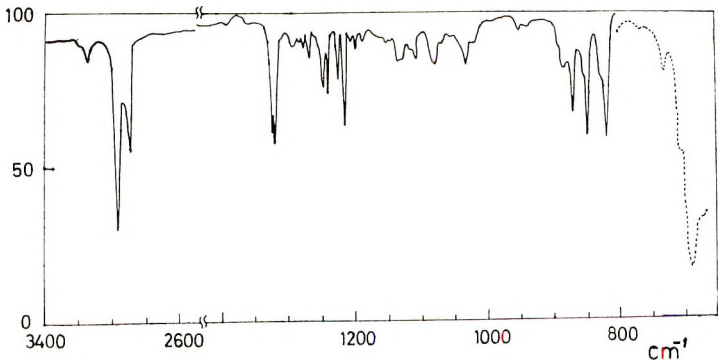


Fig. 1. Infrared spectrum of the thermal dimer of 2-vinylthiophene: (——) in $CCl_4$; (· ·) in $CS_2$.

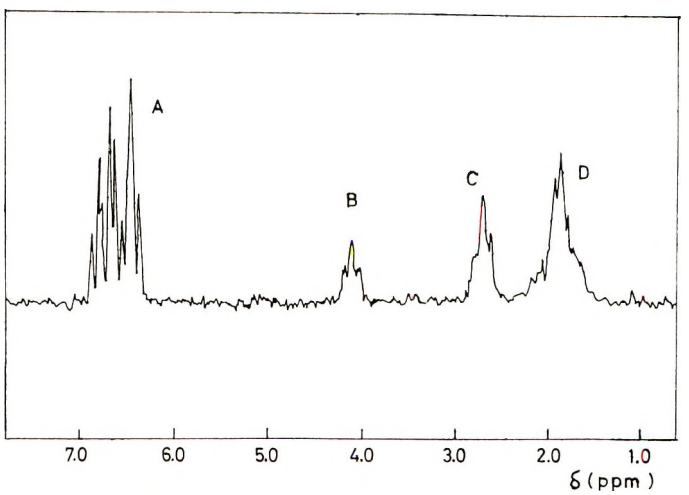


Fig. 2. NMR spectrum of the thermal dimer of 2-vinylthiophene. $CCl_4$ solution, TMS internal standard.

## Time–Conversion Relation and Formation of the Dimer

Table II and Figure 3 give the time–conversion relation at 100°C. The conversion increased with the polymerization period, and the product consisted of approximately equal amounts of the methanol-soluble and methanolinsoluble fractions. The product of Table II, run 6 was further investigated. On removing the solvent the methanol-soluble fraction gave colorless crystals, mp 78.5–81.0°C, which was identified as the Diels-Alder dimer mentioned above, on the basis of its molecular weight (221), elemental analysis, infrared spectroscopy, and gas chromatography. The methanol-in-

TABLE II
Bulk Polymerization at 100°C

| Run no. | Monomer, g | Polymerization period, min | Polymer obtained, g | | Conversion, % |
|---|---|---|---|---|---|
| | | | Soluble in $CH_3OH$ | Insoluble in $CH_3OH$ | |
| 1 | 1.494 | 45 | — | — | 8.75[a] |
| 2 | 1.647 | 90 | — | — | 12.40[a] |
| 3 | 0.675 | 123 | — | — | 12.14[a] |
| 4 | 0.848 | 300 | 0.078 | 0.095 | 20.32 |
| 5 | 1.173 | 600 | 0.198 | 0.179 | 32.20 |
| 6 | 4.860 | 1500 | 0.995 | 1.457 | 50.47 |
| 7 | 0.653 | 1800 | 0.160 | 0.146 | 46.85 |

[a] Determined by gas chromatography of the unreacted monomer.

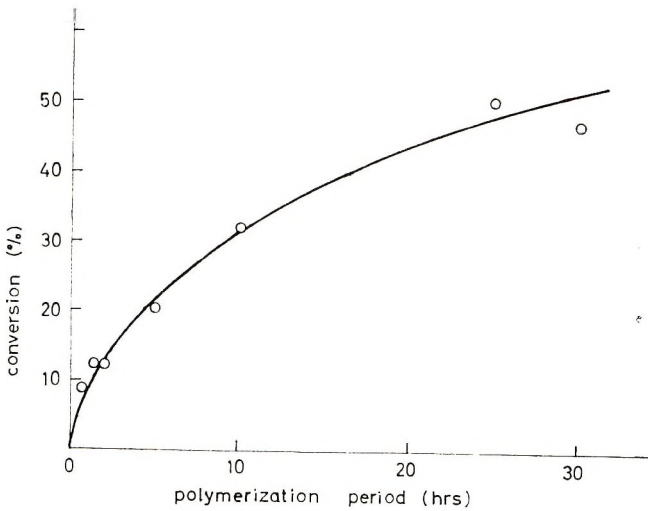


Fig. 3. Time–conversion curve at 100°C.

soluble fraction gave an infrared spectrum which was identical with that of polyvinylthiophene, and its molecular weight was 3900. Thus, in thermal polymerization of bulk monomer at 100°C, the polymer and the Diels-Alder type dimer were obtained in approximately equal amounts, as in eq. (1), and other products, 1,2-disubstituted cyclobutane and linear dimers as in the thermal oligomerization of styrene,[6,7] were not formed.

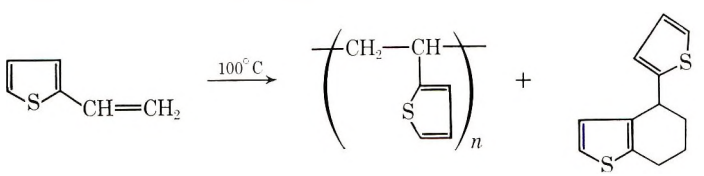


(1)

The subsequent polymerizations were carried out at lower temperatures in order to avoid the complexity which would arise from the dimer formation.

In fact, the methanol-soluble fraction was recovered only in trace amounts in the polymerizations at 80 and 60°C.

## Effect of Monomer Concentration on the Rate of Polymerization

Table III shows the effect of monomer concentration on the overall rate of the thermal polymerization at 59.7°C with benzene used as diluent. The logarithmic plots of rate versus monomer concentration were linear as shown in Figure 4. Its slope (2.46) indicated that the overall rate was proportional to the 2.5 power of monomer concentration.

TABLE III
Dependence of Overall Rate of Polymerization on Monomer Concentration at 59.7°C

| Run no. | Monomer, g | Benzene, g | Monomer concentration, mole/l.[b] | Polymerization period, min | Conversion, % | Overall rate $\times 10^6$, mole/l.-sec |
|---|---|---|---|---|---|---|
| 1[a] | 0.803 | 0 | 9.17 | 825 | 8.70 | 16.10 |
| 2 | 2.019 | 0 | 9.16 | 617 | 7.44 | 18.40 |
| 3 | 1.052 | 0.346 | 6.56 | 1402 | 10.07 | 7.85 |
| 4 | 1.910 | 0.920 | 5.79 | 1441 | 5.25 | 3.52 |
| 5 | 1.744 | 1.536 | 4.44 | 1833 | 7.58 | 3.06 |
| 6 | 1.128 | 1.444 | 3.60 | 2480 | 7.02 | 1.70 |

[a] Polymerization temperature: 59.0°C.

[b] Densities were calculated by using the following equations: for benzene,[8] $d_4^t = 0.9004 - 0.00109t$ for 2-vinylthiophene, $d_4^t = 1.062 - 0.000885t$ (obtained from $d_4^{20} = 1.044$[9] assuming a temperature coefficient equal to that of styrene[10]).

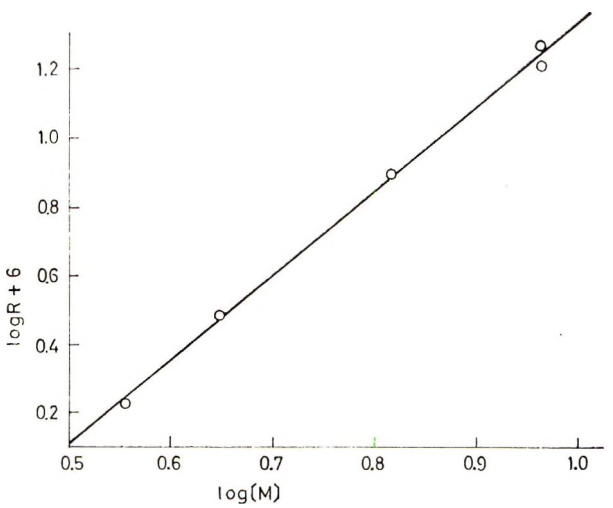


Fig. 4. Dependence of the overall rate on the monomer concentration at 59.7°C.

## Activation Energy of the Thermal Polymerization

Thermal polymerizations of bulk 2-vinylthiophene were carried out at several temperatures between 55 and 100°C. The results are given in Table IV. The overall rate constant $k$ was obtained from eq. (2) by dividing the overall rate $R$ by the 2.5 power of monomer concentration. Figure 5 shows the logarithmic plots of $k$ versus monomer concentration. From the slope of the linear relation was obtained the activation energy for the overall rate: 15.6 kcal/mole.

TABLE IV
Dependence of Overall Rate of Bulk Polymerization on Temperature

| Run no. | Polymerization temperature, °C | Polymerization time, min | Monomer, g | Monomer concentration, mole/l.[a] | Conversion, % | Overall rate × $10^5$, mole/l.-sec |
|---|---|---|---|---|---|---|
| 1 | 55.0 ± 0.1 | 1147 | 1.444 | 9.19 | 6.57 | 0.88 |
| 2 | 59.0 ± 0.1 | 825 | 0.803 | 9.17 | 8.70 | 1.61 |
| 3 | 59.7 ± 0.1 | 825 | 2.019 | 9.16 | 7.44 | 1.84 |
| 4 | 65.5 ± 0.1 | 600 | 1.441 | 9.11 | 6.17 | 1.56 |
| 5 | 75.0 ± 0.1 | 245 | 1.185 | 9.04 | 7.38 | 4.54 |
| 6 | 89.5 ± 0.5 | 120 | 0.669 | 8.92 | 6.15 | 7.61 |
| 7 | 100 ± 0.5 | 45 | 1.494 | 8.83 | 8.75 (4.38)[b] | 20.3 (10.2)[b] |

[a] Densities calculated as described in Table III.

[b] This value corresponds to the consumption of monomer minus dimer formation.

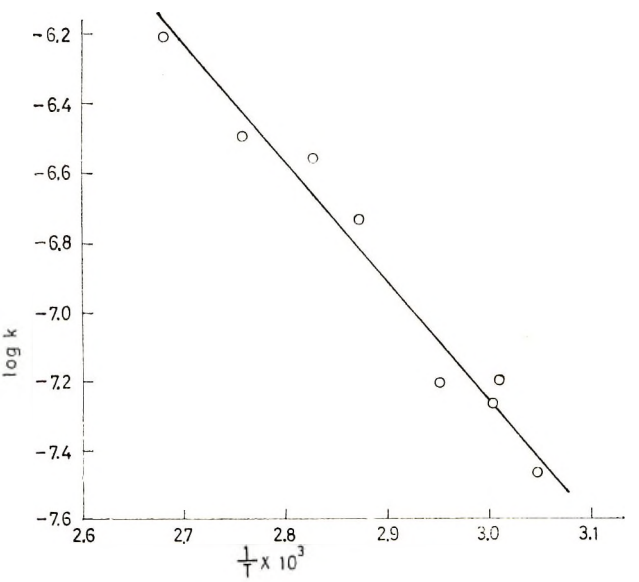


Fig. 5. Arrhenius plots.

## Chain Transfer Constant of the Dimer

The dimer which was produced during thermal polymerization, contains an active hydrogen and conceivably acts as a chain transfer agent. Thus the chain transfer constant of the dimer was determined in the radical polymerization of styrene. Table V contains the results. The transfer constant can be obtained from eq. (2) as given by Mayo:[11]

$$\frac{1}{\overline{DP}} = \frac{1}{\overline{DP}_0} + C_{dimer}\frac{[D]}{[M]} \tag{2}$$

where $\overline{DP}$ is the degree of polymerization in the presence of the transfer agent, $\overline{DP}_0$ is the degree of polymerization in the absence of the transfer agent, [D] is the concentration of the transfer agent (i.e., the thermal dimer) and $C_{dimer}$ ($= k_{tr}/k_p$) is the chain transfer constant. From the plots of $1/\overline{DP}$ versus [D]/[M] shown in Figure 6, $C_{dimer}$ was determined to be $1.1 \times 10^{-2}$.

TABLE V
Chain Transfer by the Vinylthiophene Dimer in Bulk Polymerization of Styrene[a]

| Run no. | Styrene, g[b] | (Dimer)/(Styrene) × $10^2$ | Polymer obtained, g | Conversion, % | $[\eta]_{C_6H_6}^{30°}$ | $\overline{M}_n$[c] |
|---|---|---|---|---|---|---|
| 1 | 5.29 | 0 | 0.423 | 8.00 | 0.548 | 73,300 |
| 2 | 5.29 | 0.46 | 0.443 | 8.38 | 0.532 | 70,500 |
| 3 | 5.31 | 1.43 | 0.436 | 8.22 | 0.505 | 65,500 |
| 4 | 5.32 | 2.30 | 0.441 | 8.29 | 0.486 | 62,100 |

[a] Initiator, AIBN, $2.1 \times 10^{-3}$ mole/l., polymerization temperature, 60°C; polymerization period, 2 hr.
[b] 8.25 mole/l.
[c] Calculated from[6] $\overline{M}_n = 167000[\eta]^{1.37}$.

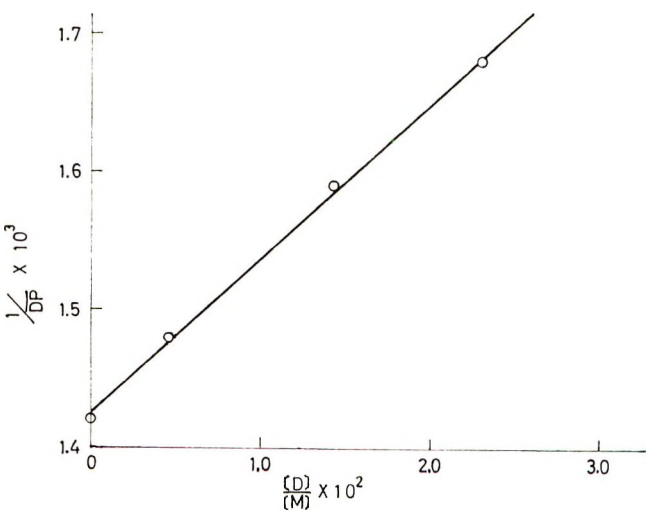


Fig. 6. Chain transfer by the thermal dimer in the bulk polymerization of styrene.

## DISCUSSION

In general, the thermal polymerization is believed to occur via the processes of initiation, propagation, and termination as follows:[12a]

Initiation: $\alpha M \rightarrow M\cdot$
with $R_i = k_i[M]^\alpha$

Propagation: $M_n^{\cdot} + M \rightarrow M\cdot_{n+1}$
with $R_p = k_p [M] [M\cdot]$.

Termination: $M_n^{\cdot} + M_m^{\cdot} \rightarrow M_{n+m}$ and/or $M_n + M_m$
with $R_t = k_t [M\cdot]^2$.

The propagation and termination processes are considered to be analogous to those of the usual radical polymerization. As for the termination process, the polystyryl radical is known to terminate predominantly by radical combination.[12b] Similarly, the propagating radical of 2-vinylfuran was assumed to undergo mostly the bimolecular termination.[13] Thus the bimolecular termination may be assumed for thermal (i.e., radical) polymerization of 2-vinylthiophene.

The overall rate of polymerization $R$ can be expressed in eq. (3):

$$R = -d[M]/dt = k[M]^n = k[M]^{\frac{\alpha}{2}+1}$$

where

$$k = k_p(k_i/k_t)^{1/2} \tag{3}$$

Since $n = 2.5$, $\alpha = 3$ from eq. (3) if benzene is considered to be simply a diluent. Then thermal initiation is concluded to be a termolecular process. The termolecular initiation has been observed for styrene by Hiatt and Bartlett[14] and for 2-vinylfuran in these laboratories.[1] The overall rate constant $k$ is expressed as follows from the Arrhenius plot of Figure 5.

$$k = 9.4 \times 10^2 \cdot \exp\{-15{,}600/RT\} \tag{4}$$

According to Flory,[12a] the activation energy for the thermal initiation can be estimated as follows. The overall activation energy of the radical polymerization of 2-vinylthiophene (benzoyl peroxide initiation) was found by Koton[15] to be 16.5 ± 0.5 kcal/mole. Assuming that the activation energy for the homolytic decomposition of benzoyl peroxide 30.0 kcal/mole[16] is equal to that for the radical initiation $E_i$, the activation energy for the thermal initiation $E_i'$ can be obtained from the comparison of overall activation energies of the initiator polymerization and the thermal polymerization ($E$ and $E'$).

$$E = E_p + 1/2(E_i - E_t) \tag{5}$$

$$E' = E_p + 1/2(E_i' - E_t) \tag{6}$$

where $E_p$ and $E_t$ are common for both polymerizations.

Thus, the activation energy for the thermal initiation is calculated to be 28.2 kcal/mole. This value is close to the corresponding activation energies of 2-vinylfuran (30.0 kcal/mole) obtained previously and of styrene (28.9 kcal/mole) obtained by Mayo.[6]

The initiation mechanism of the thermal polymerization of styrene has been discussed extensively, and two hypotheses—bimolecular initiation and termolecular initiation—have been put forward. Recently, Kirchner carried out the thermal polymerization of several deuterated styrenes and observed the decrease in the overall rate only for the *ortho-d*-substituted styrene. Thus he suggested that the hydrogen abstraction from the *ortho* position is an important step in the thermal initiation.[17] This result supports the mechanism proposed by Mayo that the Diels-Alder type dimer was involved in the thermal initiation of styrene.[7]

As mentioned above, 2-vinylthiophene thermally gave the Diels-Alder type dimer and the initiation of the thermal polymerization was found to be a termolecular process. These results strongly suggest the following initiation mechanism which is analogous to that of styrene.

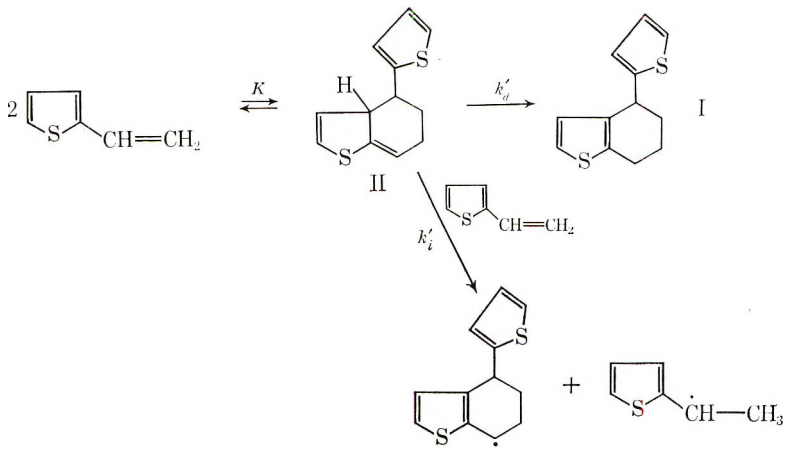


The Diels-Alder reaction of the monomer gives a dimer intermediate (II), of which hydrogen is abstracted by a third monomer molecule to form initiating radicals. The intermediate II may rearrange to a more stable dimer (I). Considering the occurrence of thermal polymerizations for styrene, 2-vinylfuran and 2-vinylthiophene, and their kinetic similarity, this mechanism may generally hold for the thermal polymerization of most vinylaromatic monomers. Vinylaromatic monomers will tend more or less to undergo the Diels-Alder dimerization. The hydrogen atom at the bridge-head in the dimer formed will readily be abstracted, or migrate, since the resonance energy of the aromatic ring is increased by these reactions. Thus, the rate of the thermal initiation will depend on the ease of formation of the unstable Diels-Alder adduct and on the ease of hydrogen abstraction from the adduct. The closeness of the activation energy of the thermal initiation of the three monomers would point to fairly constant $k'K$ values.

The same mechanism was applied to autoxidation of styrene by Dulog who considered that the initiation of the autoxidation involved the hydrogen abstraction by an oxygen molecule from the Diels-Alder dimer.[18]

On the other hand, the bimolecular initiation has been also discussed in connection with the ambiguity of the molecularity of the overall rate of thermal polymerization. Flory first considered the bimolecular biradical initiation, but rejected it on the ground that the biradical would possess an overwhelming tendency to undergo intramolecular coupling.[12a] Recently, Kirchner and Patat[19] suggested a bimolecular initiation mechanism which involved the hydrogen transfer between two styrene molecules, yielding two monoradicals. This mechanism was adopted by Gelhaar and Ueberreiter,[20] who proposed that the thermal polymerization of acenaphthylene was initiated by the bimolecular mechanism probably because of the steric reason.

Since the initiating radical in thermal polymerization is formed by abstraction of a labile hydrogen by a monomer molecule, it is conceivable that radical polymerization may be initiated by hydrogen abstraction. Thus a hydrocarbon with readily abstracted hydrogen would serve as initiator. In fact, triphenylmethane and fluorene were found to initiate polymerization of acrylonitrile at high temperatures.[21] This result may support the generality of the hydrogen abstraction by a monomer molecule as a means of the initiation of radical polymerization.

The molecular weights of poly-2-vinylthiophene obtained by thermal polymerization were at most several thousands. Since the chain transfer constant of the dimer was $1.1 \times 10^{-2}$ in polymerization of styrene, chain transfer to the dimer would be one of the major reasons for the comparatively low molecular weight obtained. Similarly, in the thermal polymerization of styrene, the molecular weight of polymer decreased rapidly with the increase in conversion at the very low conversion[22,23] and the decrease was found to be caused not by transfer to monomer[24] but by chain transfer to 1-phenyltetralin which was formed along with thermal polymerization.[25] Its chain transfer constant calculated from Müller's data[25] was $8 \times 10^{-3}$, in fair agreement with the value for the dimer of 2-vinylthiophene. The dimer I, though an effective transfer agent, does not seem to affect the kinetic pattern of termination, since addition of the dimer did not lower the conversion (Table V).

## References

1. C. Aso, T. Kunitake, Y. Tanaka, and H. Miyazaki, *Kobunshi Kagaku*, **24**, 187 (1967).
2. C. Aso, T. Kunitake, and Y. Tanaka, *Bull. Chem. Soc. Japan*, **38**, 675 (1965).
3. W. S. Emerson and T. M. Patrick, *J. Org. Chem.*, **13**, 729 (1948).
4. K. Nakanishi, *Infrared Spectroscopy*, Nankodo, Tokyo, 1960, p. 56.
5. H. Miyazaki, Master's Thesis, Kyushu University, 1966, p. 20.
6. F. R. Mayo, *J. Amer. Chem. Soc.*, **75**, 6133 (1953).
7. F. R. Mayo, *J. Amer. Chem. Soc.*, **90**, 1289 (1968).
8. Beilstein, *Handbuch der Chemie*, E II-5, p. 123.
9. R. T. Nazzaro and J. L. Bullock, *J. Amer. Chem. Soc.*, **68**, 2122 (1946).

10. M. Kotake, Ed., *Comprehensive Organic Chemistry*, Vol. 22, Asakura, Tokyo, Japan, 1958, p. 157.
11. F. R. Mayo, *J. Amer. Chem. Soc.*, **65**, 2324 (1943).
12. P. J. Flory, *Principles of Polymer Chemistry*, Cornell Univ. Press, Ithaca, New York, 1953, (a) p. 131; (b) p. 111.
13. C. Aso and Y. Tanaka, *Kobunshi Kagaku*, **21**, 373 (1964).
14. R. R. Hiatt and P. D. Bartlett, *J. Amer. Chem. Soc.*, **81**, 1149 (1959).
15. M. M. Koton, *J. Polym. Sci.*, **30**, 331 (1958).
16. Y. Yukawa, *Constants of Organic Compounds*, Asakura Shoten, Tokyo, 1963, p. 735.
17. K. Kirchner, *Makromol. Chem.*, **96**, 179 (1966).
18. L. Dulog, *Makromol. Chem.*, **76**, 119 (1964).
19. K. Kirchner and F. Patat, *Makromol. Chem.*, **37**, 251 (1960).
20. H. G. Gelhaar and K. Ueberreiter, *Kolloid Z. Z. Polymere*, **209**, 136 (1966).
21. M. Shinsenji, these laboratories, unpublished results.
22. A. Lebovits and W. C. Teach, *J. Polym. Sci.*, **47**, 527 (1960).
23. H. Benoit and C. Loucheux, *C. R. Acad. Sci.* (Paris), **251**, 382 (1960).
24. C. Henrici-Olivé and S. Olivé, *Makromol. Chem.*, **53**, 122 (1962).
25. K. F. Müller, *Makromol. Chem.*, **79**, 128 (1964).

Received December 18, 1968

JOURNAL OF POLYMER SCIENCE: PART A-1 VOL. 7, 1509–1515 (1969)

# Synthesis of Polymerizable Tetrafluorohydrazine–Diene Addition Compounds

SAMUEL F. REED, JR.,
*Redstone Research Laboratories, Rohm and Haas Company,*
*Huntsville, Alabama 35807*

## Synopsis

The reaction of tetrafluorohydrazine with alkenyl acrylates and methacrylates under appropriate conditions resulted in the isolation of olefinic bis(difluoramines) capable in some instances of undergoing free-radical-initiated polymerization and copolymerization. Monomer and polymer synthesis and characterization are discussed.

## INTRODUCTION

The tetrafluorohydrazine ($N_2F_4$)–olefin addition reaction[1] has been extended to include the reactions of $N_2F_4$ with a number of unconjugated dienes. Vinyl, allyl, and methallyl esters of acrylic and methacrylic acids were employed as the diene substrates in vapor-phase reactions conducted under flow conditions at temperature of 200–300°C. Conditions were selected to ensure mono addition of $N_2F_4$ to the diene and the formation of olefinic bisdifluoramines. Free-radical polymerization of the adducts and copolymerization with methyl methacrylate and styrene showed that the polymerizability of the monomer was dependent upon the nature of the olefinic bond. In general, their polymerization character conformed to that of similar unsubstituted monomers. This paper presents the first study describing the polymerization of vinyl compounds containing the difluoramino group.

## EXPERIMENTAL

The esters were purchased from commercial sources and distilled just prior to use in the reactions. The tetrafluorohydrazine employed was of 95% purity containing CF compounds as impurities. Infrared spectra were obtained with a Perkin-Elmer Infracord spectrophotometer using a sodium chloride prism; an Aerograph Instrument, Model A-100-C with a 5′-dinonyl phthalate on Chromosorb column was used for all gas chromatography work.

The preparative reactions were conveniently carried out in a flow reactor composed of feed lines for $N_2F_4$ and helium connected through separate

calibrated flow meters into a single line to the reactor, a copper coil 1/4 in. in diameter and 25 ft. in length. The dienes were introduced into the feed line from a calibrated power-driven syringe at a point just prior to its entrance into the heated reactor. The reactor was completely enclosed in an electrical furnace and the temperature measured by means of thermocouples placed within the furnace immediately adjacent to the reactor coil. An exit line from the reactor was passed through a series of cold traps cooled in the order −80°C, −130°C, and −196°C. In practice, the organic materials from the reactor were always collected in the −80°C trap while residual $N_2F_4$ was collected in the −196°C trap. Reactions were started by first flushing the system at a given temperature with helium, and while maintaining the helium flow at the desired level both $N_2F_4$ and diene flows were started. On completion of the reaction, the helium flow was continued for 15 min. Contents of the −196°C trap were found by mass spectroscopic analysis to be $N_2F_4$, CF compounds, and $SiF_4$. The major part of the organic materials contained in the −80°C trap were transferred through a second series of traps cooled to −80, −130, and −196°C to ensure removal of any dissolved $N_2F_4$. After opening to the air remotely, the contents of the second −80°C trap were removed and subjected to vacuum distillation. A summary of typical experimental conditions for these reactions is presented in Table I.

TABLE I
Experimental Data for $N_2F_4$–Diene Reactions

| Diene | Wt diene, flow | Helium flow rate ml/min | $N_2F_4$ flow rate ml/min | Diene flow rate, ml/min | Temp, °C | Yield adducts, g | Yield, % |
|---|---|---|---|---|---|---|---|
| Vinyl acrylate | 14.39 | 35 | 25 | 0.14 | 235 | 3.9 | 13.2 |
| Vinyl methacrylate | 14.59 | 35 | 30 | 0.13 | 230 | 10.2 | 36.3 |
| Allyl acrylate | 13.76 | 50 | 25 | 0.18 | 245 | 3.53 | 14.1 |
| Allyl methacrylate | 14.08 | 50 | 25 | 0.13 | 230 | 8.55 | 31.5 |
| Methallyl acrylate | 13.0 | 40 | 60 | 0.19 | 225 | 1.36 | 5.7 |
| Methallyl methacrylate | 13.6 | 45 | 60 | 0.20 | 235 | 2.96 | 12.5 |

Polymerization of the adducts was carried out in benzene solution with the use of azobisisobutyronitrile (AIBN) as the initiator. Each reaction was conducted by adding the adduct (0.01 mole) to 25 ml of benzene containing AIBN (0.0001 mole) in a thick-walled glass Aerosol tube, the system deaerated by passing through three freeze-thaw cycles on a vacuum line, and the reactor placed in an oil bath at 65°C for a period of 24 hr. On cooling, the solution was poured into 500 ml of methanol and the precipitated polymer collected by filtration. On drying under vacuum

the polymers were weighted. Samples for viscosity and elemental analysis were reprecipitated a second time from benzene–methanol. Viscosities of the polymers were run in acetone at 30.0°C in Ubbelohde-type viscometers.

Similar techniques were employed for the copolymerization reactions. A mixture of comonomers (0.01 mole of each) were copolymerized in benzene with 1 mole-% AIBN. Experimental conditions and isolation of copolymers were as described above.

## RESULTS

In reactions involving the alkenyl acrylate esters, a mixture of two products was obtained. These products resulted from competitive addition of $N_2F_4$ to both sites of unsaturation in the diene substrates and their relative ratio was dependent upon the reactivity of the different carbon-carbon double bonds present. Structures I and II were assigned to the two products from each reaction on the basis of the analytical data.

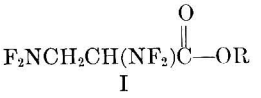

I

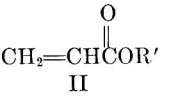

II

R = (a) —CH=CH$_2$
(b) —CH$_2$CH=CH$_2$
(c) —CH$_2$C(CH$_3$) = CH$_2$

R′ = (a) —CH(NF$_2$)CH$_2$NF$_2$
(b) —CH$_2$CH(NF$_2$)CH$_2$NF$_2$
(c) —CH$_2$C(CH$_3$)(NF$_2$)CH$_2$NF$_2$

The product ratios were determined by measurement of peak areas on gas-liquid chromatographic (GLC) analysis. Adducts of type I represented the major components of the mixtures in all reactions, varying from a ratio of 2.5:1 for the vinyl ester (Ia:IIa) to 3.5–4.0:1 for the allylic esters (Ib, Ic, IIb, IIc). Instability was noted in products of type I which displayed a tendency to eliminate HF from the carbon atom adjacent to the carbonyl group[1] upon standing at ambient temperature for several days. Storage at temperatures below 0°C reduced this decomposition to acceptable limits for short periods of time.

The methacrylate esters gave predominately products of structure III. Only the vinyl ester gave a significant quantity of a second product of structure IV. The product ratio in this reaction was approximately 11:1.

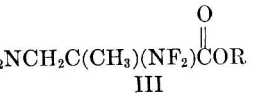

III

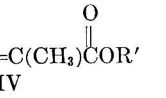

IV

R = (a) —CH=CH$_2$
(b) —CH$_2$CH=CH$_2$
(c) —CH$_2$C(CH$_3$)=CH$_2$

R′ = (a) —CH(NF$_2$)CH$_2$NF$_2$
(b) —CH$_2$CH(NF$_2$)CH$_2$NF$_2$
(c) —CH$_2$C(CH$_3$)(NF$_2$)CH$_2$NF$_2$

Both the allyl and methallyl esters yielded only trace quantities of IVb and IVc. No difficulty was experienced with the stability of these products.

All adducts were isolated either pure or as two component mixtures by distillation at reduced pressure. Yields under our experimental conditions were low (in the range 10–40%). In every instance the yield from the

methacrylate was greater than from the corresponding acrylate. Each two-component mixture was further separated in quantities sufficient for analysis by preparative gas chromatography. It was found that GLC could be employed for identification of the adducts when present in the mixtures, since adducts of type II or IV were eluted from the column before I or III. Characterization of the products was accomplished by their infrared spectra and elemental analysis (Table II). In most instances the analysis for fluorine and nitrogen were satisfactory, however, it may be noted that the values for fluorine are slightly low while nitrogen values are high in the acrylate series. These results were typical and are attributed to the occurrence of limited decomposition prior to analysis.

TABLE II
Characterization Data for $N_2F_4$–Diene Monoadducts

| Adduct | Bp, °C/mm (mixture) | Infrared absorption, cm$^{-1}$[a] C=O | C=C | Calculated F, % | N, % | Found F, % | N, % |
|---|---|---|---|---|---|---|---|
| Ia | 64–66/24 | 1782 | 1646 | 37.65 | 13.75 | 36.2 | 13.99 |
| IIa | | 1723 | 1630 | 37.65 | 13.75 | 37.8 | 13.95 |
| Ib | 68/28 | 1761 | 1651 | 35.18 | 12.96 | 34.7 | 13.32 |
| IIb | | 1721 | 1634 | 35.18 | 12.96 | 35.1 | 13.10 |
| Ic | 46–48/3 | 1759 | 1648 | 35.03 | 12.17 | 34.7 | 12.6 |
| IIc | | 1723 | 1633 | 35.03 | 12.17 | 34.9 | 12.0 |
| IIIa | 46–47/1 | 1785 | 1643 | 35.18 | 12.96 | 35.3 | 12.6 |
| IVa | | 1720 | 1637 | 35.18 | 12.96 | 34.9 | 12.8 |
| IIIb | 41/1 | 1755 | 1635 | 33.03 | 12.17 | 32.7 | 17.3 |
| IVb | 60/3 | 1757 | 1635 | 31.14 | 11.47 | 31.3 | 11.4 |

[a] $NF_2$ group absorption occurred in the region of 800–1000 cm$^{-1}$.

Polymerization studies were conducted using 2,2′-azobisisobutyronitrile as initiator. These reactions were conducted in deaerated benzene solution at 60°C for 24-hr periods. Only with adduct mixtures Ia–IIa and IIIa–IVa did homopolymerization occur to a satisfactory extent. In both instances a glasslike polymer was obtained. Copolymerization of each adduct (or mixture) with methyl methacrylate and styrene occurred readily to give copolymers containing difluoramino groups. Characterization of the polymers and copolymers was performed by measurement of intrinsic viscosity $[\eta]$ and elemental analysis (Table III).

## DISCUSSION

Under flow conditions the addition of $N_2F_4$ to the alkenyl acrylates and methacrylates occurred with formation of bisdifluoramines. Only limited quantities of the tetrakisdifluoramines were present and these were easily separated from the bisdifluoramines by distillation. No attempt was made towards the characterization of the high-boiling residues. Reaction temperatures were maintained in the range of 225–260°C to effect the

TABLE III
Characterization Data on Polymers and Copolymers of Monomeric Bis(difluoramines)

| Adduct | Co-monomer | Yield, % | [η], dl/g | Calculated | | Found | |
|---|---|---|---|---|---|---|---|
| | | | | F, % | N, % | F, % | N, % |
| Ia–IIa | — | 98 | 0.46 | 24.83 | 9.15 | 24.15 | 9.2 |
| Ia–IIa | MMA | 94 | 0.43 | 18.72 | 6.89 | 16.75 | 6.6 |
| Ia–IIa | Styrene | 87 | 0.31 | 18.54 | 6.83 | 16.9 | 6.5 |
| Ib–IIb | MMA | 63 | 0.19 | 18.09 | 6.66 | 13.4 | 5.2 |
| Ib–IIb | Styrene | 66 | 0.14 | 17.92 | 6.60 | 12.4 | 5.6 |
| Ic–IIc | MMA | 60 | 0.14 | 17.51 | 6.45 | 11.1 | 5.1 |
| Ic–IIc | Styrene | 63 | 0.11 | 17.35 | 6.39 | 10.9 | 4.9 |
| IIIa–IVa | — | 94 | 0.41 | 23.75 | 8.75 | 23.4 | 8.7 |
| IIIa–IVa | MMA | 91 | 0.39 | 18.09 | 6.66 | 17.8 | 6.4 |
| IIIa–IVa | Styrene | 84 | 0.30 | 17.92 | 6.60 | 17.8 | 6.5 |
| IIIb | MMA | 41 | 0.14 | 17.51 | 6.45 | 8.8 | 3.6 |
| IIIb | Styrene | 35 | 0.09 | 17.35 | 6.39 | 8.0 | 3.2 |
| IIIc | MMA | 40 | 0.09 | 16.96 | 6.25 | 7.1 | 2.9 |
| IIIc | Styrene | 36 | 0.07 | 16.81 | 6.19 | 6.5 | 2.6 |

addition. Under these conditions mono addition predominated to give moderate yields of the bisdifluoramines with insignificant decomposition products. At higher temperatures (>300°C), decomposition did occur, and coke formation was observed resulting at times in complete plugging of the reactor. Yields for the alkenyl acrylates ranged from 6 to 14% and from 12 to 36% for the methacrylates.

In all instances, there were competitive reactions taking place such that a mixture of two bisdifluoramines were obtained. From the yield of product and the product ratios, one can ascertain the relative reactivity of the different types of carbon–carbon double bonds to addition of $N_2F_4$. These series of compounds contain five carbon-carbon double bonds of a slightly different character. Our data indicate that the unsaturation found in the methacrylate

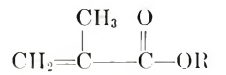

is the most reactive with the other unsaturated groups following in the order of decreasing reactivity: acrylate, $CH_2$=CHCOOR; vinyl ester, —OCH=$CH_2$; allyl —$CH_2CH$=$CH_2$; and methallyl, —$CH_2C(CH_3)$=$CH_2$. The relative reactivities are apparent when comparing the yields of methacrylates with acrylates and when comparing products of types I and III with II and IV.

The monomeric bisdifluoramines were subjected to free-radical-initiated polymerization reactions with the use of 1 mole-% 2,2′-azobisisobutyronitrile. Only product mixtures Ia–IIa and IIIa–IVa polymerized to give significant yields of polymer. In these reactions, mixtures were composed of either an acrylate or methacrylate and a vinyl ester and the polymeriza-

tion proceeded as expected following the general polymerization character of alkyl acrylates or methacrylates[2] and vinyl esters.[3] The intrinsic viscosities were 0.46 and 0.41 dl/g, respectively, which compare favorably with that of poly(methyl methacrylate) (0.49 dl/g) prepared under identical conditions. In both instances the analysis of fluorine and nitrogen were satisfactory; however, all polymerizations with the acrylate were carried out with freshly distilled monomers exhibiting limited decomposition. Nevertheless, the polyacrylates were slightly colored and continued to darken on standing indicating further decomposition.

Monomer mixtures Ib–IIb, Ic–IIc, and IIIb and IIIc did not homopolymerize to any significant extent. In all instances the polymerizations gave liquid product mixtures containing large quantities of the monomeric compounds. No attempts were made to characterize these materials. This behavior is typical of compounds containing allyl unsaturation.[4–6]

Each mixture was copolymerized with methyl methacrylate (MMA) employing a 50/50 mole ratio with 1 mol-% AIBN. Mixtures Ia–IIa and IIIa–IVa copolymerized as expected to give good yields of the copolymer showing reasonably high intrinsic viscosities and good fluorine-nitrogen analysis. When the other monomer mixtures containing high ratios of the adducts of type I or III were used as comonomers, the yield, intrinsic viscosity, and proportion of adduct entering into the polymerization decreased markedly. In general, these values were slightly lower for the methallyl monomers than for the allyl. These results may be explained by the general character of allylic compounds to undergo degradative chain transfer[4–6] when subjected to free radical polymerization.

The copolymerizations of these monomers with styrene showed the same general behavior. Mixtures Ia–IIa and IIIa–IVa copolymerized reasonably well to give copolymers possessing intrinsic viscosities near that of polystyrene (0.35 dl/g) prepared under similar conditions. Although a freshly distilled acrylate monomer mixture (Ia–IIa) was employed, the fluorine analysis was indicative of partial decomposition having occurred during the reaction. Very low molecular weight copolymers containing less than the calculated fluorine-nitrogen content were obtained from the other comonomer mixtures.

## Summary

The preparation of mixtures of monomeric bisdifluoramines from alkenyl acrylates and methacrylates and $N_2F_4$ in vapor-phase reactions conducted under flow conditions has been demonstrated. Each mixture was composed of an acrylate or methacrylate and a vinyl or allylic ester. In all instances the vinyl or allylic ester represented the major product. Polymerization of the mixtures containing the vinyl ester adducts gave high molecular weight polymers with compositions approximating that of the comonomer charge. In contrast, the allylic or methallylic ester-containing mixtures homopolymerized very poorly. A series of copolymerization

reactions of the monomeric bisdifluoramines with MMA and styrene showed that the vinyl esters copolymerized normally, whereas the allylic and methallylic esters caused pronounced lowering of the copolymer's molecular weight and the resulting composition of the copolymer showed much lower incorporation of the adduct into copolymer than present in the comonomer charge. It was apparent that the adduct mixtures from the alkenyl acrylates exhibit a tendency to decompose with loss of hydrogen fluoride.

This work was carried out under the sponsorship of the U. S. Army Missile Command Redstone Arsenal, Alabama, under Contract DA-01-021-ORD-5135.

## References

1. R. C. Petry and J. P. Freeman, *J. Org. Chem.*, **32**, 4034 (1967).
2. B. Baysal and A. V. Tobolsky, *J. Polym. Sci.*, **8**, 529 (1952).
3. F. R. Mayo and C. Walling, *Chem. Revs.*, **46**, 234 (1950).
4. P. D. Bartlett and R. Altschul, *J. Amer. Chem. Soc.*, **67**, 812, 816 (1945).
5. P. D. Bartlett and F. A. Tate, *J. Amer. Chem. Soc.*, **75**, 91 (1953).
6. A. C. R. Brown and D. G. L. James, *Can. J. Chem.*, **40**, 796 (1962).

Received November 25, 1968
Revised December 31, 1968

JOURNAL OF POLYMER SCIENCE: PART A-1 VOL. 7, 1517–1536 (1969)

# Stereospecific Polymerization of Benzyl Vinyl Ether by $BF_3 \cdot OEt_2$

HEIMEI YUKI, KOICHI HATADA, KOJI OTA, and IKUYA KINOSHITA, *Department of Chemistry, Faculty of Engineering Science, Osaka University*, and SHUNSUKE MURAHASHI, KATSUHIRO ONO, and YOSHIYUKI ITO, *Department of Polymer Science, Faculty of Science, Osaka University, Toyonaka, Osaka, Japan*

## Synopsis

Polymerization of benzyl vinyl ether was carried out by $BF_3 \cdot OEt_2$, and the effects of polymerization conditions on the stereoregularity of the polymer were studied by NMR analysis. The polymerization at −78°C in toluene gave a highly isotactic polymer. The isotacticity of the polymer was independent of the catalyst concentration but increased with a decrease in the initial monomer concentration and decreased slightly on raising the reaction temperature. When the polymerizations were carried out in toluene–nitroethane mixtures, a gradual decrease in the isotacticity and a rapid decrease in the molecular weight of the polymer were observed with increasing nitroethane in the solvent. The molecular weight of the polymer was almost constant, regardless of the catalyst concentration, and increased with increasing initial monomer concentration and decreasing polymerization temperature. When the polymerization was performed in toluene at −78°C with a small amount of water or benzyl alcohol, a linear relationship was found between the reciprocal DP of the polymer and water or benzyl alcohol concentration. The mechanisms of the initiation reaction and the stereoregulation in the polymerization were also discussed.

## INTRODUCTION

A number of papers have been published on the stereospecific polymerization of vinyl ethers.[1–5] It has been previously reported that isotactic poly(vinyl alcohol) (PVA) can be derived from crystalline poly(benzyl vinyl ether) (PBVE) which is obtained by the polymerization of benzyl vinyl ether (BVE) with boron trifluoride etherate ($BF_3 \cdot OEt_2$) at −78°C in toluene.[6]

This paper reports the analysis of tacticity in PBVE by high resolution NMR spectroscopy and the effects of the polymerization conditions on the stereoregularity of the polymer.

## EXPERIMENTAL

### Reagents

Benzyl vinyl ether was prepared from benzyl alcohol and acetylene by the catalysis of potassium hydroxide according to Reppe's method.[7] The monomer obtained was purified by heating at 60°C over sodium, then over calcium hydride, and finally over lithium aluminum hydride with stirring under dry nitrogen, and distilled *in vacuo;* bp 59.1°C/5.4 mm Hg, $n_D^{20}$ = 1.5162 (lit.[7] 1.5160). The purified BVE was sealed in ampoules under dry nitrogen and stored at −20°C.

Toluene, purified and dried by the usual method, was distilled from calcium hydride, then mixed with a small amount of *n*-BuLi (toluene solution) and redistilled in a vacuum line just before use. This purified toluene was shaken and saturated with water at 20°C and the concentration of water was calculated from its solubility in toluene.[8] This was added to the anhydrous toluene described above; the mixture was used for particular experiments as a solvent containing a known amount of water.

*n*-Hexane was purified by the usual manner and stored over metallic sodium. This was mixed with a small amount of *n*-BuLi (*n*-hexane solution) and distilled in a vacuum line just before use.

Nitroethane was purified by distillation and dried with Molecular Sieves (MS-4A). This was redistilled before use.

Methylene chloride was treated with concentrated sulfuric acid, washed with aqueous sodium hydroxide and water, dried over calcium chloride, and distilled. This was dried with a mixture of calcium hydride and Molecular Sieves (MS-4A) and distilled in a vacuum line just before use.

Pyridine purified by the usual method was dried with Molecular Sieves (MS-4A).

Acetic anhydride, benzyl alcohol, chloroform, carbon tetrachloride, and benzene were purified as usual.

Boron trifluoride etherate was purified by distillation under reduced nitrogen pressure and used as a toluene solution. The concentration was 0.468 mole/l.

Nitrogen was dried through a column packed with Molecular Sieves (MS-4A) and calcium hydride. This was further passed through the Molecular Sieves cooled to −78°C and then a solution of *n*-BuLi in liquid paraffin when it was necessary to remove traces of water and oxygen.

### Polymerization

Polymerization was carried out by one of the two following techniques.

In technique A, the reaction vessel shown in Figure 1 was used. The thermometer and the glass rod were removed. The vessel and the catalyst bulb were flushed with dry nitrogen, the monomer and the solvent were introduced into the vessel and the catalyst solution into the bulb by hypodermic syringes, and then the thermometer and the glass rod were replaced.

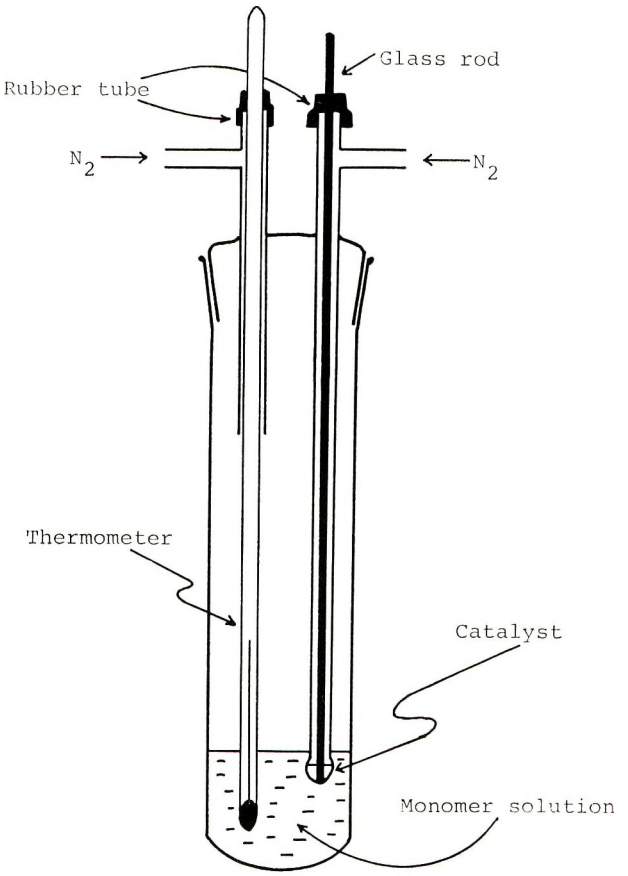


Fig. 1. Polymerization vessel.

After the monomer and the catalyst solutions were cooled to a given temperature, the glass rod was pushed down to break the bulb and the reaction vessel was shaken to mix the catalyst and the monomer solution.

In technique B, an ampoule equipped with a three-way stopcock was flushed with dry nitrogen, and then the monomer and the solvent were introduced into the ampoule with hypodermic syringes. To the monomer solutions cooled at a given temperature the catalyst solution was added by a hypodermic syringe, and the ampoule was sealed off immediately.

Generally a rapid temperature rise was observed immediately after the addition of the catalyst, and then gellike polymer was deposited in the reaction mixture. This temporary elevation of temperature was larger in technique B. Therefore, technique B was employed only in experiments in which the polymerization was carried out at an extremely low catalyst concentration with or without a small amount of water.

The polymerization was terminated by adding a small amount of ammoniacal methanol which was cooled to the same temperature as that of the

reaction mixture. If the reaction mixture gelled, it was treated in an electric mixer with ammoniacal methanol. The mixture was then poured into a large amount of methanol containing a small amount of phenyl-β-naphthylamine. The precipitated polymer was washed with the same methanol, dried *in vacuo*, and stored under an atmosphere of nitrogen at 0°C.

### Fractionation of PBVE

The polymer obtained at −78°C in toluene was a white solid having a slight elasticity at room temperature. This was refluxed in 100 parts of acetone containing a trace of phenyl-β-naphthylamine for 2 hr under nitrogen. The hot-acetone-insoluble fraction was separated by decantation from the hot supernatant solution and again extracted by 50 parts of acetone in the same manner as above. The combined acetone extracts were cooled to room temperature and allowed to crystallize overnight. Then the cold-acetone-insoluble fraction was separated by decantation and washed three times with acetone. The combined acetone solutions were concentrated *in vacuo*, and the residue was purified by reprecipitating from a small amount of toluene with methanol. The mother liquor of the reprecipitation was concentrated *in vacuo*, and the residual polymer was further reprecipitated by methanol.

### Preparation of PVA from PBVE

Through a solution of 1 g of PBVE in 100 ml of dry toluene, dry nitrogen was passed to remove oxygen dissolved in the system and then dry HBr was passed slowly at room temperature. After 20–60 min, a white precipitate appeared. The addition of HBr was continued until no increase in the amount of precipitate was observed. After 6 hr of reaction the HBr was purged off by bubbling dry nitrogen through the reaction mixture. The supernatant liquid was removed by decantation and the residual precipitate was collected by filtration with the aid of methanol. The precipitate was further immersed in 400 ml of methanol overnight, washed with methanol, and dried *in vacuo*. The PVA thus obtained was purified by reprecipitation from water with methanol. When the PVA contained a small amount of BVE units in the chain, such product could be removed by virtue of its insolubility in boiling water, although it is soluble in cold water. Usually this purified PVA still contained a trace of bromine, which was removed by a reprecipitation of the polymer from a minimum amount of cold 0.001*N* KOH aqueous solution with a large amount of methanol.

### Preparation of Poly(vinyl acetate) (PVA) from PVA

PVA (1 g) was suspended in 10 ml of dry pyridine at room temperature. After the PVA was swollen, 5 ml acetic anhydride was added, and the reaction mixture was heated at 60–70°C. The heating was continued for 1–2 hr after the polymer was dissolved. When the PVA had an extremely high isotacticity or a high molecular weight, 2–3 days heating was required for

the completion of the reaction. After reaction, the mixture was poured into 400 ml of water and the precipitated polymer was collected by filtration. The PVAc thus obtained was purified by reprecipitation from acetone with water.

### Viscosity Measurement

The intrinsic viscosity of PBVE (benzene solution) was measured at 30.0 ± 0.03°C. The viscosity of PVA was measured in water at 30.0 ± 0.03°C. Ubbelohde-type viscometers were used.

### NMR Spectra

NMR spectra were obtained with a JEOL JNM-4H-100 spectrometer at 100 MHz by using a 5–10% (w/v) sample solution containing a few per cent of tetramethylsilane as an internal standard. The spectra of PBVE and PVAc were measured in carbon tetrachloride and in chloroform, respectively, at 50°C.

### Infrared Spectra

The infrared spectra of PBVE and of PVA were taken as films on a JASCO IR-S spectrometer. The PBVE film was cast on a NaCl plate from methylene chloride solution and PVA film was cast on a KRS-6 plate from aqueous solution.

## RESULTS

### NMR Spectra and Tacticity of PBVE

In Figure 2 is shown the NMR spectrum of PBVE obtained by the polymerization with $BF_3 \cdot OEt_2$ in toluene at −78°C. The spectrum consists of four peaks corresponding to phenyl and benzylmethylene, $\alpha$ and $\beta$ protons (the respective protons on $\alpha$ and $\beta$ carbons of the vinyl monomer unit), respectively. The benzylmethylene resonance splits into three components at 5.68, 5.80, and 5.92$\tau$ and the relative intensities of these bands vary with the preparative method of the polymer. In Figure 3 are shown the slow sweeps of benzylmethylene resonances of PBVEs obtained at −78°C in toluene and in nitroethane. The relative intensity of the peak at 5.68$\tau$ in the spectrum of the polymer obtained in toluene is more intense than that obtained in nitroethane. The polymer prepared in toluene at −78°C was reported to have a predominantly isotactic structure.[6] The most intense band at 5.68$\tau$ can be assigned to benzylmethylene protons of the central monomer units in isotactic triads (*I*) and the bands at 5.80 and 5.92$\tau$ to heterotactic (*H*) and syndiotactic triads (*S*), respectively. The validity of this assignment can also be provided by a comparison of the spectra of PBVE and PVAc derived therefrom because the debenzylation of PBVE with HBr and the following acetylation of the derived PVA and PVAc does not involve racemization.[6] The fractions of triads were determined for

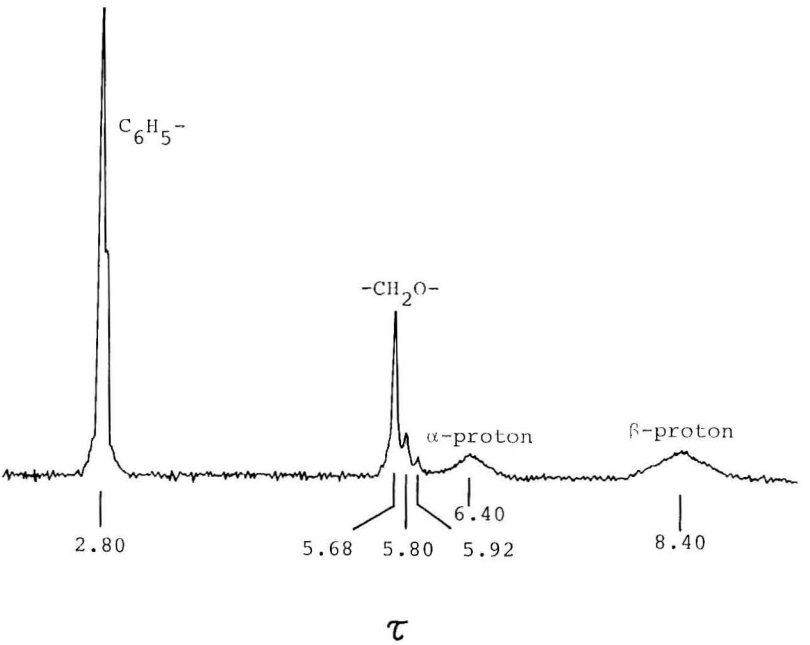


Fig. 2. NMR spectrum of PBVE obtained in toluene at −78°C with $BF_3 \cdot OEt_2$ catalyst.

PBVE and for the PVAc derived therefrom by using our assignment and that of Murahashi,[9] respectively. As shown in Table I, these two values showed a good agreement.

## Fractionation of Polymer

Each fraction separated from the PBVE obtained in toluene at −78°C was converted into PVA and its molecular weight was measured. The results are shown in Table II. Each fraction showed almost the same isotacticity, which suggests that the stereoregularity was independent of the molecular weight of polymer and the fractionation depended on the molecular weight but not on the stereoregularity of the polymer. The softening point of polymer was measured under a microscope as a temperature where the powder sample became transparent and its edges began to flow. The softening point was higher as the $\bar{P}$ of the polymer was higher.

A linear relationship was found between the logarithm of the intrinsic viscosity of PBVE and the logarithm of the degree of polymerization of the PVA derived therefrom (Fig. 4). From the equation of Nakajima and Furutati[10] [eq. (1)] on the viscosity of PVA (aqueous solution, 30.0°C) an

$$[\eta] = 7.50 \times 10^{-3} \bar{P}^{0.64} \quad (1)$$

equation [eq. (2)] for the viscosity of PBVE (toluene, 30.0°C) was obtained.

$$[\eta] = 2.14 \times 10^{-3} \bar{P}^{0.85} \quad (2)$$

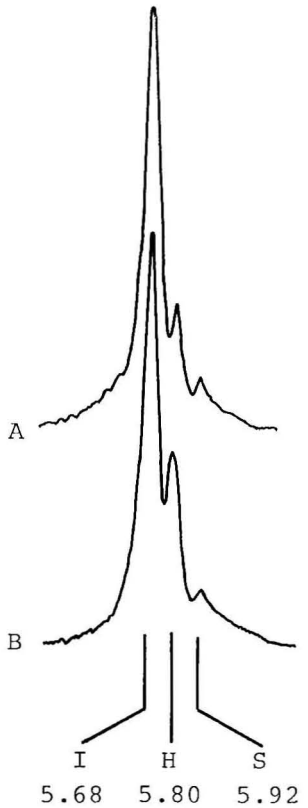


Fig. 3. NMR spectra of benzylmethylene protons of PBVE obtained at −78°C; (A) in toluene; (*B*) in $EtNO_2$.

TABLE I
Determination of Tacticities of PBVE by Different Methods

| | | | Tacticity | | | | | |
|---|---|---|---|---|---|---|---|---|
| | Polymerization | | From the benzyl methylene signals of PBVE | | | From the acetoxy-methyl signals of the derived PVAc | | |
| No. | Solvent | Temp, °C | *I*, % | *H*, % | *S*, % | *I*, % | *H*, % | *S*, % |
| K-43 | Toluene | −78 | 86 | 10 | 4 | 89 | 8 | 3 |
| K-35 | Nitroethane | −78 | 69 | 24 | 7 | 63 | 27 | 10 |

## Effect of Catalyst Concentration

The polymerization of BVE was carried out with various $BF_3 \cdot OEt_2$ concentrations at −78°C in toluene. The results are shown in Figure 5. The rate of polymerization was very large, and the polymerization at −78°C was completed within 1 hr for catalyst concentrations above $3 \times 10^{-3}$ mole/l. at a monomer concentration of 0.67 mole/l. The tacticity and the

TABLE II

Fractionation Data on PBVE Polymerized in Toluene and Degree of Polymerization ($\bar{P}$) of PVA Derived Therefrom

| No. | Fraction | Solubility | Yield, % | [η] | Softening point, °C[a] | Tacticity | | | Derived PVA | | |
|---|---|---|---|---|---|---|---|---|---|---|---|
| | | | | | | *I*, % | *H*, % | *S*, % | Yield, % | [η] | $\bar{P}$ |
| 111 | | Acetone-insol. | 72 | 1.57 | 119 | | | | 83 | 1.07 | 2320 |
| 105 | | Acetone-insol. | 78 | 3.75 | 149 | | | | 87 | 1.99 | 6100 |
| 13 | I | hot acetone-insol. | 64 | 2.16 | 125 | 73 | 21 | 6 | 71 | 1.39 | 3500 |
| | II | cold acetone-insol. | 8 | 1.45 | 113 | 74 | 19 | 7 | 77 | 0.72 | 1240 |
| | III | acetone-sol., repptd. from toluene–methanol | 21 | 0.83 | 97 | 77 | 18 | 5 | 76 | 0.71 | 1200 |
| | IV | toluene–methanol-sol.[b] | 7 | 0.35 | 90 | — | — | — | 83 | 0.35 | 410 |

[a] Softening point determined as described in Experimental section.

[b] Recovered from the mother liquor of fraction III.

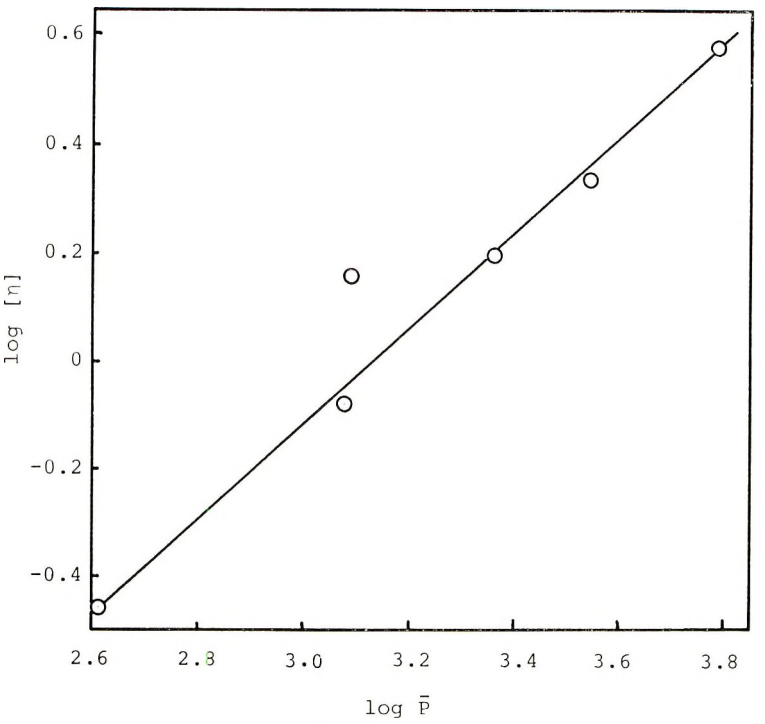


Fig. 4. Plot of log $[\eta]$ vs. log $\bar{P}$ of PBVE prepared in toluene.

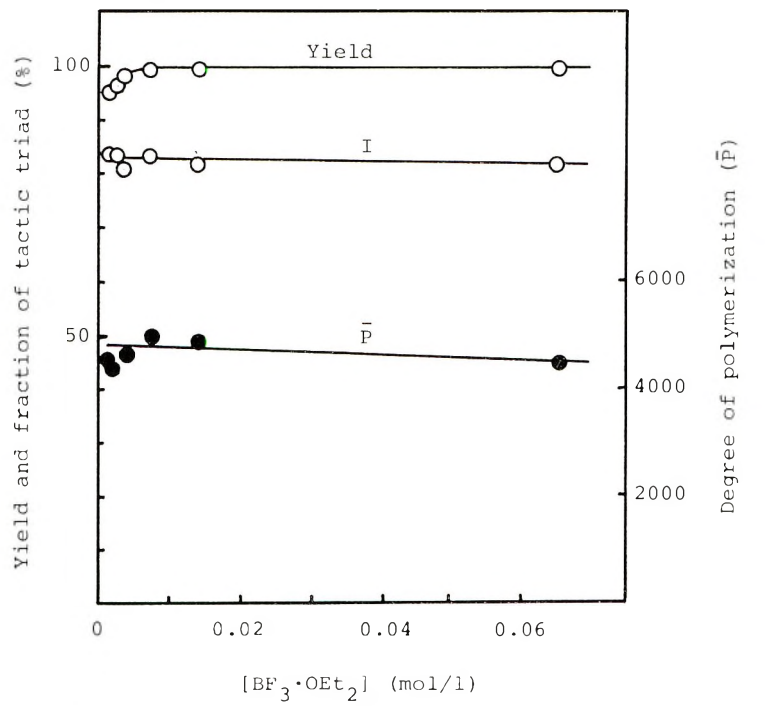


Fig. 5. Effect of catalyst concentration on yield, fraction of isotactic triad $I$, and $\bar{P}$ of the polymerization of BVE in toluene at −78°C. BVE 15.0 mmole, polymerization time 1 hr; volume of reaction mixture 22.5 ml.

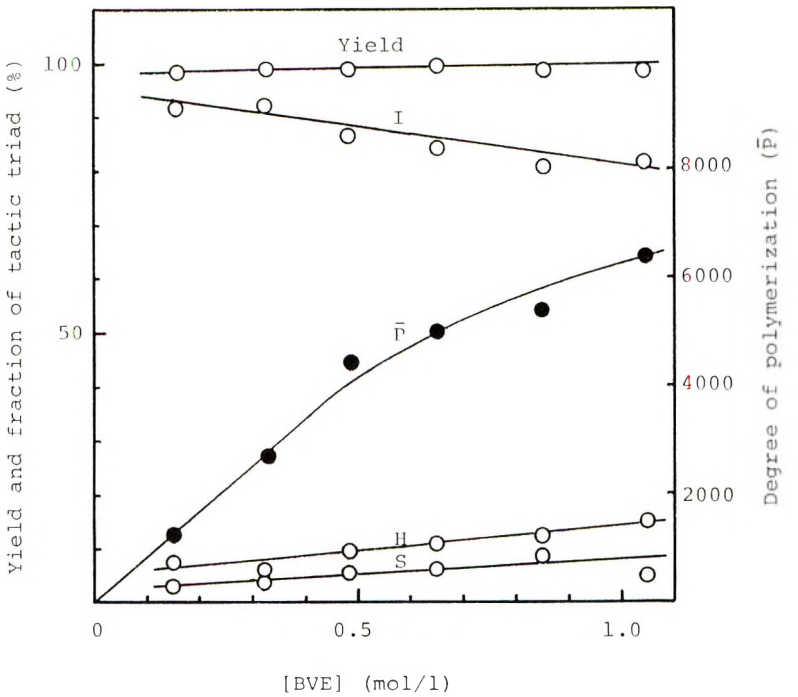


Fig. 6. Effect of monomer concentration on yield, $I$, $H$, $S$, and $P$ of the polymerization of BVE in toluene at $-78°C$. [$BF_3 \cdot OEt_2$] 0.0065 mole/l., polymerization time 1 hr; volume of reaction mixture 22.5 ml. $I$, $H$, and $S$, denote the fractions of isotactic, heterotactic, and syndiotactic triads, respectively.

molecular weight of the polymer were almost constant regardless of the catalyst concentrations.

## Effect of Monomer Concentration

The polymerization of BVE at various monomer concentrations was carried out in toluene at $-78°C$. The results are shown in Figure 6. The apparent rate of polymerization increased with the increase in the monomer concentration. The isotacticity of polymer increased with the decrease in the initial monomer concentration. An extremely high isotacticity was observed with the polymer obtained at an initial monomer concentration of 0.158 mole/l. The molecular weight of the polymer increased linearly with initial monomer concentration, at least up to 0.5 mole/l.

## Effect of Polymerization Temperature

The polymerization was carried out in toluene at various temperatures between $-96.5$ and $+18.2°C$. The results are shown in Figure 7. The isotacticity of polymer decreased only slightly with the elevation of the reaction temperature. On the other hand, a marked decrease in the molecular weight of polymer was observed at higher reaction temperatures. A

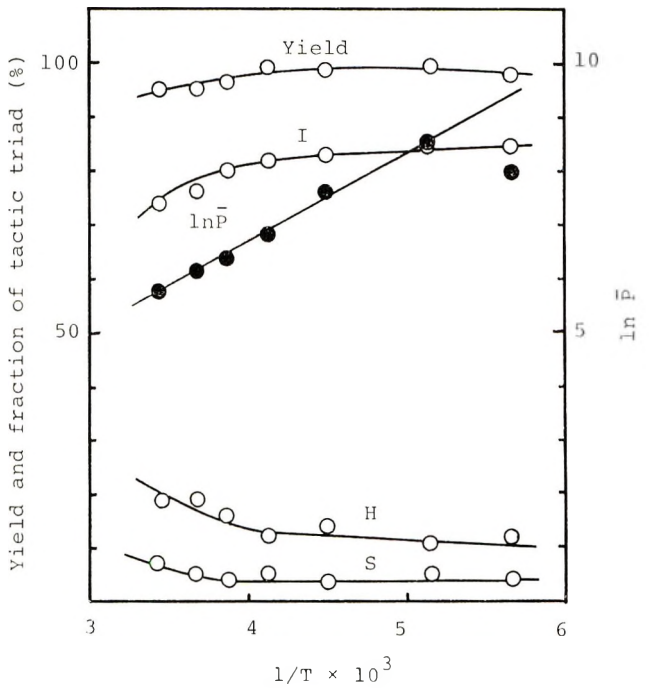


Fig. 7. Effect of temperature on yield, $I$, $H$, $S$, and $\bar{P}$ of the polymerization of BVE in toluene. BVE 15 mmole, $BF_3 \cdot OEt_2$ 0.146 mmole, volume of reaction mixture 22.5 ml, polymerization time 1 hr (3 hr at $-96.5$°C).

linear relationship was obtained between the logarithm of the degree of polymerization, ln $\bar{P}$, and the reciprocal of the reaction temperature $1/T$ (Fig. 7), and the slope showed an activation energy of $-3.4$ kcal/mole.

## Polymerization in Various Solvents

The results of the polymerization carried out in various solvents are shown in Table III. The isotacticity of polymer was slightly lower in a polar solvent. Lower polymer yields observed in the polymerizations in *n*-hexane and in diethyl ether were attributed to the low solubility of the polymer in these solvents.

The results of the polymerization in toluene–nitroethane mixtures are shown in Figure 8. A gradual decrease in the isotacticity and a rapid decrease in the molecular weight of the polymer were observed with increasing nitroethane in the solvent.

## Polymerization at Low Catalyst Concentration

The polymerization in toluene at $-78$°C was carried out at extremely low catalyst concentrations [C], such as $6.5 \times 10^{-4}$ mole/l., by means of polymerization technique B with the use of specially purified nitrogen (See Experimental section). The effect on the polymerization of a small

TABLE III
Polymerization of BVE at −78°C in Various Solvents[a]

| No. | Solvent | | | $BF_3 \cdot OEt_2$, mmole | Polymn. time, hr | Polymer | | | | |
|---|---|---|---|---|---|---|---|---|---|---|
| | Type | Dielectric constant $\epsilon$ | Temp, °C | | | Yield, % | Tacticity | | | |
| | | | | | | | *I*, % | *H*, % | *S*, % | $\bar{P}$ |
| 98[b] | *n*-Hexane | 1.890 | 20 | 0.146 | 1.2 | 12.2 | 83 | 13 | 4 | — |
| 13 | Toluene | 2.378 | 25 | 0.235 | 1.0 | 99.4 | 82 | 14 | 4 | 2320 |
| 99 | $Et_2O$ | 4.335 | 20 | 0.146 | 1.8 | 9.3 | 76 | 15 | 9 | — |
| 20 | $CH_2Cl_2$ | 9.08 | 20 | 0.235 | 1.0 | 97.5 | 76 | 21 | 3 | 520 |
| 21 | $EtNO_2$ | 28.06 | 30 | 0.235 | 1.0 | 97.5 | 67 | 26 | 7 | 500 |

[a] BVE 15 mmole, volume of the reaction mixture 22.5 ml.
[b] Polymerization was carried out at −51°C.

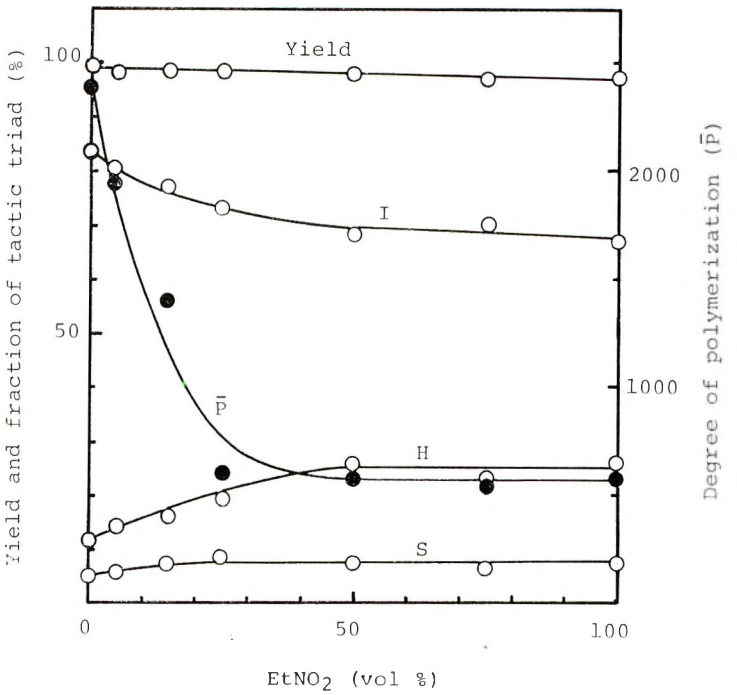


Fig. 8. Polymerization of BVE at −78°C in toluene–$EtNO_2$ mixture. BVE 15 mmole, $BF_3$·$OEt_2$ 0.235 mmole, polymerization time 1 hr, volume of reaction mixture 22.5 ml.

amount ($5.35 \times 10^{-4}$ mole/l.) of water was also investigated under the same conditions. The results are shown in Figures 9 and 10. In the polymerization at $[C] = 6.5 \times 10^{-4}$ mole/l. the rate was fairly small, and the time–conversion relationship showed a slow sigmoid curve; the molecular weight of the polymer increased as the reaction proceeded. Both the rate of polymerization and the average molecular weight of the polymer at the same yield were lower for the polymerization in the presence of water.

## Effects of Water and Benzyl Alcohol on the Polymerization

Polymerization was carried out in the presence of various amounts of water in order to investigate the effect of water on the polymerization. The experiments were done with the technique A, but with the use of the specially purified nitrogen. The results are shown in Table IV. The apparent rate of polymerization was decreased by the addition of water. However, the reaction proceeded almost to completion after a long period, even if the amount of water present was more than four times the catalyst. The temporary elevation of the temperature of the reaction mixture was observed after about 0.5 min in the absence of water and after 44 min in the system containing 0.0185 mole/l. of water ($[H_2O]/[BF_3{\cdot}OEt_2] = 2.87$ mole/mole). A linear relationship was found between the reciprocal $\bar{P}$ of polymer and water concentration (Fig. 11), but the isotacticity of polymer was almost constant, regardless of the amount of water.

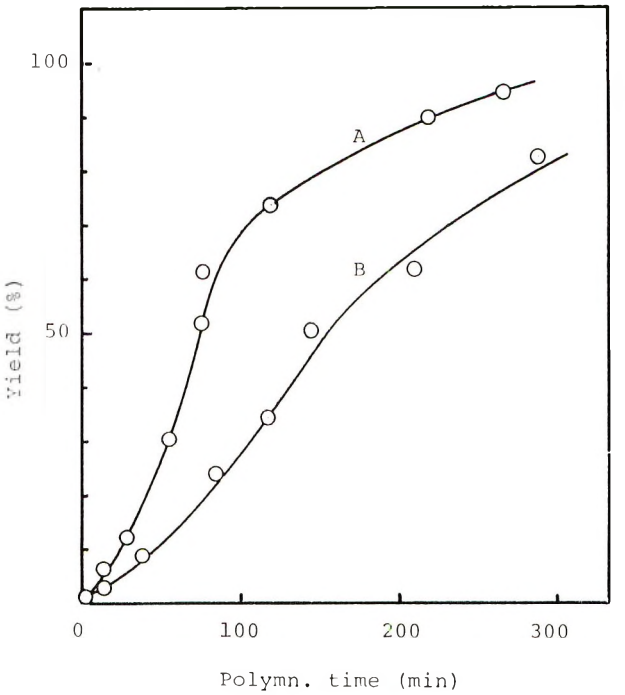


Fig. 9. Polymer yield vs. polymerization time or polymerization of BVE in toluene at −78°C: (*A*) $[H_2O]/[BF_3 \cdot OEt_2] = 0$; (*B*) $[H_2O]/[BF_3 \cdot OEt_2] = 0.823$. BVE 15 mmole, $BF_3 \cdot OEt_2$ 0.0146 mmole, volume of reaction mixture 22.5 ml.

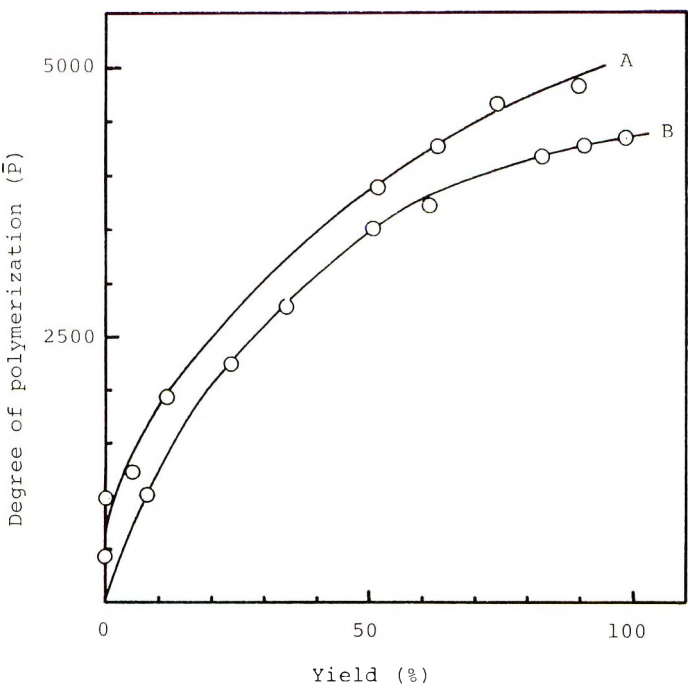


Fig. 10. Degree of polymerization vs. polymer yield for polymerization of BVE in toluene at −78°C: (*A*) $[H_2O]/[BF_3 \cdot OEt_2) = 0$; (*B*) $[H_2O]/[BF_3 \cdot OEt_2] = 0.823$. BVE 15 mmole, $BF_3 \cdot OEt_2$ 0.0146 mmole, volume of reaction mixture 22.5 ml.

TABLE IV
Effect of Water and Benzyl Alcohol (BzOH) on the Polymerization of BVE in Toluene at −78°C[a]

| No. | Additive | Additive [$BF_3 \cdot OEt_2$] mole/mole | Polymn. time, hr | Polymer Yield, % | Tacticity *I*, % | *H*, % | *S*, % | $\bar{P}$ |
|---|---|---|---|---|---|---|---|---|
| 43 | $H_2O$ | 0 | 1.0 | 97.1 | 86 | 10 | 4 | 3990 |
| 45 | | 0.96 | 1.0 | 97.6 | 86 | 8 | 6 | 1660 |
| 73 | | 1.42 | 3.25 | 89.5 | — | — | — | 780 |
| 46 | | 1.92 | 1.0 | 87.0 | 84 | 9 | 7 | 620 |
| 47 | | 2.87 | 1.0 | 82.3 | 85 | 7 | 8 | 600 |
| 76 | | 3.23 | 72.0 | 91.4 | 89 | 6 | 5 | 710 |
| 75 | | 3.81 | 72.0 | 87.6 | 83 | 10 | 7 | 930 |
| 43 | BzOH | 0 | 1.0 | 97.1 | 86 | 10 | 4 | 3990 |
| 84 | | 0.64 | 4.5 | 96.8 | 80 | 13 | 7 | 960 |
| 85 | | 1.49 | 5.0 | 90.0 | 83 | 8 | 9 | 500 |
| 81 | | 2.13 | 4.9 | 90.7 | 83 | 12 | 5 | 390 |
| 83 | | 3.19 | 6.0 | 85.1 | 85 | 8 | 7 | 352 |
| 82 | | 4.25 | 22.0 | 90.9 | 83 | 11 | 6 | 272 |

[a] BVE 15 mmole, $BF_3 \cdot OEt_2$ 0.146 mmole, volume of reaction mixture 22.5 ml.

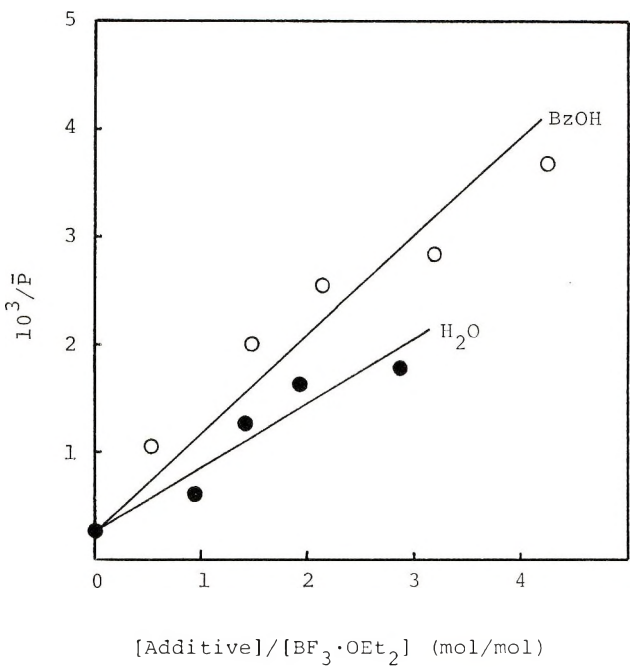


Fig. 11. Effect of water and benzyl alcohol (BzOH) on the polymerization of BVE in toluene at −78°C.

Similar results on the rate of polymerization as well as the isotacticity and the molecular weight of the polymer were obtained with the addition of benzyl alcohol instead of water (Table IV, Fig. 11).

### NMR Spectra of Catalyst System

In order to investigate the initiation reaction by $BF_3 \cdot OEt_2$ catalyst and the effect of water on this catalyst system, the NMR spectra of $BF_3 \cdot OEt_2$ and the reaction mixture of $BF_3 \cdot OEt_2$ and an equimolar amount of water or BVE were measured in toluene. The results are shown in Table V. When diethyl ether is coordinated to boron trifluoride, the methyl proton resonance shifts to higher field and the methylene resonance to lower field, and consequently the chemical shift difference $\delta$ between methyl and methylene resonances increases. With the addition of an equimolar amount of BVE to $BF_3 \cdot OEt_2$ complex the $\delta$ value decreased and became almost that of free diethyl ether. The $\delta$ value of $BF_3 \cdot OEt_2$ also decreased on addition of an equimolar amount of water, and a further decrease was observed on addition of BVE to the mixture of $BF_3 \cdot OEt_2$ and $H_2O$.

TABLE V
Investigation of the Catalyst System by NMR Spectroscopy[a]

| No. | Sample | Chemical shift of ethyl protons, $\tau$ | | |
|---|---|---|---|---|
| | | —$CH_3$ | —$CH_2$— | $\delta$[b] |
| A | $Et_2O$ | 8.87 | 6.72 | 2.15 |
| B | $BF_3 \cdot OEt_2$ | 9.07 | 6.38 | 2.69 |
| C | $BF_3 \cdot OEt_2$ + BVE[c] | 8.95 | 6.68 | 2.27 |
| D | $BF_3 \cdot OEt_2$ + $H_2O$[c] | 9.03 | 6.52 | 2.51 |
| E | $BF_3 \cdot OEt_2$ + $H_2O$ + BVE[c] | 9.02 | 6.58 | 2.44 |

[a] NMR spectra were taken at 20.5°C using a sample solution in toluene (ca. 10%) containing a few per cent of TMS as a standard.

[b] $\delta$ = (chemical shift of —$CH_3$) − (chemical shift of —$CH_2$—).

[c] Equimolar mixture.

## DISCUSSION

### Degree of Polymerization ($\bar{P}$) of PBVE

The fact that the $\bar{P}$ of PBVE produced in toluene at low temperature increased with the increase in the monomer concentration (Fig. 6) suggests that there is no or only a little chain transfer to monomer in the polymerization reaction. The $\bar{P}$ of PBVE was not affected by the catalyst concentration, but was markedly lowered by the presence of water or benzyl alcohol, which functioned as a chain-transfer agent. These results indicate that a polymer of very high molecular weight can be prepared from BVE if the reagents are sufficiently purified and water is completely excluded from the reaction mixture. It has been reported that water and alcohol are chain-transfer agents in the polymerization of vinyl ethers with $BF_3 \cdot OEt_2$ in diethyl ether at 25°C.[11]

On the other hand, in the polymerization in toluene without chain-transfer agent the $\bar{P}$ of polymer increased with increasing polymer yield, suggesting a very low rate of termination reaction at low temperature. The

marked decrease in the $\bar{P}$ of polymer with increasing reaction temperature indicates that it is necessary to minimize the temperature increase during the reaction in order to obtain a high molecular polymer. The activation energy for the polymerization $E_{\bar{P}}$, was $-3.4$ kcal/mole observed from $-78°C$ to $+20°C$. A similar value, $-3.0$ kcal/mole, has been reported for the $E_{\bar{P}}$ of the polymerization of alkyl vinyl ethers by $BF_3$·$OEt_2$ in diethyl ether at 25°C.[11]

The decrease in the $\bar{P}$ of polymer obtained in a polar solvent may not be caused by chain transfer to the solvent but by a self-termination reaction, because constant $\bar{P}$ was observed over a range of nitroethane contents in the solvent.

The low $\bar{P}$ of the polymer obtained at $-96°C$ compared with that obtained at $-78°C$ was attributed to the precipitation of polymer due to its low solubility at low temperature.

## Initiation Reaction

The sigmoid time–conversion curve obtained in the polymerization in toluene at $-78°C$ suggests that the rate of initiation is relatively lower than that of propagation. The relation between the $\bar{P}$ and the yield of polymer indicates that the effective catalyst concentration was extremely low compared with the amount of catalyst used.

Water functions as a retarder for the cationic polymerization of BVE, because it lowers the rate of polymerization, but the polymer yield reached the theoretical one even in the presence of large amounts of water if the reaction was allowed to run for a sufficiently long time. Chain transfer to water may produce unrecovered low molecular weight polymers, which are soluble in methanol. This together with the slow reinitiation after the chain transfer may be the cause of the slow apparent rate of polymerization initially in the presence of water (Fig. 9).

From the kinetic study of the polymerization of alkyl vinyl ether in diethyl ether with $BF_3$·$OEt_2$ it has been stated that the initiation of the reaction occurs with an ion-pair formed by the direct reaction between $BF_3$·$OEt_2$ and a monomer as follows:[12]

$$BF_3\cdot OEt_2 + CH_2{=}CHOR \rightarrow EtCH_2{-}\underset{\displaystyle OR}{\overset{\displaystyle |}{C}}H^+[BF_3\cdot OEt]^- \qquad (3)$$

The difference $\delta$ of the chemical shifts of methyl and methylene protons in diethyl ether corresponds approximately to the interaction between diethyl ether and $BF_3$.[13] Therefore, the results shown in Table V suggest the equilibrium (4):

$$BF_3\cdot OEt_2 + BVE \rightleftarrows BF_3\cdot BVE + Et_2O \qquad (4)$$

In the polymerization reaction the equilibrium lies mostly to the right of eq. (4) because there should be a very large excess of BVE compared to $BF_3$·$OEt_2$. The polymerization reaction may be initiated by $BF_3$·BVE as shown in eq. (5).

$$BF_3 \cdot BVE + BVE \rightarrow \left[ PhCH_2CH_2CH(OCH_2Ph) \right]^+ [BF_3 \cdot OCH{=}CH_2]^- \quad (5)$$

The $\delta$ value of $BF_3 \cdot OEt_2$ decreases on addition of an equimolar amount of water, and a further decrease of $\delta$ is observed on addition of BVE to the $BF_3 \cdot OEt_2$–$H_2O$ mixture. In the polymerization reaction the reaction shown in eq. (6) may compete with that of eq. (4), but the latter predominates.

$$BF_3 \cdot OEt_2 + H_2O \rightarrow BF_3 \cdot OH_2 + Et_2O \quad (6)$$

## Stereoregulation in Polymerization

Although a number of NMR studies of poly(alkyl vinyl ether) have been reported, the fractions of tactic triads can be readily determined from the normal spectrum only for poly(methyl vinyl ether).[14,15] In other cases special techniques, such as spin decoupling, must be used to obtain significant results.[16]

In this work we found that the NMR signal of the benzylmethylene protons in PBVE was sensitive to the stereochemical configuration and could be interpreted in terms of the triads without the need of special techniques.

Chujo[17,18] has proposed that information on the polymerization mechanism can be obtained from the relationship between the quantity, $\Delta\epsilon = -kT \log (4IS/H^2)$ and the polymerization temperature ($T$), as follows: (1) if $\Delta\epsilon = 0$ regardless of $T$, no steric contribution from a penultimate unit is considered in the polymerization; (2) when $\Delta\epsilon$ is a linear function of $T$, the penultimate effect will contribute to the polymerization mechanism; and (3) when $\Delta\epsilon$ is a complicated function of $T$, the mechanism may be interpreted neither by Bovey's single-parameter theory nor by a penultimate

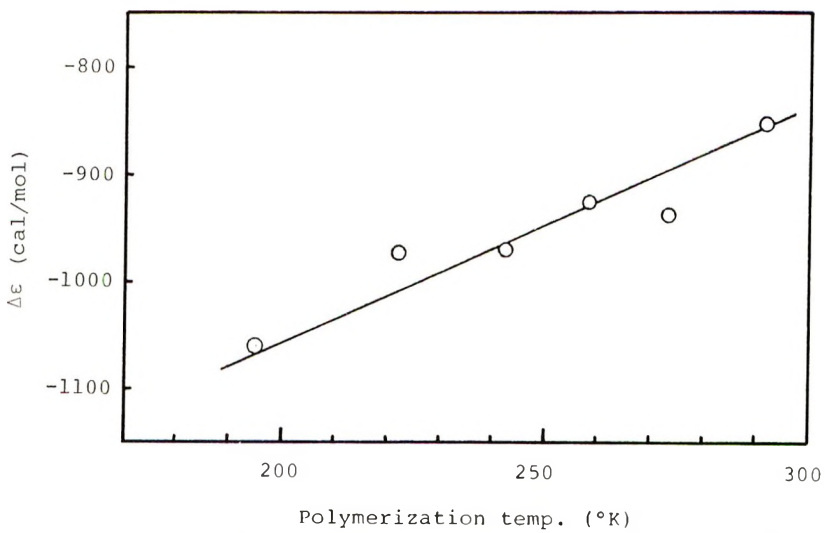


Fig. 12. $\Delta\epsilon$ vs. polymerization temperature for PBVE obtained at various temperatures in toluene.

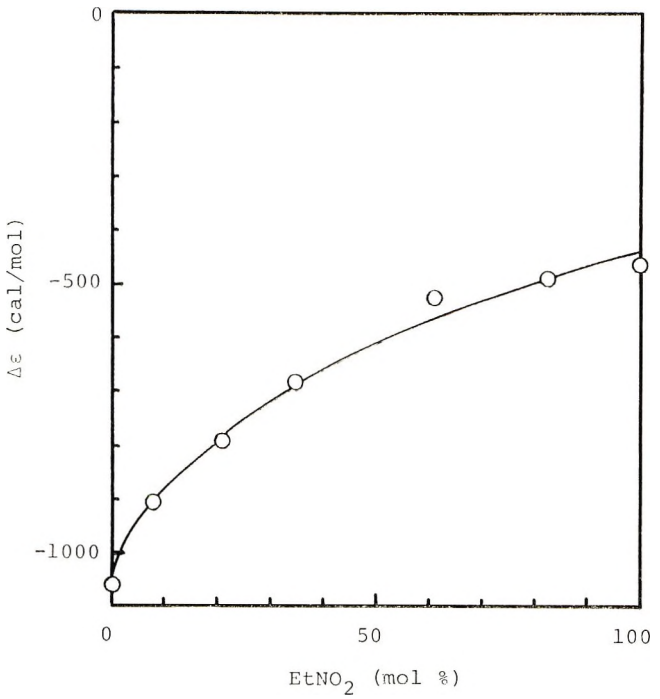


Fig. 13. $\Delta\epsilon$ vs. solvent composition for PBVE obtained in toluene–$EtNO_2$ mixture at −78°C.

effect. The mechanisms on the steric controls in the ionic polymerizations of methyl vinyl ether and methyl methacrylates have been discussed by the above treatments.[19] As shown in Figure 12, the quantity $\Delta\epsilon$ for PBVE obtained in toluene increased linearly with increasing temperature of polymerization, suggesting the existence of the penultimate effect in this stereospecific polymerization. For the polymerization in the mixture of toluene and nitroethane the $\Delta\epsilon$ value increased with increasing content of nitroethane (Fig. 13). This may suggest that the penultimate effect, if it exists in the binary solvent, decreases with increasing polarity of the poly-

TABLE VI
Fraction of Isotactic Diad in Poly(Alkyl Vinyl Ether) Obtained in Various Solvents at −78°C by $BF_3 \cdot OEt_2$

| Alkyl | Isotactic diad, % | | | Reference |
|---|---|---|---|---|
| | In toluene | In $CH_2Cl_2$ | In $EtNO_2$ | |
| Methyl | 72 | — | — | 22 |
| *tert*-Butyl | 76 | — | 48[a] | 19, 23 |
| $(Me)_3Si$— | 91 | 45[b,c] | 26[c] | 24 |
| Benzyl | 94 | 86 | 80 | This work |

[a] Calculated from infrared data.
[b] Polymerized by $Et_2AlCl$.
[c] Polymerized by $SnCl_4$.

merization medium, and this causes a depression in isotacticity of the polymer.

Generally, the low-temperature cationic polymerization of vinyl ethers in a nonpolar solvent gives an isotactic polymer. On the other hand, polymerization in a polar solvent previously yielded a syndiotactic polymer, which is explained by the free-ion propagation mechanism contrary to the ion-pair mechanism in the system in nonpolar solvent.[20,21] Thus, *tert*-butyl vinyl ether and trimethylsilyl vinyl ether form syndiotactic polymers in nitromethane and methylene chloride (Table VI). It must be noted that the polymerization of BVE produces a fairly isotactic polymer even in a polar solvent, although the penultimate effect in the stereoregulation may be smaller, as mentioned above.

The authors wish to express their sincere thanks to Mr. Yoshio Terawaki and Mr. Kazuhiko Nagata for the NMR experiments.

## References

1. C. E. Schildknecht, A. O. Zoss, S. T. Gross, H. R. Davidson, and J. M. Lambert, *Ind. Eng. Chem.*, **40**, 2104 (1948).
2. G. Natta, G. Dall'Asta, G. Mazzanti, U. Giannini, and S. Cesca, *Angew. Chem.*, **71**, 205 (1959).
3. G. Natta and G. Mazzanti, *Tetrahedron*, **8**, 86 (1960).
4. S. Okamura, T. Higashimura, and T. Watanabe, *Makromol. Chem.*, **50**, 137 (1961).
5. E. J. Vandenberg, *J. Polym. Sci. C-1*, 207 (1963).
6. S. Murahashi, H. Yuki, T. Sano, U. Yonemura, H. Tadokoro, and Y. Chatani, *J. Polym. Sci.*, **62**, No. 174, S 77 (1962).
7. W. Reppe and Mitarbeitern, *Ann.*, **601**, 84 (1956).
8. Chemical Society of Japan, ed., *Kagaku Binran Kisohen II*, Maruzen Co., 1966, p. 689.
9. S. Murahashi, S. Nozakura, M. Sumi, H. Yuki, and K. Hatada, *J. Polym. Sci. B-4*, 65 (1966).
10. A. Nakajima and K. Furutati, *Kobunshi Kagaku*, **6**, 461 (1949).
11. J. D. Coombes and D. D. Eley, *J. Chem. Soc.*, **1957**, 3700.
12. P. H. Plesch, ed., *The Chemistry of Cationic Polymerization*, Pergamon Press, 1963, p. 392.
13. K. Hatada and H. Yuki, *Tetrahedron Letters*, **1968**, 213.
14. S. Brownstein and D. M. Wiles, *J. Polym. Sci. A-2*, 1901 (1964).
15. K. C. Ramey, N. D. Field, and I. Hasegawa, *Polym. Letters*, **2**, 865 (1964).
16. K. C. Ramey, N. D. Field, and A. E. Borchert, *J. Polym. Sci. A-3*, 2885 (1965).
17. R. Chujo, *J. Phys. Soc. Japan*, **21**, 2669 (1966).
18. R. Chujo, *Makromol. Chem.*, **107**, 142 (1967).
19. Y. Ohsumi, T. Higashimura, and S. Okamura, *Kobunshi Kagaku*, **23**, 613 (1966).
20. T. Higashimura, K. Suzuki, and S. Okamura, *Makromol. Chem.*, **86**, 259 (1965).
21. S. Murahashi, S. Nozakura, and M. Sumi, *J. Polym. Sci. B-3*, 245 (1965).
22. H. Yuki, K. Hatada, and T. Suga, unpublished data.
23. K. C. Ramey, N. D. Field, and A. E. Borchert, *J. Polym. Sci. A-3*, 2885 (1965).
24. S. Murahashi, S. Nozakura, M. Sumi, H. Yuki, and K. Hatada, *Kobunshi Kagaku*, **23**, 605 (1966).

Received October 11, 1968
Revised December 31, 1968

JOURNAL OF POLYMER SCIENCE: PART A-1 VOL. , 1537–1547 (1969)

# ESR Spectra of Poly(methacrylic Acid) and Poly(methyl Methacrylate): Reinterpretation of the 9-Line Spectrum

MACHIO IWASAKI and YOSHIRO SAKAI,* *Government Industrial Research Institute, Nagoya, Hirate-machi, Kita-ku, Nagoya, Japan*

## Synopsis

The temperature dependence of the ESR spectra of poly(methacrylic acid) and poly(methyl methacrylate) $\gamma$-irradiated at room temperature was studied between $-196°C$ and $+25°C$. The conventional 9-line spectrum was observed throughout this range with no significant spectral change, in contrast to the propagating radical $\cdots CH_2—\dot{C}(CH_3)COOR$ found in methacrylic acid monomer or barium methacrylate dihydrate irradiated at $-196°C$. In addition, the irradiation of methacrylic acid monomer with a low dose at $0°C$ gave the same 13-line spectrum as that of the propagating radical obtained by the irradiation at $-196°C$, while prolonged irradiation at $0°C$ gave the same conventional 9-line spectrum as that of poly(methacrylic acid) or poly(methyl methacrylate). The conventional 9-line spectrum has a much weaker 4-line component than that of the propagating radical. The difference comes from the surrounding matrix, and the conventional 9-line spectrum is well interpreted by introducing the concept of the distribution of the conformational angle in the irregular polymer matrix. From simulation of the ESR spectrum, it was found that the intensity of the 4-line component is very sensitive to the distribution, and that the observed 9-line spectrum is well reproduced assuming a Gaussian distribution (half-height width of 5–6°) around the most probable conformation which is nearly the same as that of the propagating radical, where the conformational angles of the two C—$H_\beta$ bonds to the half-filled $p$-orbital are 55° and 65°.

## INTRODUCTION

It is well known that the radicals formed in poly(methacrylic acid) (PMAA) and poly(methyl methacrylate) (PMMA) give essentially the same 9-line ESR spectrum which consists of the so-called 5-line and 4-line components. Although a number of workers have studied this spectrum, especially in regard to the intensity ratio of the 5-line and 4-line components,[1–17] there has been some controversy whether the spectrum is due to a single species or more than two species of radicals. The latter postulation seems to be based upon the fact that the intensity ratio of the 4-line and 5-line components changes during the decay of the radicals. However, the answer to this problem has been given recently by Michel et al.,[16] who

* Present address: Department of Industrial Chemistry, Ehime University, Matsuyama, Ehime, Japan.

showed that there exists a minor but stable radical which gives a weak broad line overlapping on the major 9-line spectrum, and that the intensity ration of the 9-line spectrum itself remains constant on heat treatment. Therefore, the origin of the 9-line spectrum seems to be a single radical species.

Fisher et al.[10,11] have observed a relatively well resolved 16-line spectrum in ESR studies of the polymerization of aqueous solutions of methacrylic acid and attributed this to the propagating radical

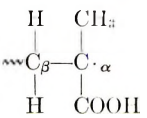

The alternation of the line width of the hyperfine components was well interpreted by the broadening of the $\sum_{\beta H} M_I = 0$ lines due to the hindered oscillation of the methylene group around the $C_\alpha$—$C_\beta$ bond (see Fig. 1). In addition, it was suggested that the conventional 9-line spectrum observed in the solid polymers is the unresolved 16-line spectrum (see Fig. 2) and is assigned to a similar propagating radical. If this is the case, one should observe the change with observation temperature of the 4-line component corresponding to the $\sum_{\beta H} M_I = 0$ lines.

Recently Bowden and O'Donnell[18] have found that the spectrum of the propagating radical trapped in irradiated barium methacrylate dihydrate at $-196$°C indeed exhibits a reversible temperature change in the solid state. They observed a 13-line spectrum at lower temperature and a 9-line spectrum at higher temperature, as is expected from the hindered oscillation model. The 13-line spectrum is essentially the same as the 16-line spectrum found by Fisher et al. in aqueous solutions, as shown in Figure 2*b*.

On the other hand, we have studied the ESR spectrum or irradiated solid methacrylic acid at $-196$°C and found that the propagating radical exhibits a 9-line spectrum at $-196$°C but a 13-line spectrum at $-24$°C (see Fig. 3),

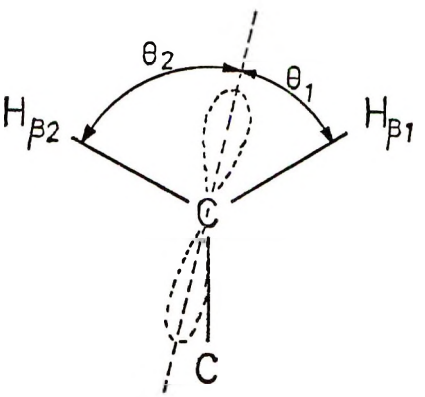


Fig. 1. Conformation of the half-filled *p*-orbital relative to the methylene protons of the propagating radical —$CH_2$—$C(CH_3)$COOR.

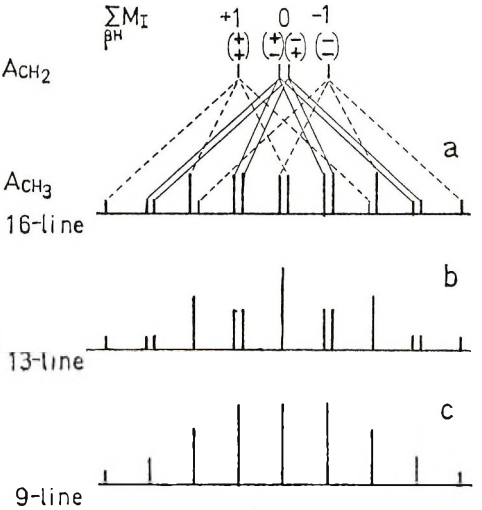


Fig. 2. Illustration of the hyperfine line structure of the radical $\cdots CH_2—\dot{C}(CH_3)$-COOR: (*a*) all the coupling constants are nonequivalent; (*b*) $A_{CH_3} = A_{\beta_1} + A_{\beta_2}$; (c) $A_{CH_3} = A_{\beta_1} + A_{\beta_2}$, and in addition, $A_{\beta_1} = A_{\beta_2}$ or there is rapid exchange of the two methylene protons.

contrary to the results with barium methacrylate dihydrate.[19] This change with observation temperature is also reversible and was well interpreted by the Bloch treatment for the two $\beta$-proton exchange in the anomalous crystalline transition at $-30°C$ which was found by the broad line NMR. As was described in our previous paper,[19] it was assumed that for the lower-temperature phase (phase II) the hindering potential barrier is lower than for the higher-temperature phase (Phase I).

Thus, all the results seem to be consistent with the hindered oscillation model of a single species of radicals. However, it should be mentioned that our 9-line spectrum found in solid methacrylic acid at $-196°C$ or that found by Bowden and O'Donnell in barium methacrylate dihydrate at higher temperature has very much stronger intensity for the 4-line component than that of the conventional 9-line spectrum. Moreover, in our previous work[19] we found that prolonged irradiation of methacrylic acid at 0°C gave the conventional 9-line spectrum which did not show the reversible change of the spectrum as mentioned above. In this connection, the present work reports further studies of this kind and compares the dependence of ESR spectra on temperature and radiation dose for radicals trapped in both solid monomers and in polymers.

## EXPERIMENTAL

Samples of MAA monomers were purified as described by Bamford et al.[8] The occluded air was removed by repeated freezing and melting at $10^{-5}$ mm Hg, and then samples were distilled into Spectrosil ESR sample

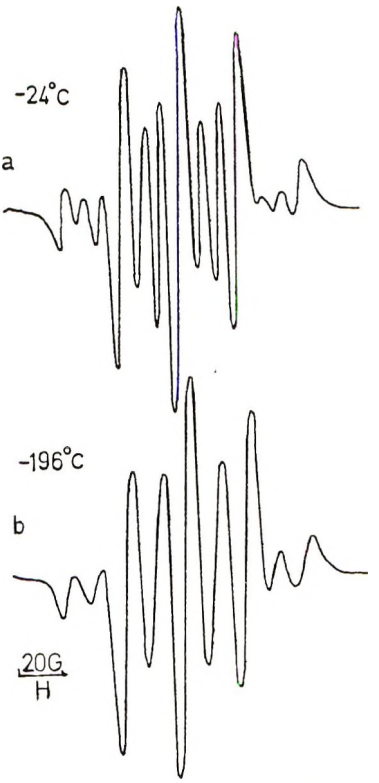


Fig. 3. Change with observation temperature of the ESR spectrum of the propagating radical $\cdots CH_2—\dot{C}(CH_3)COOH$ trapped in the MAA monomer crystals irradiated at −196°C, observed at (*a*) −24°C and (*b*) −196°C.

tubes. Irradiation was made with γ-rays from a $^{60}Co$ source at 0°C at a dose rate of $3 \times 10^4$ R/hr.

Samples of PMAA and PMMA were prepared by γ-irradiation of the respective monomers. The samples were sealed in Spectrosil ESR sample cells under vacuum of $10^{-5}$ mm Hg and then irradiated with γ-rays from a $^{60}Co$ source at room temperature. The total dose was $1.4 \times 10^6$R at a dose rate of $8.3 \times 10^4$R/hr. The ESR spectra were recorded with a Japan Electron Optics Model 3BSX spectrometer operated at 9.4 Gc/sec with 100 kc/sec modulation. The ESR measurements were carried out in the temperature range from −196 to +25°C. The simulated ESR spectra were obtained with a Japan Electron Optics Model RA-5 spectrum computer.

## RESULTS AND DISCUSSION

### Dose Dependence of ESR Spectra

The change in spectra with radiation dose at 0°C was followed for methacrylic acid. As shown in Figure 4, for the low dose ($1.5 \times 10^4$R) the

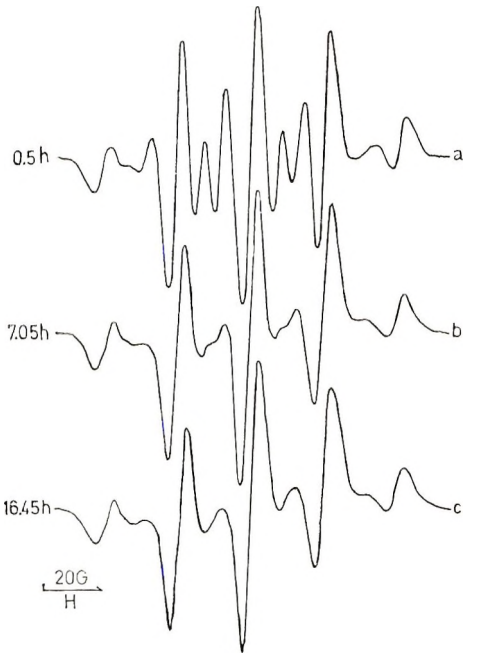


Fig. 4. Dose dependence of the ESR spectrum of the propagating radical $\cdots CH_2-\dot{C}(CH_3)COOH$ in MAA monomers irradiated at 0°C: (*a*) $1.5 \times 10^4$ R; (*b*) $21.2 \times 10^4$ R; (*c*) $49.5 \times 10^4$ R.

spectrum exhibits the same 13-line structure as that of the propagating radicals found in the same monomer irradiated at −196°C and then warmed to −24°C (see Fig. 3). However, with increasing dose, the spectrum changed gradually into the usual 9-line spectrum with a very weak 4-line component. A dose of $49.5 \times 10^4$R gave essentially the same spectrum as that obtained by the irradiation of PMAA or PMMA at room temperature (see Fig. 5).

On the other hand, studies of the solid-state polymerization of MAA showed that prolonged irradiation at 0°C gave an appreciable amount of polymer during irradiation, while post-polymerization at −24°C subsequent to pre-irradiation at −196°C was not appreciable. In-source polymerization at 0°C gave the polymer yields of 0.4, 25, and 45% for $1.5 \times 10^4$ $21.2 \times 10^4$, and $49.5 \times 10^4$R, respectively. This suggests that the propagating radical giving the 13- or 9-line spectrum which exhibits the temperature change is surrounded by the regular monomer crystals so that the spectrum is subjected to the monomer crystalline transition. However, the radical giving the conventional 9-line spectrum with the very weak 4-line component is surrounded by irregular polymer molecules. Bowden and O'Donnell[18] have also suggested the same interpretation for the time dependence of their spectrum during the post-polymerization at +50°C. The spectral change due to the crystalline transition of the surrounding monomer molecules reported in the previous paper[19] and the dose dependence of

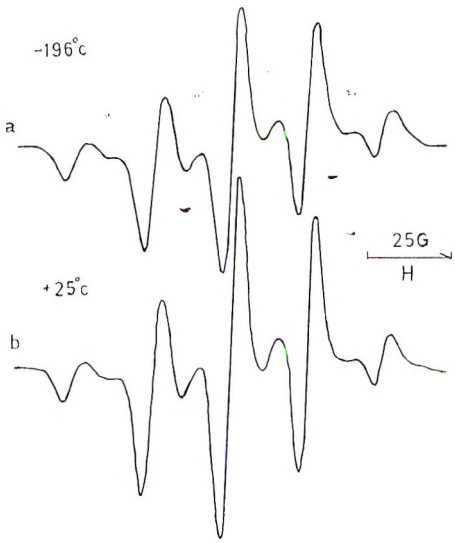


Fig. 5. Change with observation temperature of the conventional 9-line spectrum of PMAA observed at (*a*) −196°C and (*b*) +25°C.

the spectrum during the in-source polymerization definitely confirm this interpretation. The fact that the 13-line spectrum gradually changes into the conventional 9-line spectrum strongly indicates that the trapped radicals have essentially the same structure and the spectral difference comes from the surrounding matrix.

## Temperature Dependence of ESR Spectra

The temperature dependence of the spectra was measured for MAA monomers irradiated at 0°C for 19.5 × $10^4$R and for PMAA and PMMA irradiated at room temperature. The spectra have a conventional 9-line structure in the range from −196°C to +25°C. The results for PMAA are shown in Figure 5. The other cases also gave the similar spectra. Thus, the conventional 9-line spectrum not only has a different intensity of the 4-line component, but also exhibits a different temperature dependence. The small change of the spectra with temperature indicates that in the polymer matrix the structure of the trapped radicals is rigid except for the freely rotating $CH_3$ group. Usually the motion of the $CH_3$ group in radicals does not cease above −196°C.

If one assumes the rigid symmetrical conformation, that is, $\theta_1 = \theta_2 = 60°$ in Figure 1, the resulting spectrum has a much stronger 4-line component (see Fig. 7*a*). On the other hand, if one assumes the exchange of the two $\beta$-protons in the tilt conformation, one should have the weakest intensity of the 4-line component for the exchange rate $\tau^{-1} = 1/2\pi\Delta\nu_{spl}$, where $\Delta\nu_{spl}$ is the difference of the resonance frequencies for the two protons. From the modified Bloch treatment applied to the MAA monomers irradiated at −196°C,[19] it is evident that there must be a sharp temperature change for

such a condition. Therefore, the above two postulates do not account for the experimental results.

Now, as previously reported,[19] the propagating radical in the solid MAA monomers irradiated at −196°C has a conformation slightly tilted from the symmetrical structure, that is, $\theta_1 = 55°$ and $\theta_2 = 65°$ in Figure 1. In this case the trapped radicals are surrounded by the regular monomer lattice, but in the case of the conventional 9-line spectrum of PMAA or PMMA, the radicals are surrounded by irregular polymer molecules. In such a case, it is doubtful that the tilt angle is fixed at a unique position found in the MAA monomers, but it may be affected by the irregular environment of the polymer matrix, resulting in a distribution of the tilt angle. If one assumes that the surrounding matrix affects the tilt angle, one can not expect an admixture of radicals with preferred conformations because of the irregular field from the environment. From the gradual change from a 13-line to a 9-line spectrum, depending on radiation dose, it may be reasonable to assume that the most probable conformation is the same as that found in a regular monomer matrix and that the irregular environment gives some distortion from this position, depending on the irregular perturbations. Therefore, one should consider the distribution of the conformational angles around this position.

As was pointed out by Bamford et al.[17] and will be discussed later, the small deviation from the symmetrical position much the position of the $\sum_{\beta H} M_I = 0$ lines considerably but affects that of the $\sum_{\beta H} M_I = \pm 1$ lines only slightly (see Fig. 2*a*). Therefore, the distribution of the tilt angle may lower the 4-line component without affecting the 5-line component. Consequently, if one assumes that the hindering potential barrier of the oscillation around the $C_\alpha$—$C_\beta$ bond is high enough in the polymer matrix to observe little change with temperature of the spectrum, one may have a very weak 4-line component which does not change with observation temperature for such a model that the tilt angle of the $p$-orbital is distributed around the most probable position. The hindering potential barrier was estimated to be 7.2 kcal/mole in phase I of the MAA monomer matrix.[19] In the case of polymer matrix, if the barrier is around 10 kcal/mole or more, one can not observe an appreciable temperature dependence in the range from −196°C to room temperature.

## Simulation of the ESR Spectra Based on Distributed Conformation

The hyperfine lines due to the two $\beta$-protons having different coupling values should consist of four lines of equal intensity, as shown in Figure 2*a*. The outer two lines contribute to the 5-line component and the inner two lines contribute to the 4-line component of the 9-line spectrum. Assuming the $B \cos^2\theta$ rule, the coupling values $A_{\beta 1}$, $A_{\beta 2}$ for the two $\beta$ protons are expressed by

$$A_{\beta 1} = B \cos^2(\pi/3 - \alpha) \tag{1}$$

$$A_{\beta 2} = B \cos^2(\pi/3 + \alpha) \tag{2}$$

where $B = 46$G and $\alpha$ is the tilt angle from the symmetrical conformation $\theta_1 = \theta_2 = \pi/3$. As already pointed out by Bamford et al.[17] the separations $S_5(\alpha)$ and $S_4(\alpha)$ of the outer and inner lines are expressed by eqs. (3) and (4) if a small tilt angle $\alpha$ is assumed.

$$\begin{aligned} S_5(\alpha) &= A_{\beta 1} + A_{\beta 2} \\ &= (B/2)[1 + 2\alpha^2 - (2\alpha^4/3) + \ldots] \end{aligned} \tag{3}$$

$$\begin{aligned} S_4(\alpha) &= A_{\beta 1} - A_{\beta 2} \\ &= \sqrt{3}B[\alpha - (2\alpha^3/3) + \ldots] \end{aligned} \tag{4}$$

Therefore $S_5(\alpha)$ is not affected very much by the tilt angle $\alpha$, while $S_4(\alpha)$ is much affected.

Now, if one assumes the distribution of the tilt angle $\alpha$, the spectrum becomes a superposition of many conformations with different values of $\alpha$. In order to simulate such a spectrum, the following Gaussian distribution function around the most probable tilt angle $\alpha_0$ was assumed:

$$G(\alpha) = N \exp[-a(\alpha - \alpha_0)^2] \tag{5}$$

where

$$a = \ln 2/\Delta_{1/2}^2 \tag{6}$$

$$\Delta_{1/2} = \alpha_{1/2} - \alpha_0 \tag{7}$$

where $\alpha_{1/2}$ is the tilt angle at half-height and $\Delta_{1/2}$ is the half-height width of the Gaussian distribution. Therefore the resultant derivative spectrum $g'(H)$ for the radical having the distributed tilt angle may be expressed as follows:

$$g'(H) = \int_0^{\pi} g_\alpha'(H) \cdot G(\alpha) d\alpha \tag{8}$$

where $g_\alpha'(H)$ is the component derivative spectrum with the Gaussian line shape for the radical having the tilt angle $\alpha$.

In the computation of $g'_\alpha(H)$, $A_{CH_3}$ was assumed to be 22.2 G, which is the same as that of the propagating radical in the MAA monomers,[19] and the values of the $A_{CH_2}$ were calculated from eqs. (1) and (2). The $\Delta H_{msl}$ of the component spectrum $g'_\alpha(H)$ was assumed to be 6 G. As for the most probable tilt angle $\alpha_0$, it is reasonable to assume that it be equal to the value 5° of the propagating radical in the MAA monomers.[19] Figure 6 shows the simulated curves for such a model with various half-height widths $\Delta_{1/2}$ of the Gaussian distribution function. As is seen in the figure, the intensity of the 4-line component is very sensitive to the distribution of the tilt angle. If one assumes a small distribution ($\Delta_{1/2} = 5$–6°) of the tilt angle, quite satisfactory agreement with the experimental spectrum is obtained. It is quite possible that such a small range of distribution of the tilt angle actu-

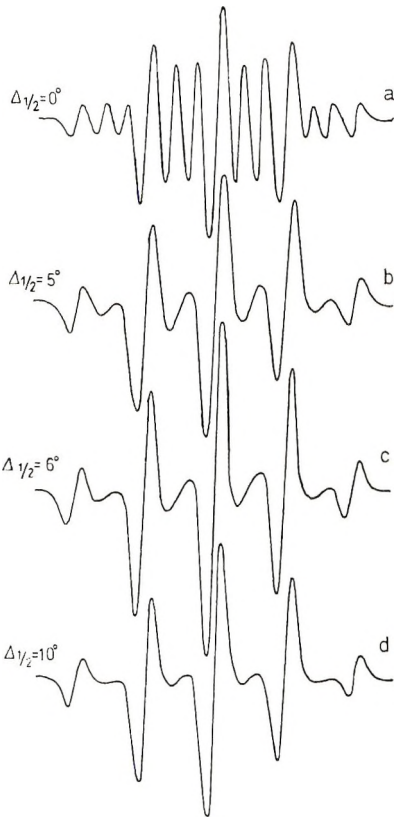


Fig. 6. Simulated ESR spectra for the radical $CH_2$—$\dot{C}(CH_3)COOR$ with a distributed conformation around the most probable position $\theta_1 = 55°$ and $\theta_2 = 65°$ with the Gaussian distribution. The half-height width $\Delta_{1/2}$ of the distribution is assumed to be (*a*) 0°, (*b*) 5°, (*c*) 6°, and (*d*) 10°.

ally exists in the polymeric system. Although it is reasonable to assume the most probable tilt angle $\alpha_0$ be 5°, tentatively $\alpha_0 = 0$, that is, the symmetrical conformation was next assumed for the same computation. The results are shown in Figure 7. In this case, one had to use the wider distribution ($\Delta_{1/2} = 10°$) to get the agreement with the experimental spectrum.

In any case, the concept of the distribution of the tilt angle in the polymeric system accounts satisfactorily for the experimental spectrum, and this concept is sometimes introduced as a factor contributing to the wide spectral line width of polymer radicals. In the present case, the 4-line component is very sensitive to the distribution, but the 5-line one is less sensitive. This is why the anomalously weak 4-line component was observed for the methacrylic radical in the polymeric system.

Although we did not compute the simulated curves with wider $\Delta_{1/2}$ than 10°, if one assumes $\Delta_{1/2}$ larger than 10° for $\alpha_0 = 5°$, it is expected that the 4-line component will be smeared out and the 5-line component will be

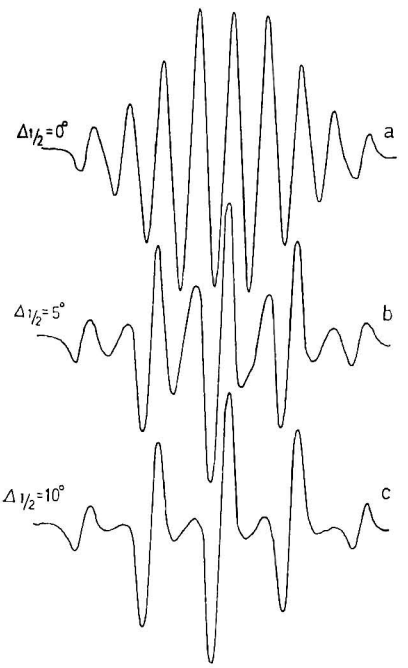


Fig. 7. Simulated ESR spectra for the radical $CH_2$—Ċ($CH_3$)COOR with a distributed conformation around the most probable position $\theta_1 = \theta_2 = 60°$ with Gaussian distribution. The half-height width $\Delta_{1/2}$ of the distribution is assumed to be (*a*) 0°, (*b*) 5°, and (*c*) 10°.

somewhat broadened. This might be the origin of the 5-line spectrum which was reported in Bowden and O'Donnell's paper. The spectrum indicated in Figure 2*d* of their paper has a weak shoulder at the position of the 4-line component and has a broader line width for the 5-line component.

In this way, the conventional 9-line spectra of PMAA and PMMA radicals are assigned to the same single radical species as the propagating radical found in the MAA monomers, and the most probable conformation of this radical is around 55° with a small distribution of the tilt angle around this position.

## CONCLUSION

The conventional 9-line spectrum of both irradiated PMAA or PMMA shows little temperature change in the range from −196°C to room temperature in contrast to the spectrum of the propagating radical found in MAA monomers or barium methacrylate dihydrate irradiated at −196°C. The conventional 9-line spectrum in the polymeric system has a very weak 4-line intensity as compared to that of the propagating radical. The difference is due to the surrounding matrix, and the conventional 9-line spectrum is well interpreted by introducing the concept of the small distribution of the con-

formational angle in the case of irregular polymer matrix. Thus, the unusual 9-line spectrum exhibiting the variation of the intensity of the 4-line component due to the experimental conditions was attributed to single radical species with such a conformation that the conformational angle has a small distribution around the most probable angle, which is nearly the same as that of the propagating radicals found in methacrylic acid monomers irradiated at −196°C.

## References


1. M. C. R. Symons, *J. Chem. Soc.*, **1959**, 277.
2. D. W. Ovenall, *Nature*, **184**, 181 (1959).
3. L. Piette, *NMR and ESR Spectroscopy*, Pergamon Press, Oxford, 1960, p. 218.
4. I. D. Campbell and F. D. Loney, *Australian J. Chem.*, **15**, 642 (1962).
5. A. Charlesby and D. K. Thomas, *Proc. Roy. Soc. (London), Ser. A*, **A269**, 104 (1962).
6. P. Kouřim and K. Vacek, *Tetrahedron Letters*, **23**, 1051 (1962).
7. M. C. R. Symons, *J. Chem. Soc.*, **1963**, 1186.
8. C. H. Bamford, G. C. Eastmond, and Y. Sakai, *Nature*, **200**, 1284 (1963).
9. A. T. Bullock and L. H. Sutcliffe, *Trans. Faraday Soc.*, **60**, 625 (1964).
10. H. Fisher, *J. Polym. Sci. B*, **2**, 529 (1964).
11. H. Fisher, *Z. Naturforsch.*, **19A**, 866 (1964).
12. M. G. Oremerod and A. Charlesby, *Polym.*, **5**, 67 (1964).
13. J. Sohma, T. Komatsu, and H. Kashiwabara, *J. Polym. Sci. B*, 287 (1965).
14. P. Kouřim and K. Vacek, *Trans. Faraday Soc.*, **61**, 415 (1965).
15. J. F. Kircher, F. A. Sliemers, R. A. Markle, W. G. Gager, and R. I. Leininger, *J. Phys. Chem.*, **69**, 189 (1965).
16. R. E. Michel, F. W. Chapman, and T. J. Mao, *J. Polym. Sci. A-1*, **5**, 677 (1967).
17. C. H. Bamford, A. Bibby, and G. C. Eastmond, *J. Polym. Sci. C*, **16**, 2417 (1967).
18. M. J. Bowden and J. H. O'Donnell, *J. Phys. Chem.*, **72**, 1577 (1968).
19. Y. Sakai and M. Iwasaki, *J. Polym. Sci. A-1*, in press.


Received November 8, 1968
Revised December 31, 1968

JOURNAL OF POLYMER SCIENCE: PART A-1 VOL. 7, 1549–1555 (1969)

# Polymerization of β-Cyanopropionaldehyde. VI. Anionic Polymerization Initiated by Aromatic Hydrocarbon–Sodium Complexes

KAZUHIKO HASHIMOTO and HIROSHI SUMITOMO,
*Faculty of Agriculture, Nagoya University,*
*Chikusa, Nagoya, Japan*

## Synopsis

Further investigation on an anionic polymerization of β-cyanopropionaldehyde was made with use of polystyryl–disodium, naphthalene–sodium, and tetraphenylethylene–disodium complexes as initiators. Styrene–β-cyanopropionaldehyde block copolymer was separated from the gross polymer obtained by the polymerization of β-cyanopropionaldehyde with polystyryl–sodium. The polymerization initiated by naphthalene–sodium and tetraphenylethylene–disodium complexes resulted in the formation of an aldol condensation-type product having a low molecular weight. It was found that initiators of weaker basicity may start the carbonyl polymerization, whereas those of stronger basicity cause the aldol condensation of β-cyanopropionaldehyde through the withdrawal of proton from the monomer.

## INTRODUCTION

It was described in the previous paper[1] that anionic polymerization of β-cyanopropionaldehyde (β-CPA) with benzophenone–alkali metal complexes was able to give poly(cyanoethyl)oxymethylene having a lower molecular weight but a higher stereoregularity and that the initiator concentration has a marked influence on the polymer yield and the stereoregularity.

The present paper is concerned with the further investigation of the anionic polymerization of β-CPA initiated by polystyryl–disodium, naphthalene–sodium, and tetraphenylethylene–disodium complexes in order to clarify the initiation mechanism and to observe the effects of the basicity of initiators on the anionic polymerization.

## EXPERIMENTAL

All procedures, including purification of materials, preparation of initiators and polymerization were carried out in a high-vacuum system ($<10^{-5}$ mm Hg). The technique employed here was the same as that previously described.[1]

## Materials

Purification of β-cyanopropionaldehyde (β-CPA) and tetrahydrofuran (THF) was as previously described.[1] Styrene was washed with a 5% aqueous potassium hydroxide and with water and dried over anhydrous sodium sulfate. After distillation under reduced pressure it was stored over calcium hydride in a high-vacuum system and distilled. Naphthalene was recrystallized from methanol after distillation under reduced pressure. Tetraphenylethylene of commercial origin was used as received.

## Preparation of Initiators

Naphthalene–sodium (Na-Naph) and tetraphenylethylene–disodium ($Na_2$-TPhE) complexes were prepared by treating solutions of naphthalene or tetraphenylethylene in THF with an excess of distilled sodium at 0°C. After one or two days the solutions were filtered. Identification of the initiators and the measurement of their concentrations were carried out in the same way as in the previous paper.[1] Polystyryl-disodium ($Na_2$-PSt) solution was quantitatively prepared by the polymerization of styrene with Na-Naph in THF. The spectrum of the solution shows an absorption at 343 mμ which is attributed to the polystyryl anion.

## RESULTS AND DISCUSSION

The results of polymerization of β-CPA with the use of $Na_2$-PSt are shown in Table I.

TABLE I
Polymerization of β-Cyanopropionaldehyde with use of Polystyrylsodium[a]

| Run no. | β-CPA, g | $Na_2$-PSt, g | $Na_2$-PSt, Mole-% (based on monomer) | Volume ratio of solvent to monomer | Polymer yield, g | Conversion of β-CPA, % |
|---|---|---|---|---|---|---|
| 46[b] | 3.35 | 1.05 | 0.39 | 11 | 1.22 | 5.0 |
| 47[c] | 3.39 | 0.87 | 0.32 | 10 | 1.34 | 13.6 |
| 49 | 16.78 | 4.97 | 0.33 | " | 5.89 | 5.5 |

[a] Conditions: $<10^{-5}$ mm Hg; −78°C; 1 day; solvent, THF.
[b] $x$, 0.14 (from yield), 0.15 (from elementary analysis).
[c] $x$, 0.35 (from yield), 0.36 (from elementary analysis).

The polymerization, accompanied by the fading of the initiator color, was observed to start immediately after the addition of the monomer solution to the initiator solution.

The polymer obtained was expected from the results of elementary and infrared analyses to consist of a mixture of polystyrene and poly(cyanoethyl)oxymethylene. Figure 1 shows the scheme and the results of elution fractionation of the mixed polymer with cyclohexane and benzene as

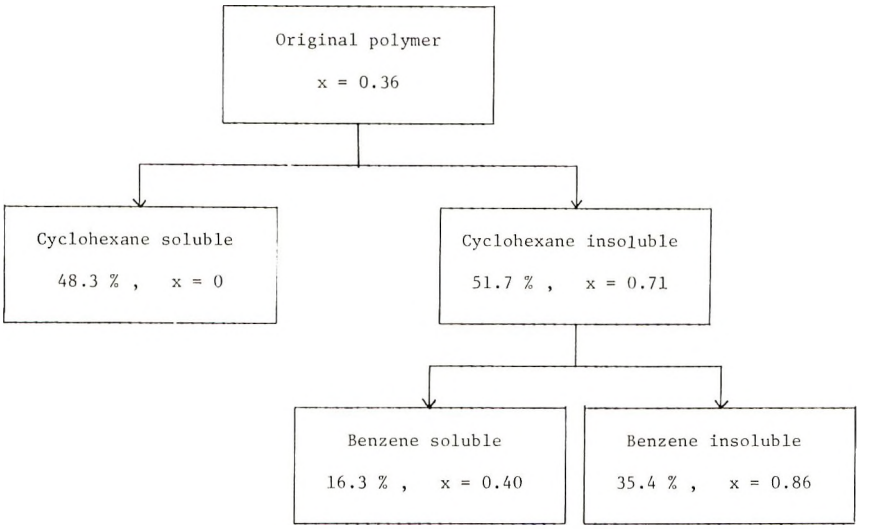


Fig. 1. Results of elution fractionation of polymer (run 47).

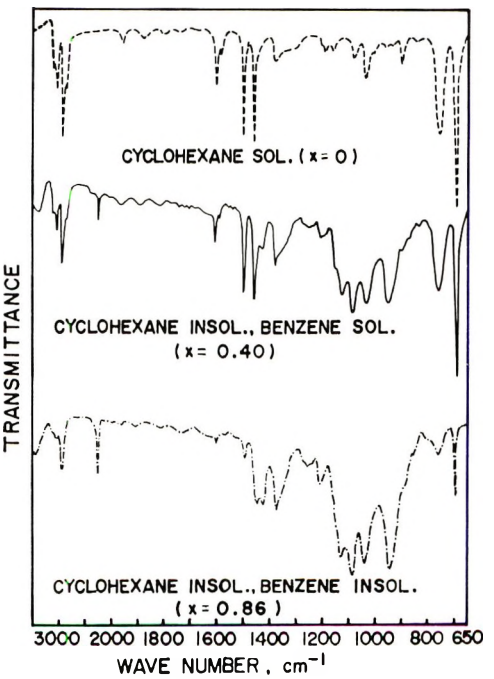


Fig. 2. Infrared spectra of polymer fractions (run 47).

solvents, where $x$ is the weight fraction of the poly(cyanoethyl)oxymethylene portion as determined by an elementary analysis.

The solubilities and infrared spectra of these fractions shown in Figure 2 suggest that the cyclohexane-soluble fraction, the cyclohexane-insoluble,

TABLE II
Polymerization of β-Cyanopropionaldehyde Initiated by Other Complexes[a]

| Run no. | β-CPA, g | Initiator | | Volume ratio of solvent to monomer | Polymer yield, g | Conversion, % | $D_{1258}/D_{1270}$ |
|---|---|---|---|---|---|---|---|
| | | Type | Mole-% (based on monomer) | | | | |
| 52 | 10.30 | Na-Naph | 0.11 | 5 | 6.55 | 63.6 | <1.00 |
| 50 | 7.35 | " | 2.11 | 5 | trace | 0 | 2.21 |
| 54 | 10.36 | " | 4.33 | 5 | 0 | 0 | — |
| 55 | 9.83 | $Na_2$-TPhE | 1.35 | 6 | 0 | 0 | — |

[a] Conditions: $<10^{-5}$ mm Hg; −78°C; 1 day; solvent, THF.

benzene-soluble fraction, and the cyclohexane-insoluble, benzene-insoluble fractions consist respectively of homopolystyrene, styrene–β-CPA block copolymer, and a mixture of block copolymer rich in poly(cyanoethyl)-oxymethylene and homopoly(cyanoethyl)oxymethylene. The copolymerization efficiency of $Na_2$-PSt calculated as [(weight of polystyrene in styrene–β-CPA block copolymer/weight of polystyrene initially used) × 100 (%)] may be estimated at about 23%, provided that all of polystyrene of the cyclohexane-soluble fraction is incorporated in the block copolymer chain.

The fact that the block copolymer was isolated suggests that the mechanism of initiation induced by carbanion conjugated with a phenyl group is of the bond-formation type. As the carbanions in benzophenone–dialkali metal complexes[1] may be conjugated with the phenyl groups, the initiation induced by them is also considered to be of the bond-formation type.

In Table II are shown the results of polymerization of β-CPA initiated by Na-Naph and $Na_2$-TPhE. It was observed that a lower initiator concentration brought on a higher yield and lower stereoregularity of polymer in the same way as the polymerization with benzophenone–alkali metal complexes.[1]

A polymerization system with a higher initial concentration of initiator produced no precipitate on treatment with a large amount of cold methanol as a precipitant. However, a very viscous, colorless, transparent liquid remained after the titration with dilute hydrochloric acid and removal of solvents and initiator residue by distillation and filtration, respectively. This material was found to have a molecular weight of about 400 (vapor pressure osmometry in dimethylformamide at 65°C) and the same contents of C, H, N and O as the β-CPA monomer.

Its infrared absorption spectrum, shown in Figure 3, shows $\nu_{O-H}$ and $\nu_{C-O}$ stretching absorption due to alcohol at about 3400 and 1134 $cm^{-1}$, respectively, as well as an absorption of $\nu_{C=O}$ stretching at 1720 $cm^{-1}$ that

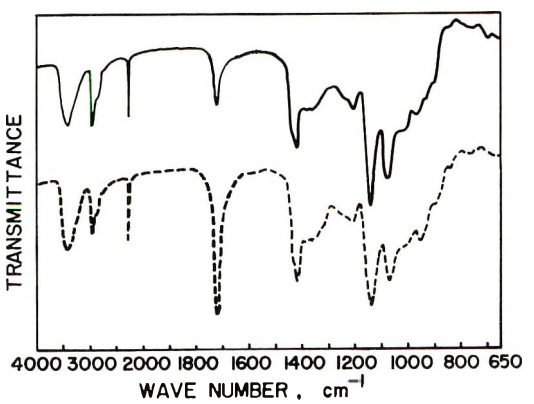


Fig. 3. Infrared spectra of byproduct of run 55: (——) byproduct of run 55; (- - - -) aldol condensation product.

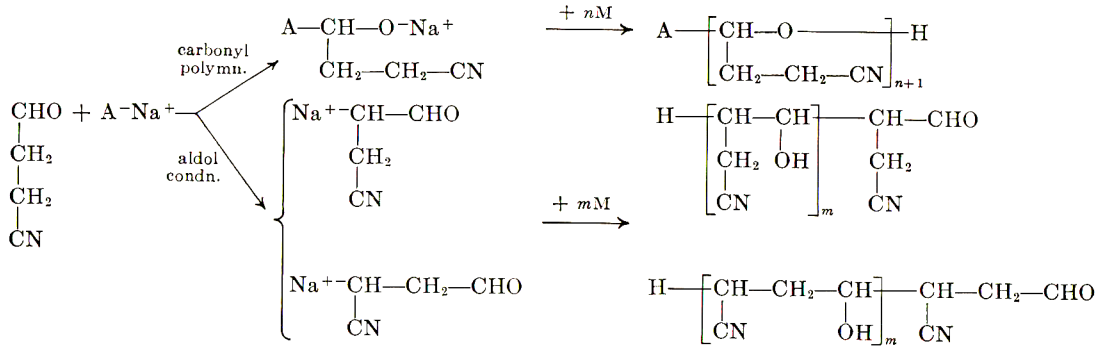


(1)

A⁻, initiator anion; M, monomer.

is weaker than in β-CPA. The dotted curve in Figure 3 shows the spectrum for the aldol condensation product obtained by the treatment of β-CPA with sodium carbonate at 0°C. From these analytical data, together with the results of NMR analysis, it is evident that the oligomeric byproduct was formed by the aldol condensation of β-CPA.

The aldol condensation of β-CPA may occur easily through the withdrawal of any active hydrogen from the monomer, followed by the addition of the carbanion produced to the carbonyl group, in competition with the main carbonyl polymerization [eq. (1)]. The detailed structure of the aldol condensation product obtained here is still not clear.

Initiators used in the investigation of the anionic polymerization of β-CPA may be divided into three groups based on their basicities, as shown in Table III.

TABLE III
Effect of Basicity of Initiators

| Group | Basicity | Initiator | Polymerization of β-CPA[a] | |
|---|---|---|---|---|
| | | | Carbonyl polymerization | Aldol condensation |
| A[b] | weak | Na-BzPh | + | − |
| B[b] | | $Na_2$-BzPh, $Li_2$-BzPh | + | − |
| C | strong | $Na_2$-TPhE, $Na_2$-PSt, Na-Naph | ± | + |

[a] + denotes frequent occurrence; ± denotes occurrence only at lower initiator concentration.

[b] Data of Sumitomo and Hashimoto.[1]

The initiators of group A and B, of comparatively weak basicity, seem to be capable of initiating the carbonyl polymerization, whereas those of group C, of stronger basicity, produce aldol condensation rather than the carbonyl polymerization. It may be that the stronger basicity of anionic initiators tends more to withdraw a proton from β-CPA, with the result that aldol condensation occurs.

## Reference

1. H. Sumitomo and K. Hashimoto *J. Polym. Sci.*, in press.

Received October 3, 1968
Revised January 14, 1969

JOURNAL OF POLYMER SCIENCE: PART A-1 VOL. 7, 1557–1566 (1969)

# High-Pressure Studies of Polymerization in Sulfur

GARY C. VEZZOLI, FRANK DACHILLE, and RUSTUM ROY,
*Materials Research Laboratory, The Pennsylvania State University, University Park, Pennsylvania 16802*

## Synopsis

By x-ray and optical studies of thermally quenched products and by differential thermal analysis under pressure the effect of high pressure on the melting and polymerization of sulfur has been investigated to 31 kb and 500°C. At least four different liquid fields have been identified. DTA experiments indicate that pressure shifts the 159°C polymerization transition first toward higher temperatures and then toward lower temperatures until it finally coincides with the melting point at a pressure of about 0.7 kb. The depolymerization temperature was found by the same technique to increase with increasing pressure up to 0.4 kb. A liquid $P$–$T$ boundary that may constitute the higher-pressure extension to the depolymerization transition has been traced up to 7.5 kb and 480°C. A very sharp, practically temperature-independent reaction in the liquid state has been located at about 9 kb extending from the liquidus to at least the limits of the apparatus at about 450°C. Evidence has been found for a possible second-order phase transformation extending from about 10 kb at 400°C to the liquidus at approximately 360°C.

## INTRODUCTION

The polymorphism of sulfur under pressure has been the subject of recent inquiry, as have been the pressure–temperature relationships regarding the structure and properties of liquid sulfur.[1–3] That there has not been even more research in this latter field is not from lack of interest but probably because of experimental difficulties encountered in maintaining molten sulfur under high pressure and analyzing the quenched product.

Gee[4] reports that at atmospheric pressure the viscosity of liquid sulfur decreases from 0.11 P at 117°C to a minimum of 0.066 P at 154°C, then rises rapidly and achieves a maximum at about 197°C, and thereafter decreases rather slowly. According to Bacon and Fanelli,[5] the viscosity increases by a factor of 2000 over the narrow temperature range of 159–166°C and achieves a maximum value at about 187°C. They find that the viscosity–heating curve practically coincides with the viscosity–cooling curve and that the maximum is decreased sharply by the presence of impurities when the sample is preheated for a relatively short period. Eisenberg[6] places the temperature of maximum viscosity at about 170°C. The abrupt rise in viscosity is attributed by Gee[4] to the simultaneous rise in concentration and in the chain length of the polymer until a maximum length of about $10^6$

atoms is achieved. As temperature continues to increase, the slow fall in viscosity he explains as a consequence of the opposing effects of decreasing polymer chain length and increasing polymer concentration.

Lewis and Randall,[7] Braune and Moller,[8] and West[9] all reported a sharp peak at 159°C in the heat capacity at atmospheric pressure as a function of temperature. The increase in the specific heat at 159°C is believed to correspond to the contribution of the heat of polymerization to the heat capacity.

Powell and Eyring[10] predicted that high pressure would contribute to a higher viscosity, since (in the liquid state) $S_8$ rings become $S_8$ chains and short chains join to form long chains upon a decrease in volume. From thermodynamic considerations, assuming an increase of molar volume on the opening of the $S_8$ ring, Eisenberg[6] has predicted that as pressure is increased, the polymerization transition of liquid sulfur will be shifted toward lower temperatures until it coincides with the melting point at 850 atm. Also from a thermodynamic argument Gee[11] pointed out that (within certain approximations) in polymeric materials resulting from ring scission, the relationships between temperature and polymer concentration are dependent on the sign of the entropy and enthalpy changes. Tobolsky and Eisenberg presented a unified theory on the equilibrium polymerization of sulfur which closely agrees with experimental data.[12]

Doi[13] showed experimentally that pressure raised the viscosity–temperature curve of sulfur. Solar and co-workers[2] observed different-colored viscous liquids (dark gray, red, yellow) corresponding to samples thermally quenched from different pressure and temperature conditions. From the above reported results it appears that sulfur offers a valuable system for the study of pressure effects on polymerization.

## EXPERIMENTAL

Differential thermal analysis under argon pressure was utilized from atmospheric pressure to 1 kb at a heating rate of 2°C/min. The sulfur was encapsulated in platinum tubes that were welded closed at both ends. Between 2.5 and 31 kb an opposed anvil high-pressure system as described by Dachille and Roy[14] was employed; the quenched samples from this were analyzed by optical and x-ray techniques.

Sample powders of 99.999+% purity were pressed into nickel rings of dimensions 0.375 in. outer diameter, 0.125 in. inner diameter, and 0.015 in. thickness. However, at pressures exceeding 18 kb these rings ruptured, presumably due to a phase transition in sulfur while still in the crystalline state. It had been found with sulfur and with similar materials that when a ring was broken, the pressure was no longer reliable. To remedy this, a ring of dimensions 0.25 in. outer diameter, 0.038 in. inner diameter, and 0.010 in. thickness was utilized at higher pressures and found effective. By comparing the melting temperature at about 17 kb determined with the 0.375-in. ring with that determined with the use of the 0.25 in. ring (at the

same pressure) it was found that a correction of +1.2 kb had to be applied to runs in which the latter ring was used.

Temperatures were measured with platinel II and chromel–alumel thermocouples and were accurate to ±3°C. Pressures in the DTA system were accurate to ±1% and in the opposed anvil system to ±5–10%. To determine the melting curve about 70 runs were required, with particular emphasis in the neighborhood of sharp curvature changes. To delineate the phase boundaries in the liquid state another 150 runs were required.

## RESULTS

Before a study of the polymerization of liquid sulfur could be conducted the melting curve had to be delineated. This curve is drawn in Figure 1 and its breadth is an expression of the degree of experimental error expected at the specific conditions of pressure and temperature. Important features of the liquidus are the maximum at 17 kb and 347 ±2°C and the possible cusp at 18 kb and 345 ±2°C. The same features were also observed by Paukov et al.[3] at about 16 kb at 310°C and 19 kb at 290°C and by Susse et al.[15] at approximately 15 kb at 300°C and 19 kb at 290°C; in both studies other high-pressure systems were used. Up to a pressure of 10 kb our experimental liquidus is in good agreement with that of Paukov and of Susse; however, above this pressure our curve corresponds more closely to the liquidus of Deaton and Blum.[16] We shall present a comparative study of experimental melting curves in another paper.

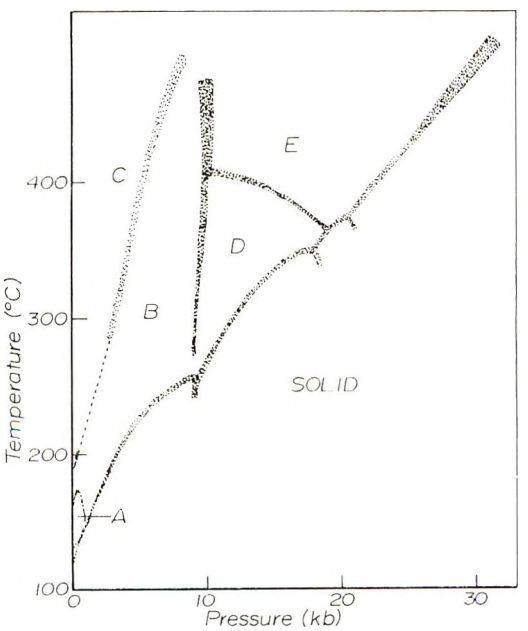


Fig. 1. Melting curve and liquid phases of sulfur from atmospheric pressure to 31 kb.

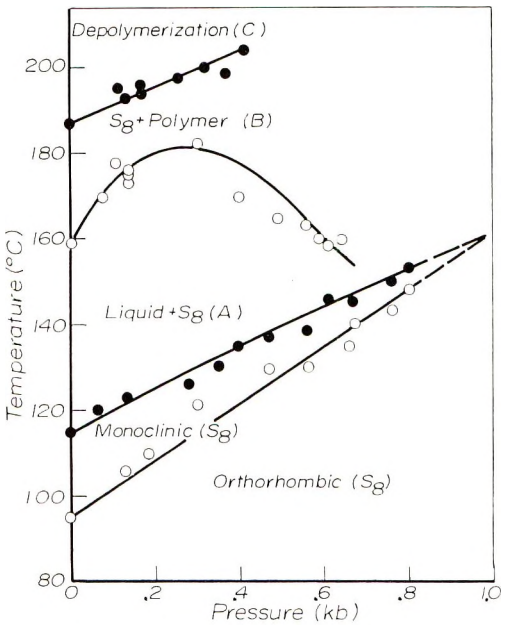


Fig. 2. Sulfur phase diagram up to 1 kb.

The orthorhombic–monoclinic and monoclinic–liquid phase boundaries (Fig. 2) were determined at elevated pressures by means of differential thermal analysis. The monoclinic phase field is quickly pinched out and appears as a wedge in equilibrium between the orthorhombic phase and the melt, roughly in agreement with the results of Tammann.[17] The polymerization temperature and its pressure variation were investigated also by DTA. This temperature was observed (see Fig. 3) to increase with increasing pressure until it achieves a rather broad maximum and then decreases as shown in Figure 2 (separating phase fields A and B). Finally, the polymerization temperature curve intersects the melting curve at a pressure extrapolated to 0.7 kb. The A–B boundary plotted in Figures 1 and 2 is drawn on the basis of DTA experiments at pressure in the up-temperature direction. In the down-temperature direction (from 200°C to 30°C) thermal responses were insufficient to determine this curve since no definite peak corresponding to the polymer → octamer transition could be found upon cooling. However, the results of Bacon and Fanelli[5] show that from viscosity criteria the polymerization transition at atmospheric pressure is found to be reversible. By DTA the pressure dependence of the depolymerization temperature was found to increase from 187°C at atmospheric pressure to 206°C at 0.41 kb. Figure 3 shows a tracing of the results of a typical DTA experiment. It was noted that the ratio between the heat effect of melting and that of polymerization was consistently about 7.5:1 at a pressure of 136 bars and about 5:1 at pressures of 300 bars and 585 bars. According to Gee,[11] at atmospheric pressure the ratio of the heat effect of

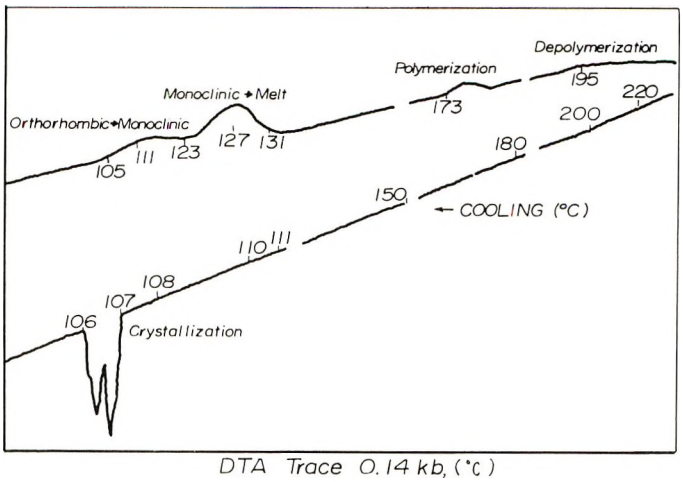


Fig. 3. DTA trace at 140 bars. The total area under the curves representing the orthorhombic–monoclinic and monoclinic–liquid heat effects is approximately equal to the total area beneath the recrystallization heat-effect. The temperature of recrystallization is delayed by 16°C presumably due to effects of supercooling and metastability.

ring opening (melting) to that of polymerization is about 10.3:1. With regard to the orthorhombic–monoclinic phase transition, however, we did not find any consistency between the ratio of its heat effect to that of melting. The reasons for this are not clear.

By the opposed anvil method experiments from 2.5 kb to 7.5 kb between 200°C and 475°C revealed a $P$–$T$ boundary that separated viscous quenched products from brittle ones. The upper limit of this boundary was set by difficulties in maintaining the sample at temperatures near and above 450°C. Samples which were thermally quenched (at pressure) from temperatures above the B–C boundary were somewhat brittle and could easily be crushed into a powder. Prompt examination with the petrographic microscope showed that the quenched product from field C consisted of orthorhombic crystallites. From the x-ray diffraction studies it appears that material C rapidly crystallizes in the orthorhombic form with reflections 1.82 Å and 2.84 Å indicating preferential orientation (See Fig. 4).

Another $P$–$T$ boundary (B → D) in liquid sulfur at 9 kb at 250°C and extending to about 10 kb at 450°C was found by the use of the opposed anvil method. Again the upper limit was set by difficulties in retaining the sample. Products thermally quenched from field B were viscous and barely "stretchable," (could not be drawn into a fiber) gave an x-ray pattern of orthorhombic sulfur with random orientations and dissolved readily in $CS_2$, whereas products quenched from the D field were highly stretchable, insoluble in $CS_2$ and also gave an x-ray pattern on "annealing" similar to that of orthorhombic sulfur, except for relative intensities and the presence of a new strong reflection at 4.52 Å (see Fig. 4). The $B$–$D$ reaction was found to be completely reversible and practically temperature-independent.

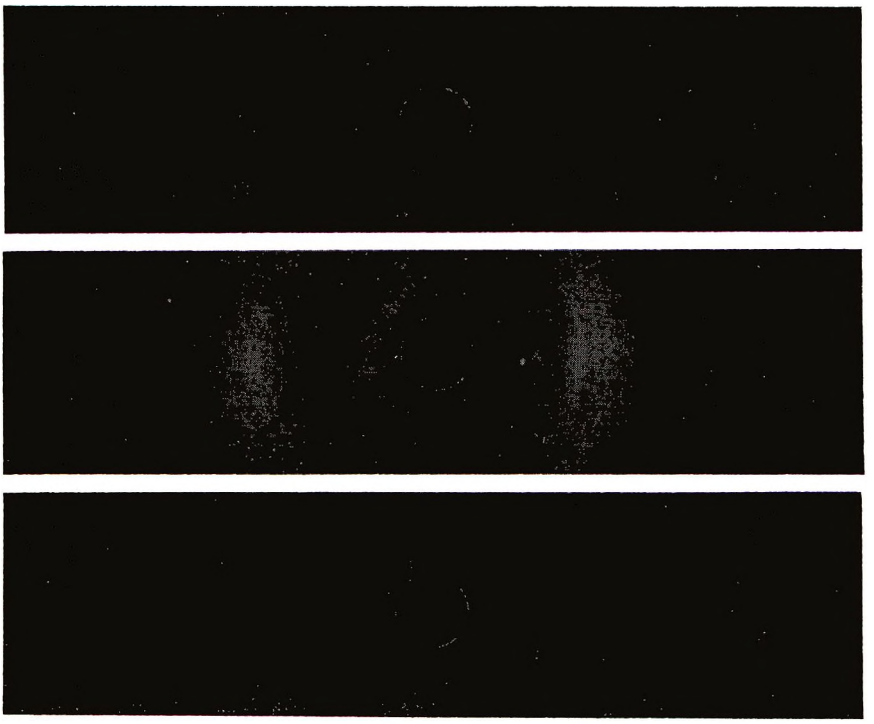

Fig. 4. X-ray diffraction patterns: (*1*) orthorhombic sulfur at room conditions; (*2*) quenched product from phase field C; (*3*) quenched product from phase field D (identical to x-ray pattern of quenched product from phase field E). Quenched products from phase field B gave an orthorhombic pattern very similar to pattern *1;* however, the orientations showed no consistency.

After holding a sample in field D for one week the quenched product was observed to be still very stretchable. Products quenched from $P$–$T$ conditions corresponding to the B–D boundary line contained both B and D.

Samples subjected to oscillating shearing stresses by the use of the shear modification of the opposed anvil system at a pressure of 13 kb and temperature of 352°C (region D) for 1–3 hr were a bright, translucent yellow and far more fluid (more liquidlike) than the brownish, highly viscous products that had not been sheared but were thermally quenched from the same $P$–$T$ conditions. Shearing, however, had no effect on changing the B–D phase boundary.

The liquid D was also quenched rapidly in pressure into the B field and then immediately thermally quenched. Similarly, the B liquid was "moved" rapidly into the D field by raising pressure followed by immediate thermal quenching. It was found that samples quenched by cooling at run pressure had the same appearance as those quenched by the above methods.

The B → D reaction in liquid sulfur, initially determined by thermal quenching at pressure, was also investigated by experiments in which pressure was rapidly released and the sample immediately removed and rapidly

cooled to room temperature. Products which were "pressure-quenched" in this manner from regions D and B were both viscous and stretchable, having an appearance very similar to polymeric sulfur formed by cooling from the melt at atmospheric pressure. Because of the small amounts of sample in each run (about 35 mg), no precise experiments could be made to determine which quenched product had the higher viscosity. Although pressure quenching did not give substantial evidence to affirm the B → D reaction, it should be noted that samples quenched by rapid pressure release (at run temperatures which are above the melting point at atmospheric pressure) are exposed for a brief time to an elevated temperature at atmospheric pressure. Thus such samples are in the stability field of a different liquid for a very short period of time and the resulting quenched product may give a very distorted picture of the real field under study.

Further experiments revealed a narrow region extending from the B–D boundary in the neighborhood of 10 kb at 400°C down to the liquidus at about 360°C and 18.5 kb from which quenched samples were viscous but barely stretchable and had the same appearance as samples thermally quenched from region B. At temperatures above this narrow region the thermally quenched product was again highly stretchable, insoluble in $CS_2$ and essentially identical to products thermally quenched from the D field. Quenched products from runs placed in this region often had both highly stretchable and "barely stretchable" material.

## DISCUSSION

Experimental evidence indicates that pressure shifts the "polymerization transition" (A → B) first to slightly higher and then to lower temperatures until it coincides with the melting point at 0.7 kb. Hence, above a pressure of about 0.7 kb sulfur must melt directly to the mixture of $S_8$ rings and diradical terminated chains as described by Eisenberg.[6] In other words, above this pressure conditions are favorable at the melting temperature for immediate chain growth. It is suspected that pressure may preferentially dampen the vibrations of the ends of the octameric chains first formed by ring scission, thereby increasing the probability for bonding with neighboring broken rings and small chains and hence promoting high polymer growth.

It might be expected, then, that the temperature necessary to break up long chains and hence reduce viscosity should increase with increasing pressure. Experimentally this appears to be the case, since the depolymerization temperature (interpreted to correspond to the maximum polymer chain length described by Gee[4]) rises with pressure as shown in Figure 2 up to 0.41 kb.

It is believed that the B–C boundary, determined at higher pressures by the opposed anvil method, is actually representative of the same depolymerization found by DTA and described above. However, DTA samples could not be rapidly quenched and compared to quenched products from the

opposed anvil system. Furthermore, the experimental limits of the two systems with regard to pressure do not overlap. However, the facts that the slopes of these two curves are about equal and that the products quenched from region C are not viscous support the suggestion that the B–C boundary is the high-pressure extension of the depolymerization boundary.

The B–D boundary cannot be a consequence of a solid-state phase transition through which the sample was quenched because as described earlier an increase or decrease in pressure sufficient to "move" the sample to the opposite side of the B–D boundary, followed by immediate thermal quenching had no visible effect on the end product. Hence, except for the small decrease in pressure while still in the liquid state, samples quenched from field D pass through the solid-phase field along the same path as those quenched from field B, yet the reaction products are strikingly different. Similarly, the same obvious difference in end products is observed in samples "moved" from field B by slight increase of pressure into field D and quenched thermally through the crystalline field along the same isobar as those samples thermally quenched directly from field D.

It is not likely that there is metastability involved in the D field because thermally quenched products which had been placed in the D field for periods of time ranging from 1 hr to 1 week had the same appearance. The fact that the product quenched from field D is insoluble in carbon disulfide suggests an analogy to the carbon disulfide-insoluble sulfur known to exist at atmospheric pressure upon slow cooling of the sulfur melt. Since the x-ray pattern of the stretchable product quenched from field D is so similar to that of orthorhombic sulfur, then by the same argument as used by Donohue and Caron,[18] it would seem extremely doubtful that this product could have the helical structure proposed by Pinkus et al.[19] for $CS_2$-insoluble sulfur at atmospheric pressure.

Although shearing the sample had no effect on changing the B–D boundary, it did cause a large decrease in the viscosity of the product thermally quenched from the D field and hence probably had some kind of inhibiting influence on polymer formation and perhaps particularly on crosslink chains.

If the B–C boundary and the depolymerization are in fact identical as suggested earlier, then phase B must consist of an equilibrium mixture of $S_8$ rings and polymer, since this mixture has been well established by others at atmospheric pressure. (Included in this mixture may be a small proportion of larger rings first formed at temperatures slightly lower than the critical polymerization temperature.)[20] Boundary B–D may then be a pressure barrier (as suggested by Powell and Eyring) above which there is a rapid increase in chain length and polymer contribution to the equilibrium mixture, both induced by a decrease in volume and reflected experimentally as a rise in "stretchability" and viscosity. On the other hand the B–D boundary may correspond to a transition to an equilibrium mixture of polymer and a ring of a different structure, perhaps six-membered. (The existence of six-

membered rings in small amounts has been established by Braune and Moller[8] at atmospheric pressure.)

The narrow zone which separates the two highly stretchable high-pressure liquids (D and E) may actually be simply a phase boundary or a boundary specifying the $P$–$T$ conditions for a polymerization reaction rather than a separate phase field. The viscosities of products quenched from this narrow zone appear to be considerably lower than the viscosities of products quenched from fields D and E (this observation as all others on viscosity was based on simple stretch tests, since no exact viscosity measurements could be made). Hence plotting relative viscosity along an isobar or isotherm connecting fields D and E would show a discontinuous minimum at a temperature or pressure corresponding to the intersection of the isobar or isotherm with the D–E boundary zone. It is interesting that at atmospheric pressure when the viscosity of the liquid is about minimum at the critical polymerization temperature of 159°C, the specific heat achieves a sharp and discontinuous maximum or peak.[7–9] If an analogy may be ventured, and the same type of discontinuous maximum in specific heat accompanies the minimum viscosity believed to be found along the D–E boundary, then this boundary would represent that of a second-order phase transformation in which the second derivative of Gibbs free energy with respect to pressure or temperature changes discontinuously. Then an increase in specific heat would be the contribution of the heat of the reaction D → E.

In studying the polymerization of liquid sulfur at pressures too high for our differential thermal analysis apparatus to be employed, emphasis had to be placed on the viscosities of the quenched products of the opposed anvil runs. Basing certain phase boundaries on these viscosity criteria is by no means unjustified, since as Bridgman[21] as well as others[4,10,22] pointed out that viscosity must be a function of the liquid structural interlocking. Bridgman's contentions that relative variations of viscosity as a function of temperature are much more pronounced at higher pressures and that the largest pressure effects on viscosity are found in those materials with the most complicated molecular structures are well borne out in sulfur with its complex eight-membered puckered rings and n-membered chains. Thus, it is valid to speak of phases of different molecular structure in the liquid state because, again as stated by Bridgman, with respect to viscosity the molecule continues to behave and function as a unit, even when the volume is greatly reduced by the application of high pressure, and as the Andrade[22] theory suggests, viscosity is a measure of a temporary "freezing-together" of molecules in the liquid state into larger aggregates which have a more nearly crystalline character over a short range.

Notwithstanding the qualitative viscosity data, it is not known at the moment whether boundaries B–D and D–E represent phase boundaries in the liquid state, or correspond to polymerization reactions. Products quenched from $P$–$T$ conditions on these boundaries show in each case the presence of two materials, and thus suggest that D and E are separate

phases. However, since we are dealing with nominally homogeneous equilibrium and have no data with regard to the ring-chain concentration of the liquids, we cannot affirm in the strict sense the existence of different phases in the liquid state. Thus whether or not reactions B $\rightleftharpoons$ D and D $\rightleftharpoons$ E are phase changes or polymerization reactions is still subject to inquiry.

We are indebted to Dr. Della M. Roy for helpful discussions and reading the manuscript and to H. Jeffrey Bender for laboratory assistance.

This research is supported by the National Science Foundation, contract number GK-1686X.

## References

1. T. Baak, *Science*, **148**, 1220 (1965).
2. C. Sclar, L. Carrison, W. Gager, and O. Stewart, *J. Phys. Chem. Solids*, **27**, 1339 (1966).
3. I. Paukov, E. Tonkov, and D. Mirinskiy, *Dokl. Akad. Nauk SSSR*, **164**, 588 (1965).
4. G. Gee, *Trans. Faraday Soc.*, **48**, 515 (1952).
5. R. Bacon and R. Fanelli, *J. Am. Chem. Soc.*, **65**, 639 (1943).
6. A. Eisenberg, *J. Chem. Phys.*, **39**, 1852 (1963).
7. G. Lewis and M. Randall, *J. Am. Chem. Soc.*, **33**, 476 (1911).
8. H. Braune and O. Möller, *Z. Naturforsch.*, **9a**, 210 (1954).
9. E. West, *J. Am. Chem. Soc.*, **81**, 29 (1959).
10. R. Powell and H. Eyring, *J. Am. Chem. Soc.*, **65**, 648 (1943).
11. G. Gee, in *Inorganic Polymers* (International Symposium on Inorganic Polymers, July, 1961), special publication No. 15, The Chemical Society, London, 1961, p. 67.
12. A. Tobolsky and A. Eisenberg, *J. Am. Chem. Soc.*, **81**, 780 (1959).
13. T. Doi, *Rev. Phys. Chem. Japan*, **33**, 41 (1963).
14. F. Dachille and R. Roy, in *The Physics and Chemistry of High Pressures*, Society of Chemical Industry, London, 1962, pp. 77–85.
15. C. Susse, R. Epain, and B. Vodar, *J. Chim. Phys. (France)*, **63**, 1502 (1966).
16. B. Deaton and F. Blum, *Phys. Rev.*, **137**, A1131 (1965).
17. G. Tammann, *Ann. Phys.*, **3**, 178 (1900).
18. J. Donohue and A. Caron, *J. Polym. Sci.*, **50**, S-17 (1961).
19. A. Pinkus, J. Kim, J. McAtee, and C. Concilio, *J. Polym. Sci.*, **40**, 581 (1959).
20. F. Fairbrother, G. Gee, and G. Merrall, *J. Polym. Sci.*, **16**, 459 (1955).
21. P. Bridgman, *The Physics of High Pressure*, G. Bell and Sons, Ltd., London, 1931, p. 354.
22. C. Andrade, Nat.: (a) 125, 309 (March 1, 1930); (b) 125, 582 (April 12, 1930).

Received January 6, 1969
Revised January 31, 1969

# NOTES

## *Further Remarks on Butadiene Polymerization with Nickel–Organic Halide Systems*

Recently we have found that systems consisting of reduced nickel and some organic halides could selectively induce radical and cationic polymerizations, depending on the kinds of the vinyl monomers used.[1,2] When these initiator systems, especially those of reduced nickel and methylchlorosilanes, were used for butadiene polymerization in benzene, polymers composed of predominantly *cis*-1,4 structure were obtained.[3]

In the present work, the effects of halide components in the initiator systems and of the solvents were further investigated. These materials were found to affect markedly the microstructure of the resulting polybutadienes.

### EXPERIMENTAL

Butadiene, benzene, and the reduced nickel were the same as used in the previous paper.[3] Tetrahydrofuran was purified by the usual method and distilled prior to use. Organic halides were distilled before use, except that carbon tetrabromide and iodoform were reagent-grade materials used without further purification. The polymerization of butadiene and the characterization of the resulting polymers were also as described in the previous paper.[3]

### RESULTS AND DISCUSSION

Some of the results are given in Table I, from which it was found that the systems of reduced nickel and carbon tetrachloride and chloroform could also induce the polymerization. The *cis*-1,4 contents of the resulting polymers were lower than those obtained by using methylchlorosilanes.[3]

All polymers were found to contain no gel fraction. It was noted that the microstructure of the resulting polybutadienes was significantly influenced by the kinds of halides and solvents used. When chlorides and bromides were used as halide components in benzene, polymers composed largely of the *cis*-1,4 units were obtained. However, with bromides and iodides in tetrahydrofuran, the polymers were predominantly of the *trans*-1,4 type.

These effects of solvents and halides on the microstructure of the resulting polybutadienes are very similar to those observed in the polymerizations with $\pi$-allyl nickel halides.[4] In the previous paper,[3] in which methylchlorosilanes were used as the halide component, we assumed that these *cis*-1,4 polymerizations might be performed by a coordinated cationic mechanism. From the results of Table I, it may be better to consider that the polymerizations of butadiene by these catalyst systems proceed via a $\pi$-allyl-coordinated mechanism [eq. (1)] rather than a coordinated cationic one.

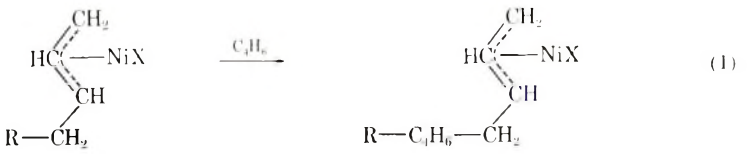


(1)

TABLE I
Polymerization of Butadiene with Reduced Nickel–Organic Halide Systems at 60°C[a]

| Halide | Solvent | Yield, % | $[\eta]$, dl/g | Microstructure, % | | |
|---|---|---|---|---|---|---|
| | | | | *cis*-1,4 | *trans*-1,4 | Vinyl |
| $CCl_4$ | Benzene | 26.2 | 0.28 | 79.0 | 16.3 | 4.7 |
| | Tetrahydrofuran | 6.5 | — | 48.6 | 35.9 | 15.5 |
| $CBr_4$ | Benzene | 15.9 | 0.06 | 65.6 | 28.9 | 5.5 |
| | Tetrahydrofuran | 14.2 | 0.08 | 21.6 | 67.0 | 11.4 |
| $CHCl_3$ | Benzene | 18.2 | — | 79.5 | 16.4 | 4.1 |
| | Tetrahydrofuran | 1.3 | — | 36.5 | 56.2 | 7.3 |
| $CHBr_3$ | Benzene | 51.3 | 0.11 | 72.5 | 25.0 | 2.5 |
| | Tetrahydrofuran | 4.1 | 0.09 | 7.2 | 71.0 | 21.8 |
| $CHI_3$ | Benzene | 12.3 | 0.03 | 25.7 | 64.0 | 10.3 |
| | Tetrahydrofuran | 45.2 | 0.31 | 6.7 | 90.4 | 2.9 |
| $C_6H_5CH_2Br$ | Benzene | 31.4 | 0.19 | 65.4 | 32.0 | 2.6 |
| | Tetrahydrofuran | 17.0 | 0.11 | 5.6 | 75.6 | 18.8 |
| $CH_2{=}CHCH_2Br$ | Benzene | 28.2 | 0.09 | 66.8 | 27.6 | 5.6 |
| | Tetrahydrofuran | 3.4 | 0.06 | 26.6 | 66.4 | 7.0 |

[a] Time 24 hr; monomer 5 ml.; solvent 5 ml.; reduced nickel 0.5 g.; halide 1 mmole.

Here R and X represent alkyl and halide groups in the alkyl halides used, respectively. Work on more detailed mechanisms is in progress.

## REFERENCES

1. T. Otsu, S. Aoki, M. Nishimura, M. Yamaguchi, and Y. Kusuki, *J. Polym. Sci. B*, **5**, 835 (1967).

2. T. Otsu, S. Aoki, M. Nishimura, M. Yamaguchi, and Y. Kusuki, *J. Polym. Sci. A-1*, in press.

3. T. Otsu and M. Yamaguchi, *J. Polym. Sci. A-1*, **7**, 387 (1969).

4. L. Porri, G. Natta, and M. C. Gallazzi, in *International Symposium on Macromolecular Chemistry, Prague* (*J. Polym. Sci. C*, **16**, O. Wichterle and B. Sedláček, Eds., Interscience, New York, 1967, p. 2525.

Shiuzo Aoki
Shizuo Kubota
Takayuki Otsu

Department of Applied Chemistry
Faculty of Engineering
Osaka City University
Sumiyoshi-ku, Osaka, Japan

Received October 29, 1968
Revised January 22, 1969

## *Synthesis of 2,5-Dimethyl-2,4-Hexadiene*

A catalytic process for the synthesis of 2,5-dimethyl-2,4-hexadiene (I) from 2,2,4-trimethyl-3 penten-1-ol (II) via homoallylic rearrangement has been devised. Diene(I) can be prepared by magnesium coupling of methallyl chloride,[1] but this method requires a mole of metal per mole of diene and expensive solvents. We have observed that the dehydration II → I occurs smoothly at 120–150°C over $Al_2O_3$ or $Al_2O_3/SiO_2$ catalysts.

The diene(I), an important intermediate in pyrethrin synthesis, has been homopolymerized,[2] copolymerized with isobutene[3] with the use of Lewis acid catalysts, and forms a 1:1 radical-initiated copolymer with maleic anhydride.[1]

That catalytic dehydration of II → I would be feasible was inferred from the solvolytic behavior of derivatives of II, obtained byMeerwein-Pondorf-Verley reduction of 2,2,4-trimethyl-3-pentenal, yield 54%, bp 170°C, $n_D^{20} = 1.547$, (reported[4] bp 170°C). Prior to the publication of Wilcox and Nealy[5] we also had observed the solvolytic rearrangement of the *p*-toluenesulfonate and *p*-nitrobenzoate esters of II to 2,5-dimethyl-2-4-hexadiene (I). In confirmation of their results, acetolysis of II-tosylate (II-OTS) gave diene (I), unrearranged II-acetate, and the rearranged acetate of III. Similarly,

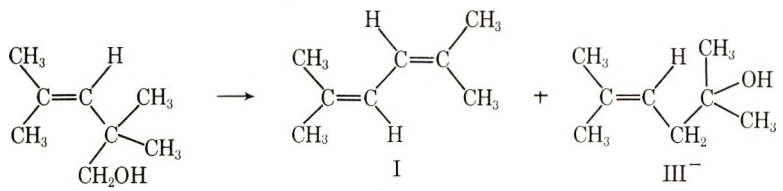

II I III

solvolysis in 50% aqueous ethanol yielded diene (I), rearranged alcohol (III), and the corresponding III-ethyl ether in the ratios (VPC) of 3:9:1. Solvolysis in aqueous pyridine of II-tosylate yielded diene (I) and the hexenol (III). Cyclopropane and cyclobutane ring products were not detected. Solvolysis of II-tosylate in aqueous diglyme in the presence of $BH_4^{\ominus}$ ion,[6] extraction with pentane and distillation gave a mixture of at least five components, bp 114–122°C in the ratio (VPC) of 70:18:3:3:2. The NMR spectrum of the distillate, assumed to show the major component, is consistent with its formulation as chiefly 2,5-dimethyl-2-hexene (reported[7] bp 112°C). We noted further that in an attempt to convert the alcohol (II) to chloride by using thionyl chloride in pyridine or in ether in the presence of potassium carbonate, the diene (I) and 2,2,4,4-tetramethyltetrahydrofuran were the only isolable products. The action of concentrated sulfuric acid on II gave the latter furan derivative exclusively. All compounds reported were identified by analysis and from their NMR spectra.

These results led us to attempt the catalytic dehydration of the homoallylic alcohol. Dehydration was readily accomplished by percolation of pure II over Houdry S-90 (87.5% $SiO_2$, 12.5% $Al_2O_3$, previously dried at 200°C in nitrogen) at 120–150°C under nitrogen. The products were collected in a Dry Ice trap, extracted with ether or pentane, dried, and distilled. Yields of 20–30% of diene (I) and the tetramethyltetrahydrofuran were consistently obtained. The dehydration of cyclopropylmethyl carbinol occurs over alumina at 265–300°C to give comparable yield of vinylcyclopropane.[8] In most instances dehydration of primary alcohols requires temperatures of 350°C or higher.[9,10] The low temperature required for diene (I) formation by catalytic dehydration and the occurrence of primary acetate in the acetolysis products of II-OTS are strong indications of a resonance stabilized intermediate(s) of the cyclopropyl carbinyl and/or bicyclobutonium type. The pattern of methyl substitution appears to favor products derived from ring-opened tertiary carbonium ions. It seems likely that the furan arises from the reaction of II with water at the catalyst surface by protonation of the double bond and ring closure.

The dehydration/rearrangement of II → I was observed as low as 90°C over Houdry S-90 (10% yield). At 200°C and higher, extensive carbonization took place. Traces of diene product were found with the use of $Al_2O_3$ at 100°C. Silica at 200°C gave 5% of diene I and traces of diene were observed using Linde 4A Molecular Sieves as catalyst. Treatment of 2,2,4-trimethyl-3-penten-1-ol with boric acid in refluxing benzene gave tris(2,2,4-trimethyl-3-penten-1-yl) borate. The borate was unchanged on heating at 300°C.

## References

1. A. Henne and A. Turk, *J. Amer. Chem. Soc.*, **64**, 827 (1942).
2. F. B. Moody, paper presented at American Chemical Society Meeting, 1965; *Polymer Preprints*, **12**, No. 2, 285 (1965).
3. J. K. Hecht, C. S. Marvel, and T. W. Campbell, *J. Polym. Sci. A-1*, **5**, 1487 (1967).
4. H. J. Hagemeyer, D. C. Holl, and M. A. Perry, U. S. Pat. 2,941,011.
5. C. F. Wilcox and D. L. Nealy, *J. Org. Chem.*, **28**, 3450 (1963).
6. H. C. Brown and H. M. Bell, *J. Org. Chem.*, **27**, 1928 (1962).
7. *Physical Properties of Chemical Compounds*, Vol. II, American Chemical Society Special Publication, Washington, D.C. 1959, p. 331.
8. V. A. Slabey, *J. Amer. Chem. Soc.*, **73**, 4930 (1952).
9. M. E. Winfield, *Catalysis*, Vol. VII, Reinhold, New York, 1960.
10. K. Kearby, *Ind. Eng. Chem.*, **32**, 1607 (1940).

R. G. Tonkyn*

Union Carbide Corporation
Chemicals Plastics Division
Bound Brook, New Jersey 08805

Received January 31, 1969

* Present address
Betz Laboratories, Inc.
Trevose, Pa. 19047